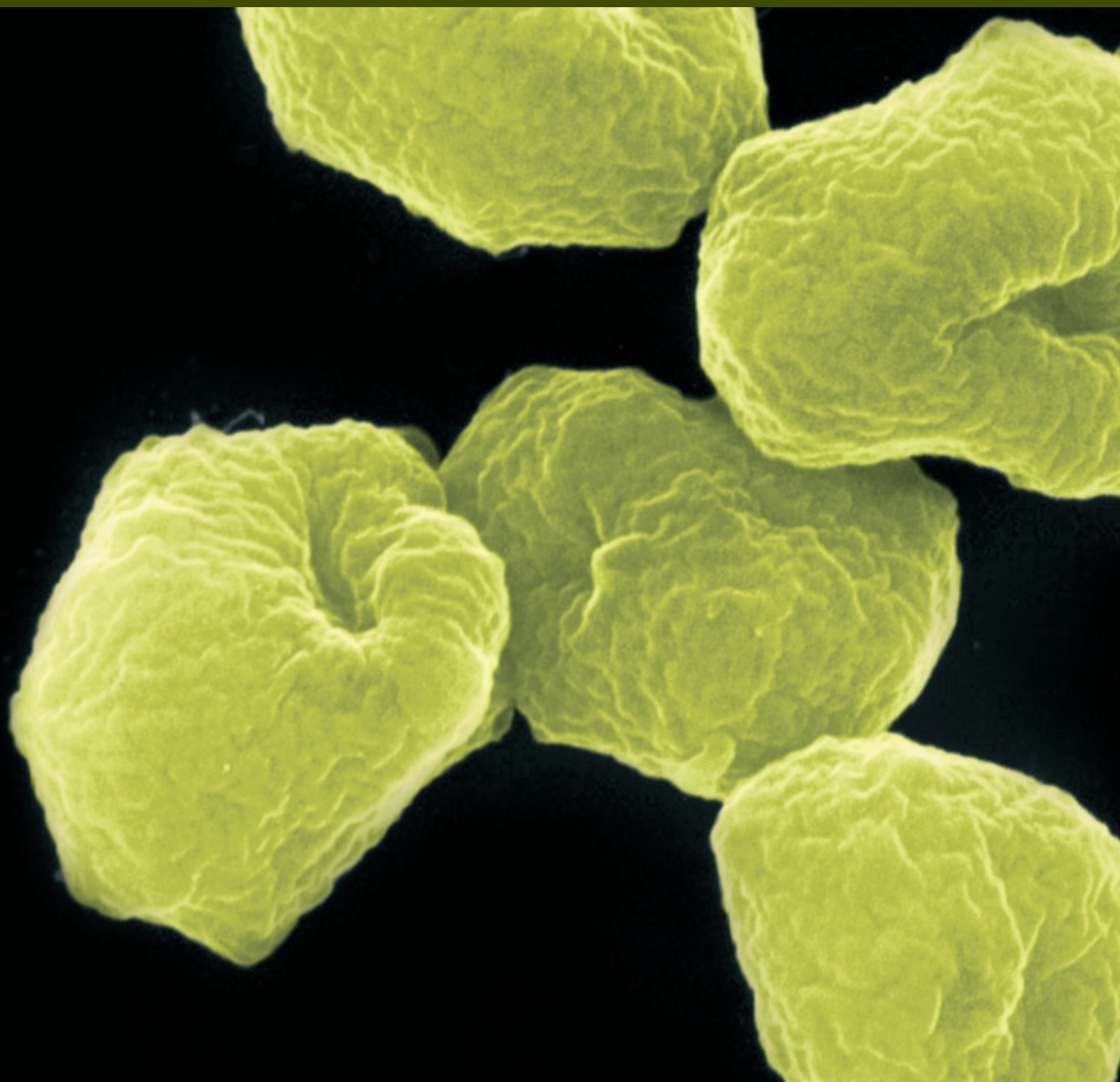# Archaea in Past and Present Geobiochemical Processes and Elemental Cycles

Guest Editors: Michael Hoppert, Martin Krüger, Joachim Reitner, and Charles Cockell

Archaea in Past and Present Geobiochemical Processes and Elemental Cycles

Archaea in Past and Present Geobiochemical Processes and Elemental Cycles

Guest Editors: Michael Hoppert, Martin Krüger, Joachim Reitner, and Charles Cockell

Editorial Board

Contents

Editorial

Archaea in Past and Present Geobiochemical Processes and Elemental Cycles

Michael Hoppert,[1,2] Martin Krüger,[3] Joachim Reitner,[2,4] and Charles Cockell[5]

[1] Institute of Microbiology and Genetics, Georg-August-University Göttingen, 37077 Göttingen, Germany
[2] Courant Research Centre Geobiology, Georg-August-University Göttingen, 37077 Göttingen, Germany
[3] Federal Institute for Geosciences and Resources, 30655 Hannover, Germany
[4] Department of Geobiology (Geoscience Institute), Georg-August-University Göttingen, 37077 Göttingen, Germany
[5] UK Centre for Astrobiology, School of Physics and Astronomy, University of Edinburgh, Edinburgh EH9 3JZ, UK

Correspondence should be addressed to Michael Hoppert; mhopper@gwdg.de

For a long time, Archaea have been considered as an ancient prokaryotic group comprising specialists restricted to narrow ecological niches. This opinion might have been supported by the characteristics of the first well-investigated isolates, being strictly anaerobic (methanogens), halophilic (haloarchaea), or thermophilic (various groups). This is, however, just the tip of the iceberg. Archaea are abundant in all ecosystems. Representatives of the whole domain span the widest range of ecological adaptations from psychrophilic to hyperthermophilic. They tolerate the widest range of pH as well as salt concentrations and use all types of substrates comprising all kinds of organic molecules as well as reduced inorganic compounds.

Nowadays, a multitude of experimental tools is available allowing researchers to study the important role of Archaea and other microorganisms in environmental processes. Most important, analysis of environmental DNA and RNA opens a direct way to assess diversity in specific habitats. The pioneering findings of Carl R. Woese for assessing microbial taxonomy by ribosomal RNA sequence analysis and comparison, together with recently developed powerful amplification and sequencing techniques, widely opened the doors for detection of new hitherto unknown archaeal groups. In particular, the phyla Crenarchaeota and Thaumarchaeota and their significance in environmental cycles could be determined by these techniques. Other tools gain in importance for the assessment of environmental processes. With the increasing availability of annotated genomes, the analysis

of metagenomes and metaproteomes becames possible and now helps us to understand the metabolic processes and networks within microbial communities. The identification of lipids allows bulk quantification of specific prokaryotic groups in recent habitats and even in fossil settings. Finally, microscopic techniques along with functional analysis helps us to understand some of these environmental processes also at structural levels, for example, in microbial mats.

This special issue of the journal Archaea addresses several aspects of the metabolic, structural, and ecological diversity of Archaea from a wide range of research fields.

The contributions by B. Wemheuer et al. point out the diversity of Bacteria and Archaea in hot springs from the Kamchatka Peninsula, revealing the dominance of Proteobacteria, Thermotogae, and Thaumarchaeota. In a second publication, B. Wemheuer et al. address the diversity in a marine habitat with haloarchaea (Halobacteria) as the predominant archaeal group. One of the key processes in sediments is methanogenesis. M. R. Torres-Alvarado et al. show in their study the changes in the abundance and activity of methanogens during dry and rainy seasons in tropical estuarine sediments. The contribution of L. A. Fernández-Güelfo et al. addresses the directed processes of methanogenesis in an anaerobic reactor suitable for wastewater treatment. The whole anaerobic food chain at different temperatures was evaluated by A. Siggins et al. in an anaerobic reactor with trichloroethylene as a substrate. X. L. H. Lim et al. used the lipid archaeol in anoxic water saturated soil as

a biomarker for the biomass of methanogens. Another marker for methanogens was evaluated by C. Wrede et al. for microbial biofilms. Methyl coenzyme M reductase was detected in situ by respective antibodies and was found to be a suitable indicator for the enzymes catalyzing methanogenesis as well as the reverse pathway anaerobic oxidation methane (AOM). Another research article by C. Wrede et al. addresses iron biomineralization in the course of AOM. Finally, a review article on Archaea in symbiosis briefly summarizes the diverse symbiotic interactions of Archaea with organisms of all other domains.

We hope that this issue will support to the statement stressed previously: Archaea, being as diverse as Bacteria, make their contribution to all important global elemental cycles.

Michael Hoppert
Martin Krüger
Joachim Reitner
Charles Cockell

Research Article

Deposition of Biogenic Iron Minerals in a Methane Oxidizing Microbial Mat

Christoph Wrede,[1,2] Sebastian Kokoschka,[1] Anne Dreier,[1,3] Christina Heller,[4,5] Joachim Reitner,[3,4] and Michael Hoppert[1,4]

[1] *Institute of Microbiology and Genetics, Georg-August-University, Grisebachstr. 8, 37077 Göttingen, Germany*

[2] *Hannover Medical School, Institute of Functional and Applied Anatomy, Carl-Neuberg-Str. 1, 30625 Hannover, Germany*

[3] *Courant Centre Geobiology, Georg-August-University, Goldschmidtstr. 3, 37077 Göttingen, Germany*

[4] *Geoscience Centre Göttingen, Georg-August-University, Goldschmidtstr. 3, 37077 Göttingen, Germany*

[5] *Federal Institute for Geosciences and Natural Resources, Stilleweg 2, 30655 Hannover, Germany*

Correspondence should be addressed to Christoph Wrede; cwrede@gwdg.de

The syntrophic community between anaerobic methanotrophic archaea and sulfate reducing bacteria forms thick, black layers within multi-layered microbial mats in chimney-like carbonate concretions of methane seeps located in the Black Sea Crimean shelf. The microbial consortium conducts anaerobic oxidation of methane, which leads to the formation of mainly two biomineral by-products, calcium carbonates and iron sulfides, building up these chimneys. Iron sulfides are generated by the microbial reduction of oxidized sulfur compounds in the microbial mats. Here we show that sulfate reducing bacteria deposit biogenic iron sulfides extra- and intracellularly, the latter in magnetosome-like chains. These chains appear to be stable after cell lysis and tend to attach to cell debris within the microbial mat. The particles may be important nuclei for larger iron sulfide mineral aggregates.

1. Introduction

Frequently, biofilm formation in marine and freshwater systems is accompanied by precipitation of minerals. These minerals are also structurally integrative parts of the microbial biofilm [1]. In most cases, mineral precipitates are deposited in close contact to and in interaction with organic macromolecules, that is, carbohydrates and/or proteins [2]. Formation of a biomineral in a microbial biofilm may be detrimental to the organisms which is mainly due to the enclosure of the living biomass by mineral precipitates. However, also positive effects, for example, when lithified precipitates provide a matrix or scaffold for the microbial biomass, may be expected. It has also been considered that beneficial effects predominate, for example, when biominerals act as chemical filters or shield UV radiation [3]. It is known that, in certain cases, biological macromolecules influence solubility of minerals (e.g., by buffering the aqueous environment or by chelating ions) and may direct the formation of a mineral matrix in a more or less specific way. As a consequence, the shape of biomineral deposits varies considerably at narrow scales and seemingly similar environmental conditions [4].

Mineral deposits caused by the activity of microorganisms are mostly based on either carbonates or silicates [4]. These mineral phases are regularly intermixed with other organic or mineralic compounds (overviews in [2, 5]). A special case of these organomineral precipitations is microbialite formation during anaerobic oxidation of methane (AOM). AOM is conducted by various groups of archaea in a metabolic pathway reverting methanogenesis [6]. Mostly, sulfate reducing bacteria (SRB) participate in AOM [7–9]. The role of SRB is still not fully understood, though is generally accepted that, along with the oxidation of methane, sulfate is reduced: $CH_4 + SO_4^{2-} \rightarrow HCO_3^- + HS^- + H_2O$ [8, 10]. As a result, carbonate phases (calcite and aragonite) and iron sulfides are generated as byproducts of the metabolic process.

It is is known that AOM occurs worldwide in anoxic sediments when methane and electrons acceptors are available (e.g., [11]). The formation of large (several centimeters and bigger) carbonate concretions depends on high methane concentrations under hydrostatic pressure and on the presence of sulfate [8, 9, 12]. In the anaerobic water column of the Black Sea, huge carbonate concretions have been observed at the Crimean shelf [8]. The carbonate buildups may be considered as highly porous "fixed bed" bioreactors, allowing the percolation of methane and the exchange of sea water. The outer and inner surfaces of these carbonate buildups are covered by complex microbial mats, primarily formed by the organisms involved in AOM.

In previous investigations, distinct layers in these microbial mats were discriminated. On the surface, exposed to the sea water, a black layer consists mainly of aggregates between methane-oxidizing archaea of the ANME-2 group and sulfate reducing bacteria (SRB). SRB of this mat type often exhibit intracytoplasmic magnetosome-like chains of greigite precipitations [8, 13, 14]. Our results imply that greigite magnetosomes are one sink for (otherwise toxic) sulfides. These particles were found inside SRB but were also present in the extracellular matrix of the biofilm.

2. Materials and Methods

Microbial mat samples were collected in 2001 during a cruise with the Russian R/V Professor Logachev in the methane seep area located in the GHOSTDABS field (Black Sea north east the Crimean shelf). These samples have already been subjected to extended geochemical and structural analyses [9, 14]. Specific antibodies, directed against methyl-coenzyme M reductase (MCR), the key enzyme of (reverse) methanogenesis, were generated after purification of MCR as essentially described according to [15] by immunization of rabbits following established protocols (e. g., [16] and, the references therein). Specificity of the antibody was extensively studied for methanogenic archaea and reverse methanogens as already described [14, 16, 17].

For microscopic analyses, the samples were chemically fixed in a 4.0% (v/v) aqueous formaldehyde solution (from a 10%, w/v, stock solution, pH 8.0, freshly prepared from paraformaldehyde) and stored in 100 mM PBS (phosphate buffered saline, pH 7.0) at 4°C until further use. The material was then washed several times in PBS and cut to small fragments of about 200 μL volume. Samples were then chemically fixed in a 0.5% (v/v) glutardialdehyde solution (in 100 mM PBS) for 2 h. The samples were then processed as described [18], for electron and light microscopy, and finally cut in ultrathin or semithin sections of either 100–300 nm or 1 μm in thickness. Semithin sections were transferred, with the aid of a transfer loop, on microscope slides, and ultrathin sections were picked up with Formvar-coated grids. For light microscopy, the sections were treated either with an anti-MCR antibody or with the lectin concanavalin A (ConA) coupled to fluorescent marker molecules (Sigma-Aldrich, Deisenhofen, Germany) as described [18]. The lectin ConA IV coupled to Alexa Fluor 546 as fluorescence marker

(Molecular Probes, Eugene, OR, USA) was used in 1/1000 working concentration dilutions in PBS supplemented with 1 mM $CaCl_2$ and $MnCl_2$ (lectin buffer). The sections were mounted on glass slides by heat fixation at 60°C for 15 min and then incubated for 30 min at room temperature. After this, the lectin dilution was soaked off, and the sections were briefly rinsed in pure lectin buffer and covered with coverslips. For immunofluorescence microscopy, the heat-fixed semithin sections were incubated with the antiserum (dil. 1/1000 with PBS, pH 7.5) for 2 h. The sections were rinsed three times in 100 μL drops of PBS (supplemented with 0.01% Tween 20) and incubated with a secondary goat anti-rabbit antibody, coupled to Alexa Fluor 546 fluorescent dye (Molecular Probes, Eugene, OR, USA), diluted 1 : 250 [14]. The rinsing steps were repeated. Fluorescence microscopy was performed with an Axio Scope light microscope using filter set 43 (BP: 545/25, FT 570, LP: 605/70) and the AxioVision software package (Zeiss, Göttingen, Germany). For comparison, phase contrast images were taken and were digitally merged with fluorescence images.

For transmission electron microscopy, ultrathin sections obtained from five distinct samples were mounted on Formvar-coated 300 mesh specimen grids. Immunolocalization with antibodies directed against MCR was performed as described. Mounted sections were stained with phosphotungstic acid (3%, w/v), if not stated otherwise [14]. Electron microscopy was performed in a Zeiss EM 902 transmission electron microscope (Zeiss, Oberkochen, Germany), equipped with a eucentric goniometer stage. Images were recorded with a 1 KB digital camera. Detection and enhancement of colloidal gold markers in digitized electron micrographs were performed as described [19]. Electron energy loss spectroscopy (EELS) of iron-containing particles was performed essentially as described in [20], with the aid of the analysis V software package (Olympus-SIS, Münster, Germany). Electron energy loss was measured between 655 eV and 751 eV. The L2 (720.6 eV) and L3 (708.0 eV) edges, observed for pure iron minerals, were represented by one broad peak at approximately 715 eV of the deposits in embedded and ultrathin sectioned biofilms.

Goniometry was performed by tilting 300 nm sections ±60 degrees with 1-degree increments. Tomograms were performed with the EM3D 2.0 software package (Department of Neurobiology, Stanford University [21]).

3. Results and Discussion

Two layers of microbial mats retrieved from the the Black Sea Crimean shelf have been identified as important for AOM: the orange (or pink) layer and the black layer. The orange layer consists of various cell morphotypes [8, 22]. Most of them were identified as ANME-1 archaea. ANME-1 cells are morphologically similar to the filamentous methanogens *Methanospirillum* and *Methanosaeta*; these cells are covered by a tight and very rigid protein sheath [23]. Sulfate reducing bacteria were present in large clusters, but not in direct contact with ANME-1 cells [8]. Visually, the black layer could be clearly distinguished from other layers. In contrast

(a)

(b)

(c)
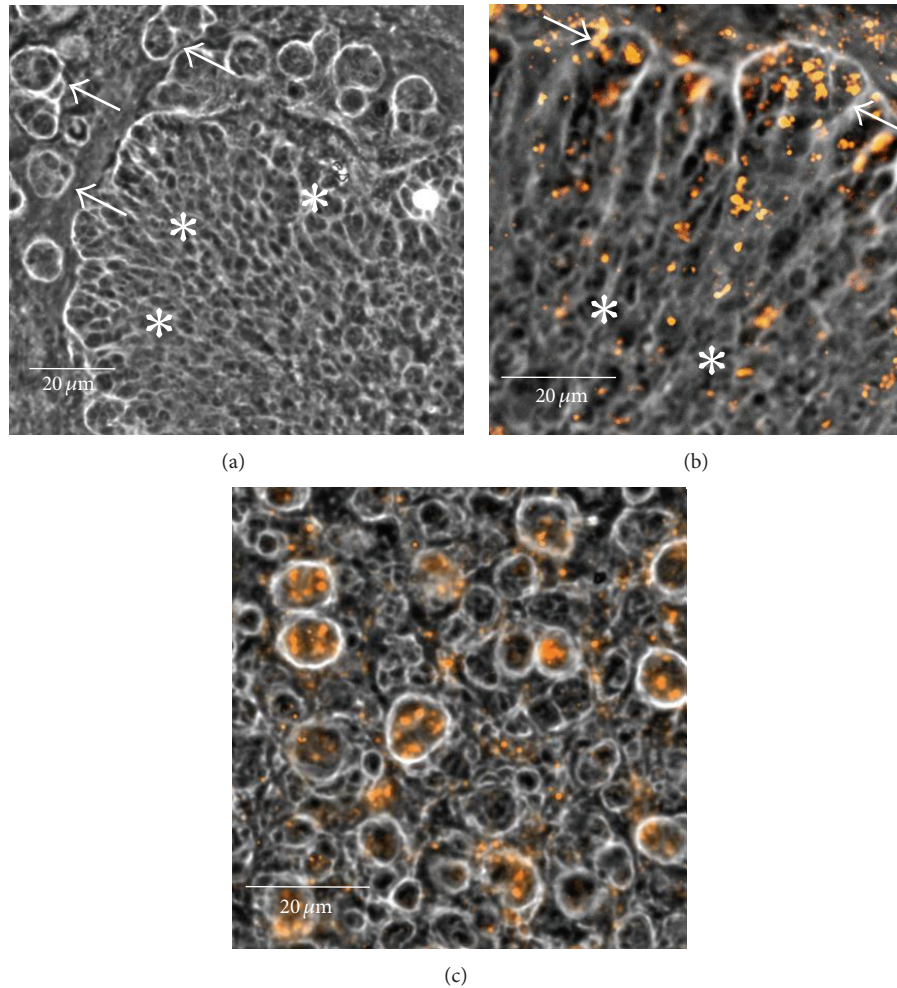
FIGURE 1: Light micrographs of semithin sections after immunofluorescence staining with anti-MCR antibodies (merged fluorescence/phase contrast images). (a) One large, cauliflower-like aggregate (lower right, the whole aggregate marked by three asterisks) surrounded by small globular aggregates (arrows) in an unstained semithin section (phase contrast microscopy). (b) Periphery of a large aggregate. The cell density at the periphery of the aggregate (arrows) is higher than in the central area (asterisks). (c) Small aggregates after fluorescence staining.

to the orange layer, the black layer consists of aggregates formed by ANME-2 and SRB of the DSS group [8, 24, 25]. Immunofluorescence labelling of MCR, performed on resin sections, marks the position of the MCR-expressing ANME-2 inside large cauliflower-shaped aggregates, consisting of thousands of cells visible in a section (Figure 1(a), asterisks, Figure 1(b)). Similar labelling experiments have been also performed on the same samples with antibodies directed against the dissimilatory adenosine-5′-phosphosulfate (APS) reductase, along with the identification of the respective gene in the microbial mat samples [14]. APS reductase is a key enzyme of sulfate reduction and could be localized in the magnetosome-bearing cell type (see below), identified as SRB.

In addition to these large cauliflower-shaped aggregates, also a smaller globular-shaped aggregate type of 5–20 labeled ANME-2 cells was identified (Figure 1(c)). This aggregate type is located in the surrounding (Figure 1(a), arrows) and in the center of the cauliflower-shaped features. All aggregates are separated by areas of low cell densities. It has to be noted that not all cells visible in the depicted sections are labelled, since markers do only bind to cells with their cytoplasm exposed to the section surface. In the large type of aggregates, cells are not completely randomly distributed; higher cell densities are observable at the periphery, separated in irregular lobes (Figure 1(b), arrows). Both types of aggregates consist of ANME-2/SRB consortia [8, 14, 22]. The electron micrographs in Figure 2 show ANME-2 (immunogold labelled) and SRB (nearly unlabeled) in a globular aggregate, surrounded by multiple layers of extracellular material. The gaps between the large aggregates are filled with EPS [18]. These gaps show a distinct lectin labelling (Figure 3(a), arrows), in contrast to the unlabeled extracellular surrounding of the ANME-2/SRB consortia. Various morphotypes of prokaryotic cells could be detected in these empty spaces (Figure 3(b), cf. [14]), including thin filaments of several μm in length and 200 nm in diameter (arrows in Figure 3(b)). Some filaments still contain a dark stained

(a)

(b)
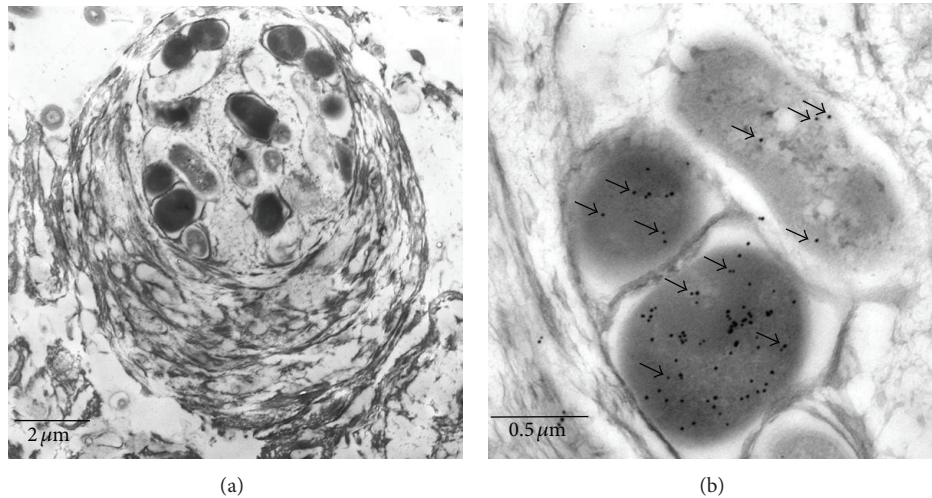
FIGURE 2: Immunoelectron microscopy. (a) Electron microscopy of a typical small aggregate (cf. Figure 1(c)), consisting of ANME-2/SRB. Several single cells are surrounded by a thick multilayered mucilage. (b) Detail of the aggregate as depicted in (a). The MCR expressing ANME-2 cells are labelled with small gold dots (black arrows point to some dots); the SRB (upper right cell) show a low background labelling (black arrows).

(a)

(b)
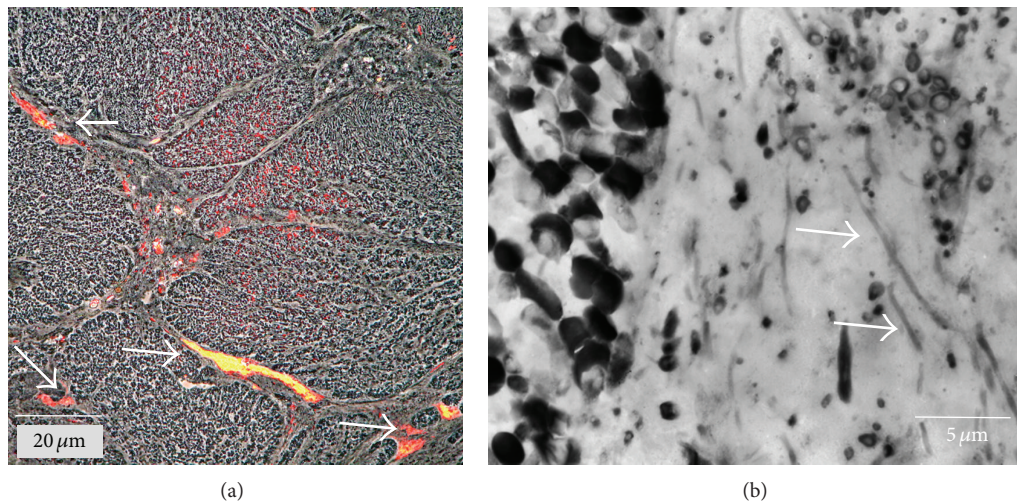
FIGURE 3: Appearance of gaps between large aggregates. (a) Overview: large patches outside aggregates show intense fluorescence (arrows) after staining with fluorescently labeled ConA lectin. (b) Electron micrograph of a 300 nm thick section from the aggregate periphery with intact cells (left) and cell debris embedded in EPS (right). Arrows point to long filaments.

matrix, putatively cytoplasmic contents. Shallowly stained filaments likely represent empty cell envelopes (Figures 4(b), 5(a), and 5(b)).

Within these large, cauliflower-shaped aggregates, SRB exhibit peculiar cytological features. Apart from occasionally observed intracytoplasmic membranes, intracellular magnetosome-like particles, arranged in straight rows and composed of greigite, were observed frequently [8, 14]. Here, we show that these chains appear to be stable after cell death and cell lysis, but exhibit structural modifications. In intact cells, chains are arranged in straight rows, mostly as parallel pairs (Figure 4(b), inset, Figure 4(c)). Figure 4(c) shows

magnetosome chains in unstained sections; that is, the cells, though still present and morphologically intact, are invisible here. Basically, three variants of magnetosome-like chains could be observed. These variants may represent three stages of development. In a (putatively) early stage, chains appear to be absent (Figure 4(a)). During aggregate development, the organisms deposit intracellular chains (Figures 4(b) and 4(c)). Finally, the organisms get lysed, and in stained sections, just the magnetosomes and some cell debris are still present; the free chains still mark the positions of the SRB in the aggregate (Figure 4(d)); distances between these deposits are similar to the distances between magnetosome chains in
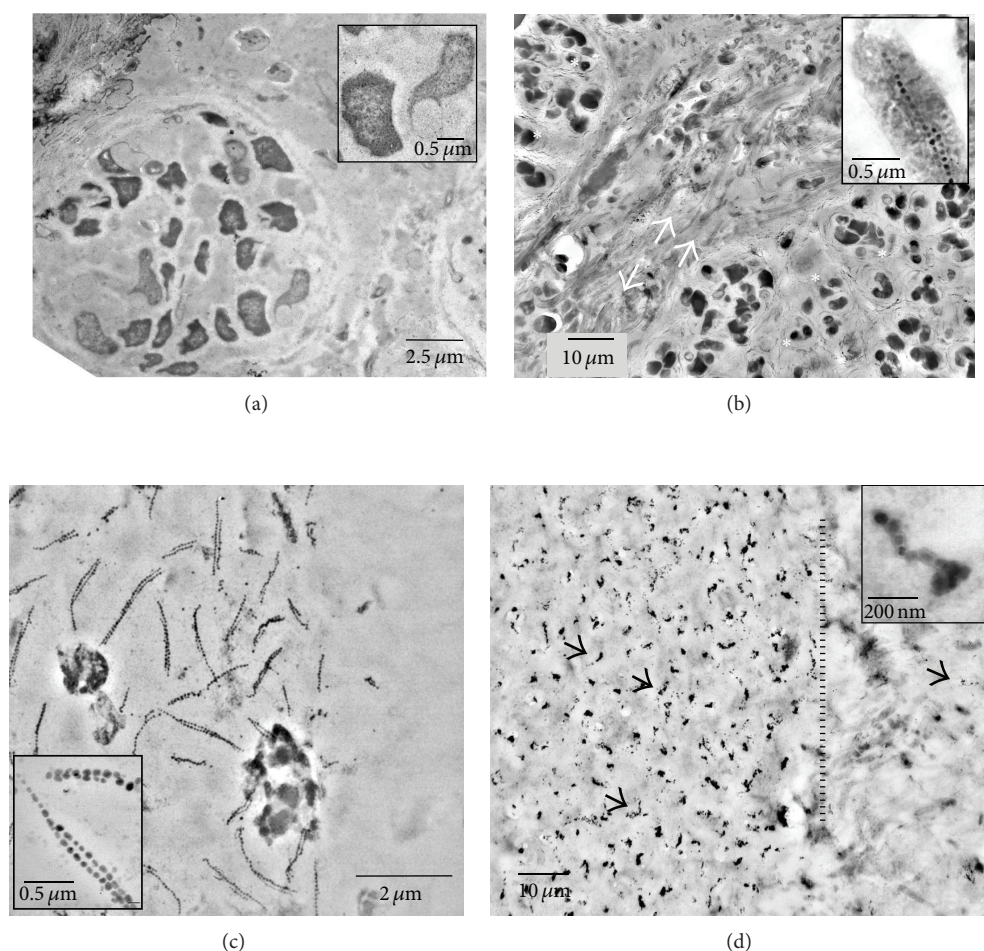
FIGURE 4: Aggregates in different stages of magnetosome-like chain formation. (a) ANME-2/SRB aggregate without visible precipitates. (b) Periphery of a large aggregate (asterisk), with gap between aggregates (arrows). Cells with multiple magnetosome-like chains (inset; see also (c)). Note cell debris, mainly consisting of envelopes from filamentous cells (arrows), outside the aggregates. (c) Periphery of an intact aggregate as depicted in (b) (unstained section; cells are invisible), showing the position of straight magnetosome chains inside cells. (d) ANME-2/SRB aggregate after cell lysis (cells are absent in spite of staining, compare (c)), with magnetosome chains still in place (some chains are marked by arrows). The inset shows a single chain. The dotted line marks the border of the aggregate (right of the dotted line). Some chains are found outside the area of the aggregate.

neighboured intact cells (Figure 4(c)). Chains of the same size are also intermixed with the cell debris in the gaps between the ANME-2/SRB aggregates; here they appear to be attached to cell envelopes of filamentous morphotypes (Figure 5(a)). Mostly, the chains exhibit curves and wrinkles, perhaps due to the loss of their intracellular scaffolding structure (cf. [26]), though also straight chains are observable. Figures 5(b) and 5(c) show particles of increased size, from 30 nm to up to 100 nm in diameter. The particles appear to be attached to the filamentous morphotype (Figure 5(c)). Larger agglomerations of these particles are found near 0.5 μm sized microcrystals (arrows in Figure 5(d)), similar to particles forming pyrite framboids (cf. [7]). It is unclear if the greigite magnetosomes contribute, in the end, to the formation of these crystals and/or framboidal pyrite

(e.g., [7, 27, 28]), but the contribution of free magnetosome chains to the iron sulfide minerals in the black layer appears to be obvious. In particular, the "reactive" surfaces of prokaryotic cell envelopes are involved in binding and accumulation of these particles. Figure 6 summarizes our observations and proposes a schematic sequence of the observed features. Active consortia may not contain magnetosome-like chains in the beginning (a), but in most of the aggregates, well-developed chains are present ((b) and (c)). The involvement of these magnetosomes in chemotaxis appears to be doubtful, since the SRB are immotile during all stages of biofilm development. It may be speculated that the particles are, in this case, an intracellular "dead end" storage granule, accumulating iron sulfides as waste product from sulfate reduction (cf. [29]). It has to be expected that not all reduced

(a)

(b)

(c)

(d)
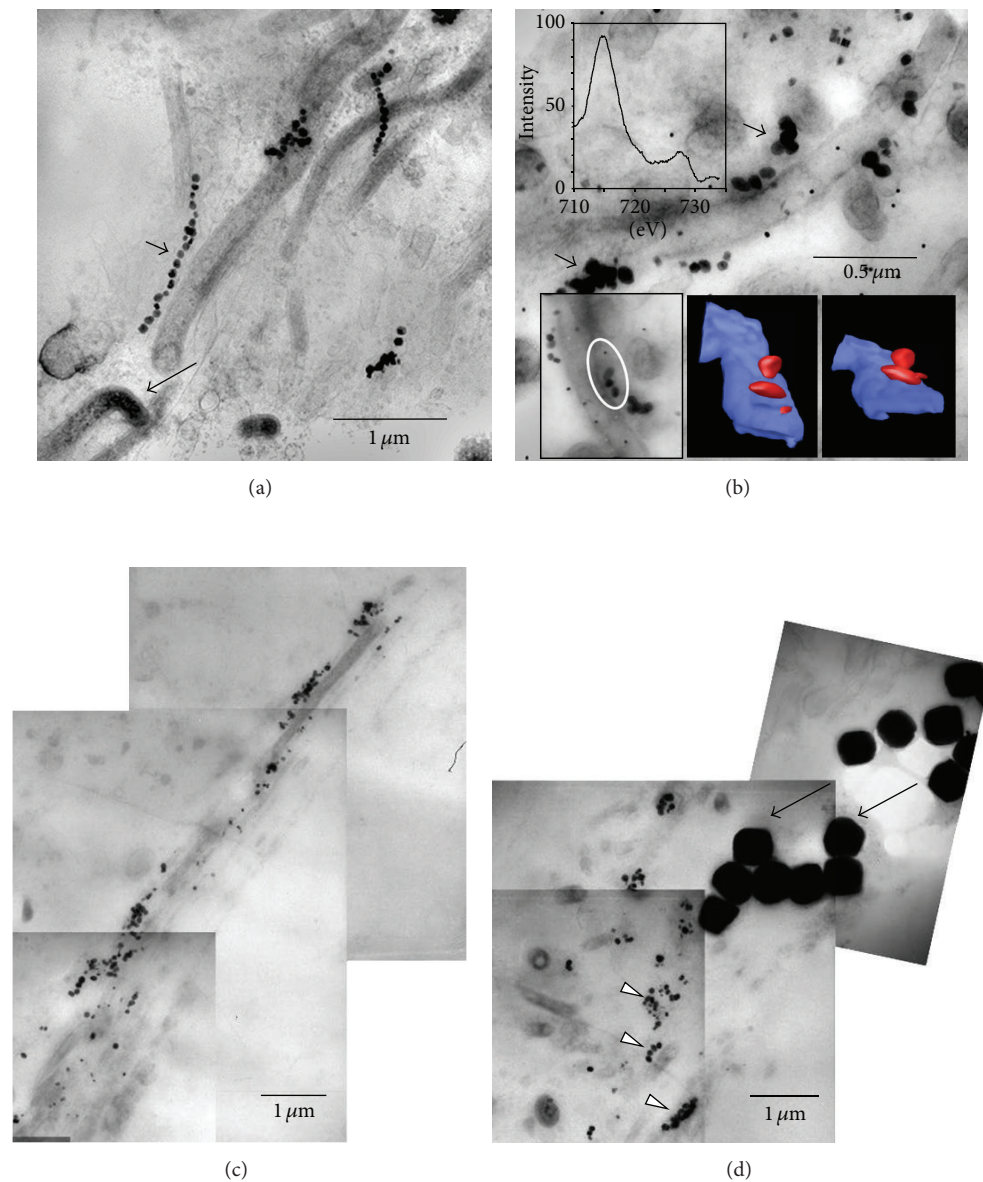
FIGURE 5: Extracellular magnetosome-like features. (a) Extracellular magnetosome chains (short arrow) bound to filamentous cell envelopes. Occasionally, also intact organisms, filled with dark cytoplasm, are visible (long arrow). (b) Particles (arrows), double in size of magnetosomes close or attached to filaments. The EELS spectrum (upper left inset) shows the energy loss at the Fe L2/L3 edges. The lower right insets show a tomogram of a small section (encircled) as depicted in the lower left inset (blue: cell envelope, red: particles). The small dots represent randomly distributed colloidal gold particles (no markers) necessary for image alignment of the tilted sections. (c) Overview image showing aggregates of the particles adjacent to filamentous envelopes. (d) Aggregates of particles (arrowheads) and typical microcrystals from framboidal pyrite (arrows).

sulfur compounds end up inside cells and, as known from other sulfate reducing bacteria, sulfides are also deposited outside cells. However, intracellular deposition may be also a rapid way to keep the concentration of sulfides as low as possible. It is obvious that both syntrophic partners die and lyse (possibly all cells at the same time) leaving the magnetosome chains as still visible remains (d) inside the aggregates. Free chains (e) migrate, by diffusion in the matrix outside the aggregate bind to a specific type of cell envelope (f), and lose their chain-like appearance and regular size (g).

Conflict of Interests

The authors declare that they have no conflict of interests.
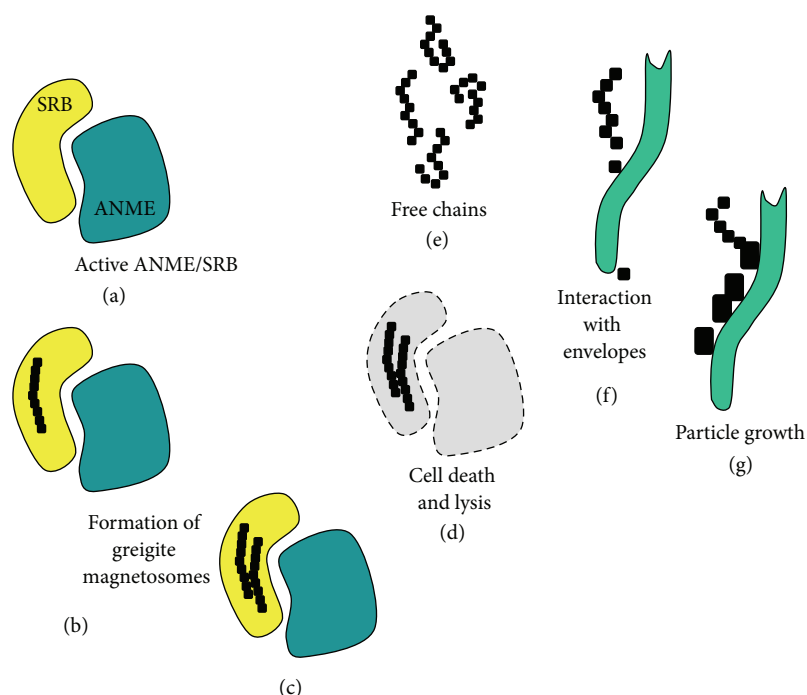
FIGURE 6: Turnover of magnetosome-like chains in the black layer. See Section 3 for further explanation.

Acknowledgments

References

[1] R. V. Burne and L. S. Moore, "Microbialites: organosedimentary deposits of benthic microbial communities," *Palaios*, vol. 2, no. 3, pp. 241–254, 1987.

[2] A. W. Decho, "Microbial biofilms in intertidal systems: an overview," *Continental Shelf Research*, vol. 20, no. 10-11, pp. 1257–1273, 2000.

[3] V. R. Phoenix and K. O. Konhauser, "Benefits of bacterial biomineralization," *Geobiology*, vol. 6, no. 3, pp. 303–308, 2008.

[4] D. S. S. Lim, B. E. Laval, G. Slater et al., "Limnology of Pavilion Lake, B. C., Canada: characterization of a microbialite forming environment," *Fundamental and Applied Limnology*, vol. 173, no. 4, pp. 329–351, 2009.

[5] P. U. P. A. Gilbert, M. Abrecht, and B. H. Frazer, "The organic-mineral interface in biominerals," *Reviews in Mineralogy and Geochemistry*, vol. 59, pp. 157–185, 2005.

[6] S. J. Hallam, N. Putnam, C. M. Preston et al., "Reverse methanogenesis: testing the hypothesis with environmental genomics," *Science*, vol. 305, no. 5689, pp. 1457–1462, 2004.

[7] J. Peckmann, A. Reimer, U. Luth et al., "Methane-derived carbonates and authigenic pyrite from the northwestern Black Sea," *Marine Geology*, vol. 177, no. 1-2, pp. 129–150, 2001.

[8] J. Reitner, J. Peckmann, M. Blumenberg, W. Michaelis, A. Reimer, and V. Thiel, "Concretionary methane-seep carbonates and associated microbial communities in Black Sea sediments," *Palaeogeography, Palaeoclimatology, Palaeoecology*, vol. 227, no. 1–3, pp. 18–30, 2005.

[9] J. Reitner, J. Peckmann, A. Reimer, G. Schumann, and V. Thiel, "Methane-derived carbonate build-ups and associated microbial communities at cold seeps on the lower Crimean shelf (Black Sea)," *Facies*, vol. 51, no. 1–4, pp. 66–79, 2005.

[10] J. T. Milucka, T. G. Ferdelman, L. Polerek et al., "Zero-valent sulphur is a key intermediate in marine methane oxidation," *Nature*, vol. 491, no. 7425, pp. 541–546, 2012.

[11] K. U. Hinrichs and A. Boetius, "The anaerobic oxidation of methane: new insights in microbial ecology and biogeochemistry," in *Ocean Margin Systems*, G. Wefer, D. Billet, D. Hebbeln, B. B. Jørgensen, M. Schlüter, and T. van Weering, Eds., pp. 457–477, Springer, Heidelberg, Germany, 2002.

[12] W. Michaelis, R. Seifert, K. Nauhaus et al., "Microbial reefs in the black sea fueled by anaerobic oxidation of methane," *Science*, vol. 297, no. 5583, pp. 1013–1015, 2002.

[13] C. T. Lefèvre, N. Menguy, F. Abreu et al., "A cultured greigite-producing magnetotactic bacterium in a novel group of sulfate-reducing bacteria," *Science*, vol. 334, no. 6063, pp. 1720–1723, 2011.

[14] C. Wrede, V. Krukenberg, A. Dreier, J. Reitner, C. Heller, and M. Hoppert, "Detection of metabolic key enzymes of methane turnover processes in cold seep microbial biofilms," *Geomicrobiology Journal*, vol. 30, no. 3, pp. 214–227, 2013.

[15] M. Hoppert and F. Mayer, "Electron microscopy of native and artificial methylreductase high-molecular-weight complexes in strain Go 1 and Methanococcus voltae," *FEBS Letters*, vol. 267, no. 1, pp. 33–37, 1990.

[16] I. J. Braks, M. Hoppert, S. Roge, and F. Mayer, "Structural aspects and immunolocalization of the F420-reducing and non-F420-reducing hydrogenases," *Journal of Bacteriology*, vol. 176, no. 24, pp. 7677–7687, 1994.

[17] M. Krüger, A. Meyerdierks, F. O. Glöckner et al., "A conspicuous nickel protein in microbial mats that oxidize methane anaerobically," *Nature*, vol. 426, no. 6968, pp. 878–881, 2003.

[18] C. Wrede, C. Heller, J. Reitner, and M. Hoppert, "Correlative light/electron microscopy for the investigation of microbial mats from Black Sea Cold Seeps," *Journal of Microbiology Methods*, vol. 73, no. 2, pp. 85–91, 2008.

[19] M. Kämper, S. Vetterkind, R. Berker, and M. Hoppert, "Methods for in situ detection and characterization of extracellular polymers in biofilms by electron microscopy," *Journal of Microbiological Methods*, vol. 57, no. 1, pp. 55–64, 2004.

[20] R. Bauer, "Electron spectroscopic imaging: an advanced technique for imaging and analysis in transmission electron microscopy," *Methods in Microbiology*, vol. 20, pp. 113–146, 1988.

[21] D. Ress, M. L. Harlow, M. Schwarz, R. M. Marshall, and U. J. McMahan, "Automatic acquisition of fiducial markers and alignment of images in tilt series for electron tomography," *Journal of Electron Microscopy*, vol. 48, no. 3, pp. 277–287, 1999.

[22] C. Heller, M. Hoppert, and J. Reitner, "Immunological localization of coenzyme M reductase in anaerobic methane-oxidizing archaea of ANME 1 and ANME 2 type," *Geomicrobiology Journal*, vol. 25, no. 3-4, pp. 149–156, 2008.

[23] T. J. Beveridge, G. D. Sprott, and P. Whippey, "Ultrastructure, inferred porosity, and gram-staining character of Methanospirillum hungatei filament termini describe a unique cell permeability for this archaeobacterium," *Journal of Bacteriology*, vol. 173, no. 1, pp. 130–140, 1991.

[24] A. Boetius, K. Ravenschlag, C. J. Schubert et al., "A marine microbial consortium apparently mediating anaerobic oxidation methane," *Nature*, vol. 407, no. 6804, pp. 623–626, 2000.

[25] L. Schreiber, T. Holler, K. Knittel, A. Meyerdierks, and R. Amann, "Identification of the dominant sulfate-reducing bacterial partner of anaerobic methanotrophs of the ANME-2 clade," *Environmental Microbiology*, vol. 12, no. 8, pp. 2327–2340, 2010.

[26] A. Scheffel, M. Gruska, D. Faivre, A. Linaroudis, J. M. Plitzko, and D. Schüler, "An acidic protein aligns magnetosomes along a filamentous structure in magnetotactic bacteria," *Nature*, vol. 440, no. 7080, pp. 110–114, 2006.

[27] J. Schieber, "Sedimentary pyrite: a window into the microbial past," *Geology*, vol. 30, no. 6, pp. 531–534, 2002.

[28] L. C. W. MacLean, T. Tyliszczak, P. U. P. A. Gilbert et al., "A high-resolution chemical and structural study of framboidal pyrite formed within a low-temperature bacterial biofilm," *Geobiology*, vol. 6, no. 5, pp. 471–480, 2008.

[29] M. Pósfai, B. M. Moskowitz, B. Arató et al., "Properties of intracellular magnetite crystals produced by *Desulfovibrio magneticus* strain RS-1," *Earth and Planetary Science Letters*, vol. 249, no. 3-4, pp. 444–455, 2006.

Research Article

Microbial Diversity and Biochemical Potential Encoded by Thermal Spring Metagenomes Derived from the Kamchatka Peninsula

Bernd Wemheuer,[1] Robert Taube,[1] Pinar Akyol,[1] Franziska Wemheuer,[2] and Rolf Daniel[1]

[1] *Department of Genomic and Applied Microbiology and Goettingen Genomics Laboratory, Institute of Microbiology and Genetics, Georg-August-University Goettingen, Grisebachstraße 8, 37077 Goettingen, Germany*

[2] *Section of Agricultural Entomology, Department for Crop Sciences, Georg-August-University Goettingen, Grisebachstraße 6, 37077 Goettingen, Germany*

Correspondence should be addressed to Rolf Daniel; rdaniel@gwdg.de

Volcanic regions contain a variety of environments suitable for extremophiles. This study was focused on assessing and exploiting the prokaryotic diversity of two microbial communities derived from different Kamchatkian thermal springs by metagenomic approaches. Samples were taken from a thermoacidophilic spring near the Mutnovsky Volcano and from a thermophilic spring in the Uzon Caldera. Environmental DNA for metagenomic analysis was isolated from collected sediment samples by direct cell lysis. The prokaryotic community composition was examined by analysis of archaeal and bacterial 16S rRNA genes. A total number of 1235 16S rRNA gene sequences were obtained and used for taxonomic classification. Most abundant in the samples were members of *Thaumarchaeota*, *Thermotogae*, and *Proteobacteria*. The Mutnovsky hot spring was dominated by the Terrestrial Hot Spring Group, *Kosmotoga*, and *Acidithiobacillus*. The Uzon Caldera was dominated by uncultured members of the Miscellaneous Crenarchaeotic Group and *Enterobacteriaceae*. The remaining 16S rRNA gene sequences belonged to the *Aquificae*, *Dictyoglomi*, *Euryarchaeota*, *Korarchaeota*, *Thermodesulfobacteria*, *Firmicutes*, and some potential new phyla. In addition, the recovered DNA was used for generation of metagenomic libraries, which were subsequently mined for genes encoding lipolytic and proteolytic enzymes. Three novel genes conferring lipolytic and one gene conferring proteolytic activity were identified.

1. Introduction

Sites of volcanic activity can be found all over the world and even under the sea. Volcanic regions provide a variety of different environments for extremophilic archaeal and bacterial microorganisms. Well-known examples of such extreme environments are terrestrial surface hot springs. With respect to geographical, physical, environmental, and chemical characteristics, hot springs are unique sites for extremophilic microorganisms [1–3]. Extremophiles inhabiting hot springs are considered to be the closest living descendants of the earliest life forms on Earth [4, 5]. Therefore, these springs provide insights into the origin and evolution of life. In addition, thermophiles and hyperthermophiles

produce a variety of hydrolytic enzymes such as lipases, glycosidases, peptidases and other biomolecules, which are of industrial interest [6–8]. For example, Hotta et al. [9] found an extremely stable carboxylesterase in the hyperthermophilic archaeon *Pyrobaculum calidifontis* VA1, and Arpigny et al. [10] identified a novel heat-stable lipolytic enzyme in *Sulfolobus acidocaldarius* DSM 639.

Especially in extreme environments, most microorganisms are reluctant to cultivation-based approaches [11, 12]. Therefore, culture-independent metagenomic strategies are promising approaches to assess the phylogenetic composition and functional potential of microbial communities living in extreme environments [7, 13, 14]. For example, Simon et al. studied the prokaryotic community in glacier ice and found a

highly diverse bacterial community [15]. In 1998, Hugenholtz et al. [1] investigated the bacterial diversity in the Obsidian Pool in Yellowstone National Park and identified several new bacterial candidate divisions. The same pool and two others were studied later by Meyer-Dombard et al. [16]. They encountered diverse bacterial and archaeal communities in all three hot springs.

In the present study, we investigated the phylogenetic composition and metabolic potential of two microbial communities derived from two extreme sites of the Kamchatka peninsula, which is located in the Far East of Russia. The Kamchatka peninsula comprises an area of approximately $472,300 \, \text{km}^2$ and is described as the *land of fire* by its first explorers due to the high density of volcanoes and associated volcanic phenomena. For example, the largest active volcano of the northern hemisphere, the Klyuchevskaya Sopka, is located on the Kamchatka Peninsula. Sediment samples analyzed in this study were taken from two hot springs providing a thermoacidophilic (70°C, pH 3.5–4) or a thermophilic (81°C, pH 7.2–7.4) environment. The composition of the prokaryotic communities of the two Kamchatkian hot springs was assessed by 16S rRNA gene analysis. In addition, metagenomic libraries were generated and screened for novel biocatalysts.

2. Materials and Methods

2.1. Sampling and DNA Extraction. Two sediment samples were taken from the hot springs located on the Kamchatka peninsula in summer 2001. The first sample was collected from a thermoacidophilic spring (70°C, pH 3.5–4) at the Mutnovsky volcano (52.453 N, 158.195 E). The second sample was taken from a thermophilic spring (81°C, pH 7.2–7.4) in the Uzon Caldera (54.5 N, 159.967 E). The chemical analysis of both sediment samples is shown in Table 1.

DNA was extracted as described by Zhou et al., 1996 [17]. The concentration of the recovered DNA was quantified using a NanoDrop ND-1000 spectrophotometer (PEQLAB, Erlangen, Germany).

2.2. Amplification of 16S rRNA Genes and Generation Clone Libraries. To assess the prokaryotic community structure, archaeal and bacterial 16S rRNA genes were amplified by PCR and analyzed. The PCR reaction mixture (50 μL) contained 2.5 μL of 10-fold Mg-free *Taq* polymerase buffer, 200 μM of each of the four deoxynucleoside triphosphates, 1.75 mM $MgCl_2$, 0.4 μM of each primer, 1 U of *Taq* DNA polymerase (Fermentas, St. Leon-Rot, Germany), and approximately 25 ng of recovered DNA as a template. Prokaryotic 16S rRNA genes were amplified with the following set of primers: 8F 5$'$-AGAGTTTGATCMTGGC-3$'$ [18] and 1114R 5$'$-GGG-TTGCGCTCGTTRC-3$'$ [19], A800F 5$'$-GTAGTCCYGGCY-GTAAAC-3$'$ [20] and A1530R 5$'$-GGAGGTGATCCAGCC-G-3$'$ [21], and Arch8F 5$'$-TCCGGTTGATCCTGCCGG-3$'$ [15] and Arch958R 5$'$-YCCGGCGTTGAMTCCAATT-3$'$ [22]. The following thermal cycling scheme was used: initial denaturation at 94°C for 2 min, 25 cycles of denaturation at 94°C for 1.5 min, annealing at 56°C (8F and 1114R), 51°C

(A800F and A1530R), or 55°C (Arch8F and 958R), followed by extension at 72°C (1 min for 1 kb). The final extension was carried out at 72°C for 10 min. Negative controls were performed by using the reaction mixture without template. The obtained PCR products were purified using the Wizard SV Gel and PCR clean up system (Promega, Madison, USA) and subsequently cloned into pCR2.1-TOPO as recommended by the manufacturer (Invitrogen, Carlsbad, USA). The resulting recombinant plasmids were used to transform *Escherichia coli* TOP 10 cells. A total of 1271 insert-carrying plasmids were isolated from randomly selected *E. coli* clones. The insert sequences were determined by the Göttingen Genomics Laboratory (Göttingen, Germany).

2.3. Analysis of 16S rRNA Genes. To assess the prokaryotic community structure, the retrieved 16S rRNA gene sequences were analyzed using QIIME [23]. The obtained 16S gene sequences were edited using gap4 [24] and initially checked for the presence of chimeric sequences using Mallard [25], Bellerophon [26], and Chimera Check [27]. Remaining

TABLE 1: Chemical analysis of the two investigated sediment samples (DM: dry matter, DIN: in accordance with the DIN (German Institute for Standardization) norm, VDLUFA: Association of German Agricultural Analytic and Research Institutes).

Element	Method	Mutnovsky (mg/kg DM)	Uzon Caldera (mg/kg DM)
Aluminum	DIN ISO 22036	22000	13000
Arsenic	DIN ISO 22036	21	590
Barium	DIN ISO 22036	20	120
Beryllium	DIN ISO 22036	<0.20	<0.20
Boron	DIN ISO 22036	<3.0	8.7
Cadmium	DIN ISO 22036	<0.10	<0.10
Calcium	DIN ISO 22036	23000	17000
Chromium	DIN ISO 22036	580	320
Cobalt	DIN ISO 22036	45	11
Copper	DIN ISO 22036	240	22
Iron	DIN ISO 22036	97000	27000
Lead	DIN ISO 22036	5.7	<2.0
Magnesium	DIN ISO 22036	2800	4200
Manganese	DIN ISO 22036	150	440
Nickel	DIN ISO 22036	270	150
Phosphorus	DIN ISO 22036	230	130
Potassium	DIN ISO 22036	120	530
Sodium	DIN ISO 22036	110	1200
Strontium	DIN ISO 22036	24	40
Titanium	DIN ISO 22036	1100	870
Vanadium	DIN ISO 22036	82	57
Zinc	DIN ISO 22036	73	42
pH (CaCl$_2$)*	VDLUFA-Method A 5.1.1	6.4	6.8
TOC	DIN EN 13137	1.06	0.67

*pH values of the two sediments were measured in situ.

sequences were clustered employing the UCLUST algorithm [28] and the following QIIME scripts: pick_otus.py and pick_rep_set.py. The sequences were clustered in operational taxonomic units (OTUs) at 1, 3, and 20% genetic dissimilarity.

The phylogenetic composition of the prokaryotic communities in both samples was determined using the QIIME assign_taxonomy.py script. A BLAST alignment [29] against the most recent SILVA ARB database [30] was performed. Sequences were classified with respect to the taxonomy of their best hit in the ARB database. Finally, OTU tables were generated. Rarefaction curves, Shannon indices [31], and Chao1 indices [32] were calculated employing QIIME. In addition, the maximal number of OTUs (n_{max}) was estimated for each sample using the Michaelis-Menten-fit alpha diversity metrics included in the QIIME software package.

One sequence per OTU (1% genetic distance) was further used for the construction of phylogenetic trees. Sequences were imported into the most recent SSU Ref SILVA database of the ARB program package [33]. Multiple sequence alignments were checked manually and improved by employing the ARB editor tool. Phylogenetic trees were created by employing the maximum parsimony algorithm implemented in ARB. The robustness of obtained tree topologies was evaluated by bootstrap analysis with 100 resemblings.

2.4. Construction of Small-Insert Metagenomic Libraries. To exploit the biochemical potential, metagenomic small-insert libraries were generated. Due to the low DNA recovery, starting material for the generation of these libraries was obtained by multiple displacement amplification employing the GenomiPhi V2 DNA Amplification Kit (GE Healthcare, Munich, Germany). To improve cloning efficiency, hyperbranched structures were resolved and the DNA was inserted into pCR-XL-TOPO (Invitrogen) as described by Simon et al. [34]. In this way, two metagenomic libraries were generated.

2.5. Screening for Hydrolytic Activity and Identification of Corresponding Genes. The constructed metagenomic libraries were screened for genes conferring lipolytic or proteolytic activity using a function-driven approach. The constructed libraries were used to transform *E. coli* DH5α cells. Recombinant cells were plated on LB agar plates containing either 1% tributyrin (lipolytic activity) [35] or 2% skim milk (proteolytic activity) [36]. Plates were incubated at 37°C for up to two weeks. Hydrolytic activity is indicated by halo formation. To determine the substrate specificity of the protease-producing clones, skim milk was replaced by 0.3% (w/v) azocasein, azoalbumin, or elastin-Congo red. Insert sequences of recombinant plasmids derived from positive clones were determined by the Göttingen Genomics Laboratory. The retrieved insert sequences were edited employing gap4 [24], and putative ORFs were annotated using Artemis (version 11.0) [37].

2.6. Cloning of Genes Conferring Lipolytic or Proteolytic Activity into Expression Vectors and Purification of the Corresponding Gene Products. For enzyme production of

lipolytic proteins, identified genes were cloned into pET101-TOPO according to the Champion pET101 directional TOPO Expression Kit (Invitrogen). In this way, sequences encoding a His$_6$ tag and a V5 epitope provided by the vector were added to the 3′ end of the coding regions. Alternative start codons were replaced by ATG. *Escherichia coli* BL21 Star (DE3) (Invitrogen) was used as a host for enzyme production. The production was performed as recommended by the manufacturer. Subsequently, recombinant cells were harvested by centrifugation, washed with Tris buffer (30 mM, pH 8.0), and resuspended in 50 mmol L^{-1} of sodium phosphate buffer containing 0,3 mol L^{-1} NaCl (pH 8.0). The cells were disrupted employing a French Press (1.38×10^8 Pa). Subsequently, the extract was cleared by centrifugation at 14,000 g and 4°C for 45 min. The supernatant was used as a source for soluble proteins. Recombinant proteins were purified using the Protino Ni-TED 2000 packed columns (Macherey-Nagel, Düren, Germany) as recommended by the manufacturer. Protein preparations were dialyzed using sodium phosphate buffer (50 mM, pH 7.5) to remove residual imidazole. Protein concentration in the purified sample was determined with Roti-Quant (Carl Roth, Karlsruhe, Germany) as suggested by the manufacturer. The purity of the protein preparations was analyzed by SDS-polyacrylamide gel electrophoresis according to Laemmli [38].

For protein production of the putative protease, the corresponding gene (*pepBW1*) was cloned into pBAD/Myc-His (Invitrogen) using a modified fusion method [39]. The gene was amplified in two PCR reactions with the following two sets of primer pairs containing synthetic sites (underlined) for cloning into the vector: pair 1, 5′-CATGGTGTTCAAT-AAATATGTCTT-3′ and 5′-CTAGGGTAGACTTAACGC-3′ and pair 2, 5′-GTGTTCAATAAATATGTCTTATT-3′ and 5′-CGCTAGGGTAGACTTAACGC-3′. After mixing, denaturation, and hybridization, four different hybridization products are formed of which one contained overhangs complementary to vector digested with *Nco*I (Fermentas) and *Bsp*119I (Fermentas). The preligation mixture (10 μL) contained 1 μL O-buffer (Fermentas) and approximately 50 ng of each PCR product. To create the appropriate overhangs for cloning, the following thermal cycling scheme was used: denaturation at 95°C for 3 min, 4 cycles of reannealing at 65°C for 2 min, and reannealing at 25°C for 15 min. The ligation reaction mixture (20 μL) contained the preligation mixture, 1 μL of O-Buffer (Fermentas), 1 μL ATP (10 mM), 1 U of T4 DNA ligase, and 10 ng of pBAD/Myc-His digested with *Nco*I and *Bsp*119I. The reaction was incubated at 16°C overnight and inactivated by heating at 65°C for 10 min. The resulting recombinant plasmids were then used to transform *E. coli* top 10 cells.

2.7. Characterization of Lipolytic Activity. Determination of enzyme specificity against different triacylglycerides was determined by growing *E. coli* BL21 (DE3) harboring the recombinant plasmids on LB agar plates containing triacylglycerides with different chain length (C4 to C18). Plates were supplemented with IPTG to a final concentration of 0.1 mM to induce gene expression.

For quantitative analysis, p-nitrophenyl esters with various chain lengths were used as described by Rashamuse et al. [40]. Routine esterase activity assays were performed by measuring the release of p-nitrophenol from a p-nitrophenyl (p-NP) ester at 410 nm using a Cary 100 UV-Vis spectrophotometer (Varian, Palo Alto, USA) with a Peltier temperature controller. Unless otherwise described, enzyme activity was measured at 50°C in Tris-HCl (50 mmol L^{-1}; pH 7.5) with p-NP caprylate (1 mmol L^{-1}; dissolved in 2-propanol) as a substrate. p-NP caprylate was used as a substrate in the standard assay because of its stability at high temperatures and alkaline pH values. Enzyme activity of EstBW2 was determined with p-NP butyrate as the enzyme showed no activity with the other substrates tested. Therefore, temperature and pH dependence of EstBW2 were not measured above 75°C and pH 8. All measurements were performed in triplicate.

To determine substrate specificity, enzyme activity was measured at standard assay conditions employing the following p-NP esters of various chain lengths: p-NP acetate (C2), p-NP butyrate (C4), p-NP caprylate (C8), p-NP caprate (C10), p-NP laurate (C12), and p-NP palmitate (C16).

The temperature dependence of enzyme activity was determined between 20 and 95°C under standard assay conditions. To compensate temperature effects on pH values, buffers were preheated to set-point temperature and adjusted using Tris buffer (50 mmol L^{-1}). Thermostability was measured by incubating the enzyme at different temperatures over various time periods. Enzyme activity was subsequently measured under standard assay conditions. Optimal pH values for enzyme activity were measured under standard assay conditions employing different overlapping buffer solutions (50 mM): sodium acetate buffer (pH 4 and 5), sodium phosphate buffer (pH 5, 6, and 7), Tris-HCl (pH 7, 8, and 9), CHES (pH 9 and 10), and CAPS (pH 10 and 11).

The effect of different detergents on enzyme activity was determined by under standard assay conditions in the presence of 1 mM AgNO$_3$, 1 mM CaCl$_2$, 1 mM CoCl$_2$, 1 mM cetyltrimethylammonium bromide (CTAB), 1 mM CuCl$_2$, 1 mM ethylenediaminetetraacetic acid (EDTA), 1 mM FeCl$_3$, 1 mM KCl, 1 mM MgCl$_2$, 1 mM MnCl$_2$, 1 mM NaCl, 1 mM NiSO$_4$, 1 mM Sodium Dodecyl Sulfate (SDS), 1 mM ZnCl$_2$, 0.01% (v/v) Tween 80, or 0.01% (v/v) 2-Mercaptoethanol. The serine dependence of the recovered lipolytic enzymes was validated under standard assay conditions by incubation in the presence of 1 mM phenylmethylsulfonyl fluoride (PMSF). In addition, we analyzed the significance of the determined effects on enzyme activity. As the enzyme tests were performed in triplicate, we assumed that all measured enzyme activities were normally distributed. The variance homogeneity was tested employing the F-test, and the significance of the detergent effects was subsequently tested either with the Student's t-test (homogenous variances) or the Welch's t test (heterogeneous variances). All statistical analyses were performed in R [41].

2.8. Nucleotide Sequence Accession Numbers. The 16S rRNA gene sequences have been deposited in GenBank under accession numbers HM149792–HM150618. Nucleotide

sequences of the four identified genes have been deposited in GenBank under the accession numbers HM063743 (plpBW1), HM063744 (estBW1), HM063745 (estBW2), and HM063746 (pepBW1).

3. Results

3.1. Sampling and Chemical Properties of the Investigated Sediments. Sediment samples were collected from two Kamchatkian hot springs. The springs were located near the Mutnovsky volcano (Mutnovsky sample) and in the Uzon Caldera (Uzon sample), which represent a thermoacidophilic (70°C, pH 3.5–4) and a thermophilic (81°C, pH 7.2–7.4) environment, respectively. Both investigated sediments were chemically distinct from each other (Table 1). The Mutnovsky sample contained higher Al, Ca, Co, Cu, Fe, Pb, and Zn concentrations than the Uzon sample. For As, B, Ba, K, Mn, and Na concentrations, the opposite was recorded. The concentrations of Cr, Mg, Ni, Sr, P, Ti, and V and the total organic carbon contents were almost identical in both samples.

3.2. Isolation of Metagenomic DNA and Construction of Metagenomic Libraries. To assess the prokaryotic diversity and metabolic potential by metagenomic approaches, environmental DNA was extracted from both samples. Approximately, 2.7 μg DNA per 10 g sediment was recovered from both samples. After removal of remaining salts, archaeal and bacterial 16S rRNA genes were amplified from the purified DNA. The resulting PCR products were used for the generation of 16S rRNA gene libraries. A total of 1271 clones were sequenced from these libraries. After quality filtering and removal of potential chimeric sequences, 1235 high-quality 16S rRNA gene sequences were obtained (536 for the Mutnovsky sample, 699 for the Uzon sample). The DNA from both samples was also used to construct metagenomic libraries. The Mutnovsky library comprised approximately 479,000 plasmids with an average insert size of 5.3 kb. The percentage of insert-carrying plasmids was 74%. The Uzon library consisted of approximately 117,000 plasmids with an average insert size of 4 kb. The percentage of insert-carrying plasmids was 85%. In summary, the generated small-insert metagenomic libraries harbored approximately 2.27 Gbp of cloned environmental DNA.

3.3. Archaeal Community Structures. We were able to assign 265 16S rRNA gene sequences of both samples to the domain *Archaea*. The classified sequences were affiliated to four different archaeal phyla (Figure 1). The *Thaumarchaeota* was the most abundant archaeal phylum in both samples (57% and 68% of all sequences, resp.). Most of the sequences were affiliated to Miscellaneous Crenarchaeotic Group nowadays belonging to the recently proposed *Thaumarchaeota* (37%). Another abundant thaumarchaeotic group was the Terrestrial Hot Spring Group (24.7%). The majority of the remaining sequences of the Mutnovsky sample were affiliated to uncultured members of the *Euryarchaeota* (34.7%), which were only detected in this sample. The majority of the
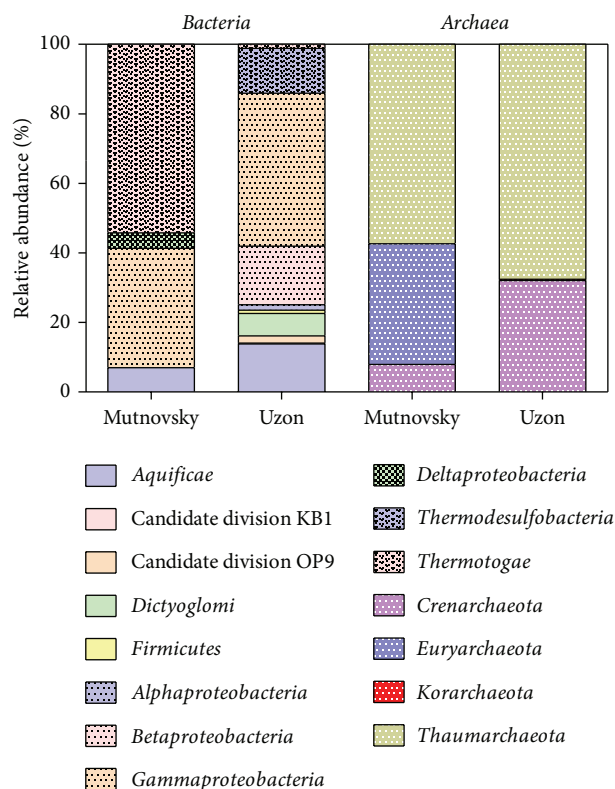
FIGURE 1: Relative sequence abundances of different archaeal and bacterial phyla and proteobacterial classes.

remaining Uzon sequences belonged to the *Crenarchaeota* (32.1%). Sequences were affiliated to known genera such as *Sulfophobococcus* (12.1%), *Thermofilum* (6.8%), *Ignisphaera* (5.3%), and to *Desulfurococcus kamchatkensis* (4.2%). The archaeal phylum *Korarchaeota* was only identified in the Uzon sample (1 sequence).

3.4. Diversity and Species Richness of Archaeal Communities. To determine the archaeal diversity and richness, rarefaction analyses were performed with QIIME. The observed OTU numbers in the Mutnovsky sample and the Uzon sample were 33 and 13 (1% genetic distance), 25 and 11 (3% genetic distance), and 7 and 5 (20% genetic distance), respectively (Table 2). The maximal expectable number of clusters for both samples was determined based on the Michaelis-Menten fit metrics. On average, more than 90% of the entire archaeal community was covered by the surveying effort. Shannon indices of the Mutnovsky and Uzon sample were 1.83 and 2.96 (1% genetic distance), 2.70 and 1.83 (3% genetic distance), and 0.86 and 1.87 (20% genetic distance), respectively. These indicated low archaeal diversity in the investigated samples. Comparison of the rarefaction analyses with the number of OTUs determined by Chao1 richness estimator revealed that, at 1 and 3% genetic distance, the rarefaction curves were almost saturated (Figure 4). Thus, the majority of the estimated richness was recovered by the surveying effort (Table 2).

3.5. Bacterial Community Structures. We were able to assign 271 sequences for Mutnovsky and 434 sequences for Uzon sample to the domain *Bacteria*. The classified sequences were affiliated to three and eight different bacterial phyla and candidate divisions in the Mutnovsky sample and the Uzon sample, respectively (Figure 1). The *Thermotogae* was the most abundant bacterial phylum in the Mutnovsky sample (54%). This phylum was almost absent in the Uzon sample (1%). Interestingly, all sequences in the Mutnovsky sample were further affiliated to uncultured members of the genus *Kosmotoga*. This genus was completely absent in the Uzon Caldera. The *Proteobacteria* were the second most abundant phylum in the Mutnovsky sample (39%) and the most abundant one in the Uzon Caldera sample (62%). Most of these sequences were further assigned to *Acidithiobacillus caldus* ATCC 51756 (28%) in the Mutnovsky sample and different genera within the *Enterobacteriacaeae* (41%) in the Uzon sample. The *Aquificae* were the third most abundant phylum in the Uzon sample (13.4%). The corresponding sequences were assigned to *Sulfurihydrogenibium rodmanii* (9.7%) and *Thermosulfidibacter takaii* (2.8%) and uncultured members of the *Aquificae*. Another abundant bacterial phylum was *Thermodesulfobacteria* (12.9%). All the sequences belonged to the genus *Caldimicrobium*. The remaining sequences were affiliated to *Dictyoglomus thermophilum* and *Dictyoglomus turgidum* of the *Dictyoglomi* (6.5%), the Candiate division OP9 (2.1%), the *Firmicutes* (0.9%), and the Candidate division KB1 (0.2%).

3.6. Diversity and Species Richness of Bacterial Communities. The observed OTU numbers in both hot springs were 17 and 50 (1% genetic distance), 12 and 42 (3% genetic distance), and 10 and 11 (20% genetic distance) in the Mutnovsky sample and the Uzon sample, respectively (Table 2). Analysis of the maximal expectable number of clusters indicated that more than 94% of the entire bacterial community was recovered by the surveying effort. Correspondingly, comparison of the rarefaction analyses with the number of OTUs determined by Chao1 richness estimator revealed that at 1%, 3%, and 20% genetic distance, the rarefaction curves were almost saturated (Table 2, Figure 4).

3.7. Screening of Metagenomic Libraries. The two generated metagenomic libraries were employed in a function-based screening to identify novel lipolytic and proteolytic enzymes. Three novel genes encoding lipolytic enzymes (*plpBW1*, *estBW1*, and *estBW2*) and one gene encoding a proteolytic enzyme (*pepBW1*) were identified during the screening of the metagenomic library derived from the Uzon sample. No hydrolytic enzymes were identified within the metagenomic library derived from the Mutnovsky sample.

The closest relatives of all identified protein sequences originated from known thermophiles. They were similar to uncharacterized putative gene products derived from *Desulfurococcus kamchatkensis* (PepBW1), *Sulfurihydrogenibium azorense* (PlpBW1 and EstBW2), and *Thermobaculum terrenum* (EstBW1) (Table 3).
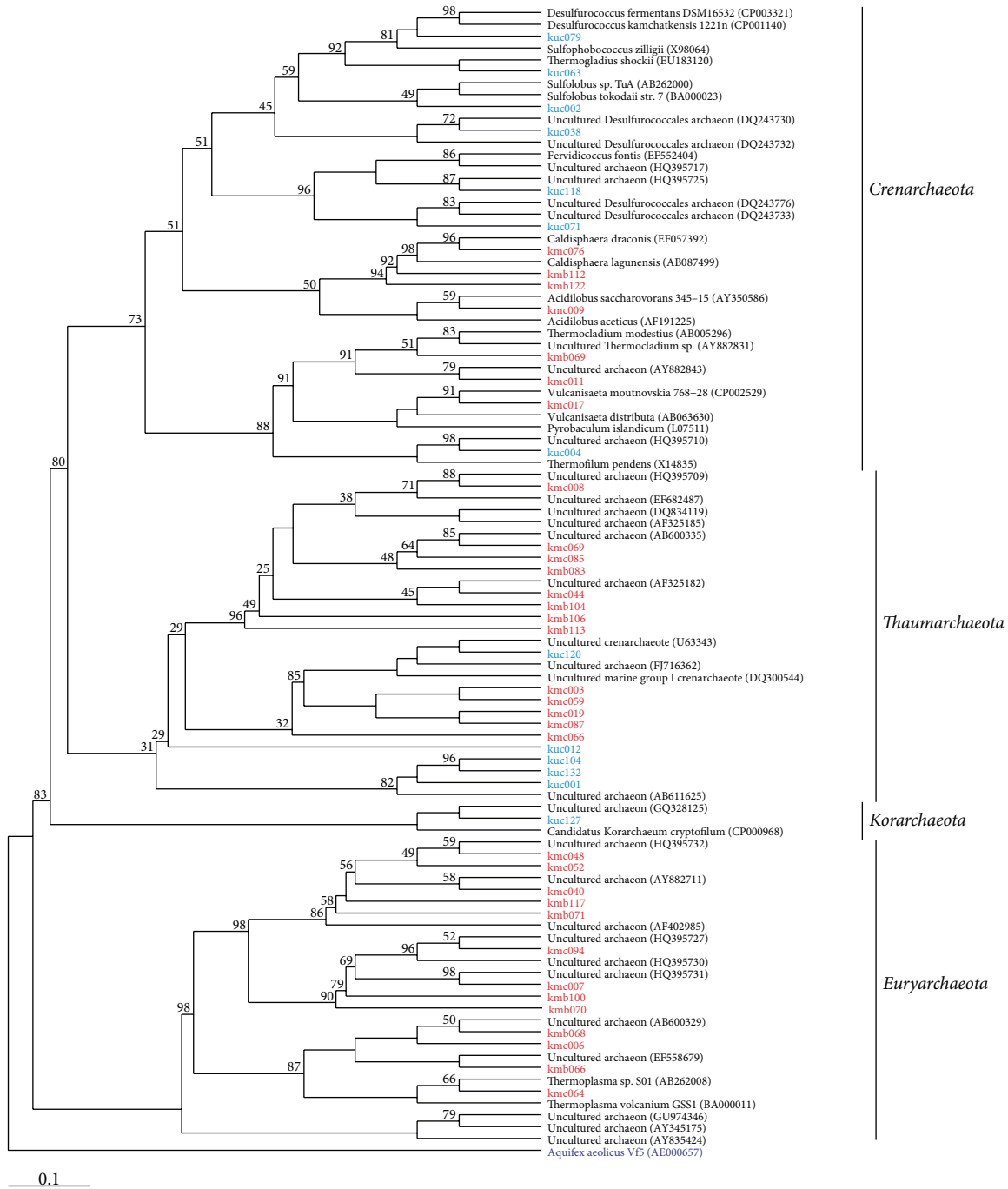
FIGURE 2: Maximum parsimony phylogenetic tree based on all archaeal 16S rRNA gene sequences. The tree was calculated using the ARB software package [33]. Sequences are characterized by sample designation (km, Kamchatka Mutnovsky; ku, Kamchatka Uzon Caldera), length of amplicon ((b), 730 bp; (c), 950 bp), number of sequence, and accession number. Sequences derived from the Mutnovsky sample are shown in red and those from the Uzon sample in blue. Numbers at branch nodes are bootstrap values (only values ≥25 are shown). The tree is rooted with the 16S rRNA gene sequence of *Aquifex aeolicus* Vf5 as an outgroup.

PlpBW1 was affiliated to the patatin-like proteins (PLPs). Four conserved domains are described for this enzyme type [42], which could all be identified within the amino acid sequence (data not shown). Interestingly, PLPs do not possess a catalytic triad. The lipolytic activity is conferred by a catalytic dyad formed by a serine residue and an aspartate residue [42]. EstBW1 and EstBW2 were affiliated to family V of lipolytic enzymes according to the classification system of Arpigny and Jaeger [43]. PepBW1 was classified employing the MEROPS database [44]. It was affiliated to the subtilisin family (family S8). Interestingly, the *pepBW1* gene sequence was almost identical to that of a putative gene encoding a
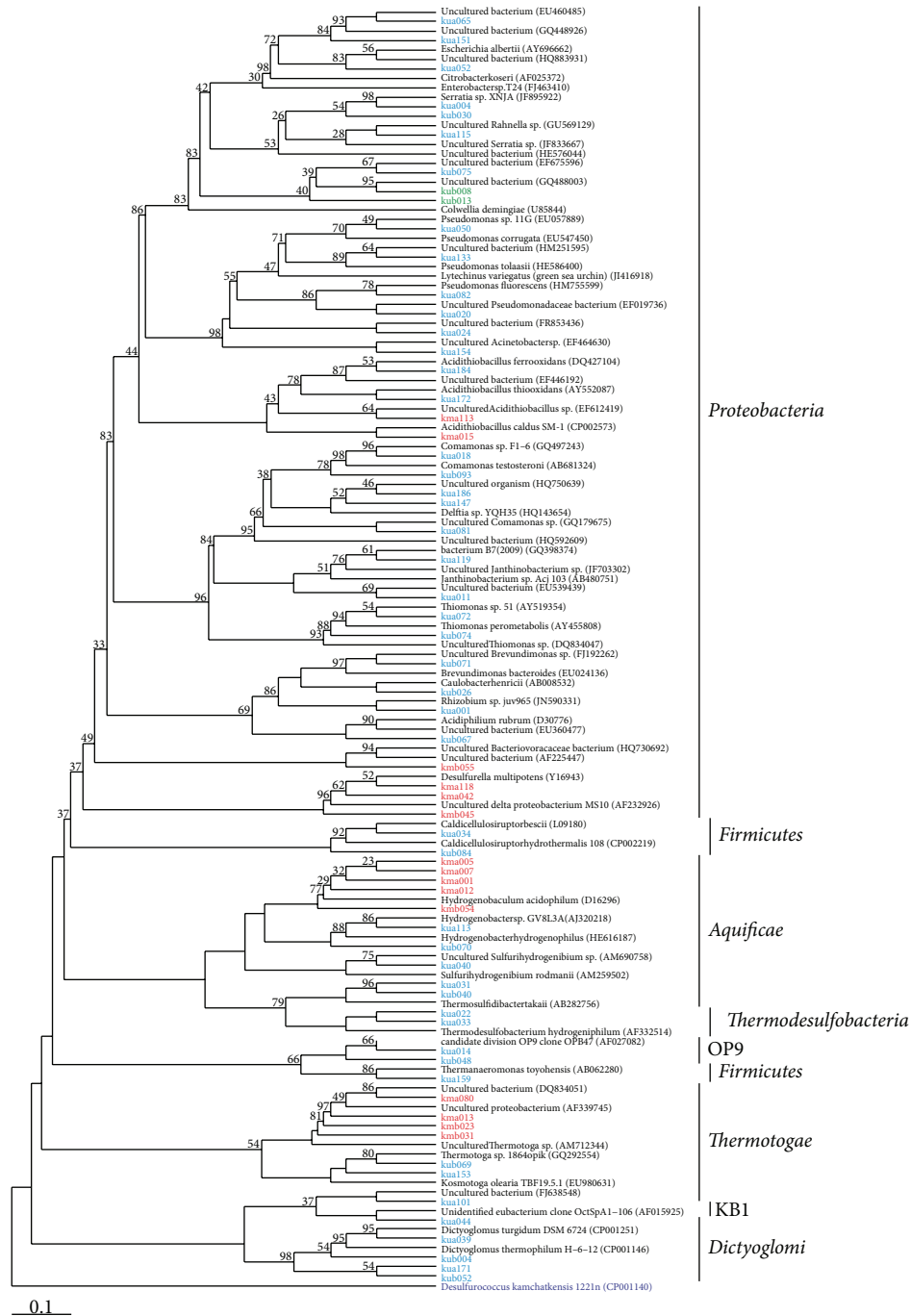
FIGURE 3: Maximum parsimony phylogenetic tree based on all bacterial 16S rRNA gene sequences. The tree was calculated using the ARB software package [33]. Sequences are characterized by sample designation (km, Kamchatka Mutnovsky; ku, Kamchatka Uzon Caldera), length of amplicon ((a), 1100 bp, (b), 730 bp), number of sequence, and accession number. Sequences derived from the Mutnovsky are shown in red and those from the Uzon Caldera in blue. OTUs shared by both sites are depicted in green. Numbers at branch nodes are bootstrap values (only values ≥25 are shown). The tree is rooted with the 16S rRNA gene sequence of *Desulfurococcus kamchatkensis* 1221n as an outgroup.

serine peptidase of *Desulfurococcus kamchatkiensis* (Table 3); *Desulfurococcus kamchatkiensis* belongs to the *Crenarchaeota* and was also isolated from a thermal spring within the Uzon Caldera [45]. In addition, the 16S rRNA gene sequence of this species was found in our 16S analysis of the Uzon sample.

3.8. Characterization of Recombinant Enzymes. To characterize all recombinant proteins, the genes conferring lipolytic and proteolytic activity were cloned into expression vectors. The recombinant *E. coli* strain containing PepBW1 was tested towards different proteins and showed proteolytic activity

TABLE 2: Prokaryotic diversity and richness at 1, 3, and 20% genetic distance. Numbers of observed OTUs as well as Shannon and Chao1 indices were calculated with QIIME [16]. The maximal number of OTUs (n_{max}) was calculated using the Michaelis-Menten-fit diversity metrics implemented in the QIIME package. Coverage was determined by dividing the observed number of OTUs with n_{max}.

Sample	Observed OTUs			Max. OTUs (n_{max})			Coverage (%)			Shannon index (H')			Chao1		
	1%	3%	20%	1%	3%	20%	1%	3%	20%	1%	3%	20%	1%	3%	20%
Archaea															
Mutnovsky	33	25	7	37.7	27.4	7.2	88	91.2	97.2	2.96	2.70	1.87	44.3	28.3	7
Uzon	13	11	5	14	11.6	5	93	94.8	100	1.83	1.67	0.86	13	11	5
Bacteria															
Mutnovsky	17	12	10	18.2	12.3	10	93.4	97.6	100	2	1.81	1.65	32	15	13
Uzon	50	42	11	62.9	52.5	11.3	95.8	80.0	97.3	2.9	2.60	1.63	69.3	56.4	11.5

TABLE 3: Novel lipolytic and proteolytic enzymes and their closest relatives in the NCBI database.

Protein	Length (amino acids)	Closest similar protein, accession no. of similar protein	Corresponding organism	E-value	Amino acid homology to the closest similar protein (% identity)
PlpBW1	250	Patatin, YP_002729059	*Sulfurihydrogenibium azorense* Az-Fu1	$9e-111$	1–250 (75%)
EstBW1	254	Alpha/beta hydrolase family protein, ZP_03857090	*Thermobaculum terrenum* ATCC BAA-798	$4e-61$	2–251 (47%)
EstBW2	191	Hypothetical protein SULAZ_0137, YP_002728134	*Sulfurihydrogenibium azorense* Az-Fu1	$2e-91$	1–188 (85%)
PepBW1	411	Subtilisin-like serine protease, YP_002428837.1	*Desulfurococcus kamchatkensis*	0	1–411 (98%)

with skim milk and elastin-Congo red but not with azoalbumin or azocasein.

The activities of the recombinant lipolytic proteins were tested towards different triacylglycerides. All proteins showed activity with tributyrin as substrate. In addition, PlpBW1 showed activity with long-chain triacylglycerides, up to trimyristin (C14). Hydrolysis of different p-nitrophenyl esters was used to further analyze the substrate specificity (Figure 5(a)). PlpBW1 and EstBW1 showed highest activity with p-NP acetate and p-NP butyrate, respectively. Both enzymes exhibit activity towards all tested p-NP esters, except p-NP palmitate. The activity decreased with increasing chain length. In contrast, EstBW2 showed only activity towards p-NP butyrate. Specific activities under standard assay conditions using the optimal substrate were 2.6 ± 0.3 U/mg (PlpBW1), 2.33 ± 0.32 U/mg (EstBW1), and 1.89 ± 0.21 U/mg (EstBW2). Based on the results, all three lipolytic enzymes are most likely carboxylesterases and not lipases.

All lipolytic enzymes were active over a wide temperature range. PlpBW1, EstBW1, and EstBW2 retained a minimum of 50% activity from 60 to 90°C, 65 to 95°C, and 40 to 75°C, respectively (Figure 5(b)). Maximal activities were recorded for PlpBW1 at 85°C, for EstBW1 at 90°C, and for EstBW2 at 65°C. We further determined the stability of the three lipolytic enzymes with respect to different temperatures. The half-lives of PlpBW1 were 45 min at 70°C, 15 min at 80°C, and 5 min at 90°C. EstBW1 exhibited half-lives of 5 h at 70°C, 2.5 h at 80°C, and a remarkable half-life of 15 min at 90°C. EstBW2 was less stable at 90°C (7 min half-live), but the activity was almost unaffected by 5 h of incubation at 70°C and 80°C (data not shown).

The pH effect on enzyme activity was measured at pH values ranging from 4 to 11 (Figure 5(c)). All enzymes exhibited high activity at neutral or alkaline pH values. Maximal activities were determined at pH 10 (PlpBW1) and pH 7 (EstBW1 and EstBW2).

Addition of EDTA, KCl, or NaCl to the reaction mixture had no significant effect on enzyme activity ($P > 0.05$), whereas all other tested detergents exhibited an effect on the activity of at least one of the recovered enzymes (Table 4). CTAB, Tween 80, and $ZnCl_2$ impacted the activities of all three enzymes significantly ($P < 0.05$). PlpBW1 showed a more than 2.5-fold higher activity in presence of CTAB, whereas EstBW1 and EstBW2 displayed a loss in activity. Tween 80 increased enzyme activity of PlpBW1 and EstBW2 but not that of EstBW1. The addition of $ZnCl_2$ decreased the activity of all three recombinant enzymes. Lipolytic activity of EstBW1 and EstBW2 was completely inhibited by the phenylmethylsulfonyl fluoride, indicating the presence of a serine residue at the active site of both enzymes. Interestingly, the activity of PlpBW1 was not affected by PMSF.

4. Discussion

4.1. Prokaryotic Community Composition in the Kamchatkian Springs. The number of metagenomic studies has been rapidly increased over the past years. Metagenomics has been
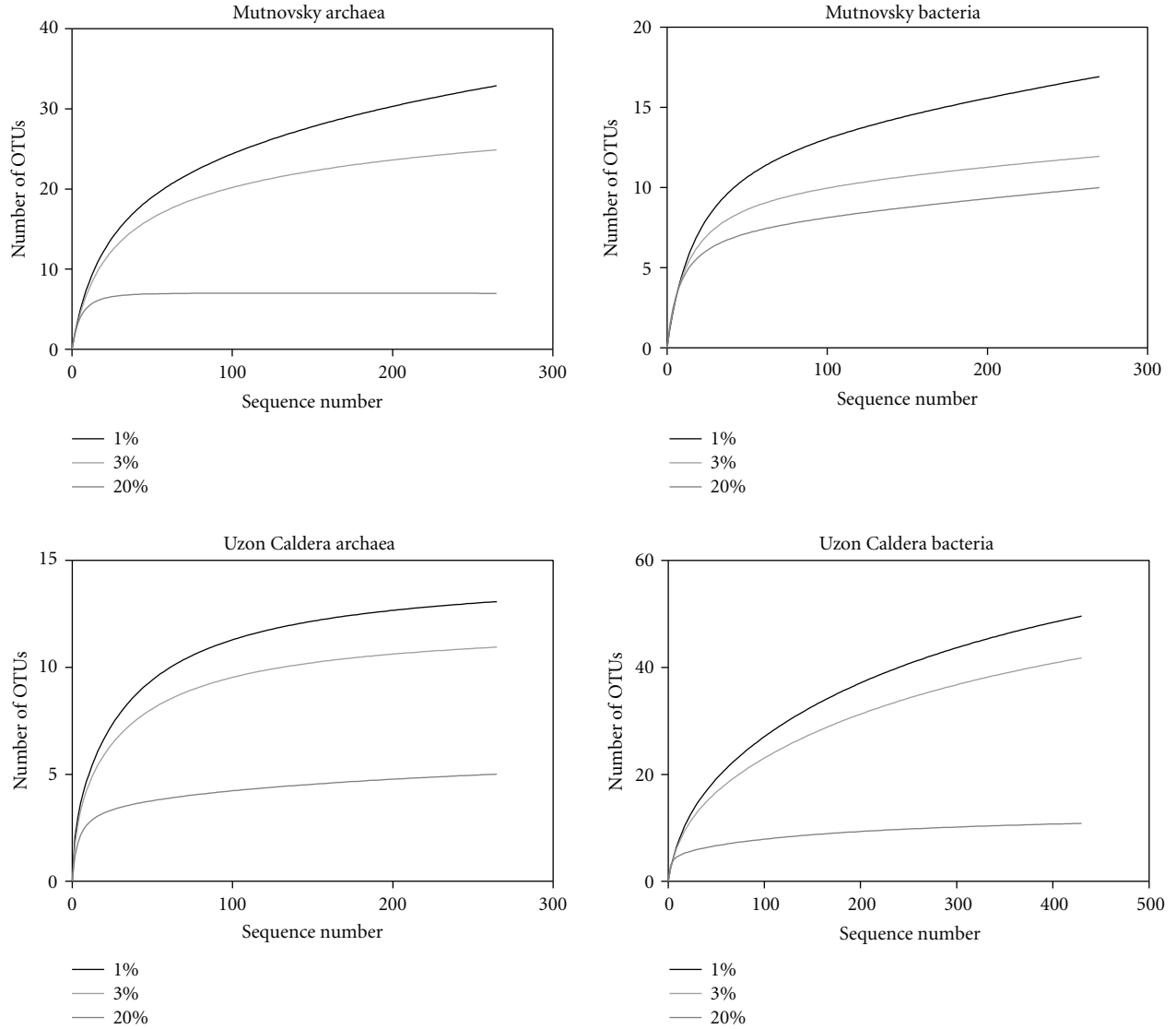
FIGURE 4: Rarefaction curves for both sampling sites. Curves were calculated at 1%, 3%, and 20% genetic distance level employing QIIME [23].

employed to assess and exploit the biodiversity of many habitats including environments of extremophiles [1, 15, 16, 46, 47]. In this study, we investigated the prokaryotic diversity of two hot springs located on the Kamchatka peninsula. We found different bacterial and archaeal communities at both sites, which were dominated by *Proteobacteria*, *Thermotogae*, and *Thaumarchaeota*.

Jackson et al. (2001) studied a mat derived from the Norris Geyser Basin, an acidic thermal spring in the Yellowstone National Park [46]. They found community pattern comparable to that in the Mutnovsky sample with one difference. They were not able to identify *Thaumarchaeota*, which is not surprising as this phylum was first proposed in 2008 [48]. Members of this phylum are not restricted to thermophilic habitats as they were originally described as mesophilic *Crenarchaeota* [48–50]. A study by Meyer-Dombard et al. (2005) investigated the prokaryotic community in three thermal springs in the Yellowstone National Park (the Silvan Spring, the Bison Pool, and the Obsidian Pool) [16]. Whereas the other pools have a rather neutral milieu, the Silvan Spring has a low pH of 5. However, the prokaryotic community structure of this acidic spring was different to that found in the acidic Mutnovsky spring sample. Meyer-Dombard et al. identified the *Crenarchaeota* as the most abundant archaeal group, whereas *Thaumarchaeota* were the most abundant group in our study. A more recent study on prokaryotic community composition of hot springs on the Tibetan Plateau also found *Thaumarchaeota* as the dominant archaeal group [48].

Analysis of the Uzon sample revealed a more diverse prokaryotic community than in the Mutnovsky sample. Only two OTUs at 1% genetic distance were shared, whereas all the other OTUs were unique for each sample (Figures 2 and 3). The observed differences in community composition between the two sampling sites might be due to the different

(a)

(b)

(c)
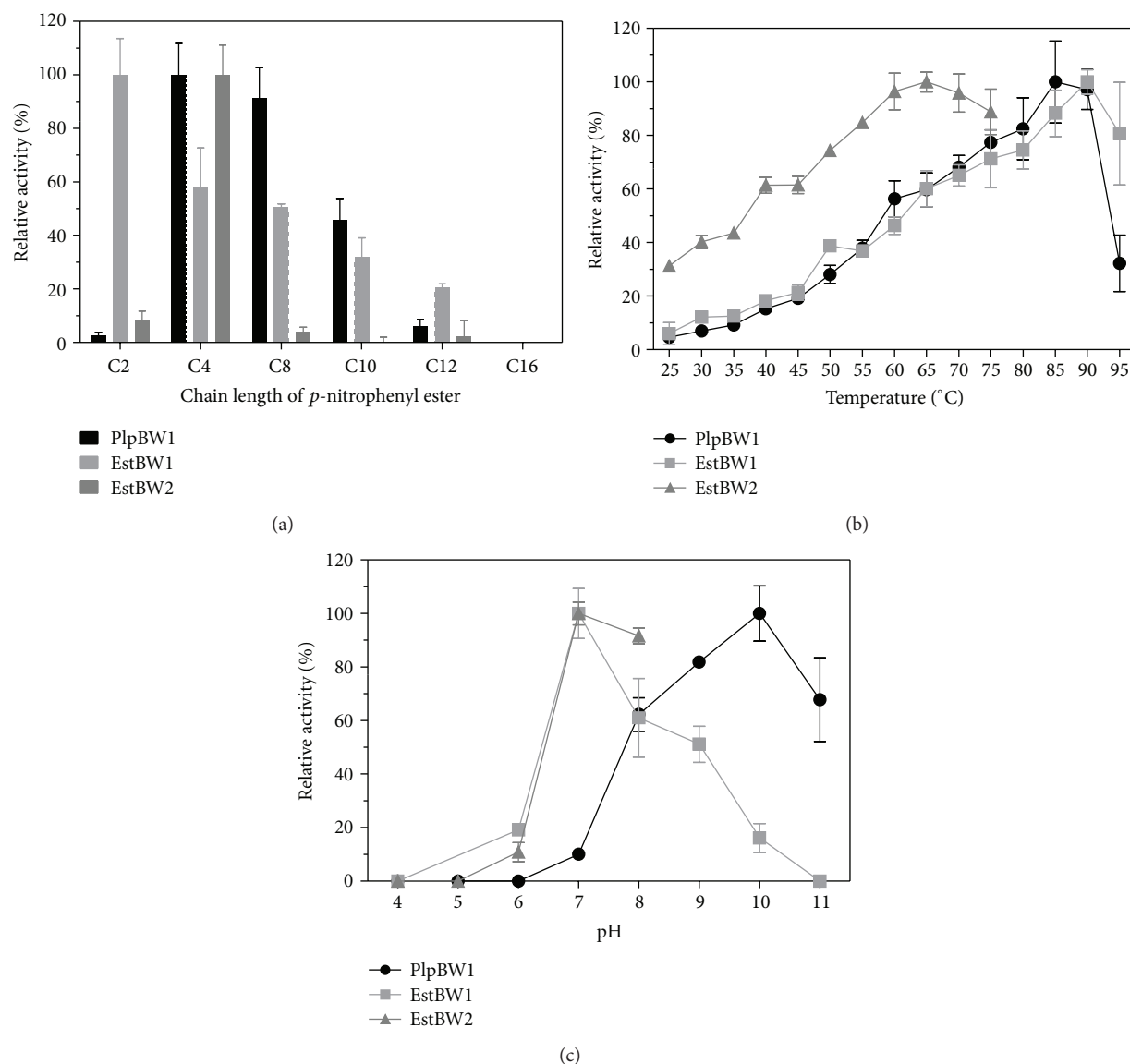
FIGURE 5: Relative activities of the three lipolytic enzymes towards different *p*-nitrophenyl esters with various chain lengths (a), at different temperatures (b), and pH values (c). The activity of estBW2 could not be measured above 75°C and pH 8 due to the instability of the *p*-NP butyrate under these conditions.

temperatures and pH values at the sites. However, Huang et al. (2011) found no statistical correlation between temperature and diversity [48].

Despite the geographical separation, the Obsidian Pool and the Uzon Caldera hot spring share a very similar community structure, as almost the same dominant archaeal and bacterial groups were identified [16]. In addition, some rare phyla were present in both samples, that is, the *Korarchaeota*. This phylum is a relatively new phylum first described by Barns et al. in 1996 [51]. Another rare bacterial group found in both samples was the Candidate division OP9. These results confirm also the presumption proposed for other extreme environments that similar environmental conditions result in similar microbial communities [15].

4.2. Hydrolytic Enzymes. In the present study, we were able to identify three novel lipolytic enzymes and one proteolytic enzyme. The determined optimal temperatures and pH values reflect the environmental conditions of the samples used for DNA isolation, indicating that the environment shapes the characteristics of the enzymes. Correspondingly, the characterized lipolytic enzymes (PlpBW1, EstBW1, and EstBW2) showed features similar to those of other metagenome-derived esterases, which were identified in thermophilic sites. Rhee et al. (2005) identified a thermophilic esterase in metagenomic libraries generated from hot spring and mud hole DNA [52]. The enzyme was active from 30 to 95°C and exhibited an optimal pH value of approximately 6.0. Tirawongsaroj et al. (2008) screened metagenomic libraries

TABLE 4: Relative activities of recombinant esterases in the presence of different chemical compounds. The effect of the additives was further tested for significance. Significant effects ($P < 0.05$) are written in bold type.

Detergent	Relative activity of PlpBW1 (%)	Relative activity of EstBW1 (%)	Relative activity of EstBW2 (%)
AgNO$_3$	106.80 ± 16.06	**34.27 ± 1.66**	**163.17 ± 4.88**
CaCl$_2$	**132.39 ± 9.63**	**85.35 ± 6.30**	97.10 ± 0.98
CoCl$_2$	**131.17 ± 5.93**	104.94 ± 7.29	**64.00 ± 5.60**
CTAB	**274.39 ± 34.52**	**40.66 ± 6.67**	**8.11 ± 3.30**
CuCl$_2$	125.48 ± 2.70	**81.03 ± 3.98**	94.20 ± 0.57
EDTA	119.45 ± 7.50	101.47 ± 10.75	96.03 ± 4.24
FeCl$_3$	106.67 ± 8.94	**53.56 ± 12.56**	99.47 ± 5.01
KCl	124.50 ± 19.51	99.29 ± 12.11	96.40 ± 5.55
2-Mercaptoethanol	84.82 ± 7.31	**0.00 ± 0.00**	78.74 ± 19.95
MgCl$_2$	**133.37 ± 7.25**	90.38 ± 13.06	101.54 ± 2.87
MnCl$_2$	72.07 ± 2.31	82.14 ± 14.16	**48.90 ± 5.22**
NaCl	131.24 ± 15.17	98.59 ± 20.07	92.42 ± 3.60
NiSO$_4$	121.86 ± 14.71	89.64 ± 4.60	**45.65 ± 8.03**
PMSF	77.49 ± 16.91	**0.08 ± 16.43**	**0 ± 4.16**
SDS	68.45 ± 17.38	**22.47 ± 9.64**	**39.49 ± 3.14**
Tween 80	**174.52 ± 2.29**	**60.70 ± 12.74**	**141.50 ± 4.94**
ZnCl$_2$	**72.01 ± 1.77**	**59.26 ± 5.72**	**8.64 ± 1.71**

Abbreviations: CTAB: cetyltrimethylammonium bromide; EDTA: ethylenediaminetetraacetic acid; SDS: sodium dodecyl sulfate; PMSF: phenylmethylsulfonyl fluoride.

derived from a Thailand hot spring and identified two novel lipolytic enzymes, of which one was also characterized as a patatin-like protein [53]. To our knowledge, PlpBW1 is the second reported patatin-like protein derived from a hot spring metagenomic library up to now [53]. In contrast to most other lipolytic enzymes containing a serine residue in the active site, PlpBW1 is not inactivated by the inhibitor PMSF [51, 54]. The effect of Zn^{2+} ions recorded for all recombinant enzymes investigated in this study was also mentioned for esterases studied by Chu et al. [54]. They also recorded a decrease of activity in presence of Zn^{2+} ions. The activity of the recovered lipolytic enzymes was positively or negatively influenced by addition of CTAB or Tween 80 (Table 4). It has been shown that these detergents can either promote or decrease activity of lipolytic enzymes by formation of micellar aggregates and monomers which then interact with hydrophobic parts of the enzymes [55].

In addition to the esterases, metagenomic libraries were mined for proteolytic activity. The identified serine peptidase, PepBW1, is the first metagenome-derived peptidase from a thermophilic environment. As PepBW1 is derived from an archaeal organism, it illustrates that screening in a heterologous host can be successful, even if the target gene originates from a different domain of life [56].

4.3. Ecology of Hot Springs.

As most studies on ecology of hot springs are targeting the prokaryotic diversity, for example, via 16S rRNA gene or other marker gene analyses, little is known on the global relevance of these extremophilic communities. Burgess et al. (2011) studied two thermal pools in the Uzon Caldera by 16S rRNA gene analysis and related some community members to different archaeal and bacterial groups, which might play a role in cycling of C, N, and S [57].

The vital role of *Archaea* in N_2 fixation and denitrification is well established [58]. The first step of nitrification, ammonium oxidation, was originally thought to be restricted to some *Proteobacteria* [59]. However, recent metagenomic studies provided evidence that *Archaea* are capable to oxidize ammonium to nitrate [58, 59]. Until recently, methanogenic *Euryarchaeota* were thought to be the only archaeal group of global relevance for element cycling. This presumption changed with the discovery of ammonia-oxidizing archaea [60], which are affiliated to the recently proposed phylum *Thaumarchaeota*. Members of this phylum contribute significantly to the global N cycle, as their high abundance and extremely low substrate threshold provides compelling evidence for a dominant role as ammonia oxidizers in open oceans [60]. In our study, we identified diverse thaumarchaeal groups in both investigated sediment samples. Thus, hot springs may also play a major role in the global N cycle.

Acknowledgments

References

[1] P. Hugenholtz, C. Pitulle, K. L. Hershberger, and N. R. Pace, "Novel division level bacterial diversity in a Yellowstone hot spring," *Journal of Bacteriology*, vol. 180, no. 2, pp. 366–376, 1998.

[2] V. T. Marteinsson, S. Hauksdóttir, C. F. V. Hobel, H. Kristmannsdóttir, G. O. Hreggvidsson, and J. K. Kristjánsson, "Phylogenetic diversity analysis of subterranean hot springs in Iceland," *Applied and Environmental Microbiology*, vol. 67, no. 9, pp. 4242–4248, 2001.

[3] T. Kvist, B. K. Ahring, and P. Westermann, "Archaeal diversity in Icelandic hot springs," *FEMS Microbiology Ecology*, vol. 59, no. 1, pp. 71–80, 2007.

[4] G. J. Olsen, C. R. Woese, and R. Overbeek, "The winds of (evolutionary) change: breathing new life into microbiology," *Journal of Bacteriology*, vol. 176, no. 1, pp. 1–6, 1994.

[5] C. R. Woese, O. Kandler, and M. L. Wheelis, "Towards a natural system of organisms: proposal for the domains Archaea, *Bacteria*, and Eucarya," *Proceedings of the National Academy of Sciences of the United States of America*, vol. 87, no. 12, pp. 4576–4579, 1990.

[6] J. Handelsman, "Metagenomics: application of genomics to uncultured microorganisms," *Microbiology and Molecular Biology Reviews*, vol. 68, no. 4, pp. 669–685, 2004.

[7] R. Daniel, "The soil metagenome—a rich resource for the discovery of novel natural products," *Current Opinion in Biotechnology*, vol. 15, no. 3, pp. 199–204, 2004.

[8] W. R. Streit, R. Daniel, and K. E. Jaeger, "Prospecting for biocatalysts and drugs in the genomes of non-cultured microorganisms," *Current Opinion in Biotechnology*, vol. 15, no. 4, pp. 285–290, 2004.

[9] Y. Hotta, S. Ezaki, H. Atomi, and T. Imanaka, "Extremely stable and versatile carboxylesterase from a hyperthermophilic archaeon," *Applied and Environmental Microbiology*, vol. 68, no. 8, pp. 3925–3931, 2002.

[10] J. L. Arpigny, D. Jendrossek, and K. E. Jaeger, "A novel heat-stable lipolytic enzyme from *Sulfolobus acidocaldarius* DSM 639 displaying similarity to polyhydroxyalkanoate depolymerases," *FEMS Microbiology Letters*, vol. 167, no. 1, pp. 69–73, 1998.

[11] R. I. Amann, W. Ludwig, and K. H. Schleifer, "Phylogenetic identification and in situ detection of individual microbial cells without cultivation," *Microbiological Reviews*, vol. 59, no. 1, pp. 143–169, 1995.

[12] P. Lorenz, K. Liebeton, F. Niehaus, and J. Eck, "Screening for novel enzymes for biocatalytic processes: accessing the metagenome as a resource of novel functional sequence space," *Current Opinion in Biotechnology*, vol. 13, no. 6, pp. 572–577, 2002.

[13] C. Elend, C. Schmeisser, C. Leggewie et al., "Isolation and biochemical characterization of two novel metagenome-derived esterases," *Applied and Environmental Microbiology*, vol. 72, no. 5, pp. 3637–3645, 2006.

[14] C. Elend, C. Schmeisser, H. Hoebenreich, H. L. Steele, and W. R. Streit, "Isolation and characterization of a metagenome-derived and cold-active lipase with high stereospecificity for (R)-ibuprofen esters," *Journal of Biotechnology*, vol. 130, no. 4, pp. 370–377, 2007.

[15] C. Simon, A. Wiezer, A. W. Strittmatter, and R. Daniel, "Phylogenetic diversity and metabolic potential revealed in a glacier ice metagenome," *Applied and Environmental Microbiology*, vol. 75, no. 23, pp. 7519–7526, 2009.

[16] D. R. Meyer-Dombard, E. L. Shock, and J. P. Amend, "Archaeal and bacterial communities in geochemically diverse hot springs of Yellowstone National Park, USA," *Geobiology*, vol. 3, no. 3, pp. 211–227, 2005.

[17] J. Zhou, M. A. Bruns, and J. M. Tiedje, "DNA recovery from soils of diverse composition," *Applied and Environmental Microbiology*, vol. 62, no. 2, pp. 316–322, 1996.

[18] G. Muyzer, A. Teske, C. O. Wirsen, and H. W. Jannasch, "Phylogenetic relationships of *Thiomicrospira* species and their identification in deep-sea hydrothermal vent samples by denaturing gradient gel electrophoresis of 16S rDNA fragments," *Archives of Microbiology*, vol. 164, no. 3, pp. 165–172, 1995.

[19] A. Wilmotte, G. Van Der Auwera, and R. De Wachter, "Structure of the 16 S ribosomal RNA of the thermophilic cyanobacterium *Chlorogloeopsis* HTF (*Mastigocladus laminosus HTF*) strain PCC7518, and phylogenetic analysis," *FEBS Letters*, vol. 317, no. 1-2, pp. 96–100, 1993.

[20] T. V. Kolganova, B. B. Kuznetsov, and T. P. Turova, "Designing and testing oligonucleotide primers for amplification and sequencing of archaeal 16S rRNA genes," *Mikrobiologiya*, vol. 71, no. 2, pp. 283–286, 2002.

[21] T. Itoh, K. I. Suzuki, and T. Nakase, "*Vulcanisaeta distributa* gen. nov., sp. nov., and *Vulcanisaeta souniana* sp. nov., novel hyperthermophilic, rod-shaped crenarchaeotes isolated from hot springs in Japan," *International Journal of Systematic and Evolutionary Microbiology*, vol. 52, no. 4, pp. 1097–1104, 2002.

[22] E. F. DeLong, "Archaea in coastal marine environments," *Proceedings of the National Academy of Sciences of the United States of America*, vol. 89, no. 12, pp. 5685–5689, 1992.

[23] J. G. Caporaso, J. Kuczynski, J. Stombaugh et al., "QIIME allows analysis of high-throughput community sequencing data," *Nature Methods*, vol. 7, no. 5, pp. 335–336, 2010.

[24] R. Staden, K. F. Beal, and J. K. Bonfield, "The Staden package, 1998," *Methods in Molecular Biology*, vol. 132, pp. 115–130, 2000.

[25] K. E. Ashelford, N. A. Chuzhanova, J. C. Fry, A. J. Jones, and A. J. Weightman, "New screening software shows that most recent large 16S rRNA gene clone libraries contain chimeras," *Applied and Environmental Microbiology*, vol. 72, no. 9, pp. 5734–5741, 2006.

[26] T. Huber, G. Faulkner, and P. Hugenholtz, "Bellerophon: a program to detect chimeric sequences in multiple sequence alignments," *Bioinformatics*, vol. 20, no. 14, pp. 2317–2319, 2004.

[27] J. R. Cole, B. Chai, T. L. Marsh et al., "The Ribosomal Database Project (RDP-II): previewing a new autoaligner that allows regular updates and the new prokaryotic taxonomy," *Nucleic Acids Research*, vol. 31, no. 1, pp. 442–443, 2003.

[28] R. C. Edgar, "Search and clustering orders of magnitude faster than BLAST," *Bioinformatics*, vol. 26, no. 19, Article ID btq461, pp. 2460–2461, 2010.

[29] C. Camacho, G. Coulouris, V. Avagyan et al., "BLAST+: architecture and applications," *BMC Bioinformatics*, vol. 10, article 421, 2009.

[30] E. Pruesse, C. Quast, K. Knittel et al., "SILVA: a comprehensive online resource for quality checked and aligned ribosomal RNA sequence data compatible with ARB," *Nucleic Acids Research*, vol. 35, no. 21, pp. 7188–7196, 2007.

[31] C. E. Shannon, "A mathematical theory of communication," *SIGMOBILE Mobile Computing and Communications Review*, vol. 5, no. 1, pp. 3–55, 2001.

[32] A. Chao and J. Bunge, "Estimating the number of species in a stochastic abundance model," *Biometrics*, vol. 58, no. 3, pp. 531–539, 2002.

[33] W. Ludwig, O. Strunk, R. Westram et al., "ARB: a software environment for sequence data," *Nucleic Acids Research*, vol. 32, no. 4, pp. 1363–1371, 2004.

[34] C. Simon, J. Herath, S. Rockstroh, and R. Daniel, "Rapid identification of genes encoding DNA polymerases by function-based screening of metagenomic libraries derived from glacial ice," *Applied and Environmental Microbiology*, vol. 75, no. 9, pp. 2964–2968, 2009.

[35] A. Henne, R. A. Schmitz, M. Bömeke, G. Gottschalk, and R. Daniel, "Screening of environmental DNA libraries for the presence of genes conferring lipolytic activity on *Escherichia coli*," *Applied and Environmental Microbiology*, vol. 66, no. 7, pp. 3113–3116, 2000.

[36] T. Waschkowitz, S. Rockstroh, and R. Daniel, "Isolation and characterization of metalloproteases with a novel domain structure by construction and screening of metagenomic libraries," *Applied and Environmental Microbiology*, vol. 75, no. 8, pp. 2506–2516, 2009.

[37] K. Rutherford, J. Parkhill, J. Crook et al., "Artemis: sequence visualization and annotation," *Bioinformatics*, vol. 16, no. 10, pp. 944–945, 2000.

[38] U. K. Laemmli, "Cleavage of structural proteins during the assembly of the head of bacteriophage T4," *Nature*, vol. 227, no. 5259, pp. 680–685, 1970.

[39] D. Tillett and B. A. Neilan, "Enzyme-free cloning: a rapid method to clone PCR products independent of vector restriction enzyme sites," *Nucleic Acids Research*, vol. 27, no. 19, pp. e26–e28, 1999.

[40] K. Rashamuse, T. Ronneburg, F. Hennessy et al., "Discovery of a novel carboxylesterase through functional screening of a pre-enriched environmental library," *Journal of Applied Microbiology*, vol. 106, no. 5, pp. 1532–1539, 2009.

[41] R Development Core Team, *R: a Language and Environment for Statistical Computing*, R Foundation for Statistical Computing, Vienna, Austria, 2005.

[42] S. Banerji and A. Flieger, "Patatin-like proteins: a new family of lipolytic enzymes present in *Bacteria*?" *Microbiology*, vol. 150, no. 3, pp. 522–525, 2004.

[43] J. L. Arpigny and K. E. Jaeger, "Bacterial lipolytic enzymes: classification and properties," *Biochemical Journal*, vol. 343, part 1, pp. 177–183, 1999.

[44] N. D. Rawlings, A. J. Barrett, and A. Bateman, "MEROPS: the peptidase database," *Nucleic Acids Research*, vol. 38, supplement 1, pp. D227–D233, 2010.

[45] I. V. Kublanov, S. K. Bidjieva, A. V. Mardanov, and E. A. Bonch-Osmolovskaya, "*Desulfurococcus kamchatkensis* sp. nov., a novel hyperthermophilic protein-degrading archaeon isolated from a Kamchatka hot spring," *International Journal of Systematic and Evolutionary Microbiology*, vol. 59, no. 7, pp. 1743–1747, 2009.

[46] C. R. Jackson, H. W. Langner, J. Donahoe-Christiansen, W. P. Inskeep, and T. R. McDermott, "Molecular analysis of microbial community structure in an arsenite-oxidizing acidic thermal spring," *Environmental Microbiology*, vol. 3, no. 8, pp. 532–542, 2001.

[47] N. Byrne, M. Strous, V. Crépeau et al., "Presence and activity of anaerobic ammonium-oxidizing *Bacteria* at deep-sea hydrothermal vents," *ISME Journal*, vol. 3, no. 1, pp. 117–123, 2009.

[48] Q. Huang, C. Dong, R. Dong et al., "Archaeal and bacterial diversity in hot springs on the Tibetan Plateau, China," *Extremophiles*, vol. 15, no. 5, pp. 549–563, 2011.

[49] C. Brochier-Armanet, S. Gribaldo, and P. Forterre, "Spotlight on the *Thaumarchaeota*," *The ISME Journal*, vol. 6, no. 2, pp. 227–230, 2012.

[50] A. Spang, R. Hatzenpichler, C. Brochier-Armanet et al., "Distinct gene set in two different lineages of ammonia-oxidizing archaea supports the phylum *Thaumarchaeota*," *Trends in Microbiology*, vol. 18, no. 8, pp. 331–340, 2010.

[51] S. M. Barns, C. F. Delwiche, J. D. Palmer, and N. R. Pace, "Perspectives on archaeal diversity, thermophily and monophyly from environmental rRNA sequences," *Proceedings of the National Academy of Sciences of the United States of America*, vol. 93, no. 17, pp. 9188–9193, 1996.

[52] J. K. Rhee, D. G. Ahn, Y. G. Kim, and J. W. Oh, "New thermophilic and thermostable esterase with sequence similarity to the hormone-sensitive lipase family, cloned from a metagenomic library," *Applied and Environmental Microbiology*, vol. 71, no. 2, pp. 817–825, 2005.

[53] P. Tirawongsaroj, R. Sriprang, P. Harnpicharnchai et al., "Novel thermophilic and thermostable lipolytic enzymes from a Thailand hot spring metagenomic library," *Journal of Biotechnology*, vol. 133, no. 1, pp. 42–49, 2008.

[54] X. Chu, H. He, C. Guo, and B. Sun, "Identification of two novel esterases from a marine metagenomic library derived from South China Sea," *Applied Microbiology and Biotechnology*, vol. 80, no. 4, pp. 615–625, 2008.

[55] V. Delorme, R. Dhouib, S. Canaan, F. Fotiadu, F. Carrière, and J. F. Cavalier, "Effects of surfactants on lipase structure, activity, and inhibition," *Pharmaceutical Research*, vol. 28, no. 8, pp. 1831–1842, 2011.

[56] S. Kocabiyik and B. Demirok, "Cloning and overexpression of a thermostable signal peptide peptidase (SppA) from *Thermoplasma volcanium* GSS1 in *E. coli*," *Biotechnology Journal*, vol. 4, no. 7, pp. 1055–1065, 2009.

[57] E. Burgess, J. Unrine, G. Mills, C. Romanek, and J. Wiegel, "Comparative geochemical and microbiological characterization of two thermal pools in the Uzon Caldera, Kamchatka, Russia," *Microbial Ecology*, vol. 63, no. 3, pp. 471–489, 2012.

[58] R. Cavicchioli, M. Z. DeMaere, and T. Thomas, "Metagenomic studies reveal the critical and wide-ranging ecological importance of uncultivated archaea: the role of ammonia oxidizers," *BioEssays*, vol. 29, no. 1, pp. 11–14, 2007.

[59] L. J. Reigstad, A. Richter, H. Daims, T. Urich, L. Schwark, and C. Schleper, "Nitrification in terrestrial hot springs of Iceland and Kamchatka," *FEMS Microbiology Ecology*, vol. 64, no. 2, pp. 167–174, 2008.

[60] M. Pester, C. Schleper, and M. Wagner, "The *Thaumarchaeota*: an emerging view of their phylogeny and ecophysiology," *Current Opinion in Microbiology*, vol. 14, no. 3, pp. 300–306, 2011.

Research Article

Localization of Methyl-Coenzyme M Reductase as Metabolic Marker for Diverse Methanogenic Archaea

Christoph Wrede,[1,2] Ulrike Walbaum,[1,3] Andrea Ducki,[1,4] Iris Heieren,[1] and Michael Hoppert[1,5]

[1] *Institute of Microbiology and Genetics, Georg-August-Universität Göttingen, Grisebachstraße 8, 37077 Göttingen, Germany*
[2] *Hannover Medical School, Institute of Functional and Applied Anatomy, Carl-Neuberg-Straße 1, 30625 Hannover, Germany*
[3] *Behavioral Ecology and Sociobiology Unit, German Primate Center, Kellnerweg 4, 37077 Göttingen, Germany*
[4] *School of Veterinary and Biomedical Sciences, Murdoch University, 90 South Street Murdoch, WA 6150, Australia*
[5] *Courant Centre Geobiology, Georg-August-Universität Göttingen, Goldschmidtstraße 3, 37077 Göttingen, Germany*

Correspondence should be addressed to Michael Hoppert; mhopper@gwdg.de

Methyl-Coenzyme M reductase (MCR) as key enzyme for methanogenesis as well as for anaerobic oxidation of methane represents an important metabolic marker for both processes in microbial biofilms. Here, the potential of MCR-specific polyclonal antibodies as metabolic marker in various methanogenic Archaea is shown. For standard growth conditions in laboratory culture, the cytoplasmic localization of the enzyme in *Methanothermobacter marburgensis*, *Methanothermobacter wolfei*, *Methanococcus maripaludis*, *Methanosarcina mazei*, and in anaerobically methane-oxidizing biofilms is demonstrated. Under growth limiting conditions on nickel-depleted media, at low linear growth of cultures, a fraction of 50–70% of the enzyme was localized close to the cytoplasmic membrane, which implies "facultative" membrane association of the enzyme. This feature may be also useful for assessment of growth-limiting conditions in microbial biofilms.

1. Introduction

Methyl-coenzyme M reductase (MCR) is the key enzyme of the final, methane-forming step in methanogenesis. The enzyme catalyses the reductive cleavage of methyl-coenzyme M (CoM-S-CH$_3$) using coenzyme B (HS-CoB) as reductant which results in the production of methane and the heterodisulfide CoM-S-S-CoB. Though the involved enzyme complexes as well as the reactants differ between *Methanosarcinales*, *Methanobacteriales,* and other groups of methanogens, the essential reaction steps are similar and require several membrane-dependent steps (see [1, 2] for review). The formation of methyl-coenzyme M is catalysed by one subunit (MtrE) of a membrane-bound complex (the N^5-methyl-tetrahydromethanopterin:coenzyme M methyltransferase) and is coupled with energy conservation via an electrochemical sodium potential across the cytoplasmic membrane (see [3] for review). Regeneration of the reductant

HS-CoB is brought about by the enzyme heterodisulfide reductase. For the regeneration of HS-CoB, reducing equivalents are needed, provided by hydrogenases and/or dehydrogenases. The reducing equivalents are either guided via a membrane-bound electron transport chain to the enzyme or are directly transferred from the hydrogenase to the heterodisulfide reductase. The reactions are also coupled to chemiosmotic mechanisms, resulting in the generation of ATP via a H$^+$-potential [4–6]. Like MtrE, the heterodisulfide reductase is a part of a membrane-bound complex. The methyl-coenzyme M reductase reaction step itself is not membrane-dependent. The enzyme has been purified from the cytoplasmic fractions of methanogenic Archaea and has been localized in the cytoplasm by immunoelectron microscopy. The catalytic reaction does not depend on the addition of membrane preparations [7–11]. A number of experiments, however, indicate that there is a certain affinity of the enzyme to the membrane [12, 13]. MCR
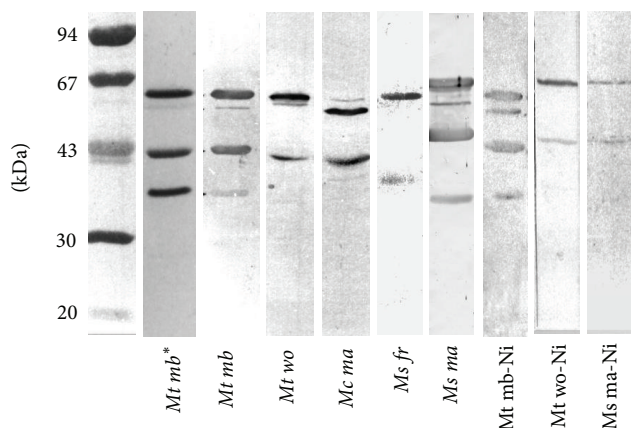
FIGURE 1: Specificity of the polyclonal serum used for immunolocalization. The slots depict crude extracts of the organisms after Western blotting of SDS gels and double-immunoperoxidase precipitation. All slots show the typical pattern of MCR. For most organisms (except *Ms ma* and *Mt mb*), only the two larger of the three MCR subunits are visible. When cells were grown on nickel-depleted media, the respective slot is marked with -Ni. The second slot (marked with an asterisk) shows a silver stained SDS-polyacrylamide gel of the purified enzyme. *Mt mb: Methanothermobacter marburgensis*, *Mt wo: Methanothermobacter wolfei*, *Mc ma: Methanococcus maripaludis*, *Ms fr: Methanosarcina mazei* (DSM 3318, formerly *Methanosarcina frisia*), *Ms ma: Methanosarcina mazei* (DSM 3647).

TABLE 1: Partitioning of MCR as revealed by immunolocalization.

Organism	Approximate doubling time (h)	Concentration of levulinic acid in the medium	% markers at the membrane
Methanothermobacter marburgensis	26	0.0	17
	35	0.05	36
	38	0.2	70
Methanothermobacter wolfei	34	0.0	15
	42	0.1	52
Methanosarcina mazei (DSM 3647)	20	0.0	32
	34	0.05	60

of *Methanothermobacter marburgensis* was located at the cytoplasmic membrane under nickel-depleted growth conditions. Also electron microscopy of vesicle preparations from *Methanobacteriales* and *Methanosarcina* showed that at least a fraction of MCR is membrane-associated. From these data, it was deduced that MCR might be part of a membrane-bound multienzyme complex [14, 15].

For the reverse process, the anaerobic oxidation of methane, a reverse operating methanogenic pathway has been postulated, with an MCR structurally very similar to the canonical enzyme [16–18]. In the postulated pathway, again, membrane binding is not necessarily required. However, as in methanogenesis, membrane association might also be of advantage, since the same membrane-dependent processes as in methanogenesis are likely [17, 19].

In *Methanobacterium thermoautotrophicum*, two different localizations of the MCR could already be shown [13]. In our study, we show that these results are also true for other methanogens, and we will discuss these results in view of immunolocalization of the key enzyme MCR for studies in environmental biofilms.

2. Materials and Methods

Methanothermobacter marburgensis (DSM 2133, formerly *Methanobacterium thermoautotrophicum*, strain Marburg), *Methanothermobacter wolfei* (DSM 2970, formerly *Methanobacterium wolfei*), and *Methanococcus maripaludis* (DSM 2067) were grown autotrophically as described [20–23]. *Methanosarcina mazei* (DSM 3318, formerly *Methanosarcina*

frisia) and *Methanosarcina mazei* (DSM 3647) were grown heterotrophically [24, 25]. Nickel-limited media did not contain nickel salts in trace element solutions and were supplemented with up to 200 mM levulinic acid (cf. Table 1). For immunolocalization, cells were grown in batch cultures at linear growth rates with approximate doubling times between 25 and 45 h (Table 1). Cell disruption was performed with a French pressure cell operated at 1,500 lb/in^2 and subsequent centrifugation by 15,000 ×g for 25 min at 4°C in order to remove cell debris. The supernatant was used for Western-blotting (see below). For protein purification, cells of *Methanothermobacter marburgensis* were grown in 14 l-fermenters with a doubling time of 2.9 h in the exponential phase on mineral salt medium and continuous gassing with H_2/CO_2 (80%/20%, v/v) as described [20]. Purification of MCR was performed according to [7]. The purified protein (MCR, i.e. the isoform I of methyl-coenzyme M reductase, Figure 1) was used for production of polyclonal antisera [26]. Protein purity and specificity of the antisera was tested by SDS polyacrylamide gel electrophoresis and Western blotting [27–29] and by immunolocalization control experiments (see below, [30]). Protein assays were performed according to [31].

Samples of an environmental methane-oxidizing biofilms were obtained and processed as described [32, 33]. Microbial mat samples were collected in 2001 during a cruise with the Russian R/V "Professor Logachev" from the methane seep area located on the NW' Shelf region (Crimean Shelf) in the Black Sea. Material for transmission electron microscopy and immunofluorescence analyses was chemically fixed in a 4.0% (w/v) formaldehyde solution and kept at 4°C in 100 mM PBS (phosphate-buffered saline, pH 7.0). The samples were washed several times in PBS and fixed in 0.3% (v/v) solution of glutardialdehyde and 0.5% (w/v) formaldehyde in PBS for 2 h at 4°C. The samples were then washed three times in PBS supplemented with 10 mM glycin. See below for subsequent dehydration and resin embedding.

Active cultures were chemically fixed anaerobically by adding 0.2% (v/v) solution of glutardialdehyde and 0.3% (w/v) formaldehyde to the active culture under anaerobic conditions. After incubation for 2 h at 4°C, the culture was centrifuged three times for 10 min at 9.000 ×g and resuspended in PBS supplemented with 10 mM glycin. Molten agar (2%, w/v, 50°C) was added to an equal volume of the
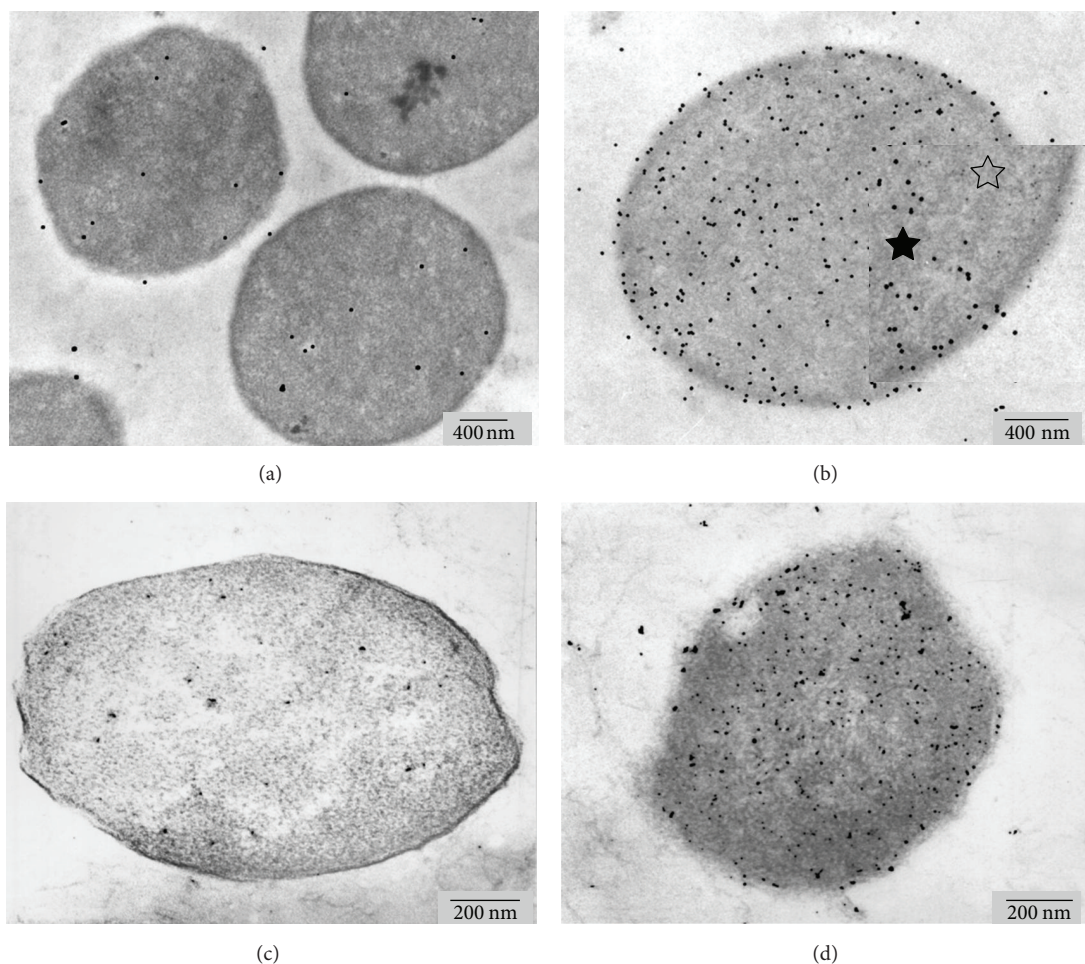
FIGURE 2: Ultrathin sections of *Methanosarcina mazei* (DSM 3318, formerly *Methanosarcina frisia* (a, b) and *Methanococcus maripaludis* (c, d) grown on media without nickel depletion. Immunolabeled cells (b, d; a, c are negative controls) show cytoplasmic localization of MCR. The inset in (b) shows an enlarged area of the image before (open star symbol) and after processing (closed star) of the gold marker.

resuspended pellet. After mixing thoroughly, the sample was allowed to solidify.

Subsequently, biofilm samples and agar-embedded culture samples were dehydrated. For dehydration, an ascending methanol series was used [30]: 15% (v/v), 30% for 15 min, 50%, 75% for 30 min, 90%, and 100% for 1 h. The temperature was successively lowered down to −35°C (steps: 15%, 30% at 0°C, 50% at −20°C, and all other steps at −35°C). Samples were then incubated in Lowicryl K4M resin dilutions in methanol (1 : 3, 1 : 2, and 3 : 1; Lowicryl resin obtained from Electron Microscopy Sciences, Hatfield, PA, USA), followed by incubation in pure resin for 1 h per step and then overnight. The blocks were transferred to small gelatin capsules (Plano, Wetzlar, Germany) containing pure resin and were polymerized for at least 48 h at −35°C and 3 d at room temperature under UV light.

Ultrathin sections of trimmed specimens (80–90 nm) were cut with glass knives in a Reichert Jung FC 4 ultramicrotome (Leica Microsystems, Wetzlar, Germany). Sections were transferred onto Formvar-coated grids [30].

For TEM immunocytochemistry, grids were placed with sections facing downwards, for 30 min on drops of 3% (w/v)

bovine serum albumin (BSA) in PBS, then for 2 h on anti-MCR antibodies (1 mg protein/mL; dilution in PBS). Negative controls were performed by incubation of the grids on PBS without the antibody.

Grids were then washed by incubation (two times 5 min) on drops of PBS containing 0.05% (v/v) Tween 20 and by incubation (5 min) on PBS without Tween, followed by a 1 h incubation step on the secondary antibody (goat anti-rabbit IgG-10 nm gold conjugate; British Biocell International Ltd., Cardiff, UK). The secondary antibody was used in a 1 : 80 dilution (in the same solutions as used for the respective primary antibodies). Again, two 5 min washing steps with PBS containing 0.05% (v/v) Tween 20, and one step with PBS was performed, followed by washing for 10 s in distilled water for desalting. Poststaining was performed with 4% (w/v) uranyl acetate solution for 3 min. All steps were conducted at room temperature.

Electron micrographs were taken, at calibrated magnifications, with a Philips EM 301 transmission electron microscope (Philips, Eindhoven, The Netherlands) operated in the conventional bright field mode and a Jeol JEM 1011 (Jeol, Eching, Germany) equipped with a Gatan Orius SC1000
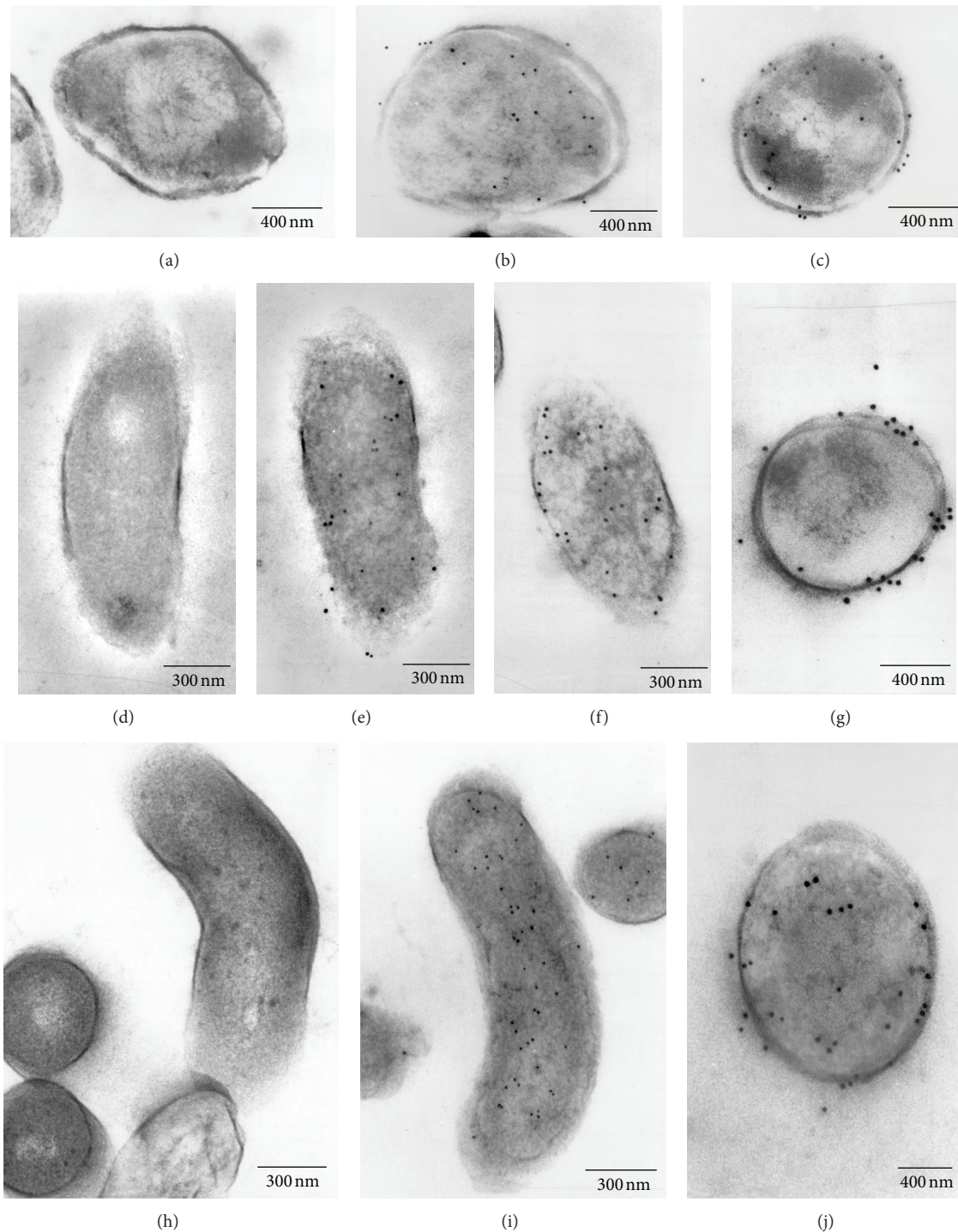
FIGURE 3: Localization of MCR in *Methanosarcina mazei* (DSM 3647; a, b, c), *Methanothermobacter marburgensis* (d–g), and *Methanother-mobacter wolfei* (h, i, j). On media without nickel depletion, the markers are localized in the cytoplasm (b, e, i). On nickel-depleted media with levulinic acid (c, f: 0.05 M; g 0.2 M; j: 0.1 M levulinic acid) a tendency to membrane localization is obvious (a, d, h are negative controls).

CCD camera (Gatan, Munich, Germany). For enhancement of gold particles of 5 nm in diameter, images were processed as follows. High-pass filtering was applied to suppress low spatial frequencies, that is, large image components with smooth contrast gradients. After readjustment of the contrast level by stretching the intensity histogram, the image was transformed by thresholding at a gray level of 100. In the black and white image, particles larger than 7 nm and smaller than 4 nm (original size) were eliminated. The resulting images depict 5 nm gold particles in pure black and white contrast.

(a)

(b)
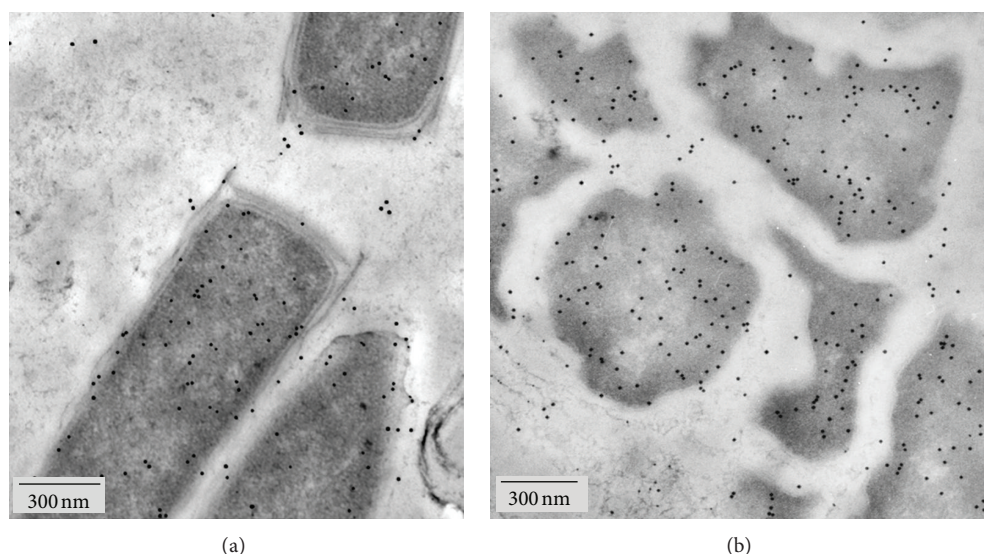
Figure 4: Localization of MCR in predominant morphotypes of microbial mats conducting AOM. Filamentous ANME-1 in the pink layer of the AOM community (a) and coccoid ANME-2 in the black layer (b) exhibit dense cytosolic MCR labelling.

Particle sizes were enlarged by a factor of 2.5 to allow an easier identification. When these images were merged with the original, a higher final contrast was gained (Figure 2(b), inset). Image processing was performed with the NIH Image software (National Institute of Health; see also [30, 34]). For statistical analysis, 20 randomly selected cells were counted. Gold markers in a range of 25 nm (original size) inside or outside the cytoplasmic membrane were referred to as "membrane associated"; all other markers inside the cell were referred to as cytoplasmic.

3. Results and Discussion

The apparent subunit molecular weights (α: 65 kDa, β: 49 kDa, and γ: 38 kDa) of the purified methyl-coenzyme M reductase correspond to the subunit molecular weights of the MCR I isoenzyme from *Methanothermobacter marburgensis* [35]. This isoform is predominant when H_2 and CO_2 supply is low and growth limiting [11]. Western blotting of crude extracts, prepared from cells that were also used for immunolocalization, revealed that the antiserum detects protein bands from a variety methanogens. The apparent sizes of these bands correspond to the expected molecular weights of the α and β subunit of MCR. In some cases, also the smallest (γ) subunit is visible (Figure 1). The same pattern has already been shown for MCR extracts obtained from anaerobic methane-oxidizing microbial mats [36]. The γ subunit of MCR is known to be less immunogenic and produces a weaker or no signal (Figure 1; [8, 15]). In some of the Western blots, a second band in the range of 67 kDa may account for the presence of the MCR isoenzyme II (MRT) in minor amounts. This enzyme exhibits a slightly smaller α subunit and a γ subunit of 33 kDa [35]. MRT was isolated from *Methanothermobacter marburgensis* [35] and from various other *Methanobacteriales* and *Methanococcales*, but as yet not from *Methanosarcinaceae* [35, 37–40].

The hydrogenotrophic methanogens investigated here were grown in batch culture with limited substrate availability. Thus, it may be expected that for those methanogens that contain, in analogy to *Methanothermobacter marburgensis*, two methyl-coenzyme M reductases, the MCR isoenzyme I is dominant [11].

Immunolocalization of MCR from *Methanosarcina mazei* (DSM 3318, formerly *Methanosarcina frisia*; Figure 2(b)), *Methanococcus maripaludis* (Figure 2(d)), *Methanosarcina mazei* (DSM 3647; Figure 3(b)), *Methanothermobacter marburgensis* (Figure 3(e)), and *Methanothermobacter wolfei* (Figure 3(i)) grown on media without depletion of nickel show that MCR antigens are distributed throughout the whole cell. For the autotrophically growing *Methanothermococcus thermolithotrophicus* (DSM 2095, formerly *Methanococcus thermolithotrophicus*) and for *Methanolobus tindarius* (DSM 2278), cytoplasmic localization of MCR has already been shown [33]. Though most of the organisms tested did not grow on nickel-depleted media, *Methanosarcina mazei* (DSM 3647), *Methanothermobacter marburgensis,* and *Methanothermobacter wolfei* grew on media without the trace element nickel and after addition of up to 0.2 M levulinic acid (final concentration) to the respective standard growth medium. Levulinic acid inhibits the biosynthesis of the nickel tetrapyrrole cofactor F430. This reduces, in addition to nickel-limitation, the expression of MCR [13, 41]. Under these conditions, the distribution of the enzyme changed; a higher amount of MCR is now located at the membrane. Table 1 summarizes the results obtained after immunolocalization. Statistical errors of individual cells counted were around 20% for all counts. Thus, the values show a clear trend, but not an exactly reproducible value. Cellular redistribution of MCR markers was most pronounced in *Methanothermobacter marburgensis* (Figures 3(f) and 3(g)). The organism may be considered as a reference for our experiments, since similar results have been

described previously [13]. Also *M. wolfei* and *M. mazei* (DSM 3647) showed redistribution of the gold marker (Figures 3(c) and 3(j)). Though the effect is less obvious than in *M. marburgensis*; 50–60% of the markers could be located at the membrane.

Samples taken from different layers of the multilayered anaerobically methane-oxidizing microbial mats [32, 36] show distinct mophotypes of methane oxidizing Archaea [33]: ANME-1 Archaea are filamentous organisms, related to *Methanomicrobiales* and are dominating in the pink-coloured layer of the microbial mat, whereas the ANME-2 Archaea of the outermost black layer are related to *Methanosarcinales* [42, 43]. Immunolocalization of MCR showed for both morphotypes intensive cytosolic labelling (Figures 4(a) and 4(b)). In this respect, the expression of MCR may not be limited in the environmental biofilm.

According to all available biochemical data, membrane association of MCR is not necessary for functioning. However, localization of the soluble enzyme in vicinity to the membrane is favourable for the whole pathway, in particular when the enzyme production is limited. Membrane binding becomes obvious, as already stated before [13], when growth conditions limit the synthesis of MCR. Putatively, the diffusion paths of the reactants are shorter and the final step of methanogenesis is more effective. We could show that this feature is not restricted to *M. marburgensis,* but appears to be true for the related *M. wolfei* as well as the phylogenetically distant *M. mazei* and may also be expected for the related methane-oxidizing Archaea. Thus the enzyme may be an interesting example for a "facultative" membrane association of proteins, with a certain capability of membrane binding, but without a specific membrane-dependent metabolic mechanism [44]. For environmental processes, location of the enzyme at the membrane may be an indirect indicator for the physiological status, in our case for nickel-limited conditions and reduced cofactor biosynthesis. According to this assumption, this does not appear to be the case for ANME-1 and ANME-2, prominent in AOM-performing microbial mats from the Black Sea (cf. Figures 4(a) and 4(b)). The images show dense cytoplasmic localization of the marker, accounting for nonlimited production of the enzyme.

Acknowledgments

References

[1] R. K. Thauer, "Biochemistry of methanogenesis: a tribute to Marjory Stephenson," *Microbiology*, vol. 144, no. 9, pp. 2377–2406, 1998.

[2] R. K. Thauer, A. K. Kaster, H. Seedorf, W. Buckel, and R. Hedderich, "Methanogenic archaea: ecologically relevant differences in energy conservation," *Nature Reviews Microbiology*, vol. 6, no. 8, pp. 579–591, 2008.

[3] G. Gottschalk and R. K. Thauer, "The Na+-translocating methyltransferase complex from methanogenic archaea," *Biochimica et Biophysica Acta*, vol. 1505, no. 1, pp. 28–36, 2001.

[4] E. Stupperich, A. Juza, M. Hoppert, and F. Mayer, "Cloning, sequencing and immunological characterization of the corrinoid-containing subunit of the N5-methyltetrahydro-methanopterin:coenzyme-M methyltransferase from *Methanobacterium thermoautotrophicum*," *European Journal of Biochemistry*, vol. 217, no. 1, pp. 115–121, 1993.

[5] U. Deppenmeier, "Redox-driven proton translocation in methanogenic archaea," *Cellular and Molecular Life Sciences*, vol. 59, no. 9, pp. 1513–1533, 2002.

[6] A. Stojanowic, G. J. Mander, E. C. Duin, and R. Hedderich, "Physiological role of the F420-non-reducing hydrogenase (MvH) from *Methanothermobacter marburgensis*," *Archives of Microbiology*, vol. 180, no. 3, pp. 194–203, 2003.

[7] R. P. Hausinger, W. H. Orme-Johnson, and C. Walsh, "Nickel tetrapyrrole cofactor F430: comparison of the forms bound to methyl coenzyme M reductase and protein free in cells of *Methanobacterium thermoautotrophicum* ΔH," *Biochemistry*, vol. 23, no. 5, pp. 801–804, 1984.

[8] I. Thomas, H.-C. Dubourguier, G. Prensier, P. Debeire, and G. Albagnac, "Purification of component C from *Methanosarcina mazei* and immunolocalization in *Methanosarcinaceae*," *Archives of Microbiology*, vol. 148, no. 3, pp. 193–201, 1987.

[9] J. Ellermann, R. Hedderich, R. Böcher, and R. K. Thauer, "The final step in methane formation. Investigations with highly purified methyl-CoM reductase (component C) from *Methanobacterium thermoautotrophicum* (strain Marburg)," *European Journal of Biochemistry*, vol. 172, no. 3, pp. 669–677, 1988.

[10] J. Ellermann, S. Rospert, R. K. Thauer et al., "Methyl-coenzyme-M reductase from *Methanobacterium thermoautotrophicum* (strain Marburg)-purity, activity and novel inhibitors," *European Journal of Biochemistry*, vol. 184, no. 1, pp. 63–68, 1989.

[11] L. G. Bonacker, S. Baudner, and R. K. Thauer, "Differential expression of the two methyl-coenzyme M reductases in *Methanobacterium thermoautotrophicum* as determined immunochemically via isoenzyme-speficic antisera," *European Journal of Biochemistry*, vol. 206, no. 1, pp. 87–92, 1992.

[12] R. Ossmer, T. Mund, and P. L. Hartzell, "Immunocytochemical localization of component C of the methylreductase system in *Methanococcus voltae* and *Methanobacterium thermoautotrophicum*," *Proceedings of the National Academy of Sciences of the United States of America*, vol. 83, no. 16, pp. 5789–5792, 1986.

[13] H. C. Aldrich, D. B. Beimborn, M. Bokranz, and P. Schönheit, "Immunocytochemical localization of methyl-coenzyme M reductase in *Methanobacterium thermoautotrophicum*," *Archives of Microbiology*, vol. 147, no. 2, pp. 190–194, 1987.

[14] F. Mayer, M. Rohde, M. Salzmann, A. Jussofie, and G. Gottschalk, "The methanoreductosome: a high-molecular-weight enzyme complex in the methanogenic bacterium strain Göl that contains components of the methylreductase system," *Journal of Bacteriology*, vol. 170, no. 4, pp. 1438–1444, 1988.

[15] M. Hoppert and F. Mayer, "Electron microscopy of native and artificial methylreductase high-molecular-weight complexes in strain Gö 1 and *Methanococcus voltae*," *FEBS Letters*, vol. 267, no. 1, pp. 33–37, 1990.

[16] M. Krüger, A. Meyerdierks, F. O. Glöckner et al., "A conspicuous nickel protein in microbial mats that oxidize methane anaerobically," *Nature*, vol. 426, no. 6968, pp. 878–881, 2003.

[17] S. J. Hallam, N. Putnam, C. M. Preston et al., "Reverse methano-genesis: testing the hypothesis with environmental genomics," *Science*, vol. 305, no. 5689, pp. 1457–1462, 2004.

[18] S. Shima, M. Krüger, T. Weinert et al., "Structure of a methyl-coenzyme M reductase from Black Sea mats that oxidize methane anaerobically," *Nature*, vol. 481, no. 7379, pp. 98–101, 2011.

[19] A. Meyerdierks, M. Kube, I. Kostadinov et al., "Metagenome and mRNA expression analyses of anaerobic methanotrophic archaea of the ANME-1 group," *Environmental Microbiology*, vol. 12, no. 2, pp. 422–439, 2010.

[20] P. Schönheit, J. Moll, and R. K. Thauer, "Growth parameters (K(s), μ(max), Y(s)) of *Methanobacterium thermoautotrophicum*," *Archives of Microbiology*, vol. 127, no. 1, pp. 59–65, 1980.

[21] H. Huber, M. Thomm, H. Konig, G. Thies, and K. O. Stetter, "*Methanococcus thermolithotrophicus*, a novel thermophilic lithotrophic methanogen," *Archives of Microbiology*, vol. 132, no. 1, pp. 47–50, 1982.

[22] N. Belay, R. Sparling, and L. Daniels, "Dinitrogen fixation by a thermophilic methanogenic bacterium," *Nature*, vol. 312, no. 5991, pp. 286–288, 1984.

[23] J. Winter, C. Lerp, and H. P. Zabel, "*Methanobacterium wolfei*, sp. nov., a new tungsten-requiring, thermophilic, autotrophic methanogen," *Systematic and Applied Microbiology*, vol. 5, no. 4, pp. 457–466, 1984.

[24] H. Hippe, D. Caspari, K. Fiebig, and G. Gottschalk, "Utilization of trimethylamine and other N methyl compounds for growth and methane formation by *Methanosarcina barkeri*," *Proceedings of the National Academy of Sciences of the United States of America*, vol. 76, no. 1, pp. 494–498, 1979.

[25] H. König and K. O. Stetter, "Isolation and characterization of *Methanolobus tindarius*, sp. nov., a coccoid methanogen growing only on methanol and methylamines," *Zentralblatt für Bakteriologie Mikrobiologie und Hygiene*, vol. 3, no. 4, pp. 478–490, 1982.

[26] E. Harlow and D. Lane, *Antibodies-A Laboratory Manual*, Cold Spring Harbor Laboratory, New York, NY, USA, 1988.

[27] U. K. Laemmli, "Cleavage of structural proteins during the assembly of the head of bacteriophage T4," *Nature*, vol. 227, no. 5259, pp. 680–685, 1970.

[28] H. Towbin, T. Staehelin, and J. Gordon, "Electrophoretic transfer of proteins from polyacrylamide gels to nitrocellulose sheets: procedure and some applications," *Proceedings of the National Academy of Sciences of the United States of America*, vol. 76, no. 9, pp. 4350–4354, 1979.

[29] H. Blum, H. Beier, and J. H. Gross, "Improved silver staining of plant proteins, RNA and DNA in polyacrylamide gels," *Electrophoresis*, vol. 8, no. 2, pp. 93–99, 1987.

[30] M. Hoppert and A. Holzenburg, *Electron Microscopy in Microbiology*, Bios Scientific, Oxford, UK, 1998.

[31] M. M. Bradford, "A rapid and sensitive method for the quantitation of microgram quantities of protein utilizing the principle of protein dye binding," *Analytical Biochemistry*, vol. 72, no. 1-2, pp. 248–254, 1976.

[32] J. Reitner, J. Peckmann, M. Blumenberg, W. Michaelis, A. Reimer, and V. Thiel, "Concretionary methane-seep carbonates and associated microbial communities in Black Sea sediments," *Palaeogeography, Palaeoclimatology, Palaeoecology*, vol. 227, no. 1–3, pp. 18–30, 2005.

[33] C. Heller, M. Hoppert, and J. Reitner, "Immunological localization of coenzyme M reductase in anaerobic methane-oxidizing archaea of ANME 1 and ANME 2 type," *Geomicrobiology Journal*, vol. 25, no. 3-4, pp. 149–156, 2008.

[34] M. Kämper, S. Vetterkind, R. Berker, and M. Hoppert, "Methods for in situ detection and characterization of extracellular polymers in biofilms by electron microscopy," *Journal of Microbiological Methods*, vol. 57, no. 1, pp. 55–64, 2004.

[35] L. G. Bonacker, S. Baudner, E. Mörschel, R. Böcher, and R. K. Thauer, "Properties of the two isoenzymes of methyl-coenzyme M reductase in *Methanobacterium thermoautotrophicum*," *European Journal of Biochemistry*, vol. 217, no. 2, pp. 587–595, 1993.

[36] C. Wrede, V. Krukenberg, A. Dreier, J. Reitner, C. Heller, and M. Hoppert, "Detection of metabolic key enzymes of methane turnover processes in cold seep microbial biofilms," *Geomicrobiology Journal*, vol. 30, no. 3, pp. 214–227, 2013.

[37] S. Rospert, D. Linder, J. Ellermann, and R. K. Thauer, "Two genetically distinct methyl-coenzyme M reductases in *Methanobacterium thermoautotrophicum* strain Marburg and delta H," *European Journal of Biochemistry*, vol. 194, no. 3, pp. 871–877, 1990.

[38] A. Lehmacher and H. P. Klenk, "Characterization and phylogeny of mcrII, a gene cluster encoding an isoenzyme of methyl coenzyme M reductase from hyperthermophilic *Methanothermus fervidus*," *Molecular and General Genetics*, vol. 243, no. 2, pp. 198–206, 1994.

[39] C. J. Bult, O. White, G. J. Olsen et al., "Complete genome sequence of the *Methanogenic archaeon, Methanococcus jannaschii*," *Science*, vol. 273, no. 5278, pp. 1058–1073, 1996.

[40] E. Springer, M. S. Sachs, C. R. Woese, and D. R. Boone, "Partial gene sequences for the A subunit of methyl-coenzyme M reductase (mcrI) as a phylogenetic tool for the family *Methanosarcinaceae*," *International Journal of Systematic Bacteriology*, vol. 45, no. 3, pp. 554–559, 1995.

[41] R. Jaenchen, H. H. Gilles, and R. K. Thauer, "Inhibition of factor F430 synthesis by levulinic acid in *Methanobacterium thermoautotrophicum*," *FEMS Microbiology Letters*, vol. 12, no. 2, pp. 167–170, 1981.

[42] K. U. Hinrichs, J. M. Hayes, S. P. Sylva, P. G. Brewert, and E. F. DeLong, "Methane-consuming archaebacteria in marine sediments," *Nature*, vol. 398, no. 6730, pp. 802–805, 1999.

[43] V. J. Orphan, C. H. House, K. U. Hinrichs, K. D. McKeegan, and E. F. DeLong, "Methane-consuming archaea revealed by directly coupled isotopic and phylogenetic analysis," *Science*, vol. 293, no. 5529, pp. 484–487, 2001.

[44] M. Hoppert and F. Mayer, "Principles of macromolecular organization and cell function in bacteria and archaea," *Cell Biochemistry and Biophysics*, vol. 31, no. 3, pp. 247–284, 1999.

Research Article

Dynamics of the Methanogenic Archaea in Tropical Estuarine Sediments

María del Rocío Torres-Alvarado,[1] Francisco José Fernández,[2] Florina Ramírez Vives,[2] and Francisco Varona-Cordero[1]

[1] *Department of Hydrobiology, Universidad Autónoma Metropolitana-Iztapalapa, Avenida San Rafael Atlixco No. 86, Colonia Vicentina, 09340 Mexico City, DF, Mexico*

[2] *Department of Biotechnology, Universidad Autónoma Metropolitana-Iztapalapa, Avenida San Rafael Atlixco No. 86, Colonia Vicentina, 09340 Mexico City, DF, Mexico*

Correspondence should be addressed to María del Rocío Torres-Alvarado; rta@xanum.uam.mx

Methanogenesis may represent a key process in the terminal phases of anaerobic organic matter mineralization in sediments of coastal lagoons. The aim of the present work was to study the temporal and spatial dynamics of methanogenic archaea in sediments of tropical coastal lagoons and their relationship with environmental changes in order to determine how these influence methanogenic community. Sediment samples were collected during the dry (February, May, and early June) and rainy seasons (July, October, and November). Microbiological analysis included the quantification of viable methanogenic archaea (MA) with three substrates and the evaluation of kinetic activity from acetate in the presence and absence of sulfate. The environmental variables assessed were temperature, pH, Eh, salinity, sulfate, solids content, organic carbon, and carbohydrates. MA abundance was significantly higher in the rainy season (10^6–10^7 cells/g) compared with the dry season (10^4–10^6 cells/g), with methanol as an important substrate. At spatial level, MA were detected in the two layers analyzed, and no important variations were observed either in MA abundance or activity. Salinity, sulfate, solids, organic carbon, and Eh were the environmental variables related to methanogenic community. A conceptual model is proposed to explain the dynamics of the MA.

1. Introduction

Coastal and marine environments, including estuaries and coastal lagoons, are characterized by large amounts of organic matter, which is mineralized primarily in sediments through anaerobic processes, sulfate reduction being the dominant metabolic pathway [1, 2]. However, although these ecosystems are the typical habitat of sulfate-reducing prokaryotes (SRP), methanogenic archaea (MA) and methane production have also been detected [3, 4].

MA are strict anaerobes that produce methane as endproduct of their metabolism. These organisms are common in anoxic environments in which electron acceptors such as nitrate and sulfate are either absents or present at low concentrations and are usually dominant in freshwater environments. In the presence of these electron acceptors, methanogenesis is outcompeted by anaerobic respiration, mainly for thermodynamic reasons [5]. MA distribution patterns and its number, as well as physical, chemical, and nutritional parameters controlling their abundance and distribution have been studied in lacustrine sediments [6] and in coastal environments [7, 8].

Most of the ecological studies assessing the structure of methanogenic communities in estuarine systems have been performed in temperate latitudes where temperature is one of the major factors regulating ecosystem function. These investigations have included an evaluation of the MA in the intertidal zone of marshes with the presence of *Spartina alterniflora*, whose roots provide organic carbon and contribute to create aerobic microhabitats [9, 10]. MA abundance has been quantified with two or three substrates, of which acetate and hydrogen have been reported as the two most important ones

(a) Coastal lagoon system of Carretas-Pereyra, Chiapas

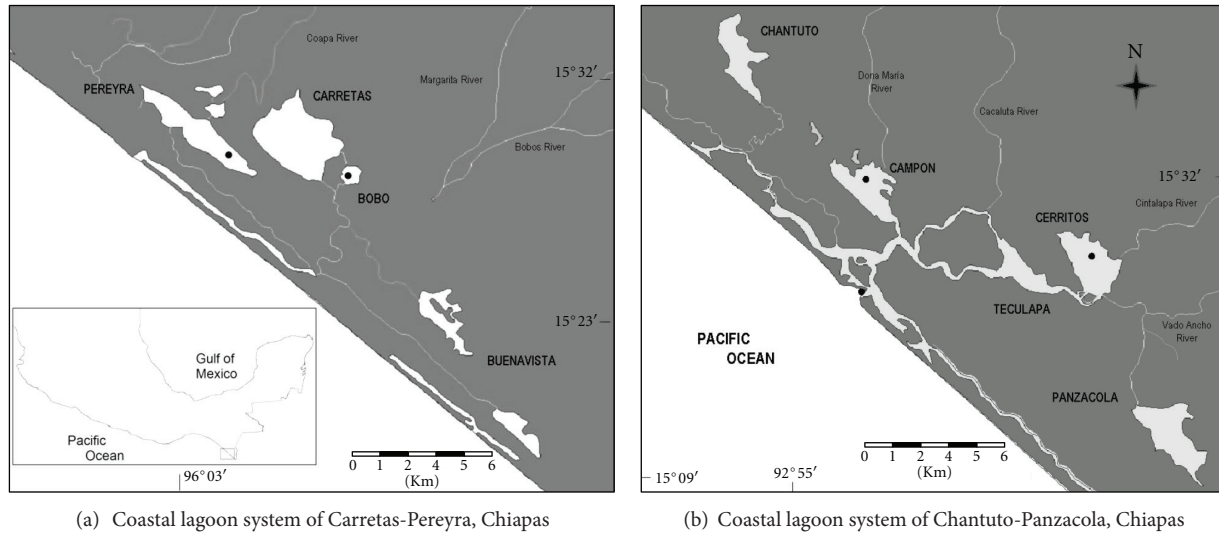(b) Coastal lagoon system of Chantuto-Panzacola, Chiapas

FIGURE 1: Study area and sampling sites (●).

[4, 11]. Additionally, it has been established that in estuaries, where a salinity gradient exists from the marine zone to a river entrance, MA are prevalent upstream in the freshwater region and decrease towards the brackish and marine ends; sulfate reduction has been identified as the key factor related to the MA distribution [7, 10, 12, 13]. Depth profiles of MA distribution have been observed, their abundance increase in deeper layers of the sediment column, because the MA are dependent on heterotrophs and fermenters during the organic matter decomposition, its decline is also related to a decrease in both sulfate concentration and redox potential [8].

In contrast to estuaries, coastal lagoons generally have restricted communication with the sea and in tropical lagoons, as a result of strong seasonal precipitation patterns, there are significant fluctuations in river discharge, and associated hydrological conditions (salinity). These variations might affect the structure of microbial communities involved in the terminal phases of the anaerobic organic matter mineralization, as well as to the biogeochemical processes related to it. In spite of its importance, studies focused on these ecosystems to assess the dynamics of anaerobic microbiota, especially MA, are scarce. It has been reported that MA using methylamines are the primary microbial components in sediments of coastal lagoons associated to mangroves, with higher densities during the summer and premonsoon [14, 15]. In another study, a peak of methane production in mangrove sediments has been recorded in the postmonsoon season [16]. In Mexico, where coastal lagoons are abundant, investigations on methanogenic communities are virtually absent; hence, the aim of the present study was to explore the spatial and temporal dynamics of the methanogenic community in sediments from two tropical coastal systems: Chantuto-Panzacola and Carretas-Pereyra, located in the Mexican southern Pacific and to propose a conceptual model on MA dynamics in sediments for the tropical coastal lagoons studied.

2. Materials and Methods

2.1. Study Site. The Chantuto-Panzacola and Carretas-Pereyra lagoon systems are located in the State of Chiapas, Mexican Pacific coast (Figure 1); they are part of the International Biosphere Reserve "La Encrucijada". The climate of the region is warm (28°C) and humid (89%) with abundant summer rainfall; annual rainfall ranges between 1,300 and 3,000 mm. The rainy season begins between May and June and continues through November; the dry season occurs from December to May [17]. Lagoon systems are characterized by high temperatures in the water column (29–35.5°C), with a variable salinity ranging from 0 to 34.5‰ in Chantuto-Panzacola and from 0 to 22.7‰ in Carretas-Pereyra, depending on the season. There is a limited exchange with the sea and a significant phosphorus supply from rivers, which favors high chlorophyll-*a* levels. Systems are bordered by mangrove forests and freshwater wetlands. Mangrove detritus results in high humic substance levels (>150 mg/L) in the rainy season [18] also recording high ammonium concentrations derived from mineralization [19].

The Chantuto-Panzacola lagoon has an area of 18,000 ha and comprises five lagoons: Chantuto, Campón, Teculapa, Cerritos, and Panzacola. In this system, samples were collected from the Cerritos and Campón lagoons (Figure 1). The Cerritos lagoon (15°09'54.4''N, 92°45'34.0''W) has a mean depth of 1.1 m in the dry season and 1.3 m during the rainy season. The Cintalapa River flows into this lagoon, contributing a volume between 66.2 m^3/s in October and 0.4 m^3/s in May (dates proportionated by the National Water Commission in Mexico). The Campon lagoon (15°12'30.0''N, 92°51'24.2''W) has a mean depth of 0.8 m in the dry season and of 0.9 m in the rainy season. The Cacaluta River flows into this lagoon, with a maximum inflow in October (144.2 m^3/s) and a minimum inflow in May (0.5 m^3/s). Sediments are a mixture of silt and sand in both lagoons.

The Carretas-Pereyra system covers an area of 3,696 ha and comprises four water bodies: Pereyra, Carretas, Bobo, and Buenavista, sampling took place in Pereyra and Bobo (Figure 1). The Pereyra lagoon ($15°31'26.1''$N, $92°51'24.2''$W) has a mean depth of 0.7 m in the dry season and 1.0 m in the rainy season. Sediment is silt-sand. The Margaritas River drains into the Pereyra lagoon (discharge volume unknown). The Bobo lagoon ($15°29'22.0''$N, $93°08'44.6''$W) has a mean depth of 0.5 m and 0.7 m in the dry and rainy seasons, respectively. It lacks freshwater inputs and sediment is silt-sand.

2.2. Sample Collection and Preparation Procedures. Sediment cores were collected with a 45 cm long and 4.5 cm wide plexiglass coring device during the dry (February, May, and early June) and rainy seasons (July, October, and November). Temperature, Eh, and pH were simultaneously measured when sampling the cores at two sediment depths (6 and 12 cm) using standard electrodes and an Ionanalizer (Conductronic pH 120). pH was measured with a glass electrode and the sediment redox potential was measured using a platinum electrode and a saturated KCl calomel reference electrode (Instrulab, Mexico). The standard potential of the reference (+198) was added to the mean value to obtain the Eh of the sediment medium. Electrodes were routinely standardized in the field using a ZoBell Solution [20]. Subsequently, samples were transported to the laboratory.

Cores obtained in each sampling station were segmented in two sections (0–6 cm and 6–12 cm) under a nitrogen atmosphere. After each section was homogenized in a plastic bag using steady shaking, subsamples were immediately taken to quantify MA. The remaining sediment was maintained under low temperature to perform physical-chemical analyses.

2.3. Microbiological Analyses. Enumeration of viable MA was performed using the Most Probable Number (MPN) method by a ten-fold dilution series (10^{-1} to 10^{-10}) for each sample using four tubes per dilution. The MPN analyses included the quantification with substrates commonly used by the different groups of MA: acetate, $CO_2 + H_2$, and methanol, with the basic medium by Balch et al. [21]. Salinity in the culture medium was adjusted with a NaCl (330 g/L) solution to obtain similar values to those measured in the original sediment sample; the pH was adjusted to 7.2 with a bicarbonate (10%) solution. Cultures were incubated at 32°C for one month. Methane was detected with a GOW-MAC Series 580 GC with a thermal conductivity detector (TCD) under the following operation conditions: column, detector, and injector temperatures of 140, 190, and 170°C, respectively; 25°C/min rate; column packed with carbosphere 80/100, helium as carrier gas at 25 mL/min; polarity of 120 mA.

In order to determine the effect of sulfate on MA for a competitive substrate, methanogenic activity was determined in a medium without sulfates (sulfate-free), using 125-mL serum bottles, with 42 mL of the Balch et al. [21] and acetate as substrate to a final concentration of 20 mM. Experiments were conducted in parallel in which the culture medium was supplemented with sulfate (final concentration 20 mM). Bottles were inoculated with 8 mL of moist sediment and incubated at 32°C in the dark for 42 days; the incubations were shaken three times per week. Each experiment was run by duplicate for each sample, including the respective controls (without acetate), with and without sulfates in the medium. Mineralization was evaluated by determining changes in acetate concentration and percent methane production in bottles. For acetate analysis, 1.5 mL samples were centrifuged at 1,120 gf for 10 min. The supernatant was filtered. A 950 μL aliquot was acidified with 50 μL of HCl (2.2 M). The acetate concentration was measured by flame ionization gas chromatography (Agilent Series 6890 Plus) using an Agilent crosslinked FFAP capillary column (15 m × 0.530 mm × 1.00 μm). Column, injection port, and FID temperatures were 120, 130, and 150°C, respectively. The temperature of the column, detector, and injector were 120, 150, and 130°C, respectively. The carrier gas was N_2 (4.5 mL/min).

2.4. Physicochemical Analyses. Sediment samples were centrifuged at 1,602.76 gf at low temperature (4-5°C) for 20 minutes to separate porewater from sediments [22]. Porewater was filtered through 0.45 μm Millipore membranes and the following parameters were determined: salinity, with an optical refractometer (American Optical); sulfate [23] and total dissolved carbohydrates, with the phenol-sulfuric acid technique [24]. Total solids and volatile solids were quantified in moist sediments [25], porosity was determinate by measuring the weight loss by drying sediment samples of know volumes and weights. Organic carbon content was measured through the method by Gaudette et al. [26] in a sediment sample dried at 60°C.

2.5. Statistical Analyses. The data matrix included MA abundances and physicochemical variables. To meet the normality assumptions, data for variables were transformed through $\log x + 1$ [27]. For the temporal analysis, variables were grouped into two climate seasons (dry and rainy); for the spatial analysis, data were grouped into two depth categories (0–6 cm and 6–12 cm). An analysis of variance (ANOVA) was conducted to test for significant differences between seasons in each system, on the one hand, and between depth categories, on the other. The significance of specific differences was assessed through the Tukey-Kramer multiple comparison test [27]. A Canonical Correspondence Analysis (CCA) was used to investigate the relationship between microbial abundance and environmental variables [28]. These analyses were conducted with the Statistica 10 (Academic) and MVSP 3.12b Software.

3. Results and Discussion

The aim of this study was to analyze the changes in the abundance and activity of MA and relate these community characteristics with some physicochemical variables to propose a conceptual model of methanogenic community dynamics in coastal lagoon sediments.

TABLE 1: Environmental variables in the coastal lagoon sediments of Chantuto-Panzacola and Carretas-Pereyra, Chiapas. Mean ± Standard deviation.

Depth	Dry season		Rainy season	
	6	12	6	12
Chantuto-Panzacola				
Temperature (˚C)	29.2 ± 1.1	28.3 ± 1.3	28.1 ± 1.5	26.7 ± 1.5
Salinity (‰)	21.3 ± 6.1	18.6 ± 5.1	2.5 ± 2.5	2.8 ± 3.1
Sulphate (mM)	11.0 ± 1.8	9.8 ± 1.2	3.8 ± 1.4	2.9 ± 0.9
pH	7.1 ± 0.1	7.0 ± 0.1	6.7 ± 0.2	6.8 ± 0.1
Eh (mV)	−206 ± 76	−356 ± 34	−104 ± 4	−286 ± 53
Total Solids (TS, g/L)	445.50 ± 120.65	338.12 ± 79.11	320.79 ± 153.2	303.50 ± 151.07
Volatile Solids (VS, g/L)	42.61 ± 20.19	47.40 ± 34.86	75.82 ± 41.0	68.76 ± 51.98
Porosity (g/cm^3)	0.3 ± 0.1	0.4 ± 0.08	0.4 ± 0.1	0.4 ± 0.1
Organic matter (%)	7.2 ± 3.4	5.9 ± 3.8	9.8 ± 5.5	5.8 ± 3.2
Organic carbon (%)	4.1 ± 2.0	3.4 ± 2.2	5.7 ± 3.1	3.3 ± 1.8
Carbohydrates (mg/L)	5.6 ± 4.0	6.5 ± 4.0	5.0 ± 1.0	5.9 ± 4.1
Carretas-Pereyra				
Temperature (˚C)	29.4 ± 0.8	28.5 ± 0.7	28.5 ± 1.9	28.3 ± 0.9
Salinity (‰)	27.3 ± 5.3	23.5 ± 3.3	4.3 ± 4.08	3.2 ± 3.8
Sulphate (mM)	13.0 ± 1.4	11.7 ± 1.3	3.5 ± 1.98	1.9 ± 1.4
pH	6.9 ± 0.1	6.8 ± 0.1	6.8 ± 0.1	6.7 ± 0.1
Eh (mV)	−296 ± 83	−411 ± 66	−152 ± 46	−369 ± 99
Total Solids (TS, g/L)	261.70 ± 135.49	229.49 ± 134.29	211.56 ± 123.36	188.41 ± 97.24
Volatile Solids (VS, g/L)	75.22 ± 35.27	85.05 ± 71.58	28.40 ± 12.90	40.39 ± 22.98
Porosity (g/cm^3)	0.2 ± 0.07	0.2 ± 0.1	0.4 ± 0.1	0.5 ± 0.1
Organic matter (%)	12.5 ± 4.5	25.4 ± 19.2	10.0 ± 4.5	15.7 ± 8.8
Organic carbon (%)	7.2 ± 4.5	14.5 ± 11.02	6.1 ± 2.6	9.03 ± 5.04
Carbohydrates (mg/L)	6.8 ± 3.6	6.0 ± 3.5	3.8 ± 1.2	5.3 ± 3.5

3.1. Environmental Variables. Conditions in the sedimentary habitat in the Chantuto-Panzacola and Carretas-Pereyra lagoon systems resulted from seasonal variations between the dry and rainy seasons. Temperature in the sediment was higher in the dry season in comparison with rainy season (Table 1); the temporal variations were significant in Chantuto-Panzacola (Table 2). Significant differences in pH were observed (Table 2). In the dry season, a greater marine influence favors neutral conditions; by contrast, in the rainy season the higher fluvial inflow decreased marine influence, and acid conditions were registered (Table 1). The redox conditions were similar to those reported for sediments from mangroves [29] and were significantly less reductive in the rainy season (Table 1) when the freshwater inflow favored sediment suspension in the water column (turbidity = 126–224 NTU), with an increase in porosity and less reduced conditions at the sediments. In the dry season redox potential decreased as a result of sediment deposition (turbidity = 31–107 NTU).

The major changes were determined in salinity and sulfate content (Tables 1 and 2). Maximum values were recorded in the dry season and minimum in the rainy season; even totally freshwater conditions existed in both systems in October (0‰). The decrease in salinity and sulfates was due to an increase in fluvial inflow and precipitation. Salinity in coastal lagoons varies according to annual cycles, which depend on the local climate, continental freshwater runoff, connection with the sea, and influence of tides. Knoppers and Kjerfve [30] point out that seasonal pulses in freshwater inflow exert a marked impact on the ecology of coastal lagoons, besides controlling salinity, increasing the water level, and holding open communication to the sea.

No significant temporal variations were observed in the concentration of total solids and organic fractions (volatile solids, organic matter, organic carbon, and carbohydrates) ($P > 0.05$); and their supply was constant through rivers and wetlands. The high rate of freshwater inflow with organic debris from land and run-off as well as from adjacent mangroves is a key factor related to the contribution of organic matter in coastal zones [31].

Spatially there was no pattern of physicochemical conditions in the sedimentary habitat as evidenced by the null significance observed for the temperature, pH, salinity and sulfates ($P > 0.05$). An exception was the Eh, which decreased significantly with depth (Tables 1 and 2). The vertical fluctuations in Eh may be attributed to a reduction in the oxygen diffusion rate in porewater as the depth of the sediment column increases [32]. There were no significant variations in solids content and organic fractions ($P > 0.05$) (Table 1). However the organic carbon content was higher in the sediment layer of 12 cm, dos Santos Fonseca et al. [33] point out that this behavior seems to result from the fact

TABLE 2: Results of the ANOVA (F) and multiple comparisons analysis (MCA) (Tukey test) of environmental and microbiological variables between seasons and sediment depth in Chantuto-Panzacola and Carretas-Pereyra. P: significance. Seasons: D: dry and R: rainy. Depth: 6 cm and 12 cm.

Variables	Season			Depth		
	F	P	MCA	F	P	MCA
Chantuto-Panzacola						
Temperature (°C)	4.66	0.0421	D > R	3.75	0.0684	—
Salinity (‰)	62.03	0.0000	D > R	0.08	0.9311	—
Sulphate (mM)	109.00	0.0000	D > R	0.45	0.5349	—
pH	28.81	0.0000	D > R	0.01	0.9427	—
Eh (mV)	4.54	0.0446	D < R	38.04	0.0000	6 < 12
MA-Acetate (cells/g)	112.38	0.0000	D < R	0.01	0.7842	—
MA-Hydrogen (cells/g)	15.10	0.0008	D < R	0.05	0.8195	—
MA-Methanol (cells/g)	5.92	0.0236	D < R	3.36	0.0528	—
Activity + SO_4 (mM acetate/g VS/day)	14.71	0.0009	D > R	1.50	0.2321	—
$CH_4 + SO_4$	66.12	0.0000	D < R	0.85	0.3085	—
$CH_4 - SO_4$	4.96	0.0364	D < R	2.17	0.0831	—
Carretas-Pereyra						
Temperature (°C)	0.97	0.3344		1.28	0.2705	—
Salinity (‰)	154.47	0.0000	D > R	0.26	0.6156	—
Sulphate (mM)	210.03	0.0000	D > R	0.45	0.5101	—
pH	10.47	0.0038	D > R	1.09	0.3088	—
Eh (mV)	3.80	0.0641	—	19.80	0.0002	6 < 12
MA-Acetate (cells/g)	4.82	0.0390	D < R	0.13	0.7193	—
MA-Hydrogen (cells/g)	9.39	0.0057	D < R	0.48	0.4952	—
MA-Methanol (cells/g)	2.71	0.1142	—	1.06	0.3142	—
Activity + SO_4 (mM acetate/g VS/day)	12.62	0.0018	D > R	0.46	0.5042	—
$CH_4 + SO_4$	15.39	0.0007	D < R	6.24	0.0204	6 < 12
$CH_4 - SO_4$	7.21	0.0135	D < R	7.88	0.0103	6 < 12

that the most labile substrate is readily used by the microbial community in the top centimeters of sediment, and the refractory fraction builds up in deeper layers, where it will be degraded slowly. The presence of refractory material (wood and phytoplankton debris identified with a light microscope Zeiss Axioscop) concentrated largely in the 6–12 cm-deep layer in Pereyra and Campón lagoons seem to support this hypothesis.

3.2. Abundance and Distribution of MA. Viable MA in the sediments of Chantuto-Panzacola and Carretas-Pereyra systems were evaluated with MPN, obtaining a range of abundance between 10^4 and 10^7 cells/g. MA density reached peak levels in the rainy season, with a significant decrease of as much as two orders of magnitude during the dry season ($P < 0.05$) (Figures 2(a)–2(c)). In the rainy season, increased freshwater input created favorable conditions for MA proliferation. In this season highest levels of MA were recorded with acetate and methanol in Chantuto-Panzacola and with methanol and H_2-CO_2 in Carretas-Pereyra. During the dry season, high MA levels were obtained with methanol in both lagoon systems; the second substrate in importance

was H_2-CO_2 and the lowest levels correspond to acetate (Table 3).

The constant occurrence of MA was probably the result of their ability to use different electron donors in an ecosystem with a constant supply of organic matter provided by the rivers and run-off from adjacent mangroves. Verma et al. [34] mentioned that the continued presence of MA in coastal lagoons is possible by the presence of "noncompetitive" substrates, (methanol and methylamines), that are used exclusively by the MA, as well as the constant availability of "competitive" substrates (acetate and hydrogen), used by methanogen and other anaerobic microorganisms.

Methanol was an important substrate in both seasons, may be released from methoxy groups during degradation of lignin. Methanol-utilizing MA have a broad substrate spectrum, can also grow on acetate, growth on H_2-CO_2 is restricted to some *Methanosarcina* species [5]. There is evidence supporting the hypothesis that cometabolism of a broad range of substrates by generalist microorganisms may confer competitive advantages [35]. Purdy et al. [13] mention that, within the methanogenic community, the presence of generalist groups implies that these are better adapted to the variations in the estuarine conditions. Additionally methanol
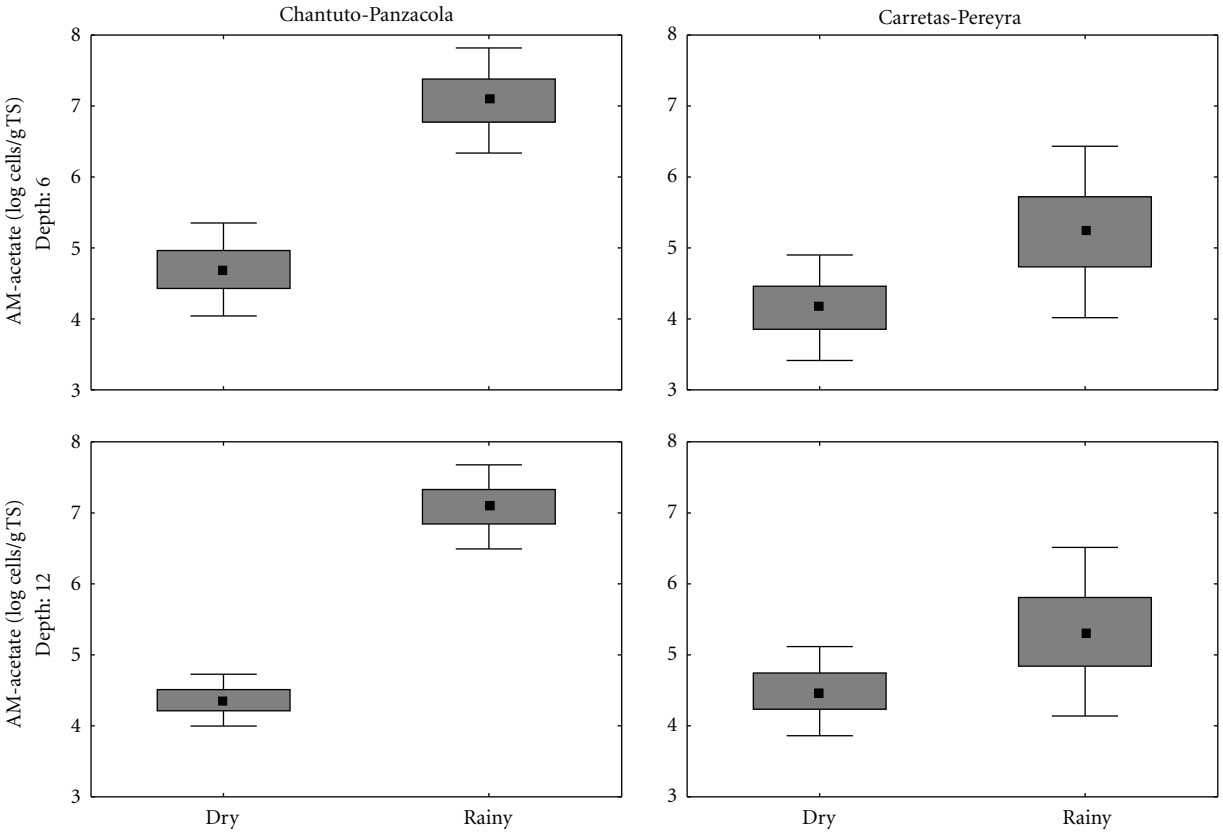
(a)
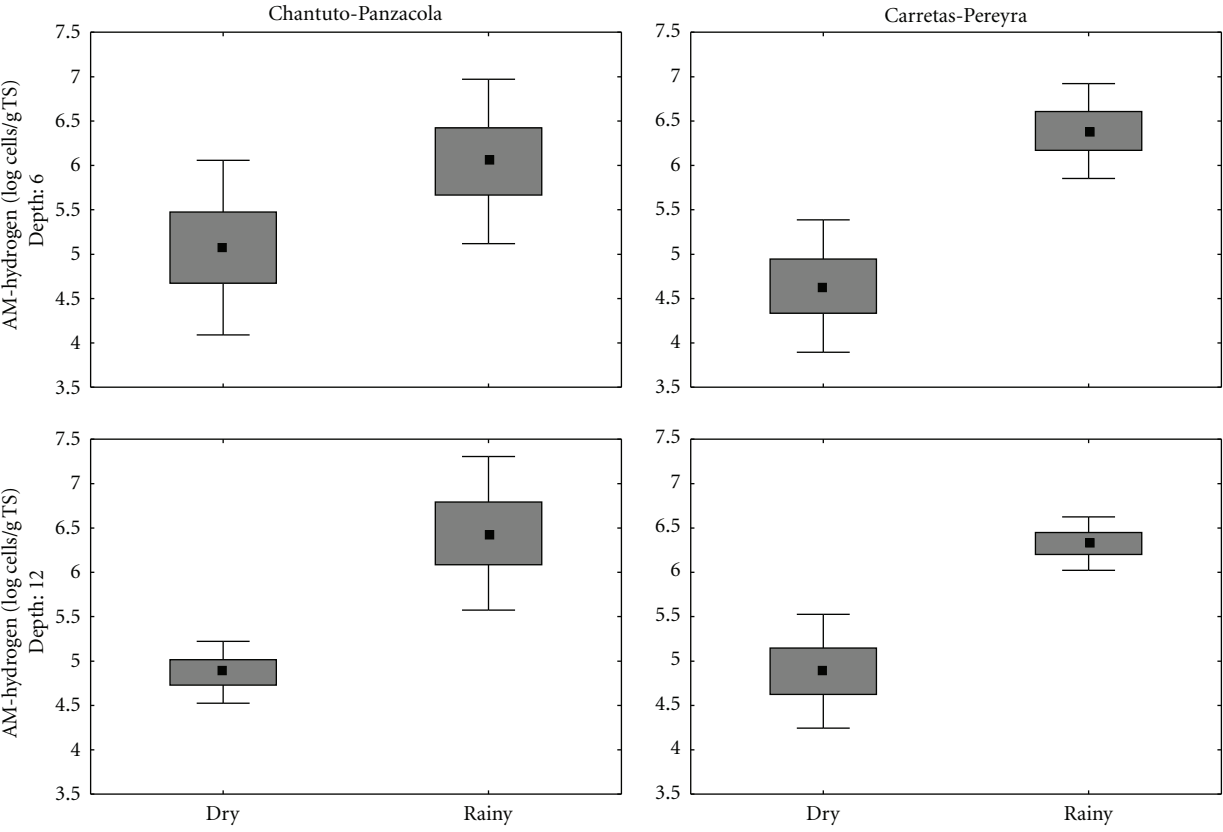
(b)

FIGURE 2: Continued.
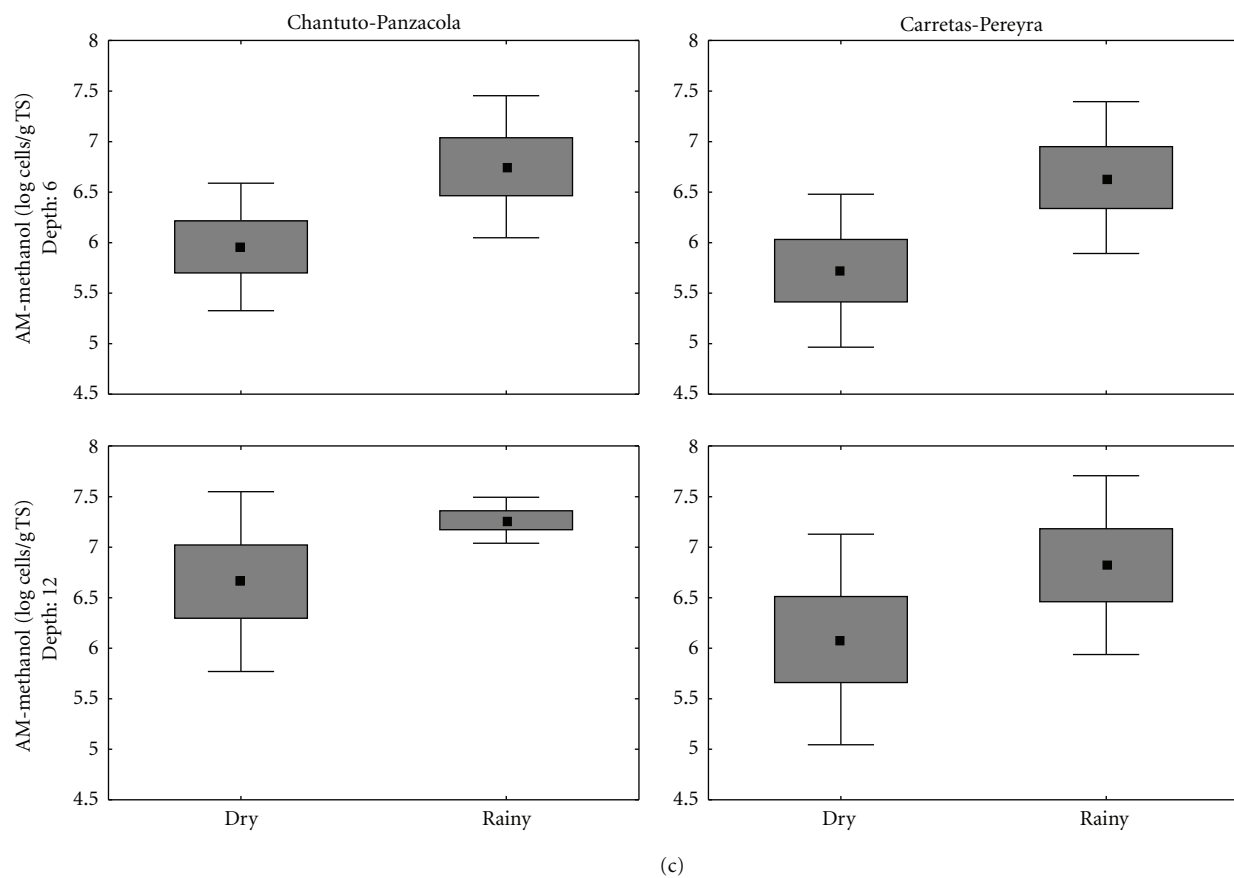
FIGURE 2: Temporal and spatial variation in the abundance of MA (log cells/g TS).

TABLE 3: Abundance of MA, acetoclastic activity, and methane production in sediments of Chantuto-Panzacola and Carretas-Pereyra, Chiapas. Mean values.

	Dry season		Rainy season	
Depth	6	12	6	12
Chantuto-Panzacola				
MA-acetate (cells/g)	1.30×10^5	2.99×10^4	2.20×10^7	2.09×10^7
MA-Hydrogen (cells/g)	1.63×10^6	9.55×10^4	9.37×10^6	8.63×10^6
MA-methanol (cells/g)	1.79×10^6	1.97×10^7	1.17×10^7	2.06×10^7
Acetate activity without SO_4^{-2} (mM acetate/g VS/day)	0.03	0.03	0.02	0.01
Acetate activity with SO_4^{-2} (mM acetate/g VS/day)	0.05	0.03	0.01	0.01
% CH_4 without SO_4^{-2}	4.81	7.91	23.50	29.73
% CH_4 with SO_4^{-2}	2.78	4.63	5.64	8.77
Carretas-Pereyra				
MA-acetate (cells/g)	4.52×10^4	6.17×10^4	1.90×10^6	1.32×10^6
MA-Hydrogen (cells/g)	1.34×10^5	1.51×10^5	4.49×10^6	2.64×10^6
MA-methanol (cells/g)	1.34×10^6	8.24×10^6	1.27×10^7	2.21×10^7
Acetate activity without SO_4^{-2} (mM acetate/g VS/day)	0.03	0.02	0.01	0.01
Acetate activity with SO_4^{-2} (mM acetate/g VS/day)	0.04	0.03	0.01	0.01
% CH_4 without SO_4^{-2}	7.83	13.01	15.42	23.47
% CH_4 with SO_4^{-2}	4.02	6.55	6.41	13.02

allows MA to maintain their populations in the presence of sulfate, which act favoring sulfate reduction. The key role of other methylated compounds was demonstrated in mangrove areas in India, where MA were quantified from methylamines [14, 15].

In the rainy season, methanol remained important, but the abundance of MA from hydrogen and acetate increased under low sulfate concentrations, hydrogen theoretically contributes 33% to total methanogenesis when carbohydrates or similar organic matter are degraded, being important in environments with high sedimentation rates ($\approx$10 cm/year) and organic carbon supplementation [36]. In the coastal lagoons studied, a high concentration of organic carbon (3.4–14.5%) was quantified, and a sedimentation rate of 6 cm/year was observed in Carretas-Pereyra. Acetate can produce approximately two thirds of total methane in freshwater sediments; however, its contribution to methane formation decreases when is consumed in other anaerobic processes as the sulfate reduction [4]. The effect of sulfate on methanogenesis was demonstrated in temperate estuaries, where the contribution of acetate for this process has been found to increase when sulfate concentration is low in freshwater zone, and the sulfate reduction decreased [7, 13]. The acetate and hydrogen are also important substrates for methanogenesis in salt marshes areas [10].

This study has revealed that acetate-utilizing and hydrogen-utilizing MA does not have a distinct vertical distribution pattern in Chantuto-Panzacola and Carretas-Pereyra sediments, whereas the methanol-based group apparently being more abundant in the 6–12 cm layer ($P = 0.05$). The presence of MA along 12 cm of sediment column seems to be a result of the availability of substrates for these microorganisms; the constant supply of different substrates favors the presence of MA at different sediment layers as also has been demonstrated in sediments of tidal flats, coastal marshes, and mangroves [8, 10, 14].

3.3. Acetoclastic Metabolic Activity. In all kinetic experiments, there was an increase in the concentration of acetate in the first days, along with other volatile fatty acids (propionate and butyrate); this pattern reveals the presence of fermentation processes in sediments. The continued presence of acetate along with other intermediaries (butyrate and propionate) is similar to that reported in other studies where methanogenesis has been assessed [37]. Acetate is an important intermediate produced during the anaerobic mineralization of organic matter, followed by propionate and other volatile fatty acids [38]. The fermentation activity is important because it releases organic substrates, such as acetate, that can be used by the MA, which cannot directly use complex organic compounds. Subsequent to the production of volatile fatty acids, acetate consumption started on day 7 in sulfate-enriched media and between days 14 and 21 in sulfate-free media. Methane production was recorded on day 21.

Acetoclastic activity in sulfate-free experiments had no significant temporary differences ($P > 0.05$) (Figures 3(a)–3(c)). The experiments with sulfate showed significant temporal fluctuations, with high values in the dry season (Table 3; Figures 3(a)–3(c)). Vertical variations did not reach statistical significance ($P > 0.05$).

Methane formation was observed in all experiments, with differences depending on the specific conditions of each medium. The addition of acetate results in an increase in methane production in relation to the amount observed in controls (no carbon supplementation).

Methane production was higher in sulfate-free media compared with sulfate-enriched media (Table 3; Figures 3(b)–3(d)). Temporal differences ($P < 0.05$) in methane production from acetate were observed in both systems. Methane levels were higher in the rainy season than in the dry season (Table 3). Significant vertical changes ($P < 0.05$) were observed only in Carretas-Pereyra: a lower production in the upper 6 cm and a higher methane production in the 6–12 cm layer (Table 3, Figures 3(b)–3(d)).

The presence of sulfate in the culture media influenced methanogenic activity. In the sulfate-free experiments a peak of acetoclastic activity was observed coupled with a rise in methane production in sediments during the rainy season and in the deep layer, suggesting that methanogenesis was favored. Studies demonstrated that potential methanogenesis from acetate was higher in the absence of sulfates [37]. By contrast, the addition of sulfate resulted in an increase of acetoclastic activity in the dry months and in the upper sediment layer, and methane production declined. In sediments of coastal lagoons and mangrove areas in India, an increase in the production and emission of methane was determined in freshwater areas compared to brackish regions. Also, methane emissions were higher in the postmonsoon season, when salinity and sulfate concentration were lower [16, 34].

3.4. Environmental Variables and MA. The correlation coefficients between environmental variables and ordination axes (interset correlation) obtained by CCA denote the relative importance of each environmental variable in the distribution of the methanogenic community. For Chantuto-Panzacola, the MA-environment correlation was 0.92 corresponded to a salinity-sulfate gradient and 0.60 for pH. CCA results for Carretas-Pereyra showed a correlation of 0.74 for pH and volatile solids, and 0.43 for volatile solids. The ordination diagram obtained by CCA showed a change in the structure of the methanogenic community with regard to certain environmental variables (Figure 4). The first axis accounted for 65.62% of total variance in Chantuto-Panzacola, corresponding to a salinity-sulfate gradient (Figure 4(a)). In the right side of the diagram, those sites with the highest sulfate concentration, temperature, and pH (dry season) were grouped, in these conditions methanol-utilizing MA were abundant. The left side of the plot-grouped sites with highest total solids content where hydrogen-utilizing MA prospered, whereas acetate-utilizing MA abound in sites with a higher porosity and less reduced conditions (Figure 4(a)). In Carretas-Pereyra, to the plot's upper left side, the first axis accounted for 29.08% of variance and salinity-sulfate, Eh and organic carbon concentration were all correlated with hydrogen-utilizing MA abundance, mainly during the rainy season. Abundance of methanol-utilizing

(a)

(b)
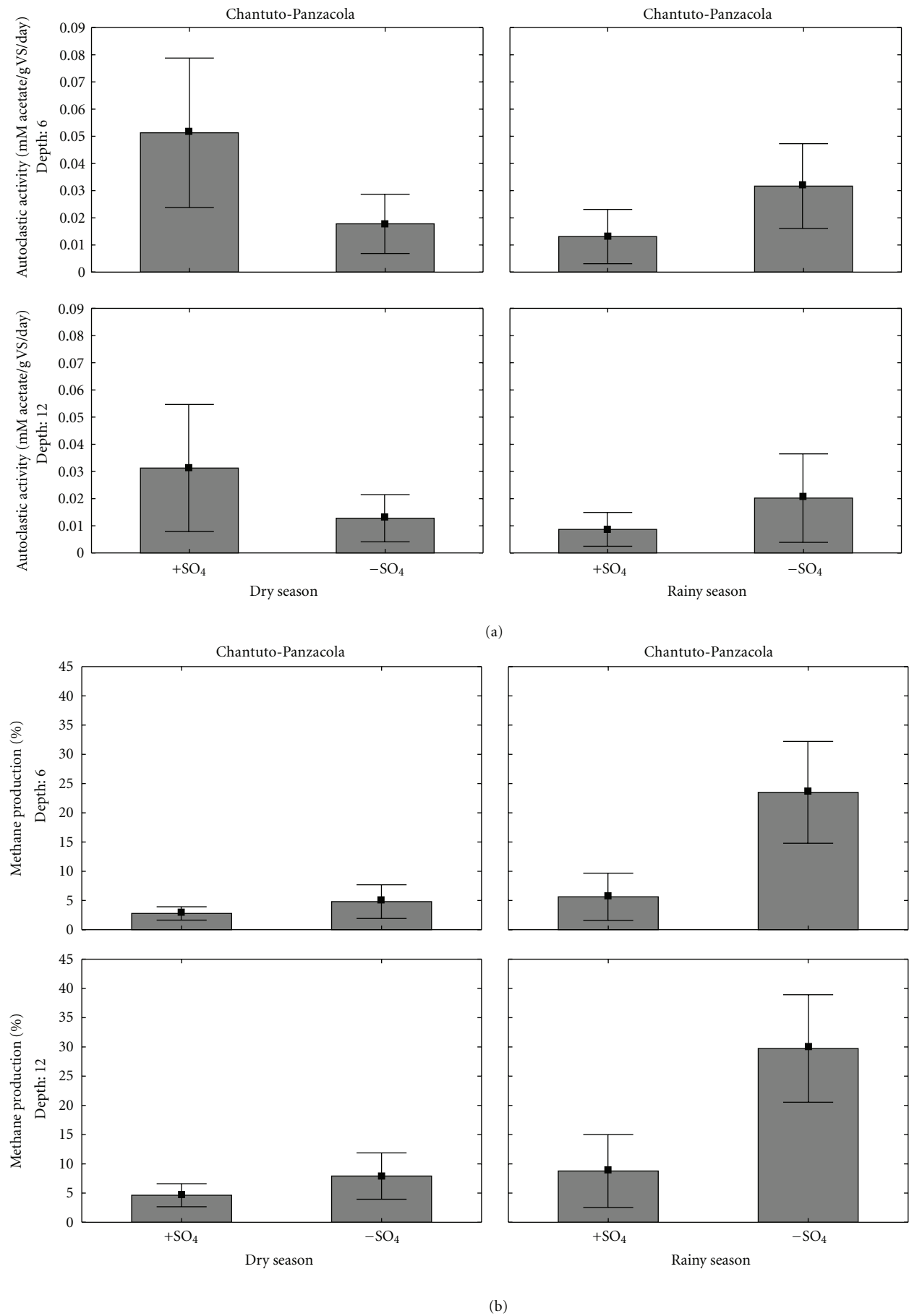
FIGURE 3: Continued.

(c)

(d)
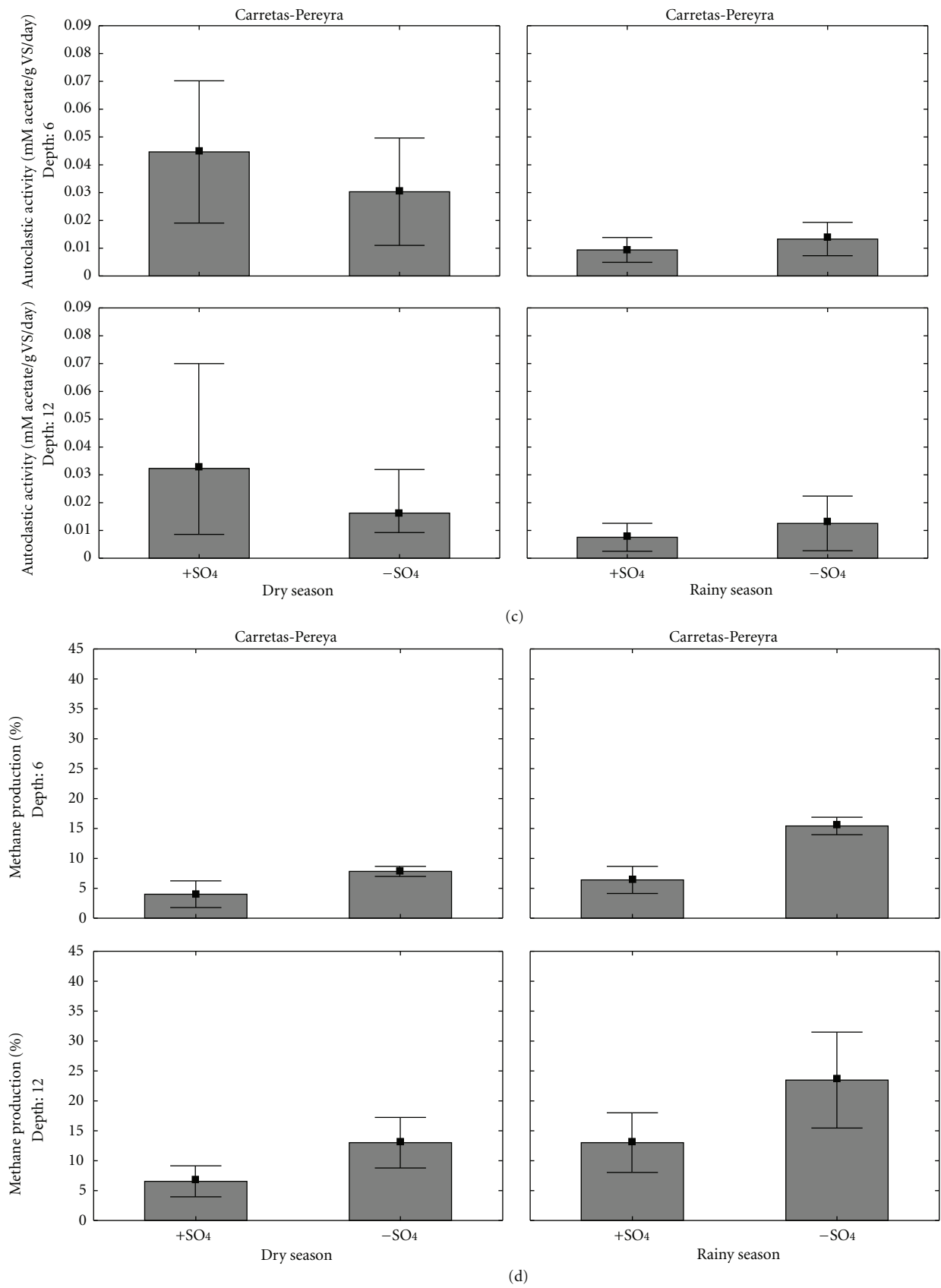
Figure 3: Temporal and spatial variations of acetoclastic activity and methane production in Chantuto-Panzacola (a, b) and Carretas-Pereyra (c, d).
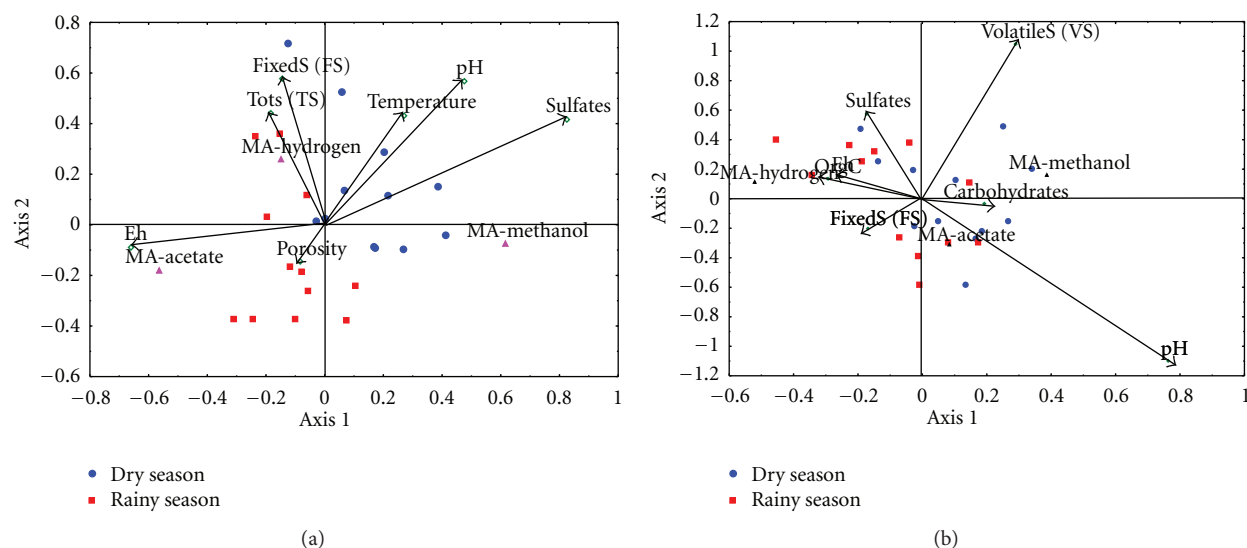
FIGURE 4: Relationship between environmental variables and methanogenic community in Chantuto-Panzacola (a) and Carretas-Pereyra (b).
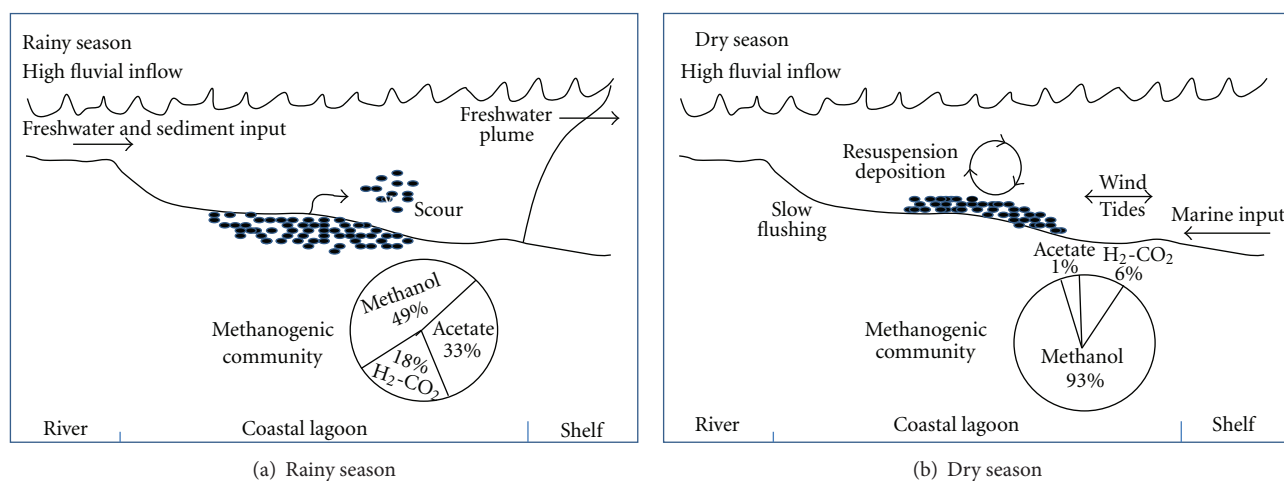
FIGURE 5: Conceptual model on MA dynamics in sediments for tropical coastal lagoons.

MA was correlated with volatile solids during the dry season and acetate-utilizing MA prospered in a pH gradient in both seasons.

The presence of sulfate significantly influenced the abundance of MA in both systems. In sulfate-rich conditions the anaerobic process that is most favored is the sulfate reduction. Elevated levels of SRP in the dry season (10^8–10^{10} cells/g) and decrease in the rainy season (10^5–10^7 cells/g) quantified in coastal lagoons studied support this hypothesis [39]. The relationship between MA and sulfate content is consistent with knowledge on these communities in sediments of temperate estuaries, tropical coastal lagoons, coastal marshes, and mangroves [7–10, 13, 14, 16].

The temperature, pH, Eh, and organic fractions were other variables contributing to the presence of MA. In this study the bacteria grew in a temperature range of 26.7–29.4°C, the optimum temperature reported for the development of methanogens is 30–32°C in tropical wetlands, whereas in mangrove sediments MA have been observed at temperature ranges between 26 and 30°C [14, 15]. The pH conditions (6.7–7.1) were favorable for methanogenic community. Mohanraju and Natarajan [15] associated the presence of MA with pH values of 6.6–7.2 in mangrove sediments, whereas in coastal marshes sediments MA were recorded in pH ranges of 6.1–7.5 [10]. The reducing (−100 to +100 mV) and highly reducing (−300 to −100 mV) characteristics of sediment also contributed to MA development, these have been reported at levels from Eh below −150 mV in coastal marshes [40].

4. Conclusions

The MA was a constant component involved in anaerobic mineralization of organic matter in the sediments of the

coastal systems Chantuto-Panzacola and Carretas-Pereyra. Their populations were active by its ability to utilize different substrates, especially methanol. In these ecosystems, changes in precipitation and its influence on fluvial inputs significantly impacted salinity and sulfate content, which was the main factor regulating the temporal dynamics of methanogenic community. In the rainy season, the increase in river inflow to lagoons produces freshwater conditions, low sulfate concentrations, sediment resuspension, and less reducing redox potentials. The environmental characteristics that prevail in this season lead to an increase in MA abundance, with the following decreasing rank by substrate: methanol > H_2-CO_2 > acetate (Figure 5(a)). Methanogenic activity from acetate is higher and results in a rise in methane production. The peak of methanogenic activity in the rainy season suggests that these ecosystems may be an important source of atmospheric CH_4 and CO_2 in this season. In the dry season, the freshwater inflow declines and salinity, sulfate, and inorganic solids content increases, along with more negative redox conditions. In this conditions a lower MA density was observed (Figure 5(b)), with the following order by substrate: methanol > acetate > H_2-CO_2. Our hypothesis is that this mechanism is cyclic and is controlled by changes associated to the seasonal fluctuations in fluvial inflow and precipitation. We considered that this model could be applied to other coastal lagoons and wetlands (mangroves) in tropical latitudes, characterized by a high organic matter concentration and a permanent river discharge, with significant seasonal variations in discharge volume. These characteristics favor the continued presence of the MA in tropical coastal systems and control their temporal dynamics. In estuaries, the absence of barriers that restrict communication with the sea difficult to apply this model because the tidal influence decreases the impact of freshwater input. In these systems the freshwater influence is more important at spatial level.

Conflict of Interests

Authors of the paper have no conflict of interests with Millipore, Statistica 10 (Academic) and MVSP (3.12b Software). The authors do not have any association with Millipore or companies who designed Statistica 10 (Academic) and MVSP (3.12b Software).

Acknowledgment

References

[1] B. B. Jørgensen, "Mineralization of organic matter in the sea bed—the role of sulphate reduction," *Nature*, vol. 296, no. 5858, pp. 643–645, 1982.

[2] M. Fukui, J. Suh, Y. Yonezawa, and Y. Urushigawa, "Major substrates for microbial sulfate reduction in the sediments of Ise Bay, Japan," *Ecological Research*, vol. 12, no. 2, pp. 201–209, 1997.

[3] D. Marty, P. Bonin, V. Michotey, and M. Bianchi, "Bacterial biogas production in coastal systems affected by freshwater inputs," *Continental Shelf Research*, vol. 21, no. 18-19, pp. 2105–2115, 2001.

[4] D. E. Canfield, E. Kristensen, and B. Thamdrup, "The methane cycle," in *Advances in Marine Biology. Aquatic Geomicrobiology*, A. Southward, P. A. Tyler, C. M. Young, and L. A. Fuiman, Eds., vol. 48, chapter 10, pp. 383–418, Elsevier, London, UK, 2005.

[5] R. K. Thauer, A. K. Kaster, H. Seedorf, W. Buckel, and R. Hedderich, "Methanogenic archaea: ecologically relevant differences in energy conservation," *Nature Reviews Microbiology*, vol. 6, no. 8, pp. 579–591, 2008.

[6] K. Zepp Falz, C. Holliger, R. Großkopf et al., "Vertical distribution of methanogens in the anoxic sediment of Rotsee (Switzerland)," *Applied and Environmental Microbiology*, vol. 65, no. 6, pp. 2402–2408, 1999.

[7] K. J. Purdy, M. A. Munson, D. B. Nedwell, and T. M. Embley, "Comparison of the molecular diversity of the methanogenic community at the brackish and marine ends of a UK estuary," *FEMS Microbiology Ecology*, vol. 39, no. 1, pp. 17–21, 2002.

[8] R. Wilms, H. Sass, B. Köpke, J. Köster, H. Cypionka, and B. Engelen, "Specific Bacterial, Archaeal, and Eukaryotic communities in tidal-flat sediments along a vertical profile of several meters," *Applied and Environmental Microbiology*, vol. 72, no. 4, pp. 2756–2764, 2006.

[9] M. J. Franklin, J. W. William, and W. B. Whitman, "Populations of methanogenic bacteria in a Georgia salt marsh," *Applied and Environmental Microbiology*, vol. 54, no. 5, pp. 1151–1157, 1988.

[10] M. A. Munson, D. B. Nedwell, and T. M. Embley, "Phylogenetic diversity of Archaea in sediment samples from a coastal salt marsh," *Applied and Environmental Microbiology*, vol. 63, no. 12, pp. 4729–4733, 1997.

[11] R. Segers and S. W. M. Kengen, "Methane production as a function of anaerobic carbon mineralization: a process model," *Soil Biology and Biochemistry*, vol. 30, no. 8-9, pp. 1107–1117, 1998.

[12] S. Takii and M. Fukui, "Relative importance of methanogenesis, sulfate reduction and denitrification in sediments of the lower Tama river," *Bulletin of Japanese Society of Microbial Ecology*, vol. 6, no. 1, pp. 9–17, 1991.

[13] K. J. Purdy, M. A. Munson, T. Cresswell-Maynard, D. B. Nedwell, and T. M. Embley, "Use of 16S rRNA-targeted oligonucleotide probes to investigate function and phylogeny of sulphate-reducing bacteria and methanogenic archaea in a UK estuary," *FEMS Microbiology Ecology*, vol. 44, no. 3, pp. 361–371, 2003.

[14] T. Ramamurthy, R. Mohanraju, and R. Natarajan, "Distribution and ecology of methanogenic bacteria in mangrove sediments of Pitchavaram, east coast of India," *Indian Journal of Marine Sciences*, vol. 19, no. 4, pp. 269–273, 1990.

[15] R. Mohanraju and R. Natarajan, "Methanogenic bacteria in mangrove sediments," *Hydrobiologia*, vol. 247, no. 1–3, pp. 187–193, 1992.

[16] H. Biswas, S. K. Mukhopadhyay, S. Sen, and T. K. Jana, "Spatial and temporal patterns of methane dynamics in the tropical mangrove dominated estuary, NE coast of Bay of Bengal, India," *Journal of Marine Systems*, vol. 68, no. 1-2, pp. 55–64, 2007.

[17] INE-SEMARNAP, *Programa de Manejo Reserva de la Biósfera La Encrucijada*, Instituto Nacional de Ecología-Secretaría del Medio Ambiente, Recursos Naturales y, Pesca, Mexico, 1999.

[18] F. J. Flores-Verdugo, F. González-Farías, D. S. Zamorano, and P. Ramírez-García, "Mangrove ecosystems of the Pacific Coast of Mexico: distribution, structure, litter fall, and detritus dynamics," in *Coastal Plant Communities of Latin America*, U. Seliger, Ed., vol. 17, pp. 269–288, Academic Press, New York, NY, USA, 1992.

[19] F. J. Flores-Verdugo, G. de la Lanza-Espino, F. Contreras-Espinosa, and C. M. Agraz-Hernández, "The tropical Pacific Coast of Mexico," in *Coastal Marine Ecosystems of Latin American, Ecological Studies*, U. Seliger and B. Kjerve, Eds., vol. 144, pp. 307–314, Springer, Berlin, Germany, 2001.

[20] D. Langmuir, "Eh-pH determination," in *Proceedings Sediments and Petrology*, R. E. Conver, Ed., p. 653, Wiley-Interscience, New York, NY, USA, 1971.

[21] W. E. Balch, G. E. Fox, L. J. Magrum, C. R. Woese, and R. S. Wolfe, "Methanogens: reevaluation of a unique biological group," *Microbiological Reviews*, vol. 43, no. 2, pp. 260–296, 1979.

[22] B. L. Howes, "Effects of sampling technique on measurements of porewater constituents in salt marsh sediments," *Limnology and Oceanography*, vol. 30, no. 1, pp. 221–227, 1985.

[23] R. W. Howarth, "A rapid and precise method for determining sulfate in seawater, estuarine waters, and sediment pore waters," *Limnology and Oceanography*, vol. 23, no. 5, pp. 1066–1069, 1978.

[24] M. Dubois, K. A. Gilles, J. K. Hamilton, P. A. Rebers, and F. Smith, "Colorimetric method for determination of sugars and related substances," *Analytical Chemistry*, vol. 28, no. 3, pp. 350–356, 1956.

[25] APHA, AWWA, and WPCF, Eds., *Standard Methods For the Examination of Water and Wastewater*, American Public Health Association, American Water Works Association and Water Pollution Control Federation, Washington, DC, USA, 2005.

[26] H. Gaudette, W. Fligh, L. Toner, and D. Folger, "An inexpensive titration method for the determination of organic carbon in recent sediments," *Journal of Sediments and Petrology*, vol. 44, no. 1, pp. 249–253, 1974.

[27] J. H. Zar, *Bioestatistical Analysis*, Prentice Hall, New York, NY, USA, 1999.

[28] C. J. F. Ter Braak, "Canonical correspondence analysis: a new eigenvector technique for multivariate direct gradient analysis," *Ecology*, vol. 67, no. 5, pp. 1167–1179, 1986.

[29] E. Lallier-Vergès, B. P. Perrussel, J. R. Disnar, and F. Baltzer, "Relationships between environmental conditions and the diagenetic evolution of organic matter derived from higher plants in a modern mangrove swamp system (Guadeloupe, French West Indies)," *Organic Geochemistry*, vol. 29, no. 5–7, pp. 1663–1686, 1998.

[30] B. Knoppers and B. Kjerfve, "Coastal lagoons of Southeastern Brazil: physical and biogeochemical characteristics," in *Estuaries of South America*, G. M. E. Perillo, M. C. Piccolo, and M. Pino-Quivira, Eds., pp. 35–66, Springer, New York, NY, USA, 1997.

[31] M. R. Preston and P. Prodduturu, "Tidal variations of particulate carbohydrates in the Mersey estuary," *Estuarine, Coastal and Shelf Science*, vol. 34, no. 1, pp. 37–48, 1992.

[32] R. W. Howarth, "Microbial processes in salt-marsh sediments," in *Aquatic Microbiology*, T. E. Ford, Ed., pp. 239–260, Blackwell Scientific Publications, Boston, Mass, USA, 1993.

[33] A. L. dos Santos Fonseca, M. Minello, C. Cardoso Marinho, and F. de Assis Esteves, "Methane concentration in water column and in pore water of a coastal lagoon (Cabiúnas Lagoon, Macaé, RJ, Brazil)," *Brazilian Archives of Biology and Technology*, vol. 47, no. 2, pp. 301–308, 2004.

[34] A. Verma, V. Subramanian, and R. Ramesh, "Methane emissions from a coastal lagoon: vembanad Lake, West Coast, India," *Chemosphere*, vol. 47, no. 8, pp. 883–889, 2002.

[35] T. Egli, "The ecological and physiological significance of the growth of heterotrophic microorganisms with mixtures of substrates," in *Advances in Microbial Ecology*, J. Gwynfryn, Ed., vol. 14, pp. 305–386, Plenum Press, New York, NY, USA, 1995.

[36] R. Conrad, "Contribution of hydrogen to methane production and control of hydrogen concentrations in methanogenic soils and sediments," *FEMS Microbiology Ecology*, vol. 28, no. 3, pp. 193–202, 1999.

[37] M. Holmer and E. Kristensen, "Coexistence of sulfate reduction and methane production in an organic-rich sediment," *Marine Ecology Progress Series*, vol. 107, no. 1-2, pp. 177–184, 1994.

[38] H. T. S. Boschker, W. de Graaf, M. Köster, L. A. Meyer-Reil, and T. E. Cappenberg, "Bacterial populations and processes involved in acetate and propionate consumption in anoxic brackish sediment," *FEMS Microbiology Ecology*, vol. 35, no. 1, pp. 97–103, 2001.

[39] M. R. Torres-Alvarado, *Determinación de la diversidad y actividad bacteriana sulfatorreductora y metanogénica en los sedimentos de dos ecosistemas estuarino-lagunares del Estado de Chiapas [Ph.D. thesis]*, Universidad Autónoma Metropolitana-Iztapalapa, México, Mexico, 2009.

[40] H. K. Kludze and R. D. DeLaune, "Methane emissions and growth of Spartina patens in response to soil redox intensity," *Soil Science Society of America Journal*, vol. 58, no. 6, pp. 1838–1845, 1994.

Review Article

Archaea in Symbioses

Christoph Wrede,[1,2] **Anne Dreier,**[1,3] **Sebastian Kokoschka,**[1] **and Michael Hoppert**[1,3]

[1] *Institute of Microbiology and Genetics, Georg-August-Universität Göttingen, Grisebachstraße 8, 37077 Göttingen, Germany*
[2] *Hannover Medical School, Institute of Functional and Applied Anatomy, Carl-Neuberg-Straße 1, 30625 Hannover, Germany*
[3] *Courant Centre Geobiology, Georg-August-Universität Göttingen, Goldschmidtstraße 3, 37077 Göttingen, Germany*

Correspondence should be addressed to Anne Dreier, anne.dreier@gmx.de

During the last few years, the analysis of microbial diversity in various habitats greatly increased our knowledge on the kingdom Archaea. At the same time, we became aware of the multiple ways in which Archaea may interact with each other and with organisms of other kingdoms. The large group of euryarchaeal methanogens and their methane oxidizing relatives, in particular, take part in essential steps of the global methane cycle. Both of these processes, which are in reverse to each other, are partially conducted in a symbiotic interaction with different partners, either ciliates and xylophagous animals or sulfate reducing bacteria. Other symbiotic interactions are mostly of unknown ecological significance but depend on highly specific mechanisms. This paper will give an overview on interactions between Archaea and other organisms and will point out the ecological relevance of these symbiotic processes, as long as these have been already recognized.

1. Introduction
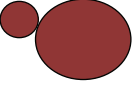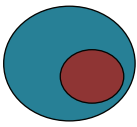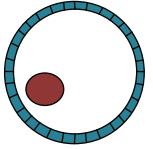
Symbiotic interactions between various groups of prokaryotes as well as between prokaryotes and eukaryotic organisms were one essential driving force of evolution, including the development of differentiated tissues in multicellular organisms [1]. Apart from the essential key events of endosymbiosis, leading to mitochondria and chloroplasts, a multitude of symbiotic interactions at various levels is an ongoing process [2]. Interestingly, most of these interactions are contributed by Bacteria, frequently by Proteobacteria [3]. Regarding parasitic or pathogenic interactions in particular, the outer envelope of the bacterial cell mediates highly specific contact to its host. Surface structures like pili, lipopolysaccharides, and outer membrane proteins may rapidly adapt to modified host tissue structures, mainly with respect to deleterious host-pathogen interactions [4]. How about Archaea? Up to now, no clearly identifiable pathogenic interactions between an Archaeon and its host have been detected, though some archaeal commensals may be indirectly involved in bacterial infections [5]. On the other hand, mutualistic symbioses have been well described, some of them with high relevance to global environmental cycles

[6]. Here we will present a short overview on interaction mechanisms known so far and relevant symbioses between Archaea and other organisms. We use the term symbiosis here in a broader sense (see Table 1); in most if not all cases the benefit of both interaction partners could not be proven, though none of these interactions appeared to be detrimental for one of the partners [7].

2. Mechanisms for Interaction with Host Cells

Apart from vertically transmitted endosymbionts, any interaction between host and symbiont depends on the surface-surface recognition. A variety of proteinaceous and polysaccharide-based surface structures are known to be involved. Surface layers are common in all Archaean groups known so far. Though their function in adhesion is up to now poorly understood, it may be expected that in particular the glycosylated surface layers are involved in adhesion. In fact, like in Bacteria, extracellular polysaccharides are known as adhesive matrix for biofilm formation [8]. As it has been described for Bacteria, filamentous protein appendages are important for adhesion of Archaean cells. Some of them appear to be unique for particular phylotypes, like the hami,

Table 1: Some examples for symbioses between Archaea and other organisms (red Archaea, green Bacteria, blue-unicellular Eukarya, and metazoans).

Symbiotic partners	Examples	Interaction	Key features
Archaeon-Archaeon	*Ignicoccus hospitalis/Nanoarchaeum equitans*	Cell-cell contact	Transfer of essential biological macromolecules from host to symbiont
Archaea-Bacteria	SM1/*Thiothrix*	Cell appendages	Sulfur redox cycling?
	ANME-Archaea/sulfate reducing Bacteria	Cell-cell contact/ no direct contact	Anaerobic methane oxidation coupled to sulfate reduction
Archaea-unicellular Eukarya	Methanogenic Archaea/Ciliates, Archamoebae	Endosymbiotic	Methanogen/hydrogenosome association, transfer of hydrogen, and/or C_1/C_2 compounds
Archaea-metazoans	Porifera-associated Thaumarchaeota	Tissue associated	Ammonia oxidation
	Diverse associations between insect and vertebrate guts	Gut microbial communities	Methanogens as a terminal part of the anaerobic food chain

highly complex proteinaceous appendages appearing like hooks. These structures are supposedly involved in the formation of a tight biofilm consisting of the euryarchaeon SM1 and a filamentous *Thiothrix*-related sulfur-oxidizing proteobacterium [9, 10] and seem to be unrelated to any other known surface appendage. Remarkably, the filamentous protein assembly ends up in a terminal hook. In addition, short prickles branch from the main filament. Though it is not known in which way interaction at the molecular level may work, a tight binding of the cells to each other and to various surfaces was shown. The filaments and an exopolysaccharide supposedly excreted by the Archaeon provide the matrix for the formation of a tight consortium between the Archaeon and the sulfur oxidizer. The shape of the consortia may vary but exhibit sort of a "string of pearl" appearance. Each pearl is in the millimeter order of magnitude and is colonized by cells of the anaerobic SM1 Archaeon in the core and a shell of the aerobic sulfur oxidizer. SM1-related sequences have been detected in low saline sulfidic water worldwide, thus a certain ecological significance is likely. The tight association is beneficial for both symbiotic partners when the Archaeon uses the sulfate generated by the sulfur oxidizes for dissimilatory sulfate reduction. The *Thiothrix* "shell" will provide anoxic conditions inside the consortium [11].

In this context another apparently unique surface structure should be mentioned. Though not involved in symbiotic interaction, hollow tubes (cannulae) composed of glycoproteins interconnect the cells of the hyperthermophilic *Pyrodictium occultum* [12]. Another uncommon structure has been described recently by cryoelectron microscopy of a microbial biofilm [13]. Cells of a member of the archaeal

group Thermoplasmatales form protuberances penetrating cells of the ultrasmall archaeal Richmond mine acidophilic organism (ARMAN).

In addition to these unique structures, interaction is frequently brought about by appendages that are also common to Bacteria. Several pilus types involved in recognition of and attachment to surfaces have been detected in Bacteria so far [4]. Yet, by far most of the archaeal pili have similarities to just the bacterial type IV pilin. Intriguingly, the archaeal flagellin is homologous to the bacterial pilin protein. The archaeal rotating flagellum is homologous to the bacterial type IV pilus secretion apparatus. Consequently, no homologies between the bacterial flagellar genes and archaeal sequences could be detected up to now [14, 15]. Also the genes of the machinery for pilus assembly have been detected in the archaeal genomes. The involvement of the appendages in attachment may differ in various groups. The flagella of *Pyrococcus furiosus* are probably motility organelles, but are also important for biofilm formation and surface attachment [16]. Flagella and pili are also necessary for the aggregate formation and surface adherence of *Sulfolobus solfataricus* [17]. As in bacteria, the pili are responsible for primary adhesion on surfaces and initiate biofilm formation. The environmental conditions for biofilm formation have been extensively studied for several *Sulfolobus* strains. Basically, temperature, pH, and iron concentrations, which are also relevant in the natural (hot spring) habitat, strongly influence biofilm development. In particular, pH and iron concentration may synergistically act on biofilm development, but in different ways in various *Sulfolobus* strains [18]. In an artificial archaeal biofilm formed by *Pyrococcus furiosus* and *Methanopyrus kandleri*,

the latter adheres to the surface (mica, glass, and others), whereas *Pyrococcus* adheres to *Methanopyrus* via flagella and/or direct contact between cells [19]. *Haloferax volcanii* uses nonmotile pili for surface attachment [20].

Pili are also involved in interactions between the Archaea and eukaryote hosts. *Methanobrevibacter*'s polar pilus-like fibers are responsible for the attachment of cells to the hindgut epithelium cuticle of the termite *Reticulitermes flavipes* [21].

Generally, a dual nature of cellular appendages (motility and attachment) is not uncommon and has been also repeatedly described for Bacteria [22, 23]. This feature is also true among Archaea, as the mentioned examples may illustrate. However, some types of cellular appendages have not been detected in Archaea. The type III secretion system (TTSS), in particular, is the essential export mechanism for bacterial flagellins and is also an important pathogenicity factor. Specific bacterial proteins are delivered to a eukaryote host after recognition by the TTSS via a hollow channel. This very specific interaction to eukaryotes may have been developed at a time in evolution, when specific signaling between pathogens and multicellular eukaryotes was evolutionary useful [24].

3. Archaeon-Archaeon Interaction

The symbiosis between the host *Ignicoccus hospitalis* and *Nanoarchaeum equitans* is well described at the structural level. *Ignicoccus*, (Desulfurococcales, Crenarchaeota) is an anaerobic, hyperthermophilic obligate chemolithoautotrophic hydrogen oxidizing Archaeon. Interestingly, cells belonging to the genus *Ignicoccus* are surrounded by a dual membrane, which appears to be a similarity to most Bacteria. However, the archaeal "outer membrane" is distinct from the composition of the known bacterial outer membranes. Most interestingly, the outer membrane of *Ignicoccus* hosts the H_2: sulfur oxidoreductase and ATPase protein complexes, that is, membrane energization takes place at this membrane and not at the inner (normally referred to as cytoplasmic) membrane as it is common in all Bacteria with a double membrane cell envelope [25]. Typical porins, homologous to those in bacterial outer membranes, are missing, which also implies that the *Ignicoccus* outer membrane is not homologous to the outer membrane of Bacteria. Instead, in *Ignicoccus hospitalis*, a unique pore-forming complex (Ihomp1) consists of nine monomers of a small unique alpha-helical protein [26]; other membrane proteins appear to be involved in the *Ignicoccus/Nanoarchaeum* symbiosis as well [27]. The symbiont *Nanoarchaeum equitans* depends obligately on the *Ignicoccus* host. The *Nanoarchaeum* cells are directly attached to the outer membrane of *Ignicoccus*. The extremely reduced genome (490 Kbp) lacks genes for essential biosynthetic pathways, such as lipid, amino acid, and nucleotide biosynthesis. Thus biological macromolecules must be provided by the *Ignicoccus* host; even transfer of ATP from host to symbiont has been discussed [28].

The relationship between *Ignicoccus* and *Nanoarchaeum* does not appear to be a true mutalistic symbiosis: though the growth parameters of either infected or uninfected

Igni-coccus cultures (containing infected cells of different degrees and uninfected cells) are the same, attached *Nanoarchaeum* cells significantly reduce the ability of *Ignicoccus* to reproduce [29].

Up to now, direct interactions between two archaeal partners appear to be extremely rare. Other species of the genus *Ignicoccus* are free living and could not be infected with the *Nanoarchaeum equitans* symbiont [29]. Though it is unlikely that interactions within the kingdom of Archaea are an exception, it has to be taken into account that interactions between largely unculturable organisms are difficult to detect. In an artificial binary biofilm between *Pyrococcus furiosus* and *Methanopyrus kandleri* hydrogen produced by *Pyrococcus* is utilized by *Methanopyrus*, which implies that mutualistic benefits may lead to stable aggregations between Archaea [18]. Upcoming in situ techniques may uncover interactions between Archaea in the near future [13].

4. Archaea-Bacteria Interactions

Under anaerobic conditions, organic compounds are degraded by the anaerobic food chain whereby the product of one group serves as a substrate for the next group within this chain. Methanogenic Archaea terminate the chain by degrading C_1 and C_2 substrates to methane and carbon dioxide.

The conversion of higher organic acids to acetate and hydrogen is endergonic, unless the hydrogen partial pressure is kept low. This may be achieved by the activity of hydrogenotrophic methanogens. This necessary coupling of hydrogen formation and uptake by syntrophic microbial consortia is termed "interspecies hydrogen transfer." A well-known consortium, "*Methanobacillus omelianskii*," was isolated several times from anaerobic sediments and sewage sludge and was regarded as a pure culture of an anaerobe converting ethanol to acetate and methane [30]. In fact, the culture consisted of a methanogenic archaeon and a Gram-negative Bacterium [31, 32]. Since then a multitude of syntrophic associations have been described, for example, with the fermentative *Acetobacterium* or *Syntrophobacter* [33, 34], with *Desulfovibrio* under low sulfate concentrations [35], but also under thermophilic conditions with *Thermoanaerobacter*, *Desulfotomaculum*, and *Pelotomaculum* [36–38] and with hydrogenotrophic methanogens as syntrophic partners. These examples show the diversity of interactions with respect to organisms and metabolic properties. Though stable aggregates and specific interactions between the syntrophic partners have been observed [39], syntrophy in interspecies hydrogen transfer is generally highly variable and may depend on the availability of substrates [40].

An important process of methane oxidation in anoxic sediments is conducted by consortia of Euryarchaeota and sulfate reducing Bacteria (SRB). The anaerobic oxidation of methane (AOM) has been first postulated by Reeburgh [41]. Up to 90% of methane produced in marine sediments is anaerobically oxidized [42], which makes AOM to an essential process in global methane turnover. However, quantitative modeling based on existing data of the few sampling sites at the ocean floor is still difficult and

the contribution of the process to global methane cycling is still a matter of debate [43]. In ocean systems, methane is either generated by methanogenesis in sediments, or abiotically by serpentinization, and may derive from methane hydrates and fossil reservoirs. In cases of high methane fluxes from large reservoirs, the AOM is usually associated with the precipitation of carbonates and sulfides. This has been particularly observed at sites of intense methane seepage, such as marine mud volcanoes and cold methane seeps; also fossil seeps were identified [44–46]. These precipitates are mostly found in sediments as carbonate-cemented plates or large tabular constructions, but also as grapestone-like concretions or even as giant columnar structures, up to several tens of meters in height, buried in the sediment [47–49]. Under anaerobic conditions, below the chemocline of anoxic ocean basins, these precipitates may form tower-like constructions in the water column, reaching several meters in height [50–52]. In most cases, tube-like or columnar towers exhibit cavities that are perfused by methane and seawater. The inner faces of these concretions are covered by remarkably complex biofilms [53–55], dominated by various representatives of the ANME Archaea (ANME: anaerobic methanotroph). The three known ANME groups are not monophyletic. ANME-1 are distantly related to Methanomicrobiales [56], while ANME-2 and ANME-3 are distantly related to Methanosarcinales [57, 58]. A fourth group has been described as ANME-2d or GoM Arc I; this group is not monophyletic with the other ANME-2 subgroups [59–61]. AOM metabolism for this novel group has not yet been proven [42]. ANME-1 and ANME-2 are the most diverse groups detected in a multitude of habitats and appear to be most relevant for AOM in anoxic environments. ANME-1 cells exhibit a cylinder-shaped morphology with an external sheath and were found only in loose association with SRB of the *Desulfococcus/Desulfosarcina* (DSS) group [53]. ANME-2 cells are coccoid and are frequently detected in consortia with SRB [55, 62]. In ANME-2a/SRB-aggregates, both cell types appear to be randomly intermixed, while ANME-2c/SRB aggregates reveal a shell-like structure with SRB at the outer shell of the aggregate. ANME-2 are usually associated with SRB of the DSS group [63, 64], but also associations with alpha-Proteobacteria, beta-Proteobacteria, or *Desulfobulbus*-related SRB and ANME-2 cells without contact to other bacteria were reported [65–71].

There is up to now no indication that the metabolism of the SRB in AOM is distinct from free-living sulfate reducing bacteria. The metabolic pathway of the ANME archaea is clearly related to methanogenesis. Intriguingly, ANME Archaea use this pathway in the reverse direction, while reducing equivalents are transferred to SRB [42, 72]. Until now, it seems that AOM with ANME Archaea is feasible just in syntrophy with sulfate reduction. A recently discovered thermophilic ANME group closely affiliated to ANME1 (ANME 1c), though may conduct AOM in contact to hydrothermal vent systems without SRB and with Fe^{3+} as putative electron acceptor. However, conclusive evidence is still missing in this case [73].

The methyl-coenzyme M reductase (MCR) catalyses in methanogenic archaea the terminal step of methane formation. In reversal, MCR is needed in a reversed methanogenic pathway for the initial step of AOM; also most of the other enzyme steps of methanogenesis operate in the reverse direction [74–76]. However, direct evidence for the reverse operation of this pathway is still lacking.

Intermediates for a necessary transfer of reducing equivalents between the syntrophic partners are still unknown. *In vitro* feeding studies excluded hydrogen, formate, acetate, methanol, and even more uncommon compounds like methylsulfides or humic acids [77–81]. The energy yield of AOM is still extremely low, compared with other anaerobic processes [82].

Recent findings indicate that the ANME Archaea are capable of both methane oxidation and sulfate reduction with elemental sulfur as an intermediate [83]. The reduced product HS_2^- may be the disproportionated by the symbiotic sulfate reducers to sulfate and HS^-. Thus, the symbioses may be less obligate than originally thought.

ANME-2 Archaea in consortia also conduct nitrogen fixation [84]. Nanometer secondary ion mass spectrometry (nano-SIMS) analysis implied the flow of nitrogen compounds from the Archaea to the sulfate reducers. Remarkably, the energy consuming nitrogen fixation is possible even under the conditions of the extremely low energy yield of AOM, though growth rates of the organisms were reduced by a factor of 20. Since AOM is a mayor sink of methane in marine sediments, nitrogen fixation by AOM may be as well a relevant process in the global nitrogen cycle. By this way, carbon, nitrogen, and sulfur cycles are linked by AOM.

Other recently described AOM processes may also be independent of archaeal groups. AOM with iron (Fe^{3+}) and mangenese (Mn^{3+}, Mn^{4+}) has been described for enrichment cultures from marine sediment samples, but a direct involvement of either archaeal or bacterial phylotypes is speculative [85]. A nitrite/nitrate dependent AOM is conducted by Bacteria (NC10 phylum, candidatus *Methylomirabilis oxyfera*; [86]). This process is clearly distinct from ANME/SRB AOM and appears to be homologous to the aerobic methane oxidation of methanotrophic Bacteria.

Another cell-cell interaction between the giant filamentous thaumarchaeote candidatus *Giganthauma karukerense* and a sulfur oxidizing gamma-Proteobacterium has been described recently [87]. A closed cell monolayer of the proteobacteria covers the surface of the large thaumarchaeote filament. It is not known in how far the cells may interact physiologically. It might be possible that the sulfur oxidizer reduces the sulfide concentration in the immediate vicinity of the host cell.

5. Interaction between Archaea and Eukarya

With respect to hitherto known mutualistic symbioses with eukaryotes, most but not all Archaea are members of the methanogenic Euryarchaeota. Methanogens are essential in the degradation of organic substrates under anaerobic conditions to methane and carbon dioxide, as terminal part of the anaerobic food chain. It is reasonable to assume that organisms with guts as anaerobic niches of nutrient decomposition harbor also methanogens as commensals.

Remarkably, a single methanogen phylotype, *Methanobrevibacter smithii*, is known to be the predominant Archaeon in the human gut microflora [88]. Symbioses between Archaea and eukaryotes, however, are not restricted to the gut anaerobic food chain. Many of the anaerobic protozoa, either free living or gut symbionts themselves, contain methanogenic Archaea as endosymbionts. These free-living protozoa are widespread in sapropels. Instead of mitochondria, they contain hydrogenosome organelles lacking a tricarboxylic acid cycle [89]. Hydrogenosomes are descendants of mitochondria. In these organelles, ATP is generated in a fermentative pathway by conversion of acetyl-CoA to acetate; the reducing power is released as molecular hydrogen [90]. Hydrogenosomes are a prerequisite for the occurrence of endosymbiotic methanogens, and hydrogenotrophic methanogens use hydrogen and carbon dioxide or formate as substrates for methanogenesis [91]. Also acetoclastic methanogens may take benefit from acetate generated by the hydrogenosome [92]. Regularly, these symbionts are transmitted vertically in the protists. Consequently, the phylotypes of the methanogens differ with respect to the protist groups and their habitats. Methanogens from free-living ciliates in freshwater habitats are related to Methanomicrobiales, whereas endosymbionts in ciliates from millipedes, cockroaches, and even frogs are Methanobacteriales [93]. However, during culturing, ciliates may also tend to lose their symbionts and also uptake of *Methanobacterium formicicum* by the ciliate *Trimyema compressum* has been reported [94]. Mechanisms of interactions between the methanogens and protists are largely unknown. Several morphological peculiarities have been described. In the free-living ciliate *Metopus contortus* polymorphic endosymbionts were observed; some cells appear to lose their cell walls and become directly attached to hydrogenosomes [95]. Also variations in size (putatively due to enlargement of cells) and stellate shape of the endosymbiont with close contact to hydrogenosomes have been observed repeatedly [96].

These results show that a peculiar crosstalk between the symbiotic partners is necessary. Like in well-studied symbiosis between eukaryotes and bacterial endosymbionts (including intracellular pathogens), protection against lysosomal digestion or cytoskeletal rearrangements of the vacuole containing the endosymbiont requires elaborate signaling pathways between host and symbiont partners [97]. It is reasonable to assume that the Archaean symbionts possess respective signaling mechanisms. However, the endosymbiotic associations between several groups of protists (Ciliata, and some representatives within groups of Archamoebae) are the only known endosymbioses so far. Thus, this way of interaction with eukaryotes does not appear to be a mainstream in archaeal life styles [98, 99].

Sponges, organisms at the evolutionary basis of the Metazoa, may be described as a diverse prokaryotic community in a eukaryote host, most of the prokaryotes with largely unknown function [100]. Though the majority of the organisms are free living in the sponge mesohyl, endosymbionts are common. Among cyanobacteria and heterotrophic bacteria, also fission yeasts have been described that are maternally transmitted via sponge eggs [101].

Archaea are ubiquitous in marine sponges, sometimes even dominant [102], though their ecological role is poorly understood. Since the composition of the archaeal community is distinct from seawater, a certain specificity of the sponge/Archaeon association must be assumed [103]. Also rather specific associations between certain archaeal phylotypes and sponges have been described. The association between a sponge and the Thaumarchaeota (formerly Crenarchaeota; [104, 105]) *Cenarchaeum symbiosum* has been first described for *Axinella mexicana* [106]. Three species of the Mediterranean *Axinella* harbor filamentous marine "group 1" Archaea colonizing the collagen surrounding the sponge spicules [107]. Marine Euryarchaeota are associated with the demosponge *Tentorium semisuberites* mesohyl [102]. The role of these symbioses is largely unknown, also with respect to the unknown ecological role of the marine Thaumarchaeota. Recent findings imply significance in the sponge nitrogen metabolism [103, 108, 109]. A vertical transmission of the ammonia-oxidizing Archaea also indicates the specificity of the symbiotic relationship [110]. Ammonia oxidizers may utilize ammonia excreted by the sponge as a metabolic end product and may thereby contribute to detoxification of the sponge tissue. This may be in particular of relevance in highly polluted areas, where high concentration of organic compounds and high ammonia concentrations affect marine biocoenoses [103].

The important role of Thaumarchaeota in nitrogen cycling, also with respect to symbioses, has been also identified in some marine mollusks: strains phylogenetically related to *Nitrosopumilus maritimus* were detected inside the tissue of the colonial ascidian *Cystodytes dellechiajei*. Here, nitrification of the Archaeon could be determined in situ [111]. Recent studies on the diversity of ammonia oxygenase genes also show that ammonia oxidizing archaeal communities differ in various coral species and are also distinct from communities in the sediment or in the water column [112, 113]. It must be expected that symbioses between other groups of marine invertebrates and Thaumarchaeota are also of relevance, in particular with respect to ammonia oxidation [114].

Among arthropods, as the largest animal phylum, only in the groups of millipedes, cockroaches, termites, and scarabs relevant methane producing species are present [93]. Methanogens represent the terminal part of the anaerobic food chain in the guts of these insects (especially termites). In this symbiosis, these Archaea utilize the main degradation products hydrogen, carbon dioxide, and acetate released by the previous steps of anaerobic lignocellulose degradation [115]. All methanogens, including the methanogen endosymbiont-bearing ciliates, are in the hindguts of these arthropods [116]. Free-living methanogens adhere to the hindgut wall. Among these big groups, a correlation between a specific diet (e.g., plant litter) and methane production could not be found, and not all members of the mentioned groups contain methanogens. However, in the group of higher termites, soil feeding termites produce more methane and contain more methanogens (according to 16S rRNA analysis) than wood feeders [117]. In the soil feeding species *Cubitermes fungifaber,* the composition of the communities

vary across the species, which does not account for a pure vertical transmission of the gut community, but a strong influence of the community in food soil [118]. Remarkably, also a *Natronococcus*-related sequence could be retrieved from the gut. Related strains are obligate haloalkaliphilic organisms of the family Halobacteriaceae, isolated from soda lakes, and are aerobic heterotrophic Archaea [119]. The *Natronococcus*-related strain may be well adapted to the first section of the hindgut (P1 part). This section provides a highly alkaline environment, reaching a pH around 12. For *Cubitermes ortognatus,* an in depth analysis of archaeal communities in four sections of the hindgut revealed remarkable distinctions in particular between the alkaline P1 part and the following P3–P5. Whereas Methanosarcinaceae–related sequences dominated in P1, they were replaced by Methanobacteriaceae-related clones in all other posterior parts of the gut. Interestingly, also Thermoplasmatales and Crenarchaeota contributed up to 40% to the archaeal community in these parts. The ecological role of these archaeal groups have to be elucidated yet.

Methanogenesis in termites is a globally relevant source of methane, with 20–29 Tg methane per year [120]. Methanogens from all ruminants produce 91–107 Tg methane per year, which is the second largest methane source after wetlands. In ruminants, methanogens are in a similar way the terminal part of the anaerobic lignocellulolytic food chains as in termite hindguts and methanogen/ruminant symbioses have been extensively studied. Some methanogens like *Methanobacterium bryantii* or *Methanobrevibacter ruminantium* were isolated from rumen fluids and were extensively studied with respect to biochemistry and energetics in methanogens, including genome analysis of *Methanobrevibacter* [121, 122]. Abundant adhesin-like sequences in the *Methanobrevibacter* genome imply intensive interactions between the methanogen and other rumen microbes. In coculture experiments with *Butyrivibrio proteoclasticus,* several *Methanobrevibacter* adhesins were upregulated and co-aggregates of both cell types were observed [122]. Interestingly, formate utilisation genes were also upregulated. Butyrate, acetate (or lactate), formate, carbon dioxide, and hydrogen gas are major fermentation products of *Butyrivibrio* during growth on xylan [123, 124]. Hydrogen and formate may be utilized by *Methanobrevibacter* in this syntrophic interaction. In addition to free-living methanogens in the rumen fluid, methanogens which are extra- and intracellularly associated with ciliate protozoa are relevant contributors to methane production. In ruminants, more than one-third of the methane may be produced by these consortia [125].

One might consider that the presence or absence of methanogens in vertebrates generally depends on the diet or the presence of specific anatomical differentiations of the gut and all herbivorous animals harbor the entire anaerobic food chain. Systematic analysis of the methane production in guts of 253 vertebrate species revealed that methane production and hence the presence of relevant amounts of methanogens does depend on the phylogenetic lineage of the animal rather than on the diet or the anatomy of the digestive system [126]. In some phylogenetic lineages like ostriches,

intestinal methanogens got lost irrespective of the diet. Methanogens are also missing within the large lineages of Carnivora/Chiroptera/Eulipotyphla (formerly Insectivora), even in herbivorous pandas (Ursidae/Carnivora). Though in all other large lineages methane producers dominate, nonproducers occur also in several "branches" of these lineages. Generally, the results imply that once the methanogens got lost in the course of evolution, they did not reappear in the descending lineages [126]. One special case with respect to the bird digestive system has drawn attention recently. The hoatzin (*Opisthocomus hoazin*) is the only known example for foregut fermentation in birds similar to the ruminants [127, 128]. The rumen methanogens found in hoatzins are more closely related to ruminant strains than to methanogens found in feces of other birds, though the composition of the methanogen community and the phylotypes themselves were still distinct from those found in ruminants [129].

In the intestines of primates, including humans, Archaea are present. *Methanobrevibacter smithii* as the dominant species draws particular attention: a syntrophic interaction between *Methanobrevibacter* and *Bacteroides thetaiotaomicron,* as studied in gnotobiotic mice, may affect the energy balance of the host [130]. *Methanobrevibacter* utilizes the *Bacteroides* fermentation product formate. This syntrophy obviously determines the expression of *Bacteroides* enzymes: the pathway directed towards formate and acetate production is upregulated, whereas alternative pathways towards propionate and butyrate are downregulated. The ongoing human microbiome project will soon update our knowledge on archaeal diversity and putative function in humans.

6. Concluding Remarks

Interactions between Archaea and other organisms are definitely as specific as interactions with symbiotic Bacteria prokaryotes. Up to now, the mechanisms of surface recognition are still poorly understood. The prominent "model" pathogens *Escherichia coli, Salmonella typhimurium, Pseudomonas aeruginosa,* and *Vibrio* spp. greatly extended our knowledge on specific interactions of Proteobacteria with animal host tissue. However, model organisms of this kind are still missing in the archaeal world, due to the lack of easy manageable molecular tools for functional studies, in particular with respect to the generation of mutant strains. In addition, we are still far away from even a rough estimate of the true sizes of the large archaeal clades. Hence, we are still unable to explore the diverse ways how Archaea may interact with each other. The description of the few very diverse cases that we know—considering the fundamental differences, for example, between *Nanoarchaeum and Ignicoccus* or the SM1 and sulfur reducer interaction—gives us an impression on the diverse ways how Archaea may interact and how diverse the mechanisms may have to be expected (see Table 1).

The symbiotic interaction between prokaryotes also leads to the question if the first eukaryote may be an offspring of a symbiotic interaction between an Archaeum and a Bacterium ([131] and references therein). Though the different roles of ancient Archaea and Bacteria are still

speculative, it becomes more and more obvious that tight symbiosis between both prokaryotic cell types also direct us to the roots of eukaryote evolution.

Acknowledgments

References

[1] G. B. West, W. H. Woodruff, and J. H. Brown, "Allometric scaling of metabolic rate from molecules and mitochondria to cells and mammals," *Proceedings of the National Academy of Sciences of the United States of America*, vol. 99, supplement 1, pp. 2473–2478, 2002.

[2] N. Klitgord and D. Segrè, "Environments that induce synthetic microbial ecosystems," *PLoS Computational Biology*, vol. 6, no. 11, Article ID e1001002, 2010.

[3] N. Dubilier, C. Bergin, and C. Lott, "Symbiotic diversity in marine animals: the art of harnessing chemosynthesis," *Nature Reviews Microbiology*, vol. 6, no. 10, pp. 725–740, 2008.

[4] D. G. Thanassi, J. B. Bliska, and P. J. Christie, "Surface organelles assembled by secretion systems of Gram-negative bacteria: diversity in structure and function," *FEMS Microbiology Reviews*, vol. 36, no. 6, pp. 1046–1082, 2012.

[5] H. P. Horz and G. Conrads, "The discussion goes on: what is the role of Euryarchaeota in humans?" *Archaea*, vol. 2010, Article ID 967271, 8 pages, 2010.

[6] C. Moissl-Eichinger and H. Huber, "Archaeal symbionts and parasites," *Current Opinion in Microbiology*, vol. 14, no. 3, pp. 364–370, 2011.

[7] J. N. Reeve and C. Schleper, "Archaea: very diverse, often different but never bad?" *Current Opinion in Microbiology*, vol. 14, no. 3, pp. 271–273, 2011.

[8] A. Koerdt, S. Jachlewski, A. Ghosh, J. Wingender, B. Siebers, and S. V. Albers, "Complementation of *Sulfolobus solfataricus* PBL2025 with an α-mannosidase: effects on surface attachment and biofilm formation," *Extremophiles*, vol. 16, no. 1, pp. 115–125, 2011.

[9] C. Moissl, C. Rudolph, and R. Huber, "Natural communities of novel archaea and bacteria with a string-of-pearls-like morphology: molecular analysis of the bacterial partners," *Applied and Environmental Microbiology*, vol. 68, no. 2, pp. 933–937, 2002.

[10] C. Moissl, R. Rachel, A. Briegel, H. Engelhardt, and R. Huber, "The unique structure of archaeal 'hami', highly complex cell appendages with nano-grappling hooks," *Molecular Microbiology*, vol. 56, no. 2, pp. 361–370, 2005.

[11] C. Rudolph, C. Moissl, R. Henneberger, and R. Huber, "Ecology and microbial structures of archaeal/bacterial strings-of-pearls communities and archaeal relatives thriving in cold sulfidic springs," *FEMS Microbiology Ecology*, vol. 50, no. 1, pp. 1–11, 2004.

[12] S. Nickell, R. Hegerl, W. Baumeister, and R. Rachel, "Pyrodictium cannulae enter the periplasmic space but do not enter the cytoplasm, as revealed by cryo-electron tomography," *Journal of Structural Biology*, vol. 141, no. 1, pp. 34–42, 2003.

[13] B. J. Baker, L. R. Comolli, G. J. Dick et al., "Enigmatic, ultrasmall, uncultivated Archaea," *Proceedings of the National Academy of Sciences of the United States of America*, vol. 107, no. 19, pp. 8806–8811, 2010.

[14] S. V. Albers, Z. Szabó, and A. J. M. Driessen, "Protein secretion in the Archaea: multiple paths towards a unique cell surface," *Nature Reviews Microbiology*, vol. 4, no. 7, pp. 537–547, 2006.

[15] M. Pohlschroder, A. Ghosh, M. Tripepi, and S. V. Albers, "Archaeal type IV pilus-like structures-evolutionarily conserved prokaryotic surface organelles," *Current Opinion in Microbiology*, vol. 14, no. 3, pp. 357–363, 2011.

[16] D. J. Näther, R. Rachel, G. Wanner, and R. Wirth, "Flagella of *Pyrococcus furiosus*: multifunctional organelles, made for swimming, adhesion to various surfaces, and cell-cell contacts," *Journal of Bacteriology*, vol. 188, no. 19, pp. 6915–6923, 2006.

[17] S. Fröls, M. Ajon, M. Wagner et al., "UV-inducible cellular aggregation of the hyperthermophilic archaeon *Sulfolobus solfataricus* is mediated by pili formation," *Molecular Microbiology*, vol. 70, no. 4, pp. 938–952, 2008.

[18] A. Koerdt, J. Gödeke, J. Berger, K. M. Thormann, and S. V. Albers, "Crenarchaeal biofilm formation under extreme conditions," *PLoS ONE*, vol. 5, no. 11, Article ID e14104, 2010.

[19] S. Schopf, G. Wanner, R. Rachel, and R. Wirth, "An archaeal bi-species biofilm formed by *Pyrococcus furiosus* and *Methanopyrus kandleri*," *Archives of Microbiology*, vol. 190, no. 3, pp. 371–377, 2008.

[20] M. Tripepi, S. Imam, and M. Pohlschröder, "*Haloferax volcanii* flagella are required for motility but are not involved in PibD-dependent surface adhesion," *Journal of Bacteriology*, vol. 192, no. 12, pp. 3093–3102, 2010.

[21] J. R. Leadbetter and J. A. Breznak, "Physiological ecology of *Methanobrevibacter cuticularis* sp. nov. and *Methanobrevibacter curvatus* sp. nov., isolated from the hindgut of the termite *Reticulitermes flavipes*," *Applied and Environmental Microbiology*, vol. 62, no. 10, pp. 3620–3631, 1996.

[22] V. B. Tran, S. M. J. Fleiszig, D. J. Evans, and C. J. Radke, "Dynamics of flagellum-and pilus-mediated association of *Pseudomonas aeruginosa* with contact lens surfaces," *Applied and Environmental Microbiology*, vol. 77, no. 11, pp. 3644–3652, 2011.

[23] A. K. Zgair and S. Chhibber, "Adhesion of *Stenotrophomonas maltophilia* to mouse tracheal mucus is mediated through flagella," *Journal of Medical Microbiology*, vol. 60, no. 7, pp. 1032–1037, 2011.

[24] U. Gophna, E. Z. Ron, and D. Graur, "Bacterial type III secretion systems are ancient and evolved by multiple horizontal-transfer events," *Gene*, vol. 312, no. 1-2, pp. 151–163, 2003.

[25] U. Küper, C. Meyer, V. Müller, R. Rachel, and H. Huber, "Energized outer membrane and spatial separation of metabolic processes in the hyperthermophilic Archaeon *Ignicoccus hospitalis*," *Proceedings of the National Academy of Sciences of the United States of America*, vol. 107, no. 7, pp. 3152–3156, 2010.

[26] T. Burghardt, D. J. Näther, B. Junglas, H. Huber, and R. Rachel, "The dominating outer membrane protein of the hyperthermophilic *Archaeum Ignicoccus hospitalis*: a novel pore-forming complex," *Molecular Microbiology*, vol. 63, no. 1, pp. 166–176, 2007.

[27] T. Burghardt, B. Junglas, F. Siedler, R. Wirth, H. Huber, and R. Rachel, "The interaction of *Nanoarchaeum equitans* with *Ignicoccus hospitalis*: proteins in the contact site between two

cells," *Biochemical Society Transactions*, vol. 37, no. 1, pp. 127–132, 2009.

[28] E. Waters, M. J. Hohn, I. Ahel et al., "The genome of *Nanoarchaeum equitans*: insights into early archaeal evolution and derived parasitism," *Proceedings of the National Academy of Sciences of the United States of America*, vol. 100, no. 22, pp. 12984–12988, 2003.

[29] U. Jahn, M. Gallenberger, W. Paper et al., "*Nanoarchaeum equitans* and Ignicoccus hospitalis: new insights into a unique, intimate association of two archaea," *Journal of Bacteriology*, vol. 190, no. 5, pp. 1743–1750, 2008.

[30] H. A. Barker, "Studies on the methane fermentation. V. Biochemical activities of *Methanobacterium omelianskii*," *Journal of Biological Chemistry*, vol. 137, no. 1, pp. 153–167, 1941.

[31] M. P. Bryant, E. A. Wolin, M. J. Wolin, and R. S. Wolfe, "*Methanobacillus omelianskii*, a symbiotic association of two species of bacteria," *Archiv für Mikrobiologie*, vol. 59, no. 1–3, pp. 20–31, 1967.

[32] C. A. Reddy, M. P. Bryant, and M. J. Wolin, "Characteristics of S organism isolated from *Methanobacillus omelianskii*," *Journal of Bacteriology*, vol. 109, no. 2, pp. 539–545, 1972.

[33] B. Eichler and B. Schink, "Oxidation of primary aliphatic alcohols by *Acetobacterium carbinolicum* sp. nov., a homoacetogenic anaerobe," *Archives of Microbiology*, vol. 140, no. 2-3, pp. 147–152, 1984.

[34] C. Wallrabenstein, E. Hauschild, and B. Schink, "*Syntrophobacter pfennigii* sp. nov., new syntrophically propionate-oxidizing anaerobe growing in pure culture with propionate and sulfate," *Archives of Microbiology*, vol. 164, no. 5, pp. 346–352, 1995.

[35] M. P. Bryant, L. L. Campbell, C. A. Reddy, and M. R. Crabill, "Growth of desulfovibrio in lactate or ethanol media low in sulfate in association with H_2 utilizing methanogenic bacteria," *Applied and Environmental Microbiology*, vol. 33, no. 5, pp. 1162–1169, 1977.

[36] A. Ben-Bassat, R. Lamed, and J. G. Zeikus, "Ethanol production by thermophilic bacteria: metabolic control of end product formation in *Thermoanaerobium brockii*," *Journal of Bacteriology*, vol. 146, no. 1, pp. 192–199, 1981.

[37] R. Klemps, H. Cypionka, F. Widdel, and N. Pfennig, "Growth with hydrogen, and further physiological characteristics of *Desulfotomaculum species*," *Archives of Microbiology*, vol. 143, no. 2, pp. 203–208, 1985.

[38] H. Imachi, Y. Sekiguchi, Y. Kamagata, S. Hanada, A. Ohashi, and H. Harada, "*Pelotomaculum thermopropionicum* gen. nov., sp. nov., an anaerobic, thermophilic, syntrophic propionate-oxidizing bacterium," *International Journal of Systematic and Evolutionary Microbiology*, vol. 52, no. 5, pp. 1729–1735, 2002.

[39] T. Shimoyama, S. Kato, S. Ishii, and K. Watanabe, "Flagellum mediates symbiosis," *Science*, vol. 323, no. 5921, p. 1574, 2009.

[40] A. J. M. Stams and C. M. Plugge, "Electron transfer in syntrophic communities of anaerobic bacteria and archaea," *Nature Reviews Microbiology*, vol. 7, no. 8, pp. 568–577, 2009.

[41] W. S. Reeburgh, "Methane consumption in Cariaco Trench waters and sediments," *Earth and Planetary Science Letters*, vol. 28, no. 3, pp. 337–344, 1976.

[42] K. Knittel and A. Boetius, "Anaerobic oxidation of methane: progress with an unknown process," *Annual Review of Microbiology*, vol. 63, pp. 311–334, 2009.

[43] P. Regnier, A. W. Dale, S. Arndt, D. E. LaRowe, J. Mogollón, and P. Van Cappellen, "Quantitative analysis of anaerobic oxidation of methane (AOM) in marine sediments: a modeling perspective," *Earth-Science Reviews*, vol. 106, no. 1-2, pp. 105–130, 2011.

[44] G. Aloisi, C. Pierre, J. M. Rouchy, J. P. Foucher, and J. Woodside, "Methane-related authigenic carbonates of Eastern Mediterranean Sea mud volcanoes and their possible relation to gas hydrate destabilisation," *Earth and Planetary Science Letters*, vol. 184, no. 1, pp. 321–338, 2000.

[45] J. Peckmann, E. Gischler, W. Oschmann, and J. Reitner, "An Early Carboniferous seep community and hydrocarbon-derived carbonates from the Harz Mountains, Germany," *Geology*, vol. 29, no. 3, pp. 271–274, 2001.

[46] G. Aloisi, I. Bouloubassi, S. K. Heijs et al., "CH_4-consuming microorganisms and the formation of carbonate crusts at cold seeps," *Earth and Planetary Science Letters*, vol. 203, no. 1, pp. 195–203, 2002.

[47] E. De Boever, D. Birgel, V. Thiel et al., "The formation of giant tubular concretions triggered by anaerobic oxidation of methane as revealed by archaeal molecular fossils (Lower Eocene, Varna, Bulgaria)," *Palaeogeography, Palaeoclimatology, Palaeoecology*, vol. 280, no. 1-2, pp. 23–36, 2009.

[48] E. De Boever, D. Birgel, P. Muchez, J. Peckmann, L. Dimitrov, and R. Swennen, "Fabric and formation of grapestone concretions within an unusual ancient methane seep system (Eocene, Bulgaria)," *Terra Nova*, vol. 23, no. 1, pp. 56–61, 2011.

[49] S. B. Ziegenbalg, D. Birgel, L. Hoffmann-Sell, C. Pierre, J. M. Rouchy, and J. Peckmann, "Anaerobic oxidation of methane in hypersaline Messinian environments revealed by ^{13}C-depleted molecular fossils," *Chemical Geology*, vol. 292-293, no. 1, pp. 140–148, 2012.

[50] J. Peckmann, A. Reimer, U. Luth et al., "Methane-derived carbonates and authigenic pyrite from the northwestern Black Sea," *Marine Geology*, vol. 177, no. 1-2, pp. 129–150, 2001.

[51] A. Y. Lein, M. V. Ivanov, N. V. Pimenov, and M. B. Gulin, "Geochemical peculiarities of the carbonate constructions formed during microbial oxidation of methane under anaerobic conditions," *Microbiology*, vol. 71, no. 1, pp. 78–90, 2002.

[52] W. Michaelis, R. Seifert, K. Nauhaus et al., "Microbial reefs in the black sea fueled by anaerobic oxidation of methane," *Science*, vol. 297, no. 5583, pp. 1013–1015, 2002.

[53] J. Reitner, A. Reimer, G. Schumann, V. Thiel, and J. Peckmann, "Methane-derived carbonate build-ups and associated microbial communities at cold seeps on the lower Crimean shelf (Black Sea)," *Facies*, vol. 51, no. 1–4, pp. 66–79, 2005.

[54] C. Wrede, C. Heller, J. Reitner, and M. Hoppert, "Correlative light/electron microscopy for the investigation of microbial mats from Black Sea Cold Seeps," *Journal of Microbiological Methods*, vol. 73, no. 2, pp. 85–91, 2008.

[55] C. Wrede, V. Krukenberg, A. Dreier, J. Reitner, C. Heller, and M. Hoppert, "Detection of metabolic key enzymes of methane turnover processes in cold seep microbial biofilms," *Geomicrobiology Journal*, vol. 30, no. 3, pp. 214–227, 2013.

[56] K. U. Hinrichs, J. M. Hayes, S. P. Sylva, P. G. Brewert, and E. F. DeLong, "Methane-consuming archaebacteria in marine sediments," *Nature*, vol. 398, no. 6730, pp. 802–805, 1999.

[57] V. J. Orphan, K. U. Hinrichs, W. Ussler III et al., "Comparative analysis of methane-oxidizing archaea and sulfate-reducing bacteria in anoxic marine sediments," *Applied and Environmental Microbiology*, vol. 67, no. 4, pp. 1922–1934, 2001.

[58] H. Niemann, T. Lösekann, D. De Beer et al., "Novel microbial communities of the Haakon Mosby mud volcano and their

role as a methane sink," *Nature*, vol. 443, no. 7113, pp. 854–858, 2006.

[59] H. J. Mills, R. J. Martinez, S. Story, and P. A. Sobecky, "Characterization of microbial community structure in Gulf of Mexico gas hydrates: comparative analysis of DNA- and RNA-derived clone libraries," *Applied and Environmental Microbiology*, vol. 71, no. 6, pp. 3235–3247, 2005.

[60] K. G. Lloyd, L. Lapham, and A. Teske, "An anaerobic methane-oxidizing community of ANME-1b archaea in hypersaline gulf of Mexico sediments," *Applied and Environmental Microbiology*, vol. 72, no. 11, pp. 7218–7230, 2006.

[61] R. J. Martinez, H. J. Mills, S. Story, and P. A. Sobecky, "Prokaryotic diversity and metabolically active microbial populations in sediments from an active mud volcano in the Gulf of Mexico," *Environmental Microbiology*, vol. 8, no. 10, pp. 1783–1796, 2006.

[62] C. Heller, M. Hoppert, and J. Reitner, "Immunological localization of coenzyme M reductase in anaerobic methane-oxidizing archaea of ANME 1 and ANME 2 type," *Geomicrobiology Journal*, vol. 25, no. 3-4, pp. 149–156, 2008.

[63] A. Boetius, K. Ravenschlag, C. J. Schubert et al., "A marine microbial consortium apparently mediating anaerobic oxidation methane," *Nature*, vol. 407, no. 6804, pp. 623–626, 2000.

[64] L. Schreiber, T. Holler, K. Knittel, A. Meyerdierks, and R. Amann, "Identification of the dominant sulfate-reducing bacterial partner of anaerobic methanotrophs of the ANME-2 clade," *Environmental Microbiology*, vol. 12, no. 8, pp. 2327–2340, 2010.

[65] V. J. Orphan, C. H. House, K. U. Hinrichs, K. D. McKeegan, and E. F. DeLong, "Multiple archaeal groups mediate methane oxidation in anoxic cold seep sediments," *Proceedings of the National Academy of Sciences of the United States of America*, vol. 99, no. 11, pp. 7663–7668, 2002.

[66] E. Durisch-Kaiser, L. Klauser, B. Wehrli, and C. Schubert, "Evidence of intense archaeal and bacterial methanotrophic activity in the Black Sea water column," *Applied and Environmental Microbiology*, vol. 71, no. 12, pp. 8099–8106, 2005.

[67] G. Eller, L. Känel, and M. Krüger, "Cooccurrence of aerobic and anaerobic methane oxidation in the water column of Lake Plußsee," *Applied and Environmental Microbiology*, vol. 71, no. 12, pp. 8925–8928, 2005.

[68] C. J. Schubert, M. J. L. Coolen, L. N. Neretin et al., "Aerobic and anaerobic methanotrophs in the Black Sea water column," *Environmental Microbiology*, vol. 8, no. 10, pp. 1844–1856, 2006.

[69] T. Treude, V. Orphan, K. Knittel, A. Gieseke, C. H. House, and A. Boetius, "Consumption of methane and CO_2 by methanotrophic microbial mats from gas seeps of the anoxic Black Sea," *Applied and Environmental Microbiology*, vol. 73, no. 7, pp. 2271–2283, 2007.

[70] A. Pernthaler, A. E. Dekas, C. T. Brown, S. K. Goffredi, T. Embaye, and V. J. Orphan, "Diverse syntrophic partnerships from deep-sea methane vents revealed by direct cell capture and metagenomics," *Proceedings of the National Academy of Sciences of the United States of America*, vol. 105, no. 19, pp. 7052–7057, 2008.

[71] K. Knittel, T. Lösekann, A. Boetius, R. Kort, and R. Amann, "Diversity and distribution of methanotrophic archaea at cold seeps," *Applied and Environmental Microbiology*, vol. 71, no. 1, pp. 467–479, 2005.

[72] T. M. Hoehler, M. J. Alperin, D. B. Albert, and C. S. Martens, "Field and laboratory studies of methane oxidation in an anoxic marine sediment: evidence for a methanogen-sulfate reducer consortium," *Global Biogeochemical Cycles*, vol. 8, no. 4, pp. 451–463, 1994.

[73] S. D. Wankel, M. M. Adams, D. T. Johnston, C. M. Hansel, S. B. Joye, and P. R. Girguis, "Anaerobic methane oxidation in metalliferous hydrothermal sediments: influence on carbon flux and decoupling from sulfate reduction," *Environmental Microbiology*, vol. 14, no. 10, pp. 2726–2740, 2012.

[74] M. Krüger, A. Meyerdierks, F. O. Glöckner et al., "A conspicuous nickel protein in microbial mats that oxidize methane anaerobically," *Nature*, vol. 426, no. 6968, pp. 878–881, 2003.

[75] S. J. Hallam, N. Putnam, C. M. Preston et al., "Reverse methanogenesis: testing the hypothesis with environmental genomics," *Science*, vol. 305, no. 5689, pp. 1457–1462, 2004.

[76] S. Scheller, M. Goenrich, R. Boecher, R. K. Thauer, and B. Jaun, "The key nickel enzyme of methanogenesis catalyses the anaerobic oxidation of methane," *Nature*, vol. 465, no. 7298, pp. 606–608, 2010.

[77] K. Nauhaus, A. Boetius, M. Krüger, and F. Widdel, "In vitro demonstration of anaerobic oxidation of methane coupled to sulphate reduction in sediment from a marine gas hydrate area," *Environmental Microbiology*, vol. 4, no. 5, pp. 296–305, 2002.

[78] K. Nauhaus, T. Treude, A. Boetius, and M. Krüger, "Environmental regulation of the anaerobic oxidation of methane: a comparison of ANME-I and ANME-II communities," *Environmental Microbiology*, vol. 7, no. 1, pp. 98–106, 2005.

[79] F. Widdel, A. Boetius, and R. Rabus, "Anaerobic biodegradation of hydrocarbons including methane," in *The Prokaryotes*, M. Dworkin, S. Falkow, E. Rosenberg, K. H. Schleifer, and E. Stackebrandt, Eds., pp. 1028–1049, Springer, New York, NY, USA, 2006.

[80] J. J. Moran, E. J. Beal, J. M. Vrentas, V. J. Orphan, K. H. Freeman, and C. H. House, "Methyl sulfides as intermediates in the anaerobic oxidation of methane," *Environmental Microbiology*, vol. 10, no. 1, pp. 162–173, 2008.

[81] G. Wegener, H. Niemann, M. Elvert, K. U. Hinrichs, and A. Boetius, "Assimilation of methane and inorganic carbon by microbial communities mediating the anaerobic oxidation of methane," *Environmental Microbiology*, vol. 10, no. 9, pp. 2287–2298, 2008.

[82] R. K. Thauer and S. Shima, "Methane as fuel for anaerobic microorganisms," *Annals of the New York Academy of Sciences*, vol. 1125, pp. 158–170, 2008.

[83] J. Milucka, T. G. Ferdelman, L. Polerecky et al., "Zero-valent sulphur is a key intermediate in marine methane oxidation," *Nature*, vol. 491, no. 7425, pp. 541–546, 2012.

[84] A. E. Dekas, R. S. Poretsky, and V. J. Orphan, "Deep-Sea archaea fix and share nitrogen in methane-consuming microbial consortia," *Science*, vol. 326, no. 5951, pp. 422–426, 2009.

[85] E. J. Beal, C. H. House, and V. J. Orphan, "Manganese- and iron-dependent marine methane oxidation," *Science*, vol. 325, no. 5937, pp. 184–187, 2009.

[86] K. F. Ettwig, M. K. Butler, D. Le Paslier et al., "Nitrite-driven anaerobic methane oxidation by oxygenic bacteria," *Nature*, vol. 464, no. 7288, pp. 543–548, 2010.

[87] F. Muller, T. Brissac, N. Le Bris, H. Felbeck, and O. Gros, "First description of giant Archaea (Thaumarchaeota) associated with putative bacterial ectosymbionts in a sulfidic marine habitat," *Environmental Microbiology*, vol. 12, no. 8, pp. 2371–2383, 2010.

[88] P. B. Eckburg, E. M. Bik, C. N. Bernstein et al., "Microbiology: diversity of the human intestinal microbial flora," *Science*, vol. 308, no. 5728, pp. 1635–1638, 2005.

[89] J. H. P. Hackstein, A. Akhmanova, B. Boxma, H. R. Harhangi, and F. G. J. Voncken, "Hydrogenosomes: eukaryotic adaptations to anaerobic environments," *Trends in Microbiology*, vol. 7, no. 11, pp. 441–447, 1999.

[90] M. Müller, M. Mentel, J. J. van Hellemond et al., "Biochemistry and evolution of anaerobic energy metabolism in eukaryotes," *Microbiology and Molecular Biology Reviews*, vol. 76, no. 2, pp. 444–495, 2012.

[91] J. J. A. Van Bruggen, K. B. Zwart, and J. G. F. Hermans, "Isolation and characterization of *Methanoplanus endosymbiosus sp. nov.*, an endosymbiont of the marine sapropelic ciliate *Metopus contortus* Quennerstedt," *Archives of Microbiology*, vol. 144, no. 4, pp. 367–374, 1986.

[92] N. Narayanan, B. Krishnakumar, V. N. Anupama, and V. B. Manilal, "*Methanosaeta sp.*, the major archaeal endosymbiont of *Metopus es*," *Research in Microbiology*, vol. 160, no. 8, pp. 600–607, 2009.

[93] J. H. P. Hackstein and T. A. van Alen, "Methanogens in the gastro-intestinal tract of animals," in *Microbiology Monographs: (Endo)Symbiotic Methanogenic Archaea*, J. H. P. Hackstein, Ed., pp. 115–142, Springer, Heidelberg, Germany, 2010.

[94] S. Wagener, C. F. Bardele, and N. Pfennig, "Functional integration of *Methanobacterium formicicum* into the anaerobic ciliate *Trimyema compressum*," *Archives of Microbiology*, vol. 153, no. 5, pp. 496–501, 1990.

[95] B. J. Finlay and T. Fenchel, "Polymorphic bacterial symbionts in the anaerobic ciliated protozoon Metopus," *FEMS Microbiology Letters*, vol. 79, no. 2-3, pp. 187–190, 1991.

[96] B. J. Finlay, T. M. Embley, and T. Fenchel, "A new polymorphic methanogen, closely related to *Methanocorpusculum parvum*, living in stable symbiosis within the anaerobic ciliate *Trimyema* sp," *Journal of General Microbiology*, vol. 139, no. 2, pp. 371–378, 1993.

[97] R. Gross, F. Vavre, A. Heddi, G. D. D. Hurst, E. Zchori-Fein, and K. Bourtzis, "Immunity and symbiosis," *Molecular Microbiology*, vol. 73, no. 5, pp. 751–759, 2009.

[98] A. Moya, J. Peretó, R. Gil, and A. Latorre, "Learning how to live together: genomic insights into prokaryote-animal symbioses," *Nature Reviews Genetics*, vol. 9, no. 3, pp. 218–229, 2008.

[99] F. Husník, T. Chrudimský, and V. Hypša, "Multiple origins of endosymbiosis within the Enterobacteriaceae (gamma-Proteobacteria): convergence of complex phylogenetic approaches," *BMC Biology*, vol. 9, no. 87, pp. 1–17, 2011.

[100] N. S. Webster and L. L. Blackall, "What do we really know about sponge-microbial symbioses," *The ISME Journal*, vol. 3, no. 1, pp. 1–3, 2009.

[101] M. Maldonado, N. Cortadellas, M. I. Trillas, and K. Rützler, "Endosymbiotic yeast maternally transmitted in a marine sponge," *The Biological Bulletin*, vol. 209, no. 2, pp. 94–106, 2005.

[102] T. Pape, F. Hoffmann, N. V. Quéric, K. Von Juterzenka, J. Reitner, and W. Michaelis, "Dense populations of Archaea associated with the demosponge *Tentorium semisuberites* Schmidt, 1870 from Arctic deep-waters," *Polar Biology*, vol. 29, no. 8, pp. 662–667, 2006.

[103] A. S. Turque, D. Batista, C. B. Silveira et al., "Environmental shaping of sponge associated archaeal communities," *PLoS ONE*, vol. 5, no. 12, Article ID e15774, 2010.

[104] C. Brochier-Armanet, B. Boussau, S. Gribaldo, and P. Forterre, "Mesophilic crenarchaeota: proposal for a third archaeal phylum, the Thaumarchaeota," *Nature Reviews Microbiology*, vol. 6, no. 3, pp. 245–252, 2008.

[105] A. Spang, R. Hatzenpichler, C. Brochier-Armanet et al., "Distinct gene set in two different lineages of ammonia-oxidizing archaea supports the phylum Thaumarchaeota," *Trends in Microbiology*, vol. 18, no. 8, pp. 331–340, 2010.

[106] C. M. Preston, K. Y. Wu, T. F. Molinski, and E. F. Delong, "A psychrophilic crenarchaeon inhabits a marine sponge: *Cenarchaeum symbiosum* gen. nov., sp. nov," *Proceedings of the National Academy of Sciences of the United States of America*, vol. 93, no. 13, pp. 6241–6246, 1996.

[107] H. Margot, C. Acebal, E. Toril, R. Amils, and J. L. Fernandez Puentes, "Consistent association of crenarchaeal Archaea with sponges of the genus *Axinella*," *Marine Biology*, vol. 140, no. 4, pp. 739–745, 2002.

[108] M. Han, F. Liu Zhang, Z. Li, and H. Lin, "Bacterial and Archaeal symbionts in the south China Sea sponge *Phakellia fusca*: community structure, relative abundance, and ammonia-oxidizing populations," *Marine Biotechnology*, vol. 14, no. 6, pp. 701–713, 2012.

[109] R. Radax, T. Rattei, A. Lanzen et al., "Metatranscriptomics of the marine sponge *Geodia barretti*: tackling phylogeny and function of its microbial community," *Environmental Microbiology*, vol. 14, no. 5, pp. 1308–1324, 2012.

[110] D. Steger, P. Ettinger-Epstein, S. Whalan et al., "Diversity and mode of transmission of ammonia-oxidizing archaea in marine sponges," *Environmental Microbiology*, vol. 10, no. 4, pp. 1087–1094, 2008.

[111] M. Martínez-García, P. Stief, M. Díaz-Valdés et al., "Ammonia-oxidizing Crenarchaeota and nitrification inside the tissue of a colonial ascidian," *Environmental Microbiology*, vol. 10, no. 11, pp. 2991–3001, 2008.

[112] J. M. Beman, K. J. Roberts, L. Wegley, F. Rohwer, and C. A. Francis, "Distribution and diversity of archaeal ammonia monooxygenase genes associated with corals," *Applied and Environmental Microbiology*, vol. 73, no. 17, pp. 5642–5647, 2007.

[113] N. Siboni, E. Ben-Dov, A. Sivan, and A. Kushmaro, "Geographic specific coral-associated ammonia-oxidizing archaea in the northern Gulf of Eilat (Red Sea)," *Microbiology Ecology*, vol. 64, no. 1, pp. 18–24, 2012.

[114] M. Pester, C. Schleper, and M. Wagner, "The Thaumarchaeota: an emerging view of their phylogeny and ecophysiology," *Current Opinion in Microbiology*, vol. 14, no. 3, pp. 300–306, 2011.

[115] M. Pester and A. Brune, "Hydrogen is the central free intermediate during lignocellulose degradation by termite gut symbionts," *The ISME Journal*, vol. 1, no. 6, pp. 551–565, 2007.

[116] J. H. P. Hackstein and C. K. Stumm, "Methane production in terrestrial arthropods," *Proceedings of the National Academy of Sciences of the United States of America*, vol. 91, no. 12, pp. 5441–5445, 1994.

[117] A. Brauman, J. Doré, P. Eggleton, D. Bignell, J. A. Breznak, and M. D. Kane, "Molecular phylogenetic profiling of prokaryotic communities in guts of termites with different feeding habits," *FEMS Microbiology Ecology*, vol. 35, no. 1, pp. 27–36, 2001.

[118] S. E. Donovan, K. J. Purdy, M. D. Kane, and P. Eggleton, "Comparison of Euryarchaea strains in the guts and food-soil of the soil-feeding termite *Cubitermes fungifaber* across

different soil types," *Applied and Environmental Microbiology*, vol. 70, no. 7, pp. 3884–3892, 2004.

[119] B. J. Tindall, H. N. M. Ross, and W. D. Grant, "*Natronobacterium* gen. nov. and *Natronococcus* gen. nov., two new genera of haloalkaliphilic archaebacteria," *Systematic and Applied Microbiology*, vol. 5, no. 1, pp. 41–57, 1984.

[120] K. L. Denman, G. Brasseur, A. Chidthaisong et al., "Couplings between changes in the climate system and biogeochemistry," in *Climate Change 2007: The Physical Science Basis. Contribution of Working Group I to the Fourth Assessment Report of the Intergovernmental Panel on Climate Change*, S. Solomon, D. Qin, M. Manning et al., Eds., pp. 500–587, Cambridge University Press, New York, NY, USA.

[121] W. B. Whitman and R. S. Wolfe, "Activation of the methylreductase system from *Methanobacterium bryantii* by ATP," *Journal of Bacteriology*, vol. 154, no. 2, pp. 640–649, 1983.

[122] S. C. Leahy, W. J. Kelly, E. Altermann et al., "The genome sequence of the rumen methanogen *Methanobrevibacter ruminantium* reveals new possibilities for controlling ruminant methane emissions," *PloS one*, vol. 5, no. 1, p. e8926, 2010.

[123] R. B. Hespell, R. Wolf, and R. J. Bothast, "Fermentation of xylans by *Butyrivibrio fibrisolvens* and other ruminal bacteria," *Applied and Environmental Microbiology*, vol. 53, no. 12, pp. 2849–2853, 1987.

[124] T. L. Miller and S. E. Jenesel, "Enzymology of butyrate formation by *Butyrivibrio fibrisolvens*," *Journal of Bacteriology*, vol. 138, no. 1, pp. 99–104, 1979.

[125] B. J. Finlay, G. Esteban, K. J. Clarke, A. G. Williams, T. M. Embley, and R. P. Hirt, "Some rumen ciliates have endosymbiotic methanogens," *FEMS Microbiology Letters*, vol. 117, no. 2, pp. 157–161, 1994.

[126] J. H. P. Hackstein, "Eukaryotic molecular biodiversity: systematic approaches for the assessment of symbiotic associations," *Antonie van Leeuwenhoek, International Journal of General and Molecular Microbiology*, vol. 72, no. 1, pp. 63–76, 1997.

[127] A. Grajal, S. D. Strahl, R. Parra, M. G. Dominguez, and A. Neher, "Foregut fermentation in the hoatzin, a neotropical leaf-eating bird," *Science*, vol. 245, no. 4923, pp. 1236–1238, 1989.

[128] F. Godoy-Vitorino, R. E. Ley, Z. Gao et al., "Bacterial community in the crop of the hoatzin, a neotropical folivorous flying bird," *Applied and Environmental Microbiology*, vol. 74, no. 19, pp. 5905–5912, 2008.

[129] A. D. G. Wright, K. S. Northwood, and N. E. Obispo, "Rumen-like methanogens identified from the crop of the folivorous South American bird, the hoatzin (*Opisthocomus hoazin*)," *The ISME Journal*, vol. 3, no. 10, pp. 1120–1126, 2009.

[130] B. S. Samuel and J. I. Gordon, "A humanized gnotobiotic mouse model of host-archaeal-bacterial mutualism," *Proceedings of the National Academy of Sciences of the United States of America*, vol. 103, no. 26, pp. 10011–10016, 2006.

[131] T. Thiergart, G. Landan, M. Schenk, T. Dagan, and W. F. Martin, "An evolutionary network of genes present in the eukaryote common ancestor polls genomes on eukaryotic and mitochondrial origin," *Genome Biology and Evolution*, vol. 4, no. 4, pp. 466–485, 2012.

Research Article

Archaeol: An Indicator of Methanogenesis in Water-Saturated Soils

Katie L. H. Lim,[1] Richard D. Pancost,[1] Edward R. C. Hornibrook,[2] Peter J. Maxfield,[1] and Richard P. Evershed[1]

[1] Organic Geochemistry Unit, Bristol Biogeochemistry Research Centre and The Cabot Institute, School of Chemistry, University of Bristol, Cantock's Close, Bristol BS8 1TS, UK
[2] Bristol Biogeochemistry Research Centre and The Cabot Institute, School of Earth Sciences, University of Bristol, Wills Memorial Building, Queen's Road, Bristol BS8 1RJ, UK

Correspondence should be addressed to Richard D. Pancost, r.d.pancost@bristol.ac.uk

Oxic soils typically are a sink for methane due to the presence of high-affinity methanotrophic *Bacteria* capable of oxidising methane. However, soils experiencing water saturation are able to host significant methanogenic archaeal communities, potentially affecting the capacity of the soil to act as a methane sink. In order to provide insight into methanogenic populations in such soils, the distribution of archaeol in free and conjugated forms was investigated as an indicator of fossilised and living methanogenic biomass using gas chromatography-mass spectrometry with selected ion monitoring. Of three soils studied, only one organic matter-rich site contained archaeol in quantifiable amounts. Assessment of the subsurface profile revealed a dominance of archaeol bound by glycosidic headgroups over phospholipids implying derivation from fossilised biomass. Moisture content, through control of organic carbon and anoxia, seemed to govern trends in methanogen biomass. Archaeol and crenarchaeol profiles differed, implying the former was not of thaumarcheotal origin. Based on these results, we propose the use of intact archaeol as a useful biomarker for methanogen biomass in soil and to track changes in moisture status and aeration related to climate change.

1. Introduction

Methane (CH_4) emission from soil is determined by the net balance of simultaneous *in situ* production of biogenic CH_4 by methanogenic *Archaea* and consumption by methanotrophic *Bacteria*. In the majority of oxic soils, methanotrophy far outweighs internal CH_4 production. The latter is assumed to be low or negligible as, although methanogens are known to survive in aerobic soils [1], they are traditionally considered strict anaerobes [2] which if present in soil are confined to anoxic microsites. Consequently, any CH_4 produced typically is oxidised before reaching the atmosphere. Nonetheless, soils exposed to wet conditions can host substantial methanogenic communities, and in some instances act as a source of CH_4 emissions, despite extended periods of oxygen exposure [3–6]. Consequently, we postulate that

in situ CH_4 production could be underestimated in such water-saturated soils, and furthermore, marginal increases in wetting caused by climate-change induced precipitation may increase the capacity of a water-saturated soil to act as a net CH_4 source rather than a sink for atmospheric CH_4. Thus, it is important to further understand the presence and distribution of microbial populations controlling CH_4 production in water-saturated soil in order to assess their potential to respond to changes in soil moisture and aeration conditions, and long-term impacts of climate change.

Membrane lipids of *Archaea* in cultures have been extensively studied and the distribution of their lipid component parts may be used for taxonomic purposes [7, 8]. Intact polar lipids (IPLs) are considered important biomarkers for living microbial biomass as polar head-groups covalently bound to the core lipid are degraded relatively quickly

upon cell lysis [9]; the resultant simple lipids are therefore expected to derive primarily from fossilised material [10–12]. Phospholipids are particularly labile [9, 13], whereas glycosidic ether lipids are more resistant to degradation [14]. Archaeal IPLs differ substantially from those synthesised by bacteria, being composed of a phosphoester or glycoside polar head group ether-bound to non-polar isoprenoid glycerol diether or tetraether core lipid [15]. The core lipid archaeol is widespread in *Archaea* from a wide range of environments. Archaeal diether core lipids have been proposed as a methanogen biomarker or to estimate quantitatively methanogen biomass in natural systems. Respective studies have predominantly been restricted to highly anaerobic environments exhibiting significant CH_4 emissions such as rice paddies [16, 17], digester sludge [18, 19], marine sediment [20], faecal material [21], permafrost [22, 23], and peatlands [24–26]. Wachinger et al. [27] observed that absolute *Archaea* cell numbers in mineral soils, calculated using the approximate ether lipid concentration 2.5 $\mu mol\,g^{-1}$ dry weight of methanogen cells [28], also reflected CH_4 productivity. Others have instead employed the analysis of intact glycerol dialkyl glycerol tetraether (GDGT) lipid distributions as evidence of living archaeal populations in soils [29, 30].

We postulate that archaeol present in soil predominantly originates from methanogens, and propose that archaeol abundance may serve as an indicator of methanogenic biomass. We investigate herein the concentration of archaeol in its free and conjugated forms with depth in three soils containing varying amounts of organic matter content and a high water content. Our study aims to gain new insights into methanogenic populations residing in oxic soil based upon the presence of archaeol in its free and conjugated forms, and by comparing the occurrence of archaeol to the thaumarchaeotal GDGT lipid, crenarchaeol.

2. Materials and Methods

Soil cores (35 or 50 cm) were collected from three Sites of Special Scientific Interest (SSSI) managed by the Countryside Council for Wales (CCW): Caeau Ton-y-Fildre (Brecknock), Cefn Cribwr Meadows (Ogwr), and Caeau Bronydd Mawr (Brecknock) (Figure 1). Sites were selected based upon data collated in a comprehensive survey of Welsh lowland grasslands [31]. Soil properties reported by Stevens et al. [31] are provided in Table 1. Sites were selected based upon organic matter content but in general were typical of moist grassland soil in Great Britain located in areas receiving a high annual input of precipitation. Vegetation at all sites was dominated by *Molinia caerulea* (purple moor grass) with rushes, such as *Juncus acutiflorus*, also being common, and to a lesser extent sedges and smaller grasses present at Cefn Cribwr Meadows.

Core sections (5 cm) were frozen after collection and freeze-dried. They were then ground with pestle and mortar and 1 to 2 g was extracted using a modified Bligh Dyer solvent containing buffered water (0.05 M KH_2PO_4; pH 7.2) : chloroform : methanol 4 : 5 : 10 (v/v/v). An aliquot of the resulting total lipid extract (TLE) was separated into

"simple lipid," "glycolipid" and "phospholipid" fractions by silica column chromatography with chloroform : acetic acid (99 : 1, v/v), acetone and MeOH, respectively [32]. We have observed that in contrast to archaeol and acyl lipids, simple GDGTs lipids only elute in the glycolipid fraction. Phospholipid and glycolipid headgroups were cleaved by hydrolysis of ether bonds using 5% HCl in MeOH [33]. Aliquots were silylated with pyridine and N,O-bis(trimethylsilyl)trifluoroacetamide (BSTFA) at 70°C for 1 hr and dissolved in hexane prior to analysis by gas chromatography-mass spectrometry (GC/MS). Archaeol was quantified relative to a 1,2-di-O-hexadecyl-*rac*-glycerol standard. Analyses were conducted in triplicate.

Soil pore water was analysed for acetic acid concentration by ion chromatography using a Dionex IC25 Ion Chromatograph. Acetic acid was isolated from 25 μL of 0.1 μm filtered pore water using two sequential IonPac HC11 analytical columns, before quantification by ion-suppressed conductivity detection. The KOH eluent flow rate was 0.2 $mL\,min^{-1}$.

Fractions were analysed by GC/MS using a ThermoQuest Finnigan Trace GC and MS instrument equipped with a nonpolar silica CP Sil5-CB column (50 m × 0.32 mm × 0.12 μm) using the following temperature program: 70°C to 130°C at 20°C min^{-1}, ramp to 300°C at 4°C min^{-1}, and held at 300°C for 10 min. The ionisation potential was 70 eV, with the scanning range *m/z* 50–650. Selected ion monitoring (SIM) of *m/z* 130, 278, and 426 was used to enhance the sensitivity of detection of archaeol.

Semi-quantitative crenarchaeol concentrations were determined using high performance liquid chromatography/atmospheric pressure chemical ionization mass spectrometry (HPLC/APCI-MS). Analyses were performed using an Accela LC system equipped with autosampler coupled to a Thermo Scientific TSQ Quantum Access. Separation of GDGTs was achieved on an Alltech Prevail Cyano column (150 × 2.1 mm; 3 μm particle size) at a flow rate of 2 mL/min, using an isocratic gradient program of hexane and hexane : isopropanol (iPA) as follows (v/v): 90 : 1 for 30 min, 87 : 73 for 5 min, 84 : 16 for 1 min, 0 : 1 for 11 min, and 9 : 1 for 13 min. APCI-MS conditions were as follows: vaporizer temperature 355°C, drying gas N_2, and temperature 200°C, capillary temperature 280°C, corona discharge current 4 μA. Crenarchaeol was detected with SIM of its protonated molecule $[M+H]^+$ by mass scanning of ion *m/z* 1292 and quantified against a C_{46} GDGT standard [34]. The relative response ratio of crenarchaeol relative to the C_{46} GDGT standard is proposed to be 1 : 1, allowing semi-quantitative concentrations to be determined.

3. Results and Discussion

Biomarker distributions at all sites were consistent with previous analyses of soil. Simple lipid and hydrolysed glycolipid fractions were typically dominated by a range of higher plant-derived lipids. In addition to fatty acids, C_{29} steroids such as 24-ethylcholest-5-en-3β-ol, 24-ethylcholesta-5,22-dien-3β-ol, and 24-ethyl-5α-cholestan-3β-ol were prominent in simple lipid fractions, which also included *n*-alkanes

TABLE 1: Soil properties at Caeau Bronydd Mawr, Cefn Cribwr Meadows, and Caeau Ton-y-Fildre [31].

| Site	Site coordinates	Texture	Dominant soil type (Avery 1980)	pH water 0–15 cm	pH water 15–30 cm	Exchange acidity (meq/100 g 105° dry soil)	Cation exchange capacity (meq/100 g 105° dry soil)	Base saturation %
Cefn Cribwr Meadows	51 55.40′N 3 40.12′W	Loamy over clay with sandy patches	Stagnogley	5.37	5.62	1.66	9.031	81.6
Caeau Bronydd Mawr	46.57′N 3 38.46′W	Loamy over clay with sandy patches	Stagnogley	4.92	4.89	1.638	5.541	70.4
Caeau Ton-y-Fildre	51 31.28′N 3 40.5′W	Humose over sandy clay	Stagnohumic gley	5.19	5.27	1.195	8.031	85.1
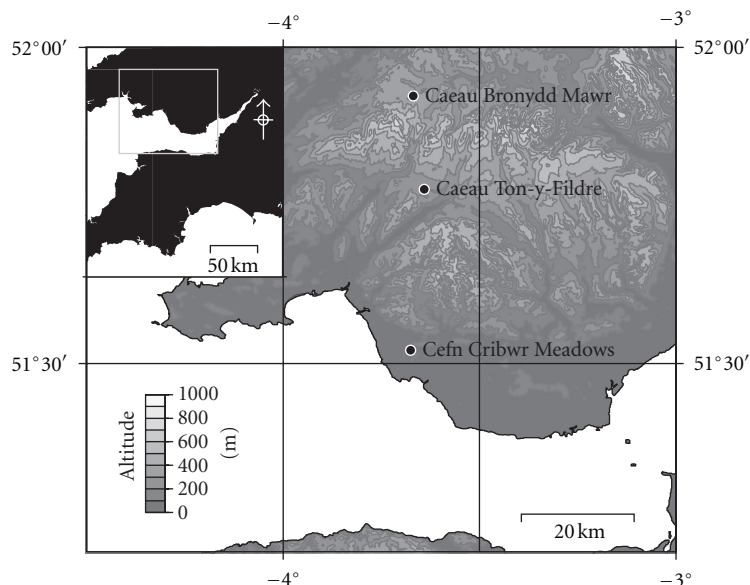
FIGURE 1: Map of Welsh sites: Caeau Ton-y-Fildre, Caeau Bronydd Mawr, and Cefn Cribwr Meadows.
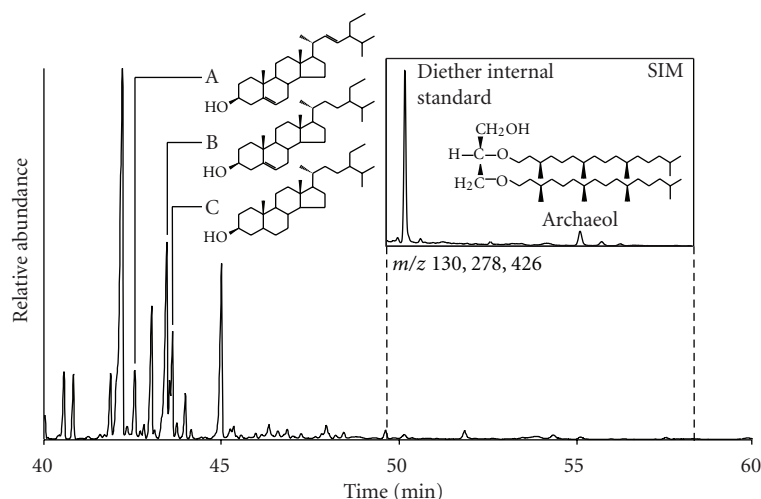

FIGURE 2: Partial total ion current (TIC) chromatogram of typical biomarker distribution at Caeau Ton-y-Fildre in simple lipid fraction. Inset: Partial chromatogram of selected ion monitoring (SIM) of m/z 130, 278, and 426 showing occurrence and structure of archaeol. A, 24-ethylcholesta-5,22-dien-3β-ol; B, 24-ethylcholest-5-en-3β-ol; C, 24-ethyl-5α-cholestan-3β-ol.

of chain length C_{25}–C_{35} with an odd-over-even predominance, and n-alkanols of chain length C_{22}–C_{34} dominated by even-carbon numbers. The latter were also present in acid-hydrolysed glycolipid fractions, in addition to mono-, di- and ω-hydroxy-fatty acids. Suites of phospholipid fatty acids (PLFAs) of bacterial origin and chain length C_{15}–C_{24} were observed in hydrolysed phospholipid fractions, with 16:0, 18:1ω7c, and 18:1ω9c being particularly abundant. Identification of 2,3-di-O-phytanyl-sn-glycerol (archaeol) was achieved by a combination of mass spectra in full scan mode and comparison of retention times in SIM mode with a 1,2-di-O-phytanyl-sn-glycerol standard (Figure 2). Archaeol was only detected in quantifiable amounts (detection limit

2 ng) at the Caeau Ton-y-Fildre site; Cefn Cribwr Meadows yielded trace concentrations in bound forms in the upper 15 cm whereas archaeol was not detected at Caeau Bronydd Mawr.

Trends in free archaeol concentrations and that bound by phosphoric and glycosidic headgroups at Caeau Ton-y-Fildre are shown in Figure 3. Archaeol bound by glycolipid sugar moieties dominates, accounting for up to 76% of the total abundance (at 10–15 cm). The relatively low proportion of free archaeol suggests either: (a) prior to the polar headgroup being lost upon cell lysis, the intact archaeol is recycled into synthesis of tetraether lipids via the head-to-head condensation of phytanyl chains, consistent with
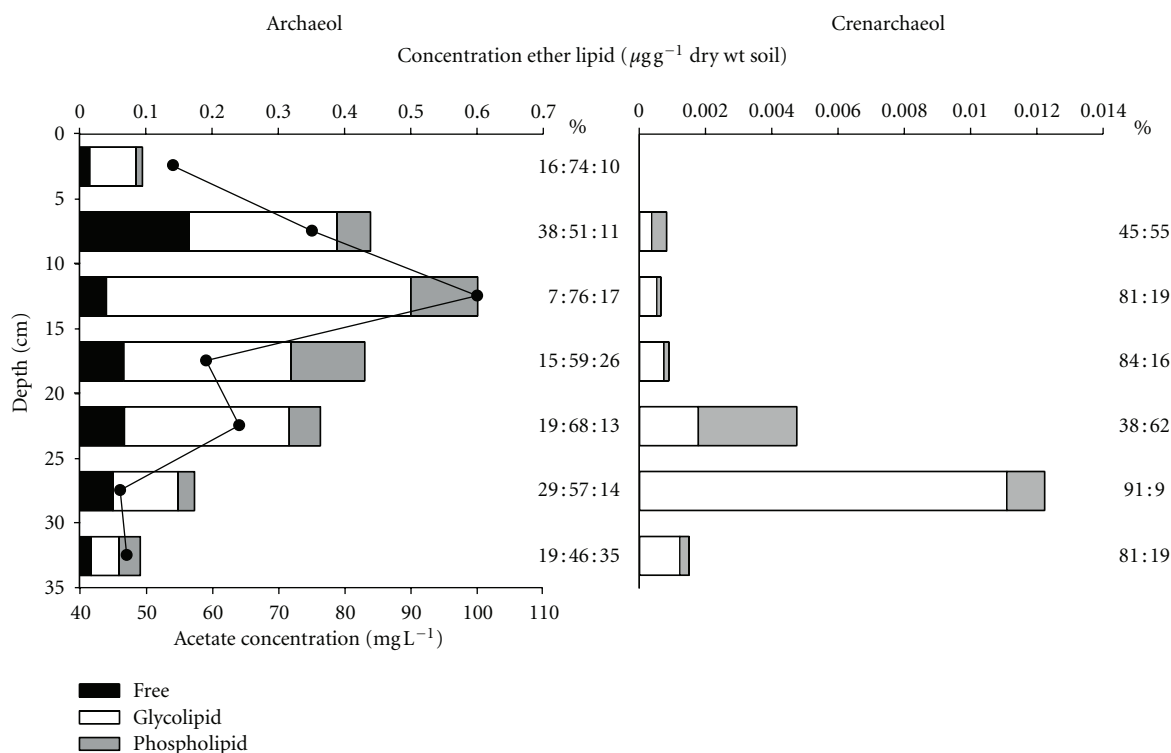
FIGURE 3: Concentrations of archaeol and crenarchaeol ($\mu g\,g^{-1}$ dry wt soil; bars; for quantification details refer to Section 2), and acetate ($mg\,L^{-1}$; circles) with depth at Caeau Ton-y-Fildre. Black, white, and dark grey bars represent free lipids and ether lipids bound by glycolipid moieties and phospholipid headgroups, respectively, in the case of archaeol; for crenarchaeol, white bars include both simple lipids and glycolipids.

biosynthetic models suggested by Nishihara et al. [35]; and/or (b) glycosidic ether lipids may form a large fraction of the fossilised pool of material due to increased resistance to degradation compared to phospholipids [14].

Archaeol bearing glycosidic headgroups also dominates over phosphorylated archaeol, again potentially indicating that the former derives from both living and fossil biomass. Alternatively, it could reflect preferential biosynthesis of the glycosidic form by soil-dwelling *Archaea*, as both glycolipid and phospholipid bound archaeol share the same diether precursor [36, 37]. Hence, the preference for glycolipid-bound archaeol may be due to the increased structural diversity and number of glycolipid structures synthesised by *Archaea* compared to that of phospholipid-bound core lipids [8, 36, 38]. This observation is consistent with previous studies showing that glycosidically-bound archaeal GDGTs rather than bacterial phospholipids are also the principal IPLs in sediments (e.g., [39]).

Since glycolipid-bound archaeol may represent both fossilised and extant biomass, we suggest trends in phospholipid archaeol concentration to be representative of living methanogenic *Archaea* distributions. The Caeau Ton-y-Fildre depth profile (Figure 3) indicates an increase in total archaeol concentration from the surface to a maximum of $0.6\,\mu g\,g^{-1}$ dry wt soil at 10–15 cm, which subsequently diminishes with depth. Although this trend is mostly reflected in the profiles of the individual fractions, the

phospholipid archaeol profile differs slightly, exhibiting maximum concentrations at 10–20 cm. The variance in depth profiles of phospholipid and glycosidic archaeol, particularly at 15–20 cm, suggests differing methanogen populations and/or more likely, that the distributions of living archaeal biomass differs from that of the fossilised biomass.

Archaeol is synthesised by a wide range euryarchaeal phenotypes [40], including methanogens, extreme halophiles and thermophilic *Archaea*. The latter two are unlikely to be present in oxic soils whereas methanogens can reside in anoxic microsites [41]. Ammonia-oxidising *Thaumarchaeota*, which dominate archaeal populations in aerobic soils [29], primarily synthesise GDGTs, specifically crenarchaeol, as opposed to archaeol [42], the former being present in the majority of soils [30]. This is in accordance with the crenarchaeol depth profile differing significantly from the archaeol profile at Caeau Ton-y-Fildre (Figure 3). Concentrations of crenarchaeol increased with depth to a maximum at 25–30 cm, in contrast to archaeol which peaked at 10–15 cm, thus implying derivation from distinct archaeal populations. Although molecular approaches suggest that thaumarchaeotal depth distributions in soil differ between sites [43], similar relationships between methanogen and *Thaumarchaeota* populations have been reported in a peat [44].

The observed downcore increase of archaeol from the surface to 15 cm likely reflects the sensitivity of

methanogenic *Archaea* to oxygen, although archaeol is not entirely absent in the uppermost 5 cm, potentially due to anaerobic conditions in microsites in periodically wet soil at shallow depth. Methanogens are known to survive in such conditions despite the presence of oxygen in soil pores [5, 45, 46]. In peat bogs, an abrupt increase in archaeol concentration coincides with the water table and hence inferred anaerobic conditions [24]. Although no water table is present in these soils, parallels can nonetheless be drawn, with the implication that maximum methanogen biomass will reflect the confluence of high organic substrate concentrations with the onset of sustained or extensive water saturation and development of anoxic microhabitats. Decreasing archaeol concentrations with depth likely reflect the depletion of substrates to support methanogenesis, a key factor for methanogen growth in anoxic environments [47]. Consistent with this observation, the overall trend in archaeol concentration is relatively similar to that of acetate concentrations in soil pore water (Figure 3). Although we note that acetate is not the only substrate that may support methanogenesis, it is known to dominate in the subsurface of organic-rich soils [48], and thus this agreement confirms the importance of organic substrates.

Quantitative detection of archaeol at Caeau Ton-y-Fildre is attributed to high moisture levels and corresponding low oxygen concentrations, which will be associated with the notably greater content of soil organic matter (SOM). The abundance of SOM was highest at 39.5% at the surface of the soil, remaining high (>30%) at 20 cm depth, subsequently decreasing to 5% at 35 cm depth (Figure 4). A high moisture level exerts a primary control of methanogenic populations, and complementing this, high SOM content and heterotrophic soil respiration collectively promote the formation of anoxic microsites in soil peds, which can host anaerobic methanogens [41, 49]. Moreover, high SOM content is likely to increase substrate availability, potentially enhancing CH_4 production [47, 50, 51]. This suggestion is supported by acetate concentrations at Caeau Ton-y-Fildre which mirror concentration trends in archaeol (Figure 3). The lower concentration of archaeol, particularly phosphorylated archaeol, at greater depths, where moisture contents remain high but acetate concentrations and SOM decrease, is evidence that both substrate availability and anoxic microsites control methanogen distribution in the soil.

The absence or very low concentration of archaeol at the other two grassland sites is somewhat enigmatic. Cefn Cribwr Meadows exhibited SOM contents greater than 20% to 15 cm depth and then decreased markedly to 5.7%. Although SOM content was only slightly lower than at Caeau Ton-y-fildre, trace quantities of archaeol were detected in the upper part of the profile, but not below this depth. At Caeau Bronydd Mawr, where SOM content was significantly lower throughout the entire core, exhibiting a maximum of 15% carbon in the shallowest sample, archaeol was absent or below detection limit at all depths. It is possible that small differences in SOM, soil texture and consequently, water retention capacity at these two sites results in less persistent anaerobic conditions within soil peds and microsites. Thus,
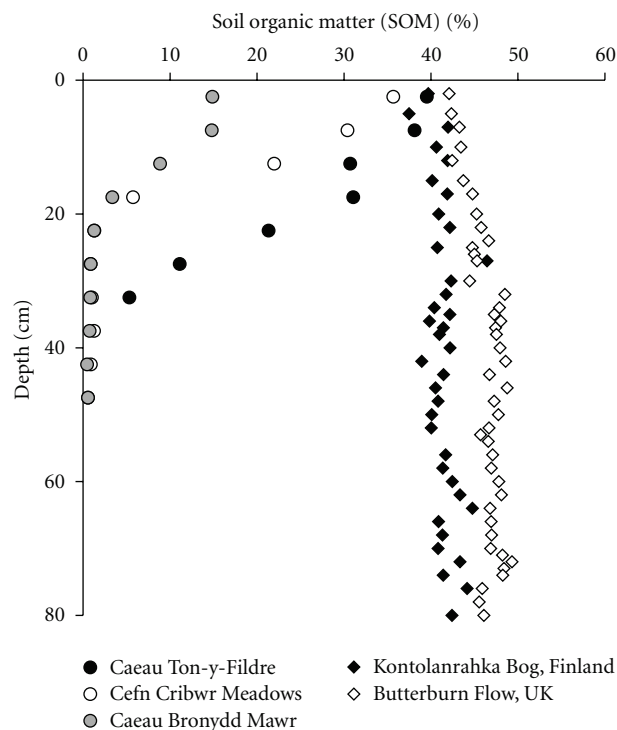

FIGURE 4: Soil organic matter (SOM) content at soil sites (dots): Caeau Ton-y-Fildre (black), Cefn Cribwr Meadows (white), Caeau Bronydd Mawr (grey); compared to peat sites [24] (diamonds): Kontolanrahka Bog, Finland (black), Butterburn Flow, UK (white).

soil moisture content appears to manifest its impact on soil methanogen biomass in multiple, inter-related ways, via its relationship to the formation of anaerobic micro-environments, influence on organic matter preservation and possibly, substrate supply to methanogens.

Figure 5 collates data from a range of sites where intact and/or free archaeol have been measured in various terrestrial environments. Data from studies reporting a combination of all archaeal diethers (e.g., hydroxyarchaeol), as opposed to solely archaeol have been excluded. Most studies of archaeol as a biomarker for methanogenic communities have predominantly focused on analyses of either free or phospholipid archaeol as tools which reflect past or modern living microbiological systems, respectively. Few studies have discussed the implications of archaeol bound by glycosidic headgroups, or all three in combination. Although glycol-ipids are more resistant to diagenesis than phospholipids, it is evident that a proportion of the glyco-archaeol most likely originates from living *Archaea*, since they have been observed in cultured methanogen lipid membranes. Thus, contributions from "dead" versus "living" biomass in natural systems are difficult to distinguish.

Regardless, our data and dataset shown in Figure 5 demonstrates that archaeol concentrations significantly increase from the SOM-lean mineral soil (Caeau Bronydd Mawr), where no archaeol is detected, to SOM-rich soils (Cefn Cribwr Meadows and Caeau Ton-y-Fildre) and per-mafrost, where significantly higher archaeol contents were
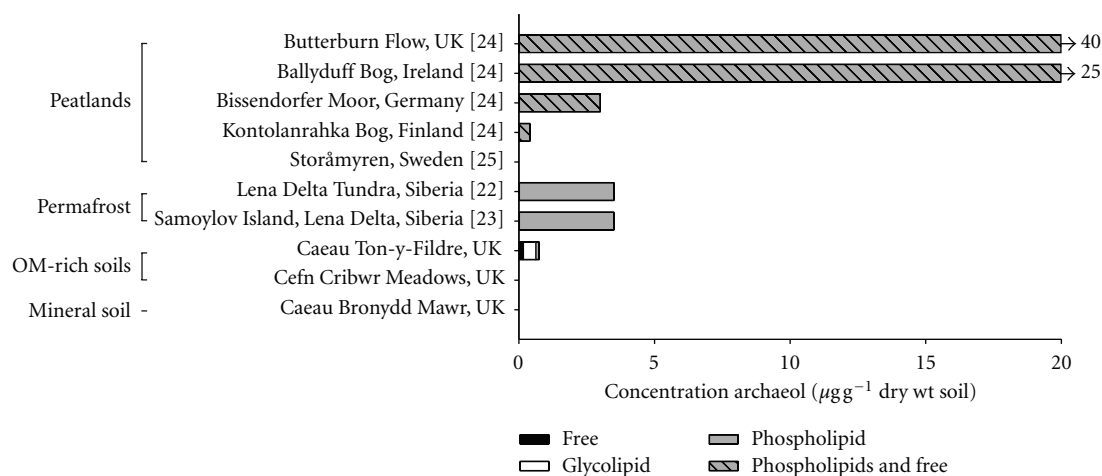
FIGURE 5: Concentration of archaeol in peat, permafrost and oxic soils (references in square brackets): free (black), glycosidic-bound (white), phospholipid-bound (grey), phospholipids and free (striped).

found, and subsequently peatlands. Highest archaeol concentrations of up to $40\,\mu g\,g^{-1}$ were observed in a British ombrotrophic bog [24], despite not including glycolipids. Although variable, archaeol concentrations in peatlands (Figure 5), where high SOM is maintained throughout the profile, are generally higher than the organic-rich soils in this study, in which the SOM abundance decreases markedly below 20 cm depth (Figure 4). Concentrations observed at Caeau Ton-y-Fildre are comparable only to higher latitude peatlands, such as the Swedish and Finnish sites [24]. Moisture content, via its impact on organic matter preservation and anoxia, may exert a significant control on soil methanogen biomass and thus could influence rates of methanogenesis in various soils [52]. Corresponding trends have been observed between archaeal phospholipids and CH_4 concentrations in permafrost [23]. It should also be noted that methanogen viability is sustained in oxic conditions, thus it cannot be excluded that biomass distributions may not reflect absolute CH_4 production rates as oxygen suppresses methanogen capability rather than disrupting community structure [53, 54].

4. Conclusions

The core lipid archaeol has been investigated as a proxy for anaerobic methanogen biomass in free and conjugated forms in depth profiles of three wet oxic soils. Archaeol was detected in quantifiable concentrations at only one site, which displayed the highest soil organic matter content. Glycosidic archaeol represented a significant proportion of total archaeol, implying accumulation as a result of its recalcitrance relative to phospholipids. Alternatively, it could simply reflect that soil methanogens predominantly biosynthesise glycosidically-bound archaeol. Trends in archaeol abundance did not reflect those of crenarchaeol, representative of ammonia-oxidising *Thaumarchaeota*, confirming an origin from differing archaeal sources. High carbon contents and increased soil moisture are thought to be the interlinked factors driving observed trends in archaeol

concentration, due to their association with development of anoxic microniches and substrate availability. Thus, while we acknowledge that future work should also consider tetraether archaeal intact polar lipids, we tentatively propose the use of archaeol as an indicator for methanogen biomass and consequently CH_4 production within terrestrial soils. This provides the potential to better understand the occurrence and prevalence of methanogenesis as a result of changes in moisture, as well as their potential for CH_4 production, and, by extension, the capacity of soils to function as a sink for atmospheric CH_4.

Acknowledgments

References

[1] D. Wagner and E. M. Pfeiffer, "Two temperature optima of methane production in a typical soil of the Elbe river marshland," *FEMS Microbiology Ecology*, vol. 22, no. 2, pp. 145–153, 1997.

[2] A. Kiener and T. Leisinger, "Oxygen sensitivity of methanogenic bacteria," *Systematic and Applied Microbiology*, vol. 4, no. 3, pp. 305–312, 1983.

[3] Y. A. Teh, W. L. Silver, and M. E. Conrad, "Oxygen effects on methane production and oxidation in humid tropical forest soils," *Global Change Biology*, vol. 11, no. 8, pp. 1283–1297, 2005.

[4] M. Keller, W. A. Reiners, and E. Veldkamp, "Pasture age effects on nitrous oxide, nitric oxide and methane emissions in the

Atlantic Lowlands of Costa Rica," *Bulletin of the Ecological Society of America*, vol. 74, p. 304, 1993.

[5] V. Peters and R. Conrad, "Sequential reduction processes and initiation of CH4 production upon flooding of oxic upland soils," *Soil Biology & Biochemistry*, vol. 28, no. 3, pp. 371–382, 1996.

[6] R. Angel, D. Matthies, and R. Conrad, "Activation of methanogenesis in arid biological soil crusts despite the presence of oxygen," *PLoS ONE*, vol. 6, no. 5, Article ID e20453, 2011.

[7] Y. Koga, M. Akagawa-Matsushita, M. Ohga, and M. Nishihara, "Taxonomic significance of the distribution of component parts of polar ether lipids in methanogens," *Systematic and Applied Microbiology*, vol. 16, no. 3, pp. 342–351, 1993.

[8] Y. Koga, H. Morii, M. Akagawa-Matsushita, and M. Ohga, "Correlation of polar lipid composition with 16S rRNA phylogeny in methanogens. Further analysis of lipid component parts," *Bioscience, Biotechnology and Biochemistry*, vol. 62, no. 2, pp. 230–236, 1998.

[9] H. R. Harvey, R. D. Fallon, and J. S. Patton, "The effect of organic matter and oxygen on the degradation of bacterial membrane lipids in marine sediments," *Geochimica et Cosmochimica Acta*, vol. 50, no. 5, pp. 795–804, 1986.

[10] P. E. Rossel, J. S. Lipp, H. F. Fredricks et al., "Intact polar lipids of anaerobic methanotrophic archaea and associated bacteria," *Organic Geochemistry*, vol. 39, no. 8, pp. 992–999, 2008.

[11] E. C. Hopmans, S. Schouten, R. D. Pancost, M. T. van der Meer, and J. S. Sinninghe Damsté, "Analysis of intact tetraether lipids in archaeal cell material and sediments by high performance liquid chromatography/atmospheric pressure chemical ionization mass spectrometry," *Rapid Communications in Mass Spectrometry*, vol. 14, no. 7, pp. 585–589, 2000.

[12] A. Pitcher, E. C. Hopmans, S. Schouten, and J. S. Sinninghe Damsté, "Separation of core and intact polar archaeal tetraether lipids using silica columns: insights into living and fossil biomass contributions," *Organic Geochemistry*, vol. 40, no. 1, pp. 12–19, 2009.

[13] D. C. White, W. M. Davis, J. S. Nickels, J. D. King, and R. J. Bobbie, "Determination of the sedimentary microbial biomass by extractible lipid phosphate," *Oecologia*, vol. 40, no. 1, pp. 51–62, 1979.

[14] S. Schouten, J. J. Middelburg, E. C. Hopmans, and J. S. Sinninghe Damsté, "Fossilization and degradation of intact polar lipids in deep subsurface sediments: a theoretical approach," *Geochimica et Cosmochimica Acta*, vol. 74, no. 13, pp. 3806–3814, 2010.

[15] C. R. Woese, O. Kandler, and M. L. Wheelis, "Towards a natural system of organisms: proposal for the domains Archaea, Bacteria, and Eucarya," *Proceedings of the National Academy of Sciences of the United States of America*, vol. 87, no. 12, pp. 4576–4579, 1990.

[16] Q. Bai, A. Gattinger, and L. Zelles, "Characterization of microbial consortia in paddy rice soil by phospholipid analysis," *Microbial Ecology*, vol. 39, no. 4, pp. 273–281, 2000.

[17] S. Asakawa, M. Akagawa-Matsushita, Y. Koga, and K. Hayano, "Communities of methanogenic bacteria in paddy field soils with long-term application of organic matter," *Soil Biology & Biochemistry*, vol. 30, no. 3, pp. 299–303, 1998.

[18] K. Demizu, S. Ohtsubo, S. Kohno, I. Miura, M. Nishihara, and Y. Koga, "Quantitative determination of methanogenic cells based on analysis of ether-linked glycerolipids by high-performance liquid chromatography," *Journal of Fermentation and Bioengineering*, vol. 73, no. 2, pp. 135–139, 1992.

[19] S. Ohtsubo, M. Kanno, H. Miyahara, S. Kohno, Y. Koga, and I. Miura, "A sensitive method for quantification of aceticlastic methanogens and estimation of total methanogenic cells in natural environments based on an analysis of ether-linked glycerolipids," *FEMS Microbiology Ecology*, vol. 12, no. 1, pp. 39–50, 1993.

[20] M. Sunamura, Y. Koga, and K. Ohwada, "Biomass measurement of methanogens in the sediments of Tokyo Bay using archaeol lipids," *Marine Biotechnology*, vol. 1, no. 6, pp. 562–568, 1999.

[21] F. L. Gill, R. J. Dewhurst, J. A. J. Dungait et al., "Archaeol—a biomarker for foregut fermentation in modern and ancient herbivorous mammals?" *Organic Geochemistry*, vol. 41, no. 5, pp. 467–472, 2010.

[22] D. Wagner, A. Lipski, A. Embacher, and A. Gattinger, "Methane fluxes in permafrost habitats of the Lena Delta: effects of microbial community structure and organic matter quality," *Environmental Microbiology*, vol. 7, no. 10, pp. 1582–1592, 2005.

[23] D. Wagner, A. Gattinger, A. Embacher, E.-M. Pfeiffer, M. Schloter, and A. Lipski, "Methanogenic activity and biomass in Holocene permafrost deposits of the Lena Delta, Siberian Arctic and its implication for the global methane budget," *Global Change Biology*, vol. 13, no. 5, pp. 1089–1099, 2007.

[24] R. D. Pancost, E. L. McClymont, E. M. Bingham et al., "Archaeol as a methanogen biomarker in ombrotrophic bogs," *Organic Geochemistry*, vol. 42, no. 10, pp. 1279–1287, 2011.

[25] H. Fritze, P. Tikka, T. Pennanen et al., "Detection of Archaeal diether lipid by gas chromatography from humus and peat," *Scandinavian Journal of Forest Research*, vol. 14, no. 6, pp. 545–551, 1999.

[26] R. D. Pancost and J. S. Sinninghe Damsté, "Carbon isotopic compositions of prokaryotic lipids as tracers of carbon cycling in diverse settings," *Chemical Geology*, vol. 195, no. 1–4, pp. 29–58, 2003.

[27] G. Wachinger, S. Fiedler, K. Zepp, A. Gattinger, M. Sommer, and K. Roth, "Variability of soil methane production on the micro-scale: spatial association with hot spots of organic material and Archaeal populations," *Soil Biology & Biochemistry*, vol. 32, no. 8-9, pp. 1121–1130, 2000.

[28] P. D. Nichols, C. A. Mancuso, and D. C. White, "Measurement of methanotroph and methanogen signature phosopholipids for use in assessment of biomass and community structure in model systems," *Organic Geochemistry*, vol. 11, no. 6, pp. 451–461, 1987.

[29] S. Leininger, T. Urich, M. Schloter et al., "Archaea predominate among ammonia-oxidizing prokaryotes in soils," *Nature*, vol. 442, no. 7104, pp. 806–809, 2006.

[30] J. W. H. Weijers, S. Schouten, O. C. Spaargaren, and J. S. Sinninghe Damsté, "Occurrence and distribution of tetraether membrane lipids in soils: implications for the use of the TEX86 proxy and the BIT index," *Organic Geochemistry*, vol. 37, no. 12, pp. 1680–1693, 2006.

[31] P. A. Stevens, S. A. Brittain, S. Hughes, T. H. Sparks, and J. Worth, "Soil/plant interactions in lowland grassland. Soil analyses and interpretation," Institute of Terrestrial Ecology, Natural Environmental Research Council, Gwynedd, 1994.

[32] L. Dickson, I. D. Bull, P. J. Gates, and R. P. Evershed, "A simple modification of a silicic acid lipid fractionation protocol to eliminate free fatty acids from glycolipid and phospholipid fractions," *Journal of Microbiological Methods*, vol. 78, no. 3, pp. 249–254, 2009.

[33] Y. Koga and H. Morii, "Special methods for the analysis of ether lipid structure and metabolism in archaea," *Analytical Biochemistry*, vol. 348, no. 1, pp. 1–14, 2006.

[34] C. Huguet, E. C. Hopmans, W. Febo-Ayala, D. H. Thompson, J. S. Sinninghe Damsté, and S. Schouten, "An improved method to determine the absolute abundance of glycerol dibiphytanyl glycerol tetraether lipids," *Organic Geochemistry*, vol. 37, no. 9, pp. 1036–1041, 2006.

[35] M. Nishihara, H. Morii, and Y. Koga, "Heptads of polar ether lipids of an archaebacterium, Methanobacterium thermoautotrophicum: structure and biosynthetic relationship," *Biochemistry*, vol. 28, no. 1, pp. 95–102, 1989.

[36] M. Kates, "Membrane lipids of archaea," in *The Biochemistry of Archaea (Archaebacteria)*, M. Kates, D. J. Kushner, and A. T. Matheson, Eds., pp. 261–292, Elsevier, Amsterdam, The Netherlands, 1993.

[37] N. Moldoveanu and M. Kates, "Biosynthetic studies of the polar lipids of Halobacterium cutirubrum. Formation of isoprenyl ether intermediates," *Biochimica et Biophysica Acta*, vol. 960, no. 2, pp. 164–182, 1988.

[38] M. Kates, "Diether and Tetraether phospholipids and Glycolipids as molecular markers for Archaebacteria (Archaea)," in *Molecular Markers in Environmental Chemistry*, R. P. Eganhouse, Ed., vol. 671 of *ACS Symposium Series*, pp. 35–48, American Chemical Society, Washington, DC, USA, 1997.

[39] J. S. Lipp, Y. Morono, F. Inagaki, and K.-U. Hinrichs, "Significant contribution of Archaea to extant biomass in marine subsurface sediments," *Nature*, vol. 454, no. 7207, pp. 991–994, 2008.

[40] Y. Koga, M. Nishihara, H. Morii, and M. Akagawa-Matsushita, "Ether polar lipids of methanogenic bacteria: structures, comparative aspects, and biosyntheses," *Microbiological Reviews*, vol. 57, no. 1, pp. 164–182, 1993.

[41] L. V. Verchot, E. A. Davidson, J. H. Cattânio, and I. L. Ackerman, "Land-use change and biogeochemical controls of methane fluxes in soils of eastern Amazonia," *Ecosystems*, vol. 3, no. 1, pp. 41–56, 2000.

[42] J. S. Sinninghe Damsté, S. Schouten, E. C. Hopmans, A. C. T. van Duin, and J. A. J. Geenevasen, "Crenarchaeol: the characteristic core glycerol dibiphytanyl glycerol tetraether membrane lipid of cosmopolitan pelagic crenarchaeota," *Journal of Lipid Research*, vol. 43, no. 10, pp. 1641–1651, 2002.

[43] M. K. Sliwinski and R. M. Goodman, "Spatial heterogeneity of crenarchaeal assemblages within mesophilic soil ecosystems as revealed by PCR-single-stranded conformation polymorphism profiling," *Applied and Environmental Microbiology*, vol. 70, no. 3, pp. 1811–1820, 2004.

[44] A. Putkinen, H. Juottonen, S. Juutinen, E.-S. Tuittila, H. Fritze, and K. Yrjälä, "Archaeal rRNA diversity and methane production in deep boreal peat," *FEMS Microbiology Ecology*, vol. 70, no. 1, pp. 87–98, 2009.

[45] F. L. Wang and J. R. Bettany, "Methane emission from Canadian prairie and forest soils under short term flooding conditions," *Nutrient Cycling in Agroecosystems*, vol. 49, no. 1–3, pp. 197–202, 1997.

[46] F. L. Wang and J. R. Bettany, "Methane emission from a usually well-drained prairie soil after snowmelt and precipitation," *Canadian Journal of Soil Science*, vol. 75, no. 2, pp. 239–241, 1995.

[47] I. Bergman, B. H. Svensson, and M. Nilsson, "Regulation of methane production in a swedish acid mire by pH, temperature and substrate," *Soil Biology & Biochemistry*, vol. 30, no. 6, pp. 729–741, 1998.

[48] E. R. C. Hornibrook, F. J. Longstaffe, and W. S. Fyfe, "Spatial distribution of microbial methane production pathways in temperate zone wetland soils: stable carbon and hydrogen isotope evidence," *Geochimica et Cosmochimica Acta*, vol. 61, no. 4, pp. 745–753, 1997.

[49] G. J. Whiting and J. P. Chanton, "Primary production control of methane emission from wetlands," *Nature*, vol. 364, no. 6440, pp. 794–795, 1993.

[50] R. T. Williams and R. L. Crawford, "Methane production in Minnesota peatlands," *Applied and Environmental Microbiology*, vol. 47, no. 6, pp. 1266–1271, 1984.

[51] D. W. Valentine, E. A. Holland, and D. S. Schimel, "Ecosystem and physiological controls over methane production in northern wetlands," *Journal of Geophysical Research-Atmospheres*, vol. 99, pp. 1563–1571, 1994.

[52] T. E. Freitag and J. I. Prosser, "Correlation of methane production and functional gene transcriptional activity in a peat soil," *Applied and Environmental Microbiology*, vol. 75, no. 21, pp. 6679–6687, 2009.

[53] S. Fetzer, F. Bak, and R. Conrad, "Sensitivity of methanogenic bacteria from paddy soil to oxygen and desiccation," *FEMS Microbiology Ecology*, vol. 12, no. 2, pp. 107–115, 1993.

[54] T. Lueders and M. Friedrich, "Archaeal population dynamics during sequential reduction processes in rice field soil," *Applied and Environmental Microbiology*, vol. 66, no. 7, pp. 2732–2742, 2000.

Research Article

RNA-Based Assessment of Diversity and Composition of Active Archaeal Communities in the German Bight

Bernd Wemheuer,[1] Franziska Wemheuer,[2] and Rolf Daniel[1]

[1] *Department of Genomic and Applied Microbiology and Göttingen Genomics Laboratory,*
 Institute of Microbiology and Genetics, Georg-August University of Göttingen, Grisebachstraße 8, 37077 Göttingen, Germany
[2] *Section of Agricultural Entomology, Department for Crop Sciences, Georg-August University of Göttingen, Grisebachstraße 6, 37077*
 Göttingen, Germany

Correspondence should be addressed to Rolf Daniel, rdaniel@gwdg.de

Archaea play an important role in various biogeochemical cycles. They are known extremophiles inhabiting environments such as thermal springs or hydrothermal vents. Recent studies have revealed a significant abundance of *Archaea* in moderate environments, for example, temperate sea water. Nevertheless, the composition and ecosystem function of these marine archaeal communities is largely unknown. To assess diversity and composition of active archaeal communities in the German Bight, seven marine water samples were taken and studied by RNA-based analysis of ribosomal 16S rRNA. For this purpose, total RNA was extracted from the samples and converted to cDNA. Archaeal community structures were investigated by pyrosequencing-based analysis of 16S rRNA amplicons generated from cDNA. To our knowledge, this is the first study combining next-generation sequencing and metatranscriptomics to study archaeal communities in marine habitats. The pyrosequencing-derived dataset comprised 62,045 archaeal 16S rRNA sequences. We identified *Halobacteria* as the predominant archaeal group across all samples with increased abundance in algal blooms. *Thermoplasmatales* (*Euryarchaeota*) and the Marine Group I (*Thaumarchaeota*) were identified in minor abundances. It is indicated that archaeal community patterns were influenced by environmental conditions.

1. Introduction

It has been calculated that one mL of oceanic sea water contains up to 10^6 different microorganisms [1]. These archaea, bacteria, protists, and unicellular fungi contribute 98% to the primary biomass production and are involved in almost all biogeochemical cycles [2]. It has been estimated that the global ocean harbors approximately 1.3×10^{28} archaeal cells and 1.3×10^{28} bacterial cells, which together constitute 63% to 90% of the entire marine picoplankton [3]. In addition, high numbers of *Archaea* have been found in marine sediments [4].

In contrast to their relatives living in extreme environments, little is known on marine *Archaea.* This is partly due to the unavailability of pure cultures. Marine *Archaea* might be involved in the oceanic nitrogen cycle as some marine *Crenarchaeota* are capable of nitrification [5]. However,

our knowledge of the archaeal role in oceanic ecology is rudimentary and their influence on global biogeochemical cycles is largely unexplored [6].

Culture-independent approaches have greatly advanced our knowledge of the diversity and ecology of marine microbial communities [7–9]. Next-generation sequencing (NGS) contributed to this advancement. For example, many different ecosystems such as soil [10, 11] or sea water [12] have been studied by DNA-based high throughput sequencing of 16S rRNA gene fragments and analysis of the obtained sequences. The main drawback of DNA-based metagenomic approaches is the inability to distinguish between active and inactive community members.

Active members and functions of microbial communities are accessible by employing RNA-based metatranscriptomic approaches. For example, Urich et al. [13] analyzed the composition and metabolic potential of active soil microbial

communities by sequencing of reverse transcribed total RNA. Other studies analyzed gene expression in ocean surface waters [8] or in a deep-sea hydrothermal plume [14]. However, mainly bacterial communities and their capabilities were analyzed in these studies.

In this paper, we investigated the composition of active archaeal communities in surface water derived from the southeastern part of the North Sea, the German Bight. The northwest of the German Bight is separated from the remaining North Sea by the Doggerbank, a large sandbank. Large coastal parts of the bight are shallow with water depths of approximately 2 to 12 meters. In our investigation, we collected seven water samples at different locations and depths in these shallow offshore areas.

The aim of our study was to assess the active archaeal community structures in the southern North Sea employing next-generation sequencing of 16S rRNA amplicons generated by reverse transcription polymerase chain reaction (RT-PCR). To our knowledge, this is the first study using this combined approach to study marine archaeal communities.

2. Material and Methods

2.1. Sampling and Sample Preparation. Seven marine water samples were taken for archaeal community analysis. Approximately 50 liters of sea water per sampling site were collected on board of the research vessel Heincke in May 2010 employing a conductivity, temperature, and depth (CTD) profiler. All sites were located in the German Bight. Sea water samples were prefiltered through a 10 μm-mesh-size nylon net and a filter sandwich consisting of a precombusted (4 h at 450°C) 47 mm-diameter glass fiber filter (Whatman GF/D; Whatman, Maidstone, UK) and a 47 mm-diameter (pore size 3.0 μm) polycarbonate filter (Nuclepore, Whatman). Bacterioplankton was harvested by filtration of 1 L prefiltered sea water through a filter sandwich consisting of a glass fiber filter (Whatman GF/F) and a 47 mm-diameter (pore size 0.2 μm) polycarbonate filter (Nuclepore, Whatman).

Additionally, marine phytoplankton samples were collected by employing a plankton net (pore size 55 μm). The composition of the algal community was determined by microscopy of the collected samples.

2.2. RNA Extraction and Purification. Total RNA was extracted as described by Weinbauer et al. [15]. One 47 mm-diameter filter (pore size 0.2 μm) was used per sample. Subsequently, RNA was purified employing the RNeasy Mini Kit as recommended by the manufacturer (Qiagen, Hilden, Germany).

To remove residual DNA from RNA samples, Ambions TURBO DNase (Invitrogen, Carlsbad, USA) was used according to the instructions of the manufacturer with one modification: subsequent to a standard reaction, 0.5 μL of TURBO DNase per 10 μg of RNA was added to the mixture, and incubation was performed at 37°C for 15 min. Phenol/Chloroform/Isoamyl alcohol (25 : 24 : 1) was used to inactivate the DNase.

The presence of remaining DNA was tested by PCR using the 16S rRNA gene as a target gene for amplification. The following two primer sets were employed: 8F/518R (5′- AGAGTTTGATCCTGGCTCAG-3′ [16] and 5′-ATTACCGCGGCTGCTGG-3′ [17]) and 1055F/1378R (5′-ATGGCTGTCGTCAGCT-3′ [18] and 5′-CGGTGTGTACA-AGGCCCGGGAACG-3′ [19]).

The PCR reaction mixture (25 μL) for amplification of the target gene contained 2.5 μL of 10-fold Mg-free *Taq* polymerase buffer (Fermentas, St. Leon-Rot, Germany), 200 μM of each of the four desoxynucleoside triphosphates, 1.75 mM MgCl$_2$, 0.4 μM of each primer, 1 U of *Taq* DNA polymerase (Fermentas), and approximately 100 ng of purified RNA sample as template. The following thermal cycling scheme was used: initial denaturation at 94°C for 2 min, 28 cycles of denaturation at 94°C for 1.5 min, annealing at 55°C for 1 min, followed by extension at 72°C for 40 s. The final extension was carried out at 72°C for 10 min.

2.3. Synthesis of cDNA from Total RNA. cDNA was synthesized from total RNA by employing the SuperScript Double-Stranded cDNA Synthesis Kit (Invitrogen) with modifications of the first strand synthesis protocol: 10 μL of total RNA (up to 5 μg) were mixed with 1 μL of random hexamer primers (Roche, Mannheim, Germany) and 1 μL dNTP mixture containing 10 mM of each of the four desoxynucleoside triphosphates. The mixture was incubated for 10 min at 70°C and chilled on ice. Four μL 5x first-strand buffer, 1 μL of 0.1 M DTT, and 1 μL RNA protect (Fermentas) were added, and the reaction mixture was incubated for 2 min at 25°C. Subsequently, 1 μL of SuperScript II reverse transcriptase was added. The reaction was incubated for 10 min at 25°C and then for 1 h at 45°C. The generated cDNA was subjected to 16S rRNA PCR.

2.4. Amplification of 16S rRNA and Pyrosequencing. To analyze archaeal diversity, the V3–V5 region of the archaeal 16S rRNA was amplified by PCR. The PCR reaction (25 μL) contained 5 μL of 5-fold Phusion GC buffer (Finnzymes, Vantaa, Finland), 200 μM of each of the four desoxynucleoside triphosphates, 1.5 mM MgCl$_2$, 4 μM of each primer (Table 1), 2.5% DMSO, 1 U of Phusion High Fidelity Hot Start DNA polymerase (Finnzymes), and approximately 50 ng of cDNA. The following thermal cycling scheme was used: initial denaturation at 98°C for 5 min, 25 cycles of denaturation at 98°C for 45 s, annealing at 68°C for 45 s, followed by extension at 72°C for 30 s. The final extension was carried out at 72°C for 5 min. Negative controls were performed by using the reaction mixture without template. Primer sequences for amplification of the V3–V5 region [20] as well as 454 adaptors with the unique MIDs for each sample are listed in Table 1. The resulting PCR products were checked for appropriate size and then purified by using the peqGOLD Gel Extraction Kit (Peqlab, Erlangen, Germany) as recommended by the manufacturer. Three independent PCR reactions were performed per sample, purified by gel extraction, and pooled in equal amounts. Quantification of the PCR products was performed using the Quant-iT dsDNA

TABLE 1: Primers used for amplification of the V3–V5 region of the archaeal 16S rRNA [20].

Sample	Primer	Sequence (5′-3′)			
		454-Adaptor (Lip-A Kit)	Key	Unique MID	Archaeal 16S rRNA specific
655	ARC344F	CGTATCGCCTCCCTCGCGCCA	TCAG	ACTGTACAGT	ACGGGGYGCAGCAGGCGCGA
658	ARC344F	CGTATCGCCTCCCTCGCGCCA	TCAG	AGACTATACT	ACGGGGYGCAGCAGGCGCGA
659	ARC344F	CGTATCGCCTCCCTCGCGCCA	TCAG	AGCGTCGTCT	ACGGGGYGCAGCAGGCGCGA
660	ARC344F	CGTATCGCCTCCCTCGCGCCA	TCAG	AGTACGCTAT	ACGGGGYGCAGCAGGCGCGA
664	ARC344F	CGTATCGCCTCCCTCGCGCCA	TCAG	ATAGAGTACT	ACGGGGYGCAGCAGGCGCGA
670	ARC344F	CGTATCGCCTCCCTCGCGCCA	TCAG	CACGCTACGT	ACGGGGYGCAGCAGGCGCGA
671	ARC344F	CGTATCGCCTCCCTCGCGCCA	TCAG	CAGTAGACGT	ACGGGGYGCAGCAGGCGCGA
All	ARC915R	CTATGCGCCTTGCCAGCCCGC	TCAG	ACAGTATATA	GTGCTCCCCGCCAATTCCT

BR Assay Kit and a Qubit fluorometer (Invitrogen) as recommended by the manufacturer. The Göttingen Genomics Laboratory determined the sequences of the 16S rRNA by using a Roche GS-FLX 454 pyrosequencer with Titanium chemistry (Roche, Mannheim, Germany).

2.5. Processing and Analysis of Pyrosequencing Derived Data Sets. Sequence data were deposited in the sequence read archive of the National Center for Biotechnology Information under accession number SRA056839. Generated 16S rRNA datasets were processed and analyzed employing the QIIME 1.4 software package and other tools [21]. The sequences were initially processed according to the denoising of 454 datasets workflow. Sequences shorter than 300 bp, with an average quality value below 25, or possessing homopolymers longer than 8 bp were removed. Afterwards, the sequences were denoised. Cutadapt was used to truncate remaining primer sequences [22]. Chimeric sequences were removed using UCHIME and the Green Genes Gold dataset as reference database [23–25].

Remaining sequences were clustered employing the UCLUST algorithm [23] and the following QIIME scripts: pick_otus.py and pick_rep_set.py. The sequences were clustered in operational taxonomic units (OTUs) at 3% and 1% genetic dissimilarity. Phylogenetic composition was determined using the QIIME assign_taxonmy.py script. A BLAST alignment [26] against the most recent Silva ARB database [27] was thereby performed. Sequences were classified with respect to the taxonomy of their best hit in the ARB database. Finally, OTU tables were generated.

2.6. Rarefaction Analysis and Diversity Analysis. Rarefaction curves, Shannon indices [28], and Chao1 indices [29] were calculated employing QIIME scripts. In addition, the maximal number of OTUs ($n_{\max}$) was estimated for each sample in R (version 2.15) [30] using the data derived from the QIIME rarefaction analysis and a nonlinear regression model based on Michaelis-Menten kinetics [31].

To compare archaeal community structures across all samples based on phylogenetic or count-based distance metrics, a principal coordinate analysis (PCoA) was performed using QIIME. The following scripts were successively used to generate a phylogenetic tree at 1% genetic distance prior to PCoA calculation: align_seqs.py (PyNAST algorithm),
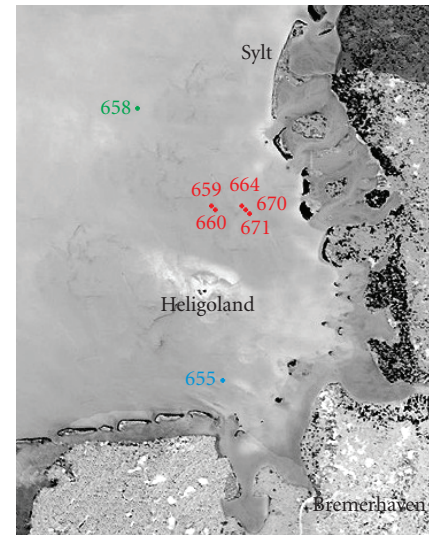
FIGURE 1: Satellite image of the German Bight showing the locations of the seven sampling sites (Image: ESA/NASA - SOHO/LASCO). Samples taken during an algal bloom (samples 659, 660, 664, 670, and 671) are shown in red. Sample 655 taken at a river outfall and sample 658 originating from outside the algal bloom in blue and green, respectively.

filter_alignment.py, and make_phylogeny.py. The tree and the respective OTU table were used to generate PCoAs employing the "beta_diversity_through_plots.py" script.

3. Results

3.1. Environmental Parameters. Marine water samples for archaeal community analysis were randomly collected at seven different locations in the German Bight (Figure 1, Table 2). Five samples (sites 659, 660, 664, 670, and 671) were taken in presence of an algal bloom. The other two samples derived from a river outfall (655) and from a site outside the algal bloom (658). The algal blooms observed during the sampling were mainly dominated by the genus *Phaeocystis*. Diatoms of the genus *Rhizosolenia* and some dinoflagellates were also identified but only in minor abundances.

TABLE 2: Parameters of sampling sites analyzed in this study.

	Site	Latitude °N	Longitude °E	Depth (m)	T (°C)	Salinity (psu)	Fluorescence (mg/m³)	Transmission (%)
655	River outfall	53°53.729	8°02.979	2	11.09	30.24	1.21	57.2
658	No bloom	54°45.754	7°26.780	2	9.73	32.71	0.49	81.23
659	Bloom	54°27.450	7°59.360	9	10.80	30.64	2.76	60.14
660	Bloom	54°27.250	8°00.110	2	10.83	30.65	1.89	72.28
664	Bloom	54°28.400	8°11.830	2	10.90	30.76	1.14	87.28
670	Bloom	54°27.570	8°12.420	2	11.43	30.83	—*	75.72
671	Bloom	54°26.940	8°12.970	2	11.70	31.04	—*	76.59

* Fluorescence was not measured due to a malfunction of the profiler.

Environmental factors at all seven sampling sites were monitored employing a CTD profiler (Table 2). Temperatures and salinities ranged from 9.73 to 11.70°C and from 30.24 to 32.71 psu, respectively. The lowest temperature and highest salinity were measured at site 658. All other sites showed similar conditions. Fluorescence was higher at bloom sites due to a higher chlorophyll concentration, whereas transmission was reduced due to a higher turbidity in the water.

3.2. Archaeal Community Structure Revealed by 16S rRNA-Based Analysis. To assess archaeal community structures, total RNA was extracted from the samples. Approximately 5 μg of total RNA per filter were extracted from each sample. After removal of contaminating DNA and small RNAs, 0.25 to 1.5 μg of RNA were used as template for cDNA synthesis. The V3–V5 region of the 16S rRNA was amplified from the generated cDNA. The resulting PCR products were subjected to pyrosequencing. Sequence processing including quality filtering, denoising, and removal of potential chimeric sequences resulted in recovery of 62,090 high quality sequences with a read length of ≥300 bp across all 7 samples. The average read length was 506 bp. The number of sequences per sample ranged from 4,301 to 23,070. We were able to assign 62,045 sequences to the domain *Archaea* and to classify all of these sequences below the domain level. The classified sequences were affiliated to three archaeal phyla with twelve archaeal classes or similar phylogenetic groups. *Euryarchaeota* was the most abundant archaeal phylum (99.25%) and *Halobacteria* the predominant class across all samples (>98.1%) (Figure 2). Most of the sequences affiliated to the *Halobacteria* (97.81%) were affiliated to uncultured members of the Deep Sea Hydrothermal Vent Group 6 (DHVEG-6) [32]. Interestingly, *Halobacteria* were more abundant in bloom samples than in other samples (Figure 2). Other archaeal groups present in all samples were the Marine Group I (*Thaumarchaeota*) [33] and the *Thermoplasamata* (*Euryarchaeota*). Sequences affiliated to the latter archaeal group belonged to the uncultured members of the CCA47 [34] group and the Marine Group II [33].

3.3. Diversity and Species Richness of Archaeal Communities. To determine the archaeal diversity and richness, rarefaction analyses were performed with QIIME [21]. Alpha diversity analysis was performed at the same level of surveying
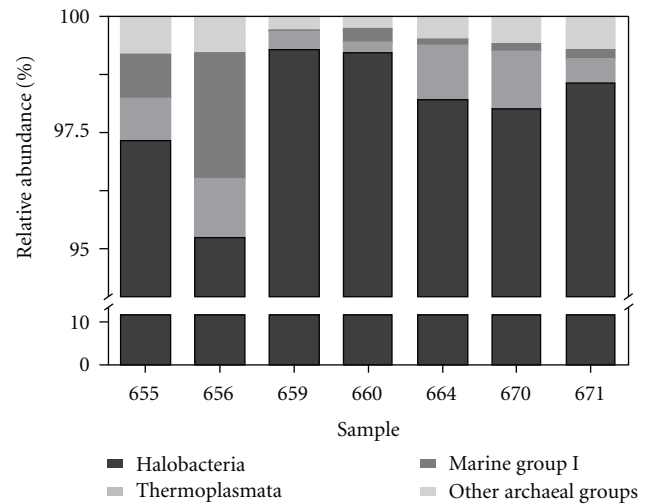

FIGURE 2: Relative sequence abundances of different archaeal phyla and classes. *Euryarchaeota*, especially *Halobacteria* (98.14%), were highly abundant. *Thermoplasmata* (0.75%) and the Marine Group 1 (0.58%) were found to some extent. All archaeal classes and groups (abundance < 0.5%) are depicted together.

effort (3100 randomly selected sequences per sample). The observed OTU number in the archaeal picoplankton ranged from 252 to 454 OTUs (1% genetic distance) and from 250 to 417 OTUs (3% genetic distance) (Table 3). The maximal expectable number of clusters for every sample was determined by nonlinear regression based on the Michalis-Menten equitation. The average OTU coverages were 62.3% and 62.6% at 1% and 3% genetic distance, respectively. Shannon indices ranged from 3.74 to 7.74 (1% genetic distance) and from 3.63 to 7.62 (3% genetic distance).

Comparison of the rarefaction analyses with the number of OTUs determined by Chao1 richness estimator revealed that at 1% and 3% genetic distances the rarefaction curves (Figure 3) were not saturated and the richness estimators indicated that 41.34% to 73.41% of the estimated richness, respectively, were recovered by the sequencing effort (Table 3). Thus, we did not survey the full extent of taxonomic diversity at these genetic distances, but a substantial fraction of the archaeal diversity within individual samples was assessed at genetic divergence of 3%.

TABLE 3: Archaeal diversity and richness values at 1% and 3% genetic distance. Numbers of observed OTUs as well as Shannon and Chao1 values were calculated with QIIME [16]. The maximal OTU number (n_{max}) in each sample was calculated by nonlinear modeling. Coverage was determined based on observed OTUs and n_{max}. To compare community structures, 3100 randomly selected sequences form every sample were used.

| Sample	Observed OTUs		Max. OTUs (n_{max})		Coverage (%)		Shannon index (H′)		Chao1	
	1%	3%	1%	3%	1%	3%	1%	3%	1%	3%
655	293	268	510	468	57.45	57.26	4.37	4.02	530	470
658	451	428	555	524	81.26	81.68	7.74	7.62	636	583
659	252	250	446	441	56.50	56.69	3.74	3.63	498	470
660	281	269	516	496	54.46	54.23	3.95	3.74	551	509
664	346	327	516	488	67.05	67.01	4.81	4.65	569	486
670	454	417	782	717	58.06	58.16	5.21	5.07	785	674
671	399	370	649	586	61.48	63.14	5.09	4.96	1227	895

(a)

(b)
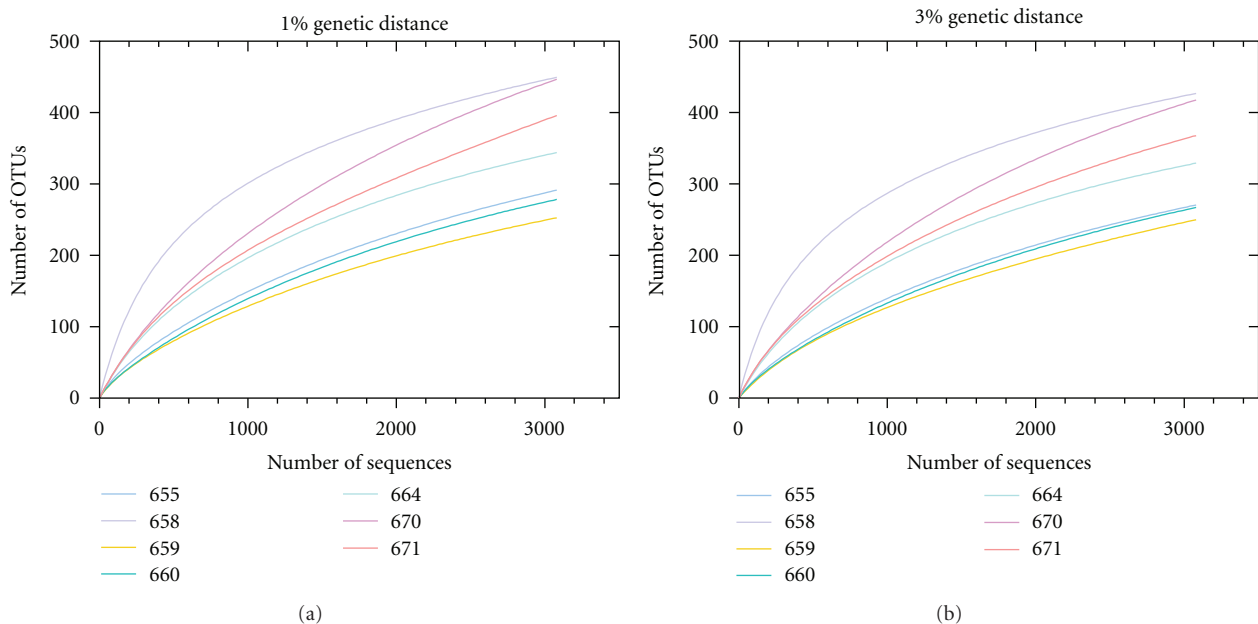
FIGURE 3: Rarefaction curves for all seven sampling sites. Curves were calculated at 1% (a) and 3% (b) genetic distance level employing QIIME [21]. Description of samplings sites is shown in Table 2.

3.4. Beta Diversity of the Bacterioplankton Community. Changes of the active bacterial community in response to different environmental conditions were examined by principal coordinate analysis (PCoA) (Figure 4). Surveying effort had no or little effect on diversity and community structure. However, the PCoA analysis revealed that all samples exhibiting similar environmental parameters such as temperature and salinity were assigned to one site of the plot. In addition, all bloom samples tend to cluster together. Sample 658 taken outside the algal bloom was completely separated from all other samples.

4. Discussion

Marine environments contain a high microbial biodiversity, and marine microbial communities play major roles in many biogeochemical cycles. Studies using culture-independent approaches have greatly contributed to our understanding of

the extent of microbial diversity [35]. Most of these studies focused on marine bacteria, whereas very little is known on the diversity and ecology of marine *Archaea*. Recent metagenomic studies provided evidence for ammonium-oxidizing *Archaea* being capable of nitrification [36]. Some marine crenarchaeal lineages are thought to be important nitrifiers in planktonic marine systems [37]. These results indicate that *Archaea* are important players in the global nitrogen cycle. However, detailed comparative ecological studies to understand archaeal community patterns and environmental drivers that shape these communities are missing [37].

This study focused on assessing the active archaeal community structure and richness in picoplankton samples derived from the German Bight by metatranscriptomic approaches. To our knowledge, this is the first study using an RNA-based approach combined with NGS to analyze archaeal community compositions. In addition, the obtained average read length (506 bp) is higher than in most other
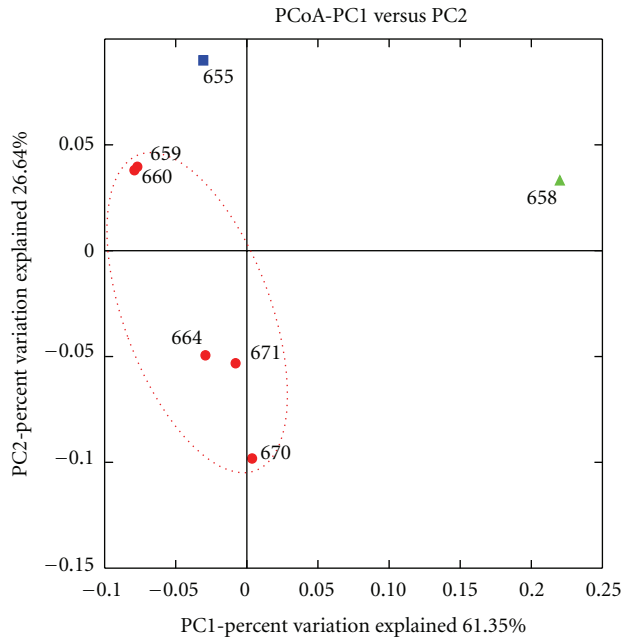
FIGURE 4: Weighted UniFrac 2D Principal Coordinate Analysis plot for beta diversity analysis. Samples taken during an algal bloom (samples 659, 660, 664, 670, and 671) are shown in red. Sample 655 taken at a river outfall and sample 658 originating from outside the algal bloom in blue and green, respectively.

studies employing NGS sequencing of 16S rRNA gene amplicons [38, 39]. The majority of sequences obtained was affiliated to the *Euryarchaeota*. Sapp et al. [40] studied marine sediments derived from the Oyster Ground (North Sea) and found high abundances of members of this phylum in their samples. We identified *Halobacteria* as the most abundant archaeal group. Members of this group can grow aerobically as well as anaerobically. Large halobacterial blooms appear reddish due to production of retinal-containing rhodopsins. Rhodopsins are photoactive membrane proteins with a highly conserved tertiary structure [41] and may serve as an additional possibility to conserve energy. This is advantageous in marine environments, as the concentration of dissolved organic matter and other nutrients is usually low [42]. Most of the halobacterial sequences analyzed in this study were affiliated to the Deep Sea Hydrothermal Vent Euryarchaeotal Group 6 (DHVE-6). This group was originally described as a hydrothermal vent lineage [43]. It was later renamed Miscellaneous Euryarchaeotic Group, as members of this group were also found in marine sediment [44] and in soil [45]. Another archaeal group found in all samples was the Marine Group I (MG-I). It was originally identified by sequencing of environmental 16S rRNA genes derived from sea water [46, 47]. Members of MG-I account for large fractions of marine prokaryotic picoplankton and prokaryotic communities in deep sea water (below 3000 m). *Thermoplasmata* were the third most abundant archaeal class in the investigated samples. Most sequences were affiliated to the CCA47 group. This group was originally identified by 16S rRNA gene analysis of oxygen-depleted marine environments [48]. Later, Ferrer et al. [34] found

members of this group in anoxic subsaline sediments. A few sequences assigned to Thermoplasmata were also affiliated to the Marine Group II. DeLong [33] suggested that members of Marine Group II (*Euryarchaeota*) are more abundant in temperate sea water than Marine Group I (*Crenarchaeota*) members. We found the opposite, as we recorded a higher abundance of Marine Group I members in the studied samples. Marine Group II members were almost absent in the investigated samples. One reason for this discrepancy might be that large parts of the German Bight are strongly influenced by tidal currents. Thus, these currents might whirl up archaeal cells from the sediment to the surface water, as most of the identified groups were originally described as inhabitants of marine sediments. Nonetheless, the number of studies targeting archaeal communities in the water column is substantially lower than that on marine sediments. Due to this knowledge gap, the habitat preference of these archaeal groups cannot be deduced definitely.

The impact of environmental conditions onto archaeal community composition and richness has been rarely studied. Auguet et al. [37] performed a general analytical approach to find community patterns of uncultured *Archaea* along environmental gradients or habitat types. Their results indicate that habitat types have a greater effect on archaeal community structures than other environmental conditions. All samples investigated in our study originated from almost the same habitat type, except for samples 655 and 658, which were collected at a river outfall region and outside of the algal bloom, respectively. Accordingly, all samples derived from the bloom showed an almost identical community composition. In addition, sample 655 showed a consimilar community structure. This indicates that similar environmental factors, such as temperature, salinity, and high nutrient availability during algal blooms or at river outfalls, have a similar impact onto composition of active archaeal communities.

Herfort et al. [49] studied archaeal communities in the southwestern North Sea via Denaturing Gradient Gel Electrophoresis (DGGE) and showed a positive correlation between the abundance of *Euryarchaeota* and chlorophyll concentrations, whereas the abundance of *Crenarchaeota* was negatively correlated with the chlorophyll concentration. Teeling et al. [50] investigated bacterial communities near Helgoland. They demonstrated that bacterial community structures were highly influenced by the presence of an algal bloom. In our study, we investigated the influence of algal blooms on archaeal diversity by PCoA. Sample taken in presence of a bloom shared a more similar community structure. This indicates that marine archaeal communities are also influenced by algal blooms or by environmental parameters correlated with bloom presence. We observed an increased number of *Halobacteria* in bloom samples. This might be correlated with the high amounts of organic matter in blooms. *Halobacteria* are the most active organisms with respect to organic matter degradation in hypersaline environments [37]. Thus the higher abundance of *Halobacteria* in algal bloom samples might indicate an involvement in marine organic matter degradation under high nutrient conditions found during algal blooms.

Due to the lack of pure cultures and large comparative investigations, robust conclusions on contributions of marine archaeal communities to biogeochemical cycles cannot be drawn. In this study, we found highly diverse and active archaeal communities in the surface water of the German Bight. Their ecological role is unknown, and further research including analyses of expressed functional genes needs to be performed to unravel the role of marine *Archaea*.

Acknowledgments

References

[1] T. P. Curtis, W. T. Sloan, and J. W. Scannell, "Estimating prokaryotic diversity and its limits," *Proceedings of the National Academy of Sciences of the United States of America*, vol. 99, no. 16, pp. 10494–10499, 2002.

[2] M. L. Sogin, H. G. Morrison, J. A. Huber et al., "Microbial diversity in the deep sea and the underexplored "rare biosphere"," *Proceedings of the National Academy of Sciences of the United States of America*, vol. 103, no. 32, pp. 12115–12120, 2006.

[3] M. B. Karner, E. F. Delong, and D. M. Karl, "Archaeal dominance in the mesopelagic zone of the Pacific Ocean," *Nature*, vol. 409, no. 6819, pp. 507–510, 2001.

[4] H. Agogué, M. Brink, J. Dinasquet, and G. J. Herndl, "Major gradients in putatively nitrifying and non-nitrifying Archaea in the deep North Atlantic," *Nature*, vol. 456, no. 7223, pp. 788–792, 2008.

[5] E. F. DeLong and D. M. Karl, "Genomic perspectives in microbial oceanography," *Nature*, vol. 437, no. 7057, pp. 336–342, 2005.

[6] S. J. Giovannoni and U. Stingl, "Molecular diversity and ecology of microbial plankton," *Nature*, vol. 437, no. 7057, pp. 343–348, 2005.

[7] T. Brinkhoff, D. Fischer, J. Vollmers et al., "Biogeography and phylogenetic diversity of a cluster of exclusively marine myxobacteria," *International Society for Microbial Ecology Journal*, vol. 6, no. 6, pp. 1260–1272, 2012.

[8] J. Frias-Lopez, Y. Shi, G. W. Tyson et al., "Microbial community gene expression in ocean surface waters," *Proceedings of the National Academy of Sciences of the United States of America*, vol. 105, no. 10, pp. 3805–3810, 2008.

[9] J. C. Venter, K. Remington, J. F. Heidelberg et al., "Environmental genome shotgun sequencing of the sargasso sea," *Science*, vol. 304, no. 5667, pp. 66–74, 2004.

[10] H. Nacke, A. Thürmer, A. Wollherr et al., "Pyrosequencing-based assessment of bacterial community structure along different management types in German forest and grassland soils," *PLoS ONE*, vol. 6, no. 2, Article ID e17000, 2011.

[11] C. Will, A. Thürmer, A. Wollherr et al., "Horizon-specific bacterial community composition of german grassland soils, as revealed by pyrosequencing-based analysis of 16S rRNA genes," *Applied and Environmental Microbiology*, vol. 76, no. 20, pp. 6751–6759, 2010.

[12] M. Vila-Costa, J. M. Gasol, S. Sharma, and M. A. Moran, "Community analysis of high- and low-nucleic acid-containing bacteria in NW Mediterranean coastal waters using 16S rDNA pyrosequencing," *Environmental Microbiology*, vol. 14, no. 6, pp. 1390–1402, 2012.

[13] T. Urich, A. Lanzén, J. Qi, D. H. Huson, C. Schleper, and S. C. Schuster, "Simultaneous assessment of soil microbial community structure and function through analysis of the metatranscriptome," *PLoS ONE*, vol. 3, no. 6, Article ID e2527, 2008.

[14] R. A. Lesniewski, S. Jain, K. Anantharaman, P. D. Schloss, and G. J. Dick, "The metatranscriptome of a deep-sea hydrothermal plume is dominated by water column methanotrophs and lithotrophs," *International Society for Microbial Ecology Journal*. In press.

[15] M. G. Weinbauer, I. Fritz, D. F. Wenderoth, and M. G. Höfle, "Simultaneous extraction from bacterioplankton of total RNA and DNA suitable for quantitative structure and function analyses," *Applied and Environmental Microbiology*, vol. 68, no. 3, pp. 1082–1087, 2002.

[16] V. I. Miteva, P. P. Sheridan, and J. E. Brenchley, "Phylogenetic and physiological diversity of microorganisms isolated from a deep greenland glacier ice core," *Applied and Environmental Microbiology*, vol. 70, no. 1, pp. 202–213, 2004.

[17] G. Muyzer, E. C. De Waal, and A. G. Uitterlinden, "Profiling of complex microbial populations by denaturing gradient gel electrophoresis analysis of polymerase chain reaction-amplified genes coding for 16S rRNA," *Applied and Environmental Microbiology*, vol. 59, no. 3, pp. 695–700, 1993.

[18] M. J. Ferris, A. Masztal, and D. H. Martin, "Use of species-directed 16S rRNA gene PCR primers for detection of Atopobium vaginae in patients with bacterial vaginosis," *Journal of Clinical Microbiology*, vol. 42, no. 12, pp. 5892–5894, 2004.

[19] M. Hartmann and F. Widmer, "Reliability for detecting composition and changes of microbial communities by T-RFLP genetic profiling," *FEMS Microbiology Ecology*, vol. 63, no. 2, pp. 249–260, 2008.

[20] Z. Yu, R. García-González, F. L. Schanbacher, and M. Morrison, "Evaluations of different hypervariable regions of archaeal 16S rRNA genes in profiling of methanogens by Archaea-specific PCR and denaturing gradient gel electrophoresis," *Applied and Environmental Microbiology*, vol. 74, no. 3, pp. 889–893, 2008.

[21] J. G. Caporaso, J. Kuczynski, J. Stombaugh et al., "QIIME allows analysis of high-throughput community sequencing data," *Nature Methods*, vol. 7, no. 5, pp. 335–336, 2010.

[22] M. Martin, "Cutadapt removes adapter sequences from high-throughput sequencing reads," *EMBnet.Journal*, vol. 17, no. 1, pp. 10–12, 2011.

[23] R. C. Edgar, B. J. Haas, J. C. Clemente, C. Quince, and R. Knight, "UCHIME improves sensitivity and speed of chimera detection," *Bioinformatics*, vol. 27, no. 16, Article ID btr381, pp. 2194–2200, 2011.

[24] P. D. Schloss, D. Gevers, and S. L. Westcott, "Reducing the effects of PCR amplification and sequencing artifacts on 16S rRNA-based studies," *PLoS ONE*, vol. 6, no. 12, Article ID e27310, 2011.

[25] T. Z. DeSantis, P. Hugenholtz, N. Larsen et al., "Greengenes, a chimera-checked 16S rRNA gene database and workbench compatible with ARB," *Applied and Environmental Microbiology*, vol. 72, no. 7, pp. 5069–5072, 2006.

[26] C. Camacho, G. Coulouris, V. Avagyan et al., "BLAST+: architecture and applications," *BMC Bioinformatics*, vol. 10, article 421, 2009.

[27] E. Pruesse, C. Quast, K. Knittel et al., "SILVA: a comprehensive online resource for quality checked and aligned ribosomal RNA sequence data compatible with ARB," *Nucleic Acids Research*, vol. 35, no. 21, pp. 7188–7196, 2007.

[28] C. E. Shannon, "A mathematical theory of communication," *SIGMOBILE Mobile Computing and Communications Review*, vol. 5, no. 1, pp. 3–55, 2001.

[29] A. Chao and J. Bunge, "Estimating the number of species in a stochastic abundance model," *Biometrics*, vol. 58, no. 3, pp. 531–539, 2002.

[30] RDevelopmentCoreTeam, *R: A Language and Environment For Statistical Computing*, 2012.

[31] L. Michaelis and M. L. Menten, "Die kinetik der invertinwirkung," *Biochemistry Zeitung*, vol. 49, no. 333–369, p. 352, 1913.

[32] J. Kan, S. Clingenpeel, R. E. Macur et al., "Archaea in Yellowstone Lake," *International Society for Microbial Ecology Journal*, vol. 5, no. 11, pp. 1784–1795, 2011.

[33] E. F. DeLong, "Oceans of archaea," *ASM News*, vol. 69, no. 10, p. 9, 2003.

[34] M. Ferrer, M. E. Guazzaroni, M. Richter et al., "Taxonomic and functional metagenomic profiling of the microbial community in the anoxic sediment of a sub-saline shallow lake (Laguna de Carrizo, Central Spain)," *Microbial Ecology*, vol. 62, no. 4, pp. 824–837, 2011.

[35] C. Simon and R. Daniel, "Metagenomic analyses: past and future trends," *Applied and Environmental Microbiology*, vol. 77, no. 4, pp. 1153–1161, 2011.

[36] R. Cavicchioli, M. Z. DeMaere, and T. Thomas, "Metagenomic studies reveal the critical and wide-ranging ecological importance of uncultivated archaea: the role of ammonia oxidizers," *BioEssays*, vol. 29, no. 1, pp. 11–14, 2007.

[37] J. C. Auguet, A. Barberan, and E. O. Casamayor, "Global ecological patterns in uncultured Archaea," *International Society for Microbial Ecology Journal*, vol. 4, no. 2, pp. 182–190, 2010.

[38] O. O. Lee, Y. Wang, J. Yang, F. F. Lafi, A. Al-Suwailem, and P. Y. Qian, "Pyrosequencing reveals highly diverse and species-specific microbial communities in sponges from the Red Sea," *International Society for Microbial Ecology Journal*, vol. 5, no. 4, pp. 650–664, 2011.

[39] J. A. Huber, D. B. Mark Welch, H. G. Morrison et al., "Microbial population structures in the deep marine biosphere," *Science*, vol. 318, no. 5847, pp. 97–100, 2007.

[40] M. Sapp, E. R. Parker, L. R. Teal, and M. Schratzberger, "Advancing the understanding of biogeography-diversity relationships of benthic microorganisms in the North Sea," *FEMS Microbiology Ecology*, vol. 74, no. 2, pp. 410–429, 2010.

[41] J. L. Spudich, C. S. Yang, K. H. Jung, and E. N. Spudich, "Retinylidene proteins: structures and functions from archaea to humans," *Annual Review of Cell and Developmental Biology*, vol. 16, pp. 365–392, 2000.

[42] M. T. Madigan and T. D. Brock, *Brock Biology of Microorganisms*, Pearson/Benjamin Cummings, San Francisco, Calif, USA, 2010.

[43] K. Takai and K. Horikoshi, "Genetic diversity of archaea in deep-sea hydrothermal vent environments," *Genetics*, vol. 152, no. 4, pp. 1285–1297, 1999.

[44] K. B. SØRensen, A. Lauer, and A. Teske, "Archaeal phylotypes in a metal-rich and low-activity deep subsurface sediment of the Peru Basin, ODP Leg 201, Site 1231," *Geobiology*, vol. 2, no. 3, pp. 151–161, 2004.

[45] K. Takai, D. P. Moser, M. DeFlaun, T. C. Onstott, and J. K. Fredrickson, "Archaeal diversity in waters from deep South African gold mines," *Applied and Environmental Microbiology*, vol. 67, no. 12, pp. 5750–5760, 2001.

[46] E. F. DeLong, "Archaea in coastal marine environments," *Proceedings of the National Academy of Sciences of the United States of America*, vol. 89, no. 12, pp. 5685–5689, 1992.

[47] J. A. Fuhrman, K. McCallum, and A. A. Davis, "Novel major archaebacterial group from marine plankton," *Nature*, vol. 356, no. 6365, pp. 148–149, 1992.

[48] T. Stoeck and S. Epstein, "Novel eukaryotic lineages inferred from small-subunit rRNA analyses of oxygen-depleted marine environments," *Applied and Environmental Microbiology*, vol. 69, no. 5, pp. 2657–2663, 2003.

[49] L. Herfort, S. Schouten, B. Abbas et al., "Variations in spatial and temporal distribution of Archaea in the North Sea in relation to environmental variables," *FEMS Microbiology Ecology*, vol. 62, no. 3, pp. 242–257, 2007.

[50] H. Teeling, B. M. Fuchs, D. Becher et al., "Substrate-controlled succession of marine bacterioplankton populations induced by a phytoplankton bloom," *Science*, vol. 336, no. 6081, pp. 608–611, 2012.

Research Article

Impact of Trichloroethylene Exposure on the Microbial Diversity and Protein Expression in Anaerobic Granular Biomass at 37°C and 15°C

Alma Siggins,[1] Anne-Marie Enright,[1] Florence Abram,[2] Catherine Botting,[3] and Vincent O'Flaherty[1]

[1] Microbial Ecology Laboratory, Department of Microbiology, School of Natural Sciences, National University of Ireland, Galway, Ireland
[2] Functional Environmental Microbiology, Department of Microbiology, School of Natural Sciences, National University of Ireland, Galway, Ireland
[3] BSRC Mass Spectrometry Facility, University of St Andrews, St Andrews KY16 9ST, UK

Correspondence should be addressed to Vincent O'Flaherty, vincent.oflaherty@nuigalway.ie

Granular biomass from a laboratory-scale anaerobic bioreactor trial was analysed to identify changes in microbial community structure and function in response to temperature and trichloroethylene (TCE). Two bioreactors were operated at 37°C, while two were operated at 15°C. At the time of sampling, one of each temperature pair of bioreactors was exposed to process failure-inducing concentrations of TCE ($60\,mg\,L^{-1}$) while the other served as a TCE-free control. Bacterial community structure was investigated using denaturing gradient gel electrophoresis (DGGE) and 16S rRNA gene clone library analysis. Temperature was identified as an important factor for bacterial community composition, while minor differences were associated with trichloroethylene supplementation. Proteobacteria was the dominant phylum in all bioreactors, while clone library analysis revealed a higher proportion of Bacteroidetes-, Chloroflexi-, and Firmicutes-like clones at 15°C than at 37°C. Comparative metaproteomics in the presence and absence of TCE was carried out by two-dimensional gel electrophoresis (2-DGE), and 28 protein spots were identified, with putative functions related to cellular processes, including methanogenesis, glycolysis, the glyoxylate cycle, and the methyl malonyl pathway. A good agreement between metaproteomic species assignment and phylogenetic information was observed, with 10 of the identified proteins associated with members of the phylum Proteobacteria.

1. Introduction

Anaerobic digestion (AD) is a sequential and cooperative microbial process, employed in engineered ecosystems for the treatment of wastes and wastewaters and for the production of biogas from biomass and organic residues [1]. Low-temperature operation of laboratory-scale anaerobic digesters has been proven feasible as a cost-effective alternative to traditional mesophilic operating temperatures for a wide range of wastewater types [2, 3]. At all applied temperature ranges, AD relies on the appropriate combination of a variety of microorganisms; complex syntrophic interactions between archaeal and bacterial species are essential for the complete degradation of organic compounds to methane [4]. In the past two decades, the nature of the microbial communities involved in low temperature AD has come under closer scrutiny, with the recognition that greater understanding of the potential and limitations of the microbial consortium could aid in process optimisation. For example, Enright et al. [5] demonstrated that a shift in methanogenic community structure observed by terminal restriction fragment length polymorphism (TRFLP) corresponded to increased hydrogenotrophic activity, while Bialek et al. [6] used statistical analysis (moving window/nonmetric multidimensional scaling) of quantitative polymerase chain reaction (qPCR) data to visualise shifts in the methanogenic communities that could be attributed to bioreactor configuration. Both of these studies, as is traditional for investigation of the microbial communities underpinning the process of anaerobic digestion, focused on the methanogens, a group of

anaerobic archaea involved in the conversion of acetate and hydrogen to methane [7]. The low biodiversity associated with methanogens in AD has facilitated the generation of functional and process-relevant information based on methanogenic community structure [8].

We have previously documented the response of the methanogenic community within anaerobic granular biomass to the presence of trichloroethylene (TCE; [9]). TCE is a potentially carcinogenic and mutagenic compound [10], which is routinely employed in the cleaning and metal degreasing industries, and can be completely dechlorinated by the process of anaerobic digestion [11]. Our previous study[9] investigated the impact of influent TCE concentrations on the stable operation of expanded granular sludge bed bioreactors at 37°C and 15°C. In order to explore the observed decrease in operational performance noted at both temperatures in response to an influent TCE concentration of 60 mg L^{-1}, specific methanogenic activity (SMA) and toxicity batch assays, in addition to qPCR analysis of the methanogenic community, were undertaken [9]. We determined that changes in the methanogenic community in response to TCE were not sufficient to result in the observed process failure, while temporal sampling revealed that changes in temperature resulted in a higher impact on the methanogenic population structure [9]. Specific methanogenic activity and toxicity assays suggested that acetoclastic methanogens were reversibly inhibited by the presence of TCE and/or its degradation derivatives, while competition by dechlorinating organisms may have limited the availability of hydrogen for hydrogenotrophic methanogenesis [9]. Although our study [9] addressed the response of the archaeal community to the presence of TCE, no changes that could definitively account for bioreactor failure at that TCE concentration were identified. Conclusions from that study were based on metabolic groups rather than specific organisms, and disparities in results between molecular and physiological data were observed [9]. Consequently, this study attempts to further investigate the structural response of the bacterial domain, and the functional response of the overall microbial community.

This study investigated the impact of TCE on both the bacterial community structure (using DGGE and 16s rRNA clone library) and the microbial community function (using 2-DGE based metaproteomics) within AD bioreactors operating at 37°C and 15°C.

2. Materials and Methods

2.1. Source of Biomass. Anaerobic granular sludge originating from four expanded granular sludge bed (EGSB) bioreactors was investigated. All bioreactors (R1–R4) were utilised for the treatment of a volatile fatty acid (VFA)-based wastewater. R1 and R2 were operated at 37°C, while R3 and R4 were operated at 15°C, with R1 and R3 supplemented with increasing concentrations of trichloroethylene (TCE; 10–60 mg L^{-1}). The prepared influent was stored in a closed system to prevent volatilisation of TCE; a nitrogen filled gas bag was used to equilibrate the pressure as the influent was pumped from the storage container to the

bioreactor. The bioreactor trial and associated performance data are presented in detail in Siggins et al. [9]. Biomass was sampled from the bioreactors on day 235, when influent TCE concentration of R1 and R3 were 60 mg L^{-1}.

2.2. Volatile Fatty Acid (VFA) Analysis. Analysis of VFA concentrations of effluent samples collected from R1–R4 throughout the trial were performed by heated (85°C) and agitated headspace, in a Varian Saturn 2000 GC/MS system, with CombiPAL autosampler (Varian Inc., Walnut Creek, CA). Separation was carried out on a Varian Capillary column, CP-WAX 58 (FFAP) CB (25 m length × 0.32 mm internal diameter × 0.2 μm film thickness, Varian). The injector volume was 2 mL and the injector temperature was maintained at 250°C. Helium was employed as the carrier gas, at a flow rate of 1 mL min^{-1}. The temperature program was as follows: 50°C (20 s) to 110°C (20 s) at a rate of 2°C min^{-1}; from 110°C to 200°C (20 s) at a rate of 20°C min^{-1}. The MS-detector was operated in the scan mode in the range of 40–150 m z^{-1} at a temperature of 210°C. Identification of VFAs was achieved by matching chromatographic retention times and spectra of standard compounds (acetic-, butyric- and propionic-acids). Calibration curves of standard VFAs were constructed and used for relative concentration of VFAs in effluent headspace samples, expressed as mg L^{-1}.

2.3. Specific Methanogenic Activity (SMA) Testing. Biomass samples were screened for metabolic capability using specific methanogenic activity (SMA) tests. These were performed using the pressure transducer technique [12, 13], in which propionate (30 mM), butyrate (15 mM), and ethanol (30 mM) were used as substrates to assay indirect methanogenesis. All assays contained 2–5 g volatile suspended solids (VSS) L^{-1} and were performed in triplicate at the bioreactor operational temperature (R1 and R2 37°C; R3 and R4 15°C). Vials without any substrate were used as controls.

2.4. Extraction of Genomic DNA. Total genomic DNA was extracted in duplicate from the four biomass samples using an automated nucleic acid extractor (Magtration 12GC, PSS Co., Chiba, Japan). Granular biomass was finely crushed using a mortar and pestle, and re-suspended in 1x phosphate buffered saline to a ratio of 1 : 4 w/v. A 100 μL aliquot of the biomass suspension was loaded per extraction. Extracted DNA was eluted in 100 μL Tris-HCl buffer (pH 8.0) and stored at −20°C.

2.5. Clone Library Analysis of 16S rRNA Genes. Bacterial clone libraries were constructed from the extracted genomic DNA; 16S rRNA genes were PCR-amplified using forward primer 27F (5′-AGA GTT TGA TCC TGG CTC AG-3′; [14]) and reverse primer 1392R (5′ ACG GGC GGT GTG TRC-3′; [15]). Reaction mixtures (50 μL) contained 1.5 mM MgCl$_2$, 5 μL 10x NH$_4$ buffer (16 mM (NH$_4$)$_2$SO$_4$, 67 mM Tris-HCl (pH 8.8 at 25°C), 0.01% Tween-20), 0.2 mM each dNTP (dATP, dCTP, dGTP, dTTP), 12.5 pmol of each primer, 2 μL template DNA, and 1U *Taq* DNA polymerase.

The PCR reactions were carried out using a touchdown PCR under the following conditions: initial denaturation at 95°C for 10 mins, followed by 10 cycles of 95°C for 60 s, annealing at 63°C for 60 s, and extension at 72°C for 120 s, where the annealing temperature was decreased by 1°C per cycle; followed by 20 cycles of denaturation at 95°C for 60 s, annealing at 52°C for 60 s, and extension at 72°C for 120 s, followed by a final 10 min extension at 72°C. Controls containing no DNA were also employed to identify amplification of contaminants, and none was detected. PCR products were ligated into the plasmid vector pCR 2.1-TOPO (Invitrogen) and the hybrid vectors were used to transform *Escherichia coli* TOP 10 competent cells, following the manufacturer's instructions. Transformants were screened using Luria-Bertani (LB) agar plates containing 50 μg mL^{-1} kanamycin. Clone libraries were constructed by growing 96 randomly selected colonies derived from each sample at 37°C overnight in 200 μL LB broth medium containing 50 μg mL^{-1} kanamycin in a 96-well plate.

2.6. Amplified rDNA Restriction Analysis (ARDRA). Ninety-six clones from each library were screened to determine if they contained the appropriately sized insert. Vector-specific M13 forward and reverse primers were used at a concentration of 12.5 pmol, with the other PCR reagents as described previously. PCR conditions were: denaturation at 95°C for 10 min; 30 cycles of: 95°C for 60 s, 55°C for 60 s, 72°C for 60 s; followed by a final extension at 72°C for 10 minutes. Five μL of the resulting PCR products were digested with 0.8 μL of the restriction endonuclease *Hae*III at 37°C for 12–16 hours. The resulting DNA fragments were resolved by electrophoresis on 3.5% (w/v) high resolution agarose and banding patterns were grouped into operational taxonomic units (OTUs).

2.7. Partial 16S rDNA Sequencing, Phylogenetic, and Statistical Analysis. Inserts from clones representing the 52 OTU's identified were sequenced on a Licor gel sequencer using vector specific M13 primers (MWG Biotech, Germany). Sequences from this study were aligned with 16S rRNA gene sequences retrieved from BLASTn and the RDP using Clustal X [16], and the phylogenetic inference package Paup* 4.0b8 was used for all phylogenetic analysis [17]. The resulting partial 16S rRNA gene sequences were deposited in the GenBank database under the accession numbers HM749844–HM749879. The Simpson index of diversity ($1 - D$) was calculated using the Primer6 software in order to compare the bacterial diversity of the four biomass samples as revealed by clone library analysis, using the algorithm ($D = \Sigma(n(n-1)/N(N-1))$), where n is the number of individuals belonging to a species in any given sample and N is the total number of individuals present in any given sample [18]. A Simpson's diversity index close to 1 means that the sample is highly diverse [18].

2.8. Denaturing Gradient Gel Electrophoresis (DGGE). DGGE analysis of bacterial 16S rRNA genes extracted from the four samples was carried as follows: initial PCR amplification used the primers 341F (5′-CCT ACG GGA GGC AGC AG-3′

[19]) and 517R (5′-ATT ACC GCG GCT GCT GG-3′ [19]), with a 40-base pair GC clamp attached to the 5' terminus of the forward primer.

The touchdown PCR program consisted of an initial denaturation at 94°C for 120 s; followed by 10 cycles of 94°C for 30 s, annealing at 65°C for 30 s, and extension at 72°C for 30 s, where the annealing temperature was decreased by 1°C per cycle; followed by 20 cycles of denaturation at 95°C for 30 s, annealing at 55°C for 30 s and extension at 72°C for 30 s, followed by a final 10 min extension at 72°C. A 40 μL aliquot of GC-clamped PCR product was loaded onto a 10% (w/v) polyacrylamide gel containing a denaturing gradient of 30–70% (where 100% denaturant contained 7 M urea, 40% formamide) and ran at 60°C and 70 V for 16 h in a D-Code system (BioRad, Hercules, CA). The DGGE gels were ethidium bromide stained and photographed under UV trans-illumination. Seventeen bands were selected for further investigation by sequencing and phylogenetic analysis. Ten of these selected bands were present in all samples and were not affected by either temperature or TCE. Six bands were present only at 15°C (R3 and R4), while one band was present only at 37°C (R1 and R2), with both conditions indicating a temperature-dependent response of the microbial community. Selected bands were excised from the gel using a sterile scalpel blade, resuspended in 200 μL of sterile water, and stored at room temperature for three hours to elute DNA from the gel for use as a PCR template. PCR reactions were performed under the conditions described above and the resulting PCR products were cloned using TOPO TA (Invitrogen). Plasmids from five randomly selected clones per reaction were extracted and 2 μL of plasmid DNA was employed as a template for PCR using the same primers and conditions as described previously. For confirmatory purpose, the products of PCR from plasmid DNA were electrophoresed on a DGGE gel in parallel with the corresponding original PCR product. Plasmids that produced bands that underwent denaturation at the same gradient concentration as the original sample, and thereby migrated the same distance through the gel, were selected and sequenced (MWG Biotech, Germany).

Sequences from this study were aligned with 16S rRNA gene sequences retrieved from BLASTn and the RDP using Clustal X [16], and the phylogenetic inference package Paup* 4.0b8 was used for all phylogenetic analysis [17]. The resulting partial 16S rRNA gene sequences were deposited in the GenBank database under the accession numbers HM749788–HM749804.

2.9. Statistical Analysis of DGGE Data. DGGE gels were analysed by creating binary matrices, where-by the presence or absence of bands in each sample were denoted with the numeric values "1" or "0", respectively. These matrices were used to calculated unweighted pair-group methods using arithmetic averages (UPGMA) similarity dendrograms using the PC-ORD 5.0 statistical package [20].

2.10. Two-Dimensional Gel Electrophoresis (2-DGE). Proteins were extracted in duplicate from 50 mL of each granular sludge sample by sonication and subsequently separated

TABLE 1: Specific Methanogenic Activity (SMA) of biomass sampled from R1 to R4 on day 235 of bioreactor trial, when influent TCE concentrations of R1 and R3 were 60 mg L^{-1} [9] Values shown are expressed as mL CH$_4$ gVSS^{-1} day^{-1} and are means of triplicates with std. errors (std. deviation/$\sqrt{n}$, $n = 3$) given in parentheses.

Temperature	Biomass	Propionate	Butyrate	Ethanol
37°C	R1 (TCE)	123 (5)	124 (3)	160 (11)
	R2 (Control)	222 (2)	160 (33)	210 (28)
15°C	R3 (TCE)	82 (5)	14 (1)	51 (5)
	R4 (Control)	164 (1)	23 (2)	48 (11)

by 2-DGE [21, 22]. Briefly, the first dimension consisted of isoelectric focusing (IEF) using 7 cm IPG strips with linear pH gradients (pH 4 to 7; Amersham). The second dimension polyacrylamide (12% w/v) gels were run in pairs along with molecular weight markers with a range of 10–225 kDa (Broad Range Protein Molecular Markers, Promega). Gels were stained overnight in GelCode 135 Blue staining reagent (Pierce) and then destained in deionised, distilled water for several hours. Twenty four gels were run corresponding to two duplicate independent extractions and three technical replicates of four samples. Gel images were processed and analysed with PDQuest-Advanced software, version 8.0.1 (BioRad). Spot counts were obtained using the spot detection wizard enabling the Gaussian model option and data normalisation was performed using the Local Regression Model, as recommended by the manufacturer. Ratios of spot intensities were determined in the presence and absence of TCE at both 37°C and 15°C. Protein expression ratios greater than two-fold were considered significant. Proteins deemed of interest were excised from the gels and identified using nanoflow liquid chromatography-electrospray ionization tandem mass spectrometry (nLC-ESI-MS/MS), as previously described [21, 22]. The MS/MS data were analysed using the Mascot 2.2 search engine (Matrix Science, London, UK) against the NCBInr database (04 March 2010, 10,530,540 sequences) with no species restriction. Positive protein identification was based on two criteria: a Mascot Mowse score of >52 (95% confidence level) and a minimum detection of two peptides per protein.

3. Results

3.1. Specific Methanogenic Activity.
At R1 and R3 influent TCE concentrations of 60 mg L^{-1}, the SMA against propionate, butyrate, and ethanol was generally lower for both TCE-supplemented bioreactors (R1 and R3) than their corresponding controls (R2 and R4; Table 1). For each of the three substrates tested, the activity of the TCE-supplemented bioreactors was higher at 37°C (R1) than at 15°C (R3; Table 1), with the same trend observed for biomass originating from the control bioreactors, with activity of R2 (37°C) higher than that of R4 (15°C) for all three substrates utilised in this assay (Table 1).

3.2. Clone Library Analysis of 16S rRNA Genes.
ARDRA was carried out on a total of 354 clones, and several temperature-related, but apparently TCE-independent, changes in the

bacterial community structure were observed (Figure 1). For example, although clones related to the phylum Proteobacteria were dominant in all bioreactors, the proportion of Proteobacteria-like clones was higher in both R1 and R2 (37°C, with and without TCE, resp.) than in R3 and R4 (15°C, with and without TCE, resp.), while the opposite was true of Bacteroidetes-, Chloroflexi-, and Firmicutes-like clones (Figure 1). The 15°C biomass samples showed higher species diversity than at 37°C, and Simpson's diversity indices were: R1 (37°C TCE) 0.7032; R2 (37°C control) 0.6384; R3 (15°C TCE) 0.8459; R4 (15°C control) 0.8462.

3.3. DGGE.
UPGMA analysis of PCR-DGGE data demonstrated that the bacterial community of the biomass statistically clustered by bioreactor operational temperature, with the 37°C bacterial communities (R1 and R2) demonstrating >80% similarity, and the 15°C bioreactors (R3 and R4) demonstrating >90% similarity, irrespective of TCE exposure (Figure 2). Furthermore, the greatest difference in the bacterial community structure of these samples was observed between the 37°C and 15°C bioreactor clusters, which established temperature as a stronger driving force in bacterial community diversity than TCE (Figure 2).

Phylogenetic analysis of the seventeen DNA fragments excised from the DGGE gel allowed the identification of organisms within the bacterial community (Figure 3). Of these seventeen bands, ten were present in all samples, of which nine were identified as being closely associated with: *Pseudomonas* (B1), *Syntrophomonas* (B2), *Geobacter* (B3 and B11), *Desulfovibrio* (B9), Syntrophaceae (B10), Myxococcales (B12), Deltaproteobacteria (B13), and Firmicutes (B14), while B7 did not group with any classified bacterial phylum (Figure 3).

Six bands were only detected at 15°C (R3 and R4) and were related to: Planctomycetes (B4), Bacteroidetes (B5), Chloroflexi (B6 and B15), Deltaproteobacteria (B16), and Spirochaetes (B17); while only B8 was present exclusively at 37°C (R1 and R2) and was identified as a Thermotogae-like species (Figure 3). Overall, six of the seventeen bands analysed were phylogenetically affiliated with Proteobacteria, (B3, B10, B11, B12, B13, B16) establishing it as the most dominant phylum (Figure 3). No bands were observed on DGGE gels that were differentially detected due to the presence or absence of TCE.

3.4. Metaproteomics.
Ninety-three distinct spots were excised and sequenced for protein identification based on protein expression ratios. Spots were selected so that proteins that were constitutively expressed, induced or repressed in the presence of TCE were all included for analysis. Of these, 46% were positively identified using nLC-ESI-MS/MS. A number of proteins were found to have migrated as several distinct spots, resulting in the positive identification of 27 unique proteins (Table 2).

Twelve proteins were associated with bacterial species, ten of which were members of the phylum Proteobacteria, with the Actinobacteria and Firmicutes each represented by one protein (Table 2). The functions of proteins originating from bacterial species were highly varied. Proteins associated with
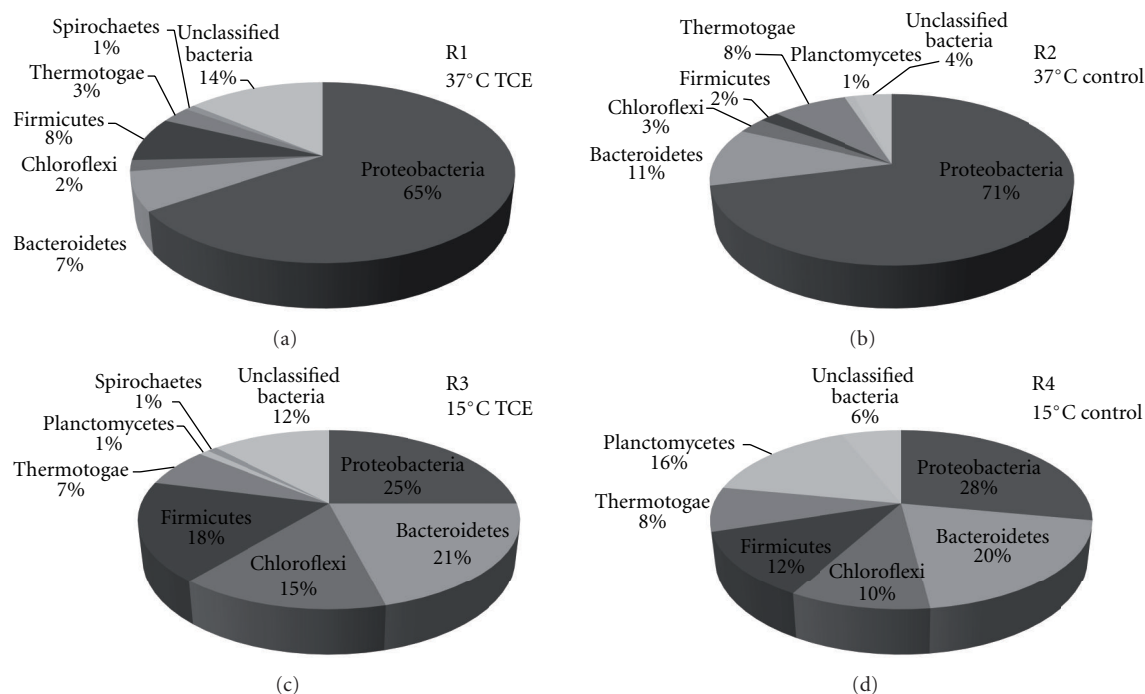
Figure 1: Diversity of bacterial clones obtained from 16S rRNA gene clone libraries. R1: 37°C TCE-supplemented; R2: 37°C control; R3: 15°C TCE-supplemented; R4: 15°C control.
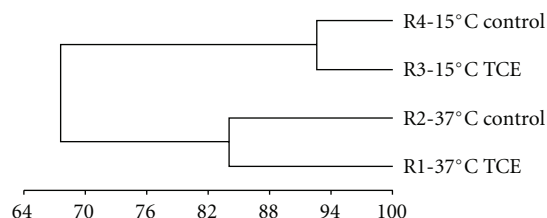

Figure 2: Bacterial UPGMA cluster analysis of 16S rDNA fragments generated from DGGE banding profiles. Percent similarity calculated by (1−Sorensons (Bray-Curtis) distance measurement) ∗ 100. R1: 37°C TCE-supplemented; R2: 37°C control; R3: 15°C TCE-supplemented; R4: 15°C control.

the metabolism of components of the influent wastewater, namely acetate (phosphate acetyltransferase) and ethanol (alcohol dehydrogenase), were identified in all samples, and were affiliated with the Proteobacteria (Table 2).

Five proteins were identified that could be involved in the degradation of glyoxylate (Table 2). Glyceraldehyde-3-phosphate dehydrogenase, an enzyme of the glycolytic pathway, was detected in all samples (Table 2), indicating that the glycolytic pathway appears to be active under all of the conditions investigated. In addition, there is evidence of activity of the methyl-malonyl pathway, as methyl malonyl-CoA mutase was detected in all samples, and was upregulated ca. 24-fold in the presence of TCE at 37°C (Table 2). Succinyl-CoA synthetase, associated with the production of succinyl-CoA, which is required for the methyl malonyl pathway, was identified in both 37°C samples, but not at 15°C (Table 2). Malate dehydrogenase, a protein of the glyoxylate cycle that converts malate to oxaloacetate, was also identified in all

samples, but was downregulated 3-fold in the presence of TCE at 15°C (Table 2). Oxaloacetate, in turn, can be converted to aspartate, which can lead to the production of L-homocysteine via the formation of O-acetyl-L-homoserine by O-acetylserine sulfhydrylase, an enzyme which was detected in all samples and was found to be upregulated in the presence of TCE at both temperatures (Table 2). O-acetylserine sulfhydrylase was assigned to *Geobacter* sp., known to be involved in TCE dechlorination [24].

The remaining nine proteins were assigned to archaeal species belonging to the orders Methanomicrobiales and Methanobacteriales, and to the family Methanosaeta (Table 2). Unsurprisingly, methanogenesis dominated the suggestedfunction of proteins originating from the archaea, with proteins involved in the production of methane from acetate (Acetyl-CoA decarbonylase) and CO_2 (coenzyme F420 dependent N5, N10 methylenetetrahydromethanopterin reductase) identified in all samples (Table 2).

In addition, several house-keeping proteins were identified, and included those involved in ATP synthesis and proteolysis, while acetate-CoA ligase was upregulated in the presence of TCE at both temperatures, which would result in increased production of acetyl-CoA (Table 2). Finally, a hypothetical protein of unknown function was detected at 37°C, and affiliated with *Methanospirillum* sp. (Table 2).

4. Discussion

Several results indicated a negative response of the bacterial community to the presence of TCE, particularly at the maximum applied concentration of 60 mg L^{-1}. For example, the accumulation of measured VFA, particularly propionic
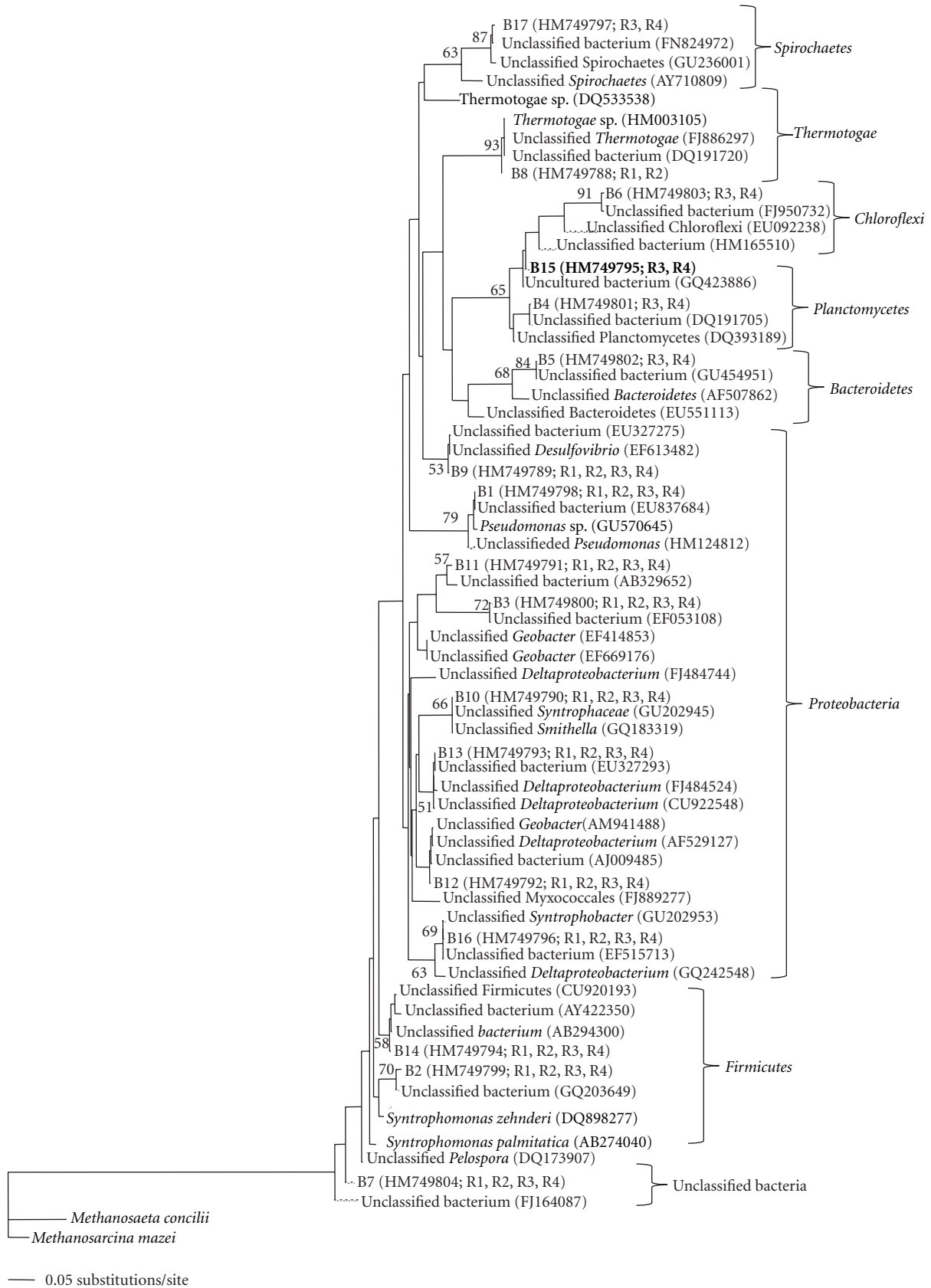
FIGURE 3: Phylogeny of bacterial sequences obtained by DGGE from R1–R4 biomass, calculated using the Kimura-2 algorithm and the neighbour-joining method [23]. Bootstrap replicates (total 100 replicate samplings) supporting the branching order are shown at relevant nodes. Accession numbers and the bioreactor biomass containing the respective bands are given in parenthesis. R1: 37°C TCE-supplemented; R2: 37°C control; R3: 15°C TCE-supplemented; R4: 15°C control.

TABLE 2: Proteins identified from bioreactor biomass. Ratio = TCE reactor spot intensity: non-TCE control reactor spot intensity, that is, positive values indicate the protein in question was expressed at a higher intensity in the TCE-supplemented reactor, and negative values indicate the protein was expressed at a higher intensity in the control reactor. N.D.: not detected.

Protein	Suggested function	Accession number	Species assignment	Classification	Mascot score	% coverage	37°C ratio	15°C ratio
Acetyl-CoA decarbonylase β-subunit	Methanogenesis from acetate	gi 116753609	Methanosaeta thermophila	Order Methanosarcinales	253	8	-1.7	-1.2
					171	8	N.D.	1.2
Co-enzyme F420 dependent N5, N10 methylenetetrahydromethanopterin reductase	Methanogenesis from CO_2	gi 1002717	Methanothermobacter thermoautotrophicus	Order Methanobacteriales	248	19	-1.4	-1.7
					166	13	-2.6	N.D.
					147	9	1.8	1
Tetrahydromethanopterin-S-methyltransferase H-subunit	Methanogenesis from CO_2	gi 116754675	Methanosaeta thermophila	Order Methanosarcinales	104	2	-3.9	N.D.
Methyl-CoM reductase I α-subunit	Methanogenesis	gi 126855	Methanothermobacter marburgensis	Order Methanobacteriales	203	8	3.2	-1.6
Methyl-CoM reductase I α-subunit	Methanogenesis	gi 284413635	Methanobacterium sp.	Order Methanobacteriales	469	25	1.2	-1.9
					396	23	N.D.	-4.6
					237	16	N.D.	-3.7
Methyl-CoM reductase I α-subunit	Methanogenesis	gi 47827047	Uncultured Methanosarcinales	Order Methanosarcinales	140	17	2.1	2.8
Methyl-CoM reductase I β-subunit	Methanogenesis	gi 126862	Methanothermobacter marburgensis	Order Methanobacteriales	393	11	N.D.	-8.3
					223	8	-2.7	N.D.
					148	9	-1.7	-1.5
Methyl-CoM reductase I β-subunit	Methanogenesis	gi 126178567	Methanoculleus marisnigri	Order Methanomicrobiales	224	5	2.8	1.3
Methyl-CoM reductase I γ-subunit	Methanogenesis	gi 116753883	Methanosaeta thermophila	Order Methanosarcinales	157	11	-2.7	4.9
Proteasome α-subunit	Proteolysis	gi 6093782	Methanosaeta thermophila	Order Methanosarcinales	206	16	-5.1	12.5
					151	12	N.D.	1.1
Thermosome	Molecular chaperone	gi 116754081	Methanosaeta thermophila	Order Methanosarcinales	272	9	-2.9	N.D. in R4
V-type ATP synthase α-subunit	ATP synthesis	gi 116754898	Methanosaeta thermophila	Order Methanosarcinales	273	10	N.D.	1.8
					217	10	-1.1	N.D.
					212	10	3.9	N.D.
					199	10	1.9	N.D.
					191	8	-5.6	1.9
Hypothetical protein Mhun-2513	Unknown	gi 88603754	Methanospirillum hungatei	Order Methanomicrobiales	1640	46	1	N.D.
Acetate-CoA Ligase	Acetyl-CoA synthesis	gi 116754497	Methanosaeta thermophila	Order Methanosarcinales	153	5	3.8	5.9
Iron-containing alcohol dehydrogenase	Ethanol metabolism	gi 77457538	Pseudomonas fluorescens	Phylum Proteobacteria	180	3	1.4	N.D.
					159	3	1	-1.7
					122	6	N.D.	1.1

TABLE 2: Continued.

| Protein	Suggested function	Accession number	Species assignment	Classification	Mascot score	% coverage	37°C ratio	15°C ratio
Phosphate acetyltransferase	Acetate metabolism	gi 95930364	*Desulfuromonas acetoxidans*	Phylum Proteobacteria	106	5	−1.4	6.5
Acetate-CoA transferase β-subunit	Acetate metabolism	gi 147678377	*Pelotomaculum thermopropionicum*	Phylum Firmicutes	304	18	1.1	N.D.
Glyceraldehyde-3-phosphate dehydrogenase type I	Glycolysis	gi 213959469	*Propionibacterium acnes*	Phylum Actinobacteria	375	17	−2	2
Methyl Malonyl-CoA mutase large subunit	Isomerisation of Succinyl-CoA	gi 116747906	*Syntrophobacter Fumaroxidans*	Phylum Proteobacteria	507	16	23.7	−1.1
Succinyl-CoA synthetase β-subunit	Formation of Succinyl-CoA	gi 116749138	*Syntrophobacter Fumaroxidans*	Phylum Proteobacteria	235	15	−1.1	N.D.
Malate dehydrogenase	Glyoxylate pathway	gi 116747908	*Syntrophobacter Fumaroxidans*	Phylum Proteobacteria	383	26	1.8	−3.1
O-acetylserine sulfhydrylase	Homocysteine production	gi 148265277	*Geobacter uraniireducens*	Phylum Proteobacteria	216	10	2.9	3.4
Chaperone protein	Macromolecule assembly	gi 85859704	*Syntrophus aciditrophicus*	Phylum Proteobacteria	555	17	N.D.	2.8
Chaperone protein DnaK	Protein folding	gi 116748478	*Syntrophobacter Fumaroidans*	Phylum Proteobacteria	230	8	−1.5	N.D.
Chaperonin GroEL	Protein folding	gi 148266317	*Geobacter uraniireducens*	Phylum Proteobacteria	620 / 326	18 / 10	−8.5 / 3.6	3.6 / N.D. in R4
Extracellular ligand binding receptor	Receptor activity	gi 116750526	*Syntrophobacter Fumaroidans*	Phylum Proteobacteria	671 / 309	28 / 17	−1.5 / 1.2	N.D. / −2.9
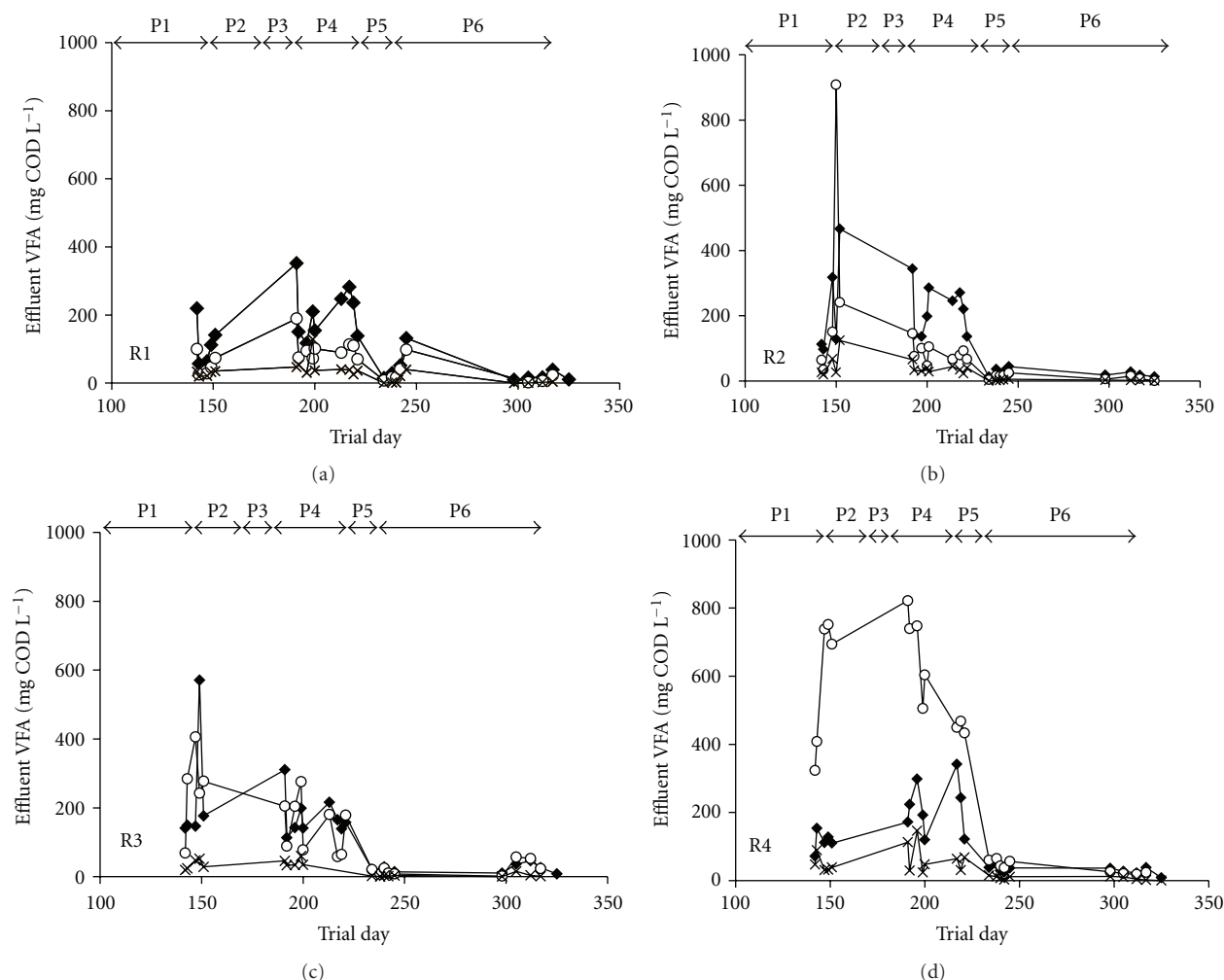
Figure 4: Effluent VFA concentrations of R1–R4: acetic acid (♦); propionic acid (○); butyric acid (-x-). R1: 37°C TCE-supplemented; R2: 37°C control; R3: 15°C TCE-supplemented; R4: 15°C control.

acid, was observed during process perturbations following the initial TCE addition and subsequent increases in TCE concentration (Figure 4). Also, SMA assays using indirect methanogenic substrates indicated that on day 235, the activities of propionate, butyrate, and ethanol utilisers were generally lower in the TCE-supplemented bioreactors than in their control counterparts (Table 1). However, analysis of the bacterial community during this study did not reveal any significant changes in the community structure that could be strongly attributed to the process failure observed in both R1 (37°C) and R3 (15°C) at influent TCE concentrations of 60 mg L^{-1} [9]. As was the case of with the archaeal population [9], it would appear that the bacterial community was not structurally affected by the addition of TCE; however the reduced activity of the syntrophic populations may have contributed to process failure.

By employing 16S rRNA gene analysis (DGGE and clone libraries) this study aimed to target the bacterial community structure and identify changes that may have been associated with temperature-and/or TCE-induced process

failure. Additionally, metaproteomic analysis of the overall microbial community was carried out in an attempt to identify proteins associated with ongoing functions in the bioreactors, including the reductive dechlorination of TCE.

The high levels of Proteobacteria-like species observed by DGGE and 16S rRNA gene clone libraries in all samples was in keeping with previous studies, which reported that Proteobacteria are commonly amongst the dominant phyla in anaerobic bioreactors [25, 26]. Analysis of the metaproteome confirmed the metabolic activity of Proteobacteria in all samples (Table 2), substantiating the importance of this phylum in the process of anaerobic digestion. Correspondingly, several key Proteobacteria species were identified by one or more of these techniques. For example, propionate-oxidising *Syntrophobacter fumaroxidans* were present in all samples, detected by both bacterial clone library (Figure 1) and DGGE analysis (Figure 3), and were associated with three of the proteins involved in the metabolic pathways outlined in Figure 5. One of these proteins, methyl malonyl CoA mutase, which is involved in the metabolism of propionate
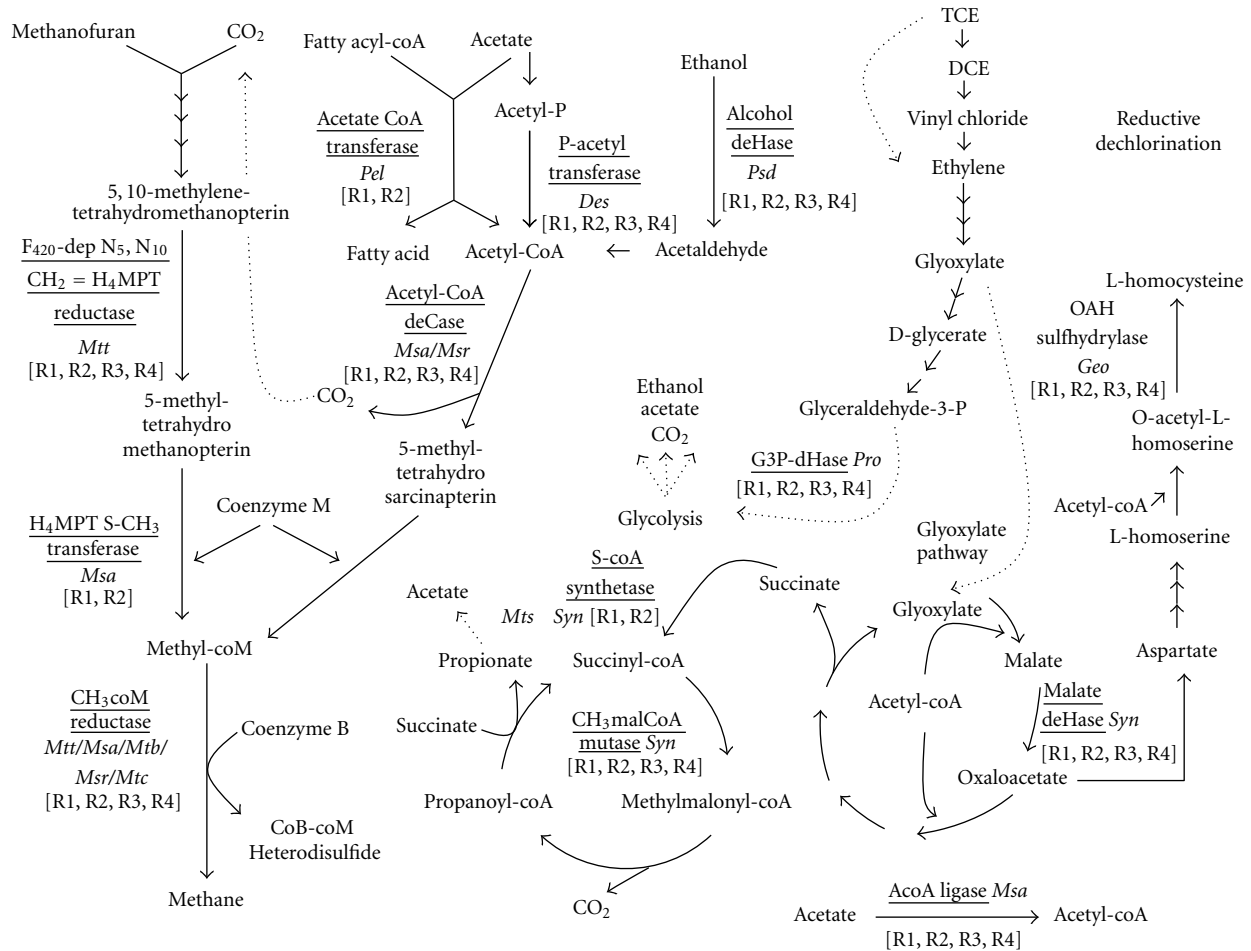
FIGURE 5: Proposed metabolic pathway for the degradation of VFA and TCE inferred from the metaproteomic data. Enzymes identified in this study are underlined. Species abbreviations are as follows: Mtt Methanothermobacter sp.; Msa Methanosaeta sp.; Mtb Methanobacterium sp.; Msr Methanosarcinales sp.; *Mtc Methanoculleus* sp.; Pel *Pelotomaculum* sp.; Des Desulfuromonas sp.; Psd *Pseudomonas* sp.; Syn *Syntrophobacter* sp.; Pro Propionibacterium sp.; *Geo Geobacter* sp. Enzymes were identified from the bioreactors indicated within square brackets, where R1: 37°C TCE-supplemented; R2: 37°C control; R3: 15°C TCE-supplemented; R4: 15°C control.

(Figure 5), was strongly induced in the presence of TCE at 37°C (Table 2), although SMA assays indicated a lower activity of propionate mediated methanogenesis in the presence of TCE (Table 1). It is possible that production of methyl malonyl CoA mutase increased in response to this metabolic bottleneck, and facilitated the stable production of CH_4 at 37°C. In addition, as oxidation of intermediate reduced organic compounds such as propionate is energetically unfavourable, *Syntrophobacter* require growth in coculture with methanogens that utilise both hydrogen and formate, such as *Methanospirillum hungatei*, thereby maintaining low concentrations of these oxidation products and allowing energy gain by all organisms involved [27, 28]. qPCR analysis using a primer/probe set specific for the order Methanomicrobiales, to which the *Methanospirillum* belong, quantified 16S rRNA gene numbers of 10^7-10^9 copies $[gVSS]^{-1}$ on day 235 [9], while specifically, *Methanospirillum hungatei* was detected by analysis of the metaproteome, and associated with a protein of unknown function (Table 2).

Clones associated with several bacterial phyla were detected at low levels in various bioreactors, for example: Bacteroidetes- and Chloroflexi-like clones were identified in all biomass samples (R1–R4; Figure 1); Spirochaetes-like clones only accounted for 1% of the clones from R1 and R3 biomass and were not detected in either R2 or R4 (Figure 1); and *Planctomycetes*-like clones were detected in R2, R3 and R4 (Figure 1). The phyla *Planctomycetes*, Bacteroidetes, Chloroflexi, and Spirochaetes were each represented by one DGGE band, which were detected in both 15°C bioreactors, but were not detected at 37°C (B4, B5, B6 and B17, resp., Figure 3). It is possible that PCR amplification for DGGE was biased against the low levels of these phyla in the bioreactors, as the amplification of a more abundant template DNA fragment has been shown to suppress the amplification of a minor template [29]. These phyla have been classically identified within bioreactors, although the exact functions of Bacteroidetes, Chloroflexi, and Spirochaetes are as of yet unknown [30]. As no proteins

affiliated with these phyla were identified in any sample (Table 2), the functions of these microbial groups in anaerobic bioreactors could not be determined from this study. The majority of the literature regarding the role of the phylum *Planctomycetes* in granular biomass focuses on the anaerobic ammonium oxidising (ANAMMOX) bacteria [31], which convert nitrate and ammonium directly to dinitrogen gas [32], although none of the known proteins associated with this process were identified in this study (Table 2).

Firmicutes-like species were detected by multiple analytical methods in all of the samples. For example, Peptococcaceae-like clones were detected in each clone library (Figure 1) while metaproteomics detected acetate-CoA transferase in both 37°C bioreactors (Table 2), which was associated with *Pelotomaculum thermopropionicum,* a thermophilic, syntrophic, propionate-oxidising bacterium of the Peptococcaceae family [33]. This species has been shown to grow in coculture with the hydrogenotrophic *Methanothermobacter thermoautotrophicus* [33], which was also found to be active in all biomass samples (Table 2). Furthermore, *Syntrophomonas* species within the Firmicutes phylum were represented by both clone library (Figure 1) and DGGE analysis (Figure 3) in all samples, and have previously been shown to grow syntrophically with *Methanospirillum* species, resulting in the formation of methane [34].

The order Desulfuromonadales, and specifically, *Geobacter* species, were detected in all samples (Figures 1 and 3), and have both been associated with the partial dechlorination of TCE to *cis*-1,2 DCE [24]. A protein associated with *Geobacter* sp., O-acetylserine sulfhydrylase, was upregulated in the presence of TCE, at both 37°C and 15°C (Table 2). O-acetylserine sulfhydrylase is involved in the production of L-homocysteine (Figure 5), which can be further converted to cysteine (involved in protein folding) or methionine (often found to interact with the lipid bilayer of membrane-spanning protein domains; [35]). It is possible then, that an increased production of O-acetylserine sulfhydrylase might lead to an increased level of L-homocysteine as a response to the action of lipophilic TCE, which may associate with the cell membrane, resulting in inhibition of cell membrane ATPases [36]. Interestingly, although *Geobacter* species have been associated with TCE dechlorination [24] and have been detected in this study through both clone library (Figure 1) and DGGE analysis (Figure 3), the use of metaproteomics allowed a suggestion for a specific function for this group to be put forward.

No proteins specifically associated with the reductive dechlorination of TCE were identified by 2-DGE analysis of the metaproteome (Table 2). One hypothesis is that as the bioreactor influent contained a much higher concentration of VFA's than TCE, it is possible that the TCE concentration induced the production of sufficient enzymes for TCE dechlorination, but was insufficient for detection by 2-DGE. Although the dechlorination of TCE was not monitored during this trial, we have previously reported the successful dechlorination of TCE to DCE (>98%) with a similar experimental design at 37°C and 15°C [37], and at temperatures as low as 7°C [38]. Similar difficulties associated with the detection of specific enzymes involved

in bioremediation pathways have been encountered with regards to hydrocarbons [39] and chemical pollutants such as toluene [40]. The absence of a matched metagenomic dataset unquestionably hinders protein identification, for example, previous studies have shown that analysis of the metaproteome of activated sludge by 2-DGE resulted in the identification of 38 proteins [41], while implementation of the 2D-nano-LC method with a metagenomic dataset led to the identification of 5029 proteins [42].

Overall, both clone library and DGGE analysis of the bioreactor bacterial populations identified a divergence from the seed biomass that could be attributed more to temperature than TCE. Specifically, UPGMA analysis of DGGE band diversity revealed that the greatest change in bacterial community development occurred between the bioreactors operating at 37°C and at 15°C (Figure 2), while at both temperatures, TCE resulted in a change of <5% between the TCE-exposed and the control biomass (Figure 2). This supports previous studies, which concluded that while analysis of bacterial population dynamics is important, it is not a reliable indicator of process events, as high levels of dynamism can be observed even during times of functional stability [43, 44].

5. Conclusions

The following conclusions can now be drawn: (1) changes in the metaproteome could be observed as a function of operational temperature and exposure to TCE; (2) according to DGGE UPGMA data, the major driver for bacterial community structure development in anaerobic bioreactors was temperature, with a limited response to the presence of TCE; (3) the detection of specific function associated proteins (such as TCE reductive dehalogenases) could have been improved by the availability of a metagenomic dataset to assist protein identification.

Acknowledgments

References

[1] G. Lettinga, "Anaerobic digestion and wastewater treatment systems," *Antonie van Leeuwenhoek, International Journal of General and Molecular Microbiology*, vol. 67, no. 1, pp. 3–28, 1995.

[2] D. Massé, Y. Gilbert, and E. Topp, "Pathogen removal in farm-scale psychrophilic anaerobic digesters processing swine manure," *Bioresource Technology*, vol. 102, no. 2, pp. 641–646, 2011.

[3] R. M. McKeown, C. Scully, T. Mahony, G. Collins, and V. O'Flaherty, "Long-term (1243 days), low-temperature (4–15°C), anaerobic biotreatment of acidified wastewaters: bioprocess performance and physiological characteristics," *Water Research*, vol. 43, no. 6, pp. 1611–1620, 2009.

[4] T. Amani, M. Nosrati, and T. R. Sreekrishnan, "Anaerobic digestion from the viewpoint of microbiological, chemical and

operational aspects—a review," *Environmental Reviews*, vol. 18, pp. 255–278, 2010.

[5] A. M. Enright, G. Collins, and V. O'Flaherty, "Temporal microbial diversity changes in solvent-degrading anaerobic granular sludge from low-temperature (15°C) wastewater treatment bioreactors," *Systematic and Applied Microbiology*, vol. 30, no. 6, pp. 471–482, 2007.

[6] K. Bialek, J. Kim, C. Lee, G. Collins, T. Mahony, and V. O'Flaherty, "Quantitative and qualitative analyses of methanogenic community development in high-rate anaerobic bioreactors," *Water Research*, vol. 45, no. 3, pp. 1298–1308, 2011.

[7] M. Tabatabaei, R. A. Rahim, N. Abdullah et al., "Importance of the methanogenic archaea populations in anaerobic wastewater treatments," *Process Biochemistry*, vol. 45, no. 8, pp. 1214–1225, 2010.

[8] Y. Liu and W. B. Whitman, "Metabolic, phylogenetic, and ecological diversity of the methanogenic archaea," *Annals of the New York Academy of Sciences*, vol. 1125, pp. 171–189, 2008.

[9] A. Siggins, A. M. Enright, and V. O'Flaherty, "Methanogenic community development in anaerobic granular bioreactors treating trichloroethylene (TCE)-contaminated wastewater at 37°C and 15°C," *Water Research*, vol. 45, no. 8, pp. 2452–2462, 2011.

[10] USEPA United States National Toxicology Program, 12th Report on carcinogens, 2011, http://ntp.niehs.nih.gov/ntp/roc/twelfth/profiles/Trichloroethylene.pdf.

[11] P. J. M. Middeldorp, M. L. G. C. Luijten, B. A. Van de Pas et al., "Anaerobic microbial reductive dehalogenation of chlorinated ethenes," *Bioremediation Journal*, vol. 3, no. 3, pp. 151–169, 1999.

[12] J. D. Coates, M. F. Coughlan, and E. Colleran, "Simple method for the measurement of the hydrogenotrophic methanogenic activity of anaerobic sludges," *Journal of Microbiological Methods*, vol. 26, no. 3, pp. 237–246, 1996.

[13] E. Colleran, F. Concannon, T. Golden et al., "Use of methanogenic activity tests to characterize anaerobic sludges, screen for anaerobic biodegradability and determine toxicity thresholds against individual anaerobic trophic," *Water Science and Technology*, vol. 25, no. 7, pp. 31–40, 1992.

[14] E. F. DeLong, "Archaea in coastal marine environments," *Proceedings of the National Academy of Sciences of the United States of America*, vol. 89, no. 12, pp. 5685–5689, 1992.

[15] D. J. Lane, B. Pace, and G. J. Olsen, "Rapid determination of 16S ribosomal RNA sequences for phylogenetic analyses," *Proceedings of the National Academy of Sciences of the United States of America*, vol. 82, no. 20, pp. 6955–6959, 1985.

[16] J. D. Thompson, T. J. Gibson, F. Plewniak, F. Jeanmougin, and D. G. Higgins, "The CLUSTAL X windows interface: flexible strategies for multiple sequence alignment aided by quality analysis tools," *Nucleic Acids Research*, vol. 25, no. 24, pp. 4876–4882, 1997.

[17] D. L. Swofford, *PAUP*. Phylogenetic Analysis Using Parsimony (* and Other Methods), Version 4*, Sinauer Associates, Sunderland, Mass, USA, 2001.

[18] E. H. Simpson, "Measurement of diversity," *Nature*, vol. 163, no. 4148, p. 688, 1949.

[19] G. Muyzer, E. C. De Waal, and A. G. Uitterlinden, "Profiling of complex microbial populations by denaturing gradient gel electrophoresis analysis of polymerase chain reaction-amplified genes coding for 16S rRNA," *Applied and Environmental Microbiology*, vol. 59, no. 3, pp. 695–700, 1993.

[20] B. McCune and J. B. Grace, *Analysis of Ecological Communities*, MjM Software, Corvallis, Ore, USA, 2002.

[21] F. Abram, E. Gunnigle, and V. O'Flaherty, "Optimisation of protein extraction and 2-DE for metaproteomics of microbial communities from anaerobic wastewater treatment biofilms," *Electrophoresis*, vol. 30, no. 23, pp. 4149–4151, 2009.

[22] F. Abram, A. M. Enright, J. O'Reilly, C. H. Botting, G. Collins, and V. O'Flaherty, "A metaproteomic approach gives functional insights into anaerobic digestion," *Journal of Applied Microbiology*, vol. 110, no. 6, pp. 1550–1560, 2011.

[23] N. Saitou and M. Nei, "The neighbor-joining method: a new method for reconstructing phylogenetic trees," *Molecular Biology and Evolution*, vol. 4, no. 4, pp. 406–425, 1987.

[24] F. E. Löffler, Q. Sun, J. Li, and J. M. Tiedje, "16S rRNA gene-based detection of tetrachloroethene-dechlorinating *Desulfuromonas* and *Dehalococcoides* species," *Applied and Environmental Microbiology*, vol. 66, no. 4, pp. 1369–1374, 2000.

[25] R. Chouari, D. Le Paslier, P. Daegelen, P. Ginestet, J. Weissenbach, and A. Sghir, "Novel predominant archaeal and bacterial groups revealed by molecular analysis of an anaerobic sludge digester," *Environmental Microbiology*, vol. 7, no. 8, pp. 1104–1115, 2005.

[26] J. J. Godon, E. Zumstein, P. Dabert, F. Habouzit, and R. Moletta, "Molecular microbial diversity of an anaerobic digestor as determined by small-subunit rDNA sequence analysis," *Applied and Environmental Microbiology*, vol. 63, no. 7, pp. 2802–2813, 1997.

[27] F. A. M. De Bok, M. L. G. C. Luijten, and A. J. M. Stams, "Biochemical evidence for formate transfer in syntrophic propionate-oxidizing cocultures of Syntrophobacter fumaroxidans and *Methanospirillum hungatei*," *Applied and Environmental Microbiology*, vol. 68, no. 9, pp. 4247–4252, 2002.

[28] X. Dong, C. M. Plugge, and A. J. M. Stams, "Anaerobic degradation of propionate by a mesophilic acetogenic bacterium in coculture and triculture with different methanogens," *Applied and Environmental Microbiology*, vol. 60, no. 8, pp. 2834–2838, 1994.

[29] S. Becker, P. Boger, R. Oehlmann, and A. Ernst, "PCR bias in ecological analysis: a case study for quantitative Taq nuclease assays in analyses of microbial communities," *Applied and Environmental Microbiology*, vol. 66, no. 11, pp. 4945–4953, 2000.

[30] G. Talbot, E. Topp, M. F. Palin, and D. I. Massé, "Evaluation of molecular methods used for establishing the interactions and functions of microorganisms in anaerobic bioreactors," *Water Research*, vol. 42, no. 3, pp. 513–537, 2008.

[31] C. J. Tang, P. Zheng, Q. Mahmood, and J. W. Chen, "Start-up and inhibition analysis of the Anammox process seeded with anaerobic granular sludge," *Journal of Industrial Microbiology and Biotechnology*, vol. 36, no. 8, pp. 1093–1100, 2009.

[32] A. Abeliovich, "Transformations of ammonia and the environmental impact of nitrifying bacteria," *Biodegradation*, vol. 3, no. 2-3, pp. 255–264, 1992.

[33] H. Imachi, Y. Sekiguchi, Y. Kamagata, A. Ohashi, and H. Harada, "Cultivation and in situ detection of a thermophilic bacterium capable of oxidizing propionate in syntrophic association with hydrogenotrophic methanogens in a thermophilic methanogenic granular sludge," *Applied and Environmental Microbiology*, vol. 66, no. 8, pp. 3608–3615, 2000.

[34] M. Hatamoto, H. Imachi, S. Fukayo, A. Ohashi, and H. Harada, "*Syntrophomonas palmitatica* sp. nov., an anaerobic syntrophic, long-chain fatty-acid-oxidizing bacterium isolated from methanogenic sludge," *International Journal of Systematic and Evolutionary Microbiology*, vol. 57, no. 9, pp. 2137–2142, 2007.

[35] J. T. Brosnan and M. E. Brosnan, "The sulfur-containing amino acids: an overview," *Journal of Nutrition*, vol. 136, no. 6, pp. 16365–16405, 2006.

[36] L. H. Lash, J. W. Fisher, J. C. Lipscomb, and J. C. Parker,"'Metabolism of trichloroethylene," *Environmental Health Perspectives*, vol. 108, no. 2, pp. 177–200, 2000.

[37] A. Siggins, A. M. Enright, and V. O'Flaherty, "Temperature dependent (37-15°C) anaerobic digestion of a trichloroethylene-contaminated wastewater," *Bioresource Technology*, vol. 102, no. 17, pp. 7645–7656, 2011.

[38] A. Siggins, A. M. Enright, and V. O'Flaherty, "Low-temperature (7°C) anaerobic treatment of a trichloroethylene-contaminated wastewater: microbial community development," *Water Research*, vol. 45, no. 13, pp. 4035–4046, 2011.

[39] F. Bastida, C. Nicolás, J. L. Moreno, T. Hernández, and C. García, "Tracing changes in the microbial community of a hydrocarbon-polluted soil by culture-dependent proteomics," *Pedosphere*, vol. 20, no. 4, pp. 479–485, 2010.

[40] M. A. Williams, E. B. Taylor, and H. P. Mula, "Metaproteomic characterization of a soil microbial community following carbon amendment," *Soil Biology and Biochemistry*, vol. 42, no. 7, pp. 1148–1156, 2010.

[41] P. Wilmes, M. Wexler, and P. L. Bond, "Metaproteomics provides functional insight into activated sludge wastewater treatment," *PLoS ONE*, vol. 3, no. 3, Article ID e1778, 2008.

[42] P. Wilmes, A. F. Andersson, M. G. Lefsrud et al., "Community proteogenomics highlights microbial strain-variant protein expression within activated sludge performing enhanced biological phosphorus removal," *The ISME Journal*, vol. 2, no. 8, pp. 853–864, 2008.

[43] A. Fernández, S. Huang, S. Seston et al., "How stable is stable? Function versus community composition," *Applied and Environmental Microbiology*, vol. 65, no. 8, pp. 3697–3704, 1999.

[44] S. McHugh, G. Collins, T. Mahony, and V. O'Flaherty, "Biofilm reactor technology for low temperature anaerobic waste treatment: microbiology and process characteristics," *Water Science and Technology*, vol. 52, no. 7, pp. 107–113, 2005.

Research Article

New Strategy for a Suitable Fast Stabilization of the Biomethanization Performance

L. A. Fernández-Güelfo,[1] C. J. Álvarez-Gallego,[1] D. Sales Márquez,[2] and L. I. Romero García[1]

[1] *Department of Chemical Engineering and Food Technology, Faculty of Science, University of Cadiz, Cadiz, 11510 Puerto Real, Spain*
[2] *Department of Environmental Technologies, Faculty of Marine and Environmental Sciences, University of Cadiz, Cadiz, 11510 Puerto Real, Spain*

Correspondence should be addressed to L. A. Fernández-Güelfo, alberto.fdezguelfo@uca.es

The start-up strategies for thermophilic anaerobic reactors usually consist of an initial mesophilic stage (35°C), with an approximate duration of 185 days, and a subsequent thermophilic stage (55°C), which normally requires around 60 days to achieve the system stabilizatio. During the first 8–10 days of the mesophilic stage, the reactor is not fed so that the inoculum, which is generally a mesophilic anaerobic sludge, may be adapted to the organic solid waste. Between mesophilic and thermophilic conditions the reactor is still not fed in an effort to prevent possible imbalances in the proces. As a consequence, the start-up and stabilization of the biomethanization performance described in the literature require, at least, around 245 days. In this sense, a new strategy for the start-up and stabilization phases is presented in this study. This approach allows an important reduction in the overall time necessary for these stages in an anaerobic continuous stirred tank reactor (CSTR) operated at thermophilic-dry conditions for treating the organic fraction of the municipal solid waste (OFMSW): 60 days versus 245 days of conventional strategies. The new strategy uses modified SEBAC technology to adapt an inoculum to the OFMSW and the operational conditions prior to seeding the CSTR.

1. Introduction

The organic fraction of municipal solid wastes (OFMSW) has been commonly treated by means of anaerobic digestion (AD) [1–3]. Among the main advantages of this biological process, the low energy consumption and sludge generation and the high hydrogen and/or methane productions must be highlighted; however, the main disadvantage is its slowness.

In order to avoid this important inconvenience and to accelerate the process with regard to the mesophilic-wet conditions (35°C, 5–10% total solids concentration), AD may be operated at thermophilic-dry (55°C, 30% total solids concentration) conditions. At these new conditions the hydrolysis phase is faster and more effective and, therefore, the overall rate of the process is improved. On the other hand, it must be noted that for the start-up and stabilization of the biomethanization process in continuous stirred tank reactor

(CSTR) for anaerobic biodegrading of OFMSW is necessary operational times extremely long.

As it is reported by the authors Bolzonella et al. [4] and Michaud et al. [5], the strategy generally employed to start-up and stabilization of thermophilic anaerobic digesters consists of two stages.

(1) A mesophilic stage (35°C) of about 185 days of operation. During the first 8–10 days the reactor is not fed in order to the inoculum (generally anaerobic mesophilic sewage sludge) may be adapted to the waste.

(2) A thermophilic stage (55°C) with an approximate duration of 60 days at least. In addition, during the mesophilic-thermophilic transition the reactor is not fed to prevent destabilization episodes.

Following this, the strategies reported in the literature have an approximate duration of about 245 days at least. This fact is mainly because the inoculum is not adapted to the type of waste and/or the operational conditions.

With specific reference to the full-scale industrial application of the AD processes, at first, because of the historical background, more reactors adopting the wet processes (<10% dry solids in the reactor) were applied; since then, dry digestion (more than 25% dry solids in the feed) has prevailed because of the reduced volume of reactors and wastewater production. Most applied technologies for dry processes are Dranco, Valorga, Linde, and Kompogas, all working in the range 30–40% of total solids in the reactor feeding [6].

About the conventional ranges of temperature of the AD processes, a total treatment capacity for solid waste organics, excluding the tonnage used for sewage sludge and manures, evolved from 122,000 ton per year in 1990 to 1,037,000 ton available or under construction by the last decade in 53 plants across Europe, an increase by 750%. Both mesophilic and thermophilic technologies have been proven, with about 38% of capacity being operated at thermophilic temperatures. All digestion plants were initially operated at mesophilic temperatures. The first thermophilic plants were dry fermentation plants and came online in 1992 and 1993. The capacity of mesophilic operation increased by 350,000 ton during 1994 through 1999, while thermophilic capacity increased by 280,000 ton or 70,000 ton and 56,000 ton per year, respectively. During some years, more mesophilic plants are added while during other years more thermophilic capacity is constructed. No clear trend can be observed. It can be expected that the increase will be level for both temperature ranges, even though more suppliers are starting to provide thermophilic digestion. Thermophilic operation was developed later but has been established as a reliable and accepted mode of fermentation. It provides the added benefit of treating the waste at higher temperatures and thereby increasing pathogen kill-off during the anaerobic phase. The added amount of heat does not seem to stop companies operating thermophilically, as higher gas production yields and rates are being claimed by various suppliers [7].

For all the above reasons, an inoculum adapted to the waste (OFMSW) and the operational conditions (thermophilic-dry AD) was obtained by mean of the modified sequencing batch anaerobic composting (SEBAC) technology. This technology and its modifications are fully detailed in the literature [8–11] and have been successfully employed to develop the AD of OFMSW with acceptable conversions in only 30 days.

The modification of the SEBAC technology used in this research is based on the interconnection of two anaerobic digesters (reactors A and B). Daily, reactors A and B are fed by means of the recirculation of the leachate generated from the other reactor. In this way the fresh organic waste (reactor A) to be digested is inoculated through recirculation of the leachate or effluent from the reactor containing the digested waste (reactor B), while the leachate generated by the reactor with fresh waste (reactor A) is recirculated to the reactor with the digested waste (reactor B). In this way a flow of

microorganisms is established to the undigested waste and of organic material to the digested waste [12].

Based on all the stated above and in order to reduce the long-time periods required for the start-up and stabilization of the biomethanization in a CSTR operated at thermophilic-dry conditions for treating OFMSW, two main goals may be defined in this work which are as follows.

(i) To obtain a suitable inoculum quickly by means of the modified SEBAC technology commented previously. This inoculum will be adapted to the OFMSW and the operational conditions typical of the thermophilic-dry AD ($55°C$ and 30% total solids concentration).

(ii) To achieve stable biomethanization performance for the thermophilic-dry AD of OFMSW in a CSTR using the inoculum obtained by the modified SEBAC technology.

2. Materials and Methods

2.1. Modified SEBAC Technology. This system consists of the interconnection of two anaerobic 25 L-reactors (Figure 1), operating under thermophilic-dry conditions ($55°C$ and 30% total solids concentration).

(i) Reactor A contains alternate layers of source selected OFMSW and pig manure with a total solids concentration of 30%. The pig manure accelerates the colonization of the OFMSW since it is a potential source of anaerobic microorganisms.

(ii) Reactor B generally contains a stabilized waste previously degraded by anaerobic digestion, with a high concentration of viable and active microorganisms [13]. In this study, anaerobic mesophilic sludge, from the anaerobic digesters of a full-scale plant for treating sewage sludge, was used.

Daily, the leachate produced in reactor A was exchanged to reactor B and an equivalent quantity of sludge from reactor B was added to reactor A. This procedure causes a flow of microorganisms from B to A and a flow of organic matter from reactor A to B. Reactors do not require agitation and the time required for effective start-up is around 30 days. The composition of the modified SEBAC reactors is shown in Table 1.

2.2. Continuous Stirred Tank Reactor (CSTR). The CSTR was initially loaded with 1.5 kg of milled and dry synthetic OFMSW (90% in total solids concentration). The moisture was adjusted using the inoculum obtained by means of the modified SEBAC technology described above. Concretely, the inoculums consisted of a 1 : 1 v/v mixture [14–16] of thermophilic sludge and leachate. In this sense, 4 litres of inoculum (2 litres of sludge + 2 litres of leachate) were required to add moisture to the synthetic OFMSW.

The compositions of the different wastes used in this study are given in Table 2. It must be noted that the synthetic OFMSW was prepared based on the nutritional requirements of the main populations of microorganisms involved in the
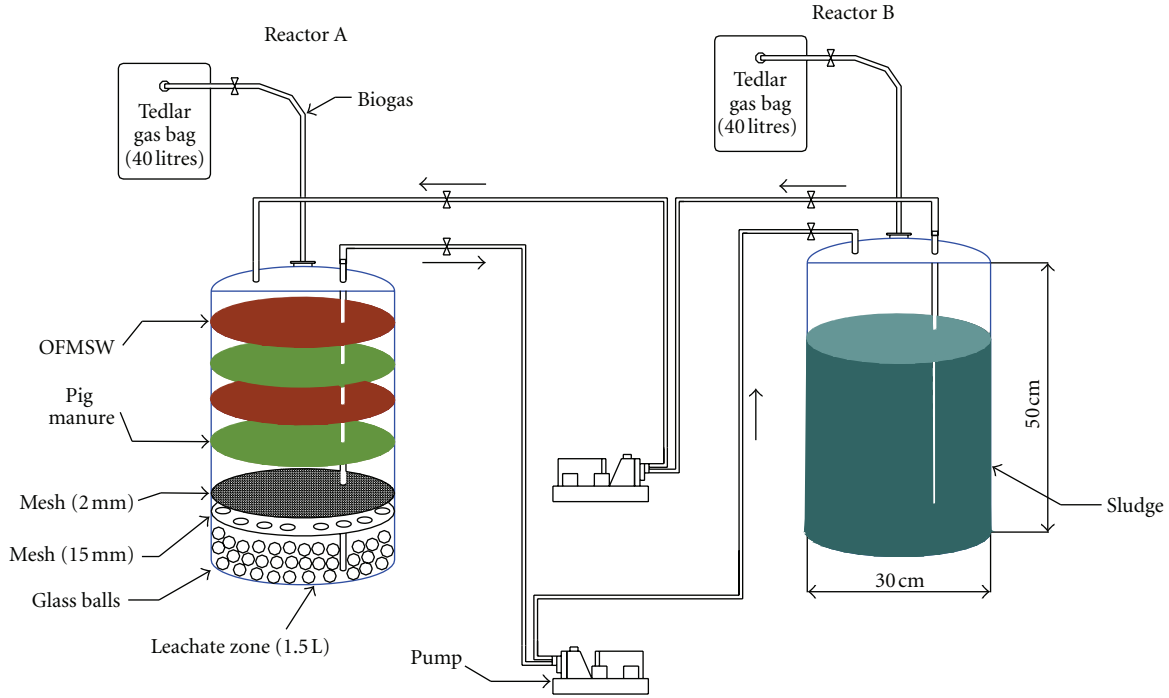
Figure 1: Flow of leachate in the modified SEBAC reactors.

Table 1: Composition of the modified SEBAC reactors.

	Wastes	Layers	Weight/layer (kg)
Reactor A	OFMSW	2	1
	Pig manure	2	1.5
Reactor B	Sludge	—	21

AD [17]. This type of feed avoids the problem of high variations in the composition of the source selected OFMSW. This aspect is important in order to determine an accurate efficiency for the process.

2.3. Processing of the OFMSW. Control of the total solid concentration of the feed is necessary to obtain a suitable level of performance for the dry AD. Therefore, pretreatment of the OFMSW samples was necessary to adjust them to the required optimum values. In this study, the samples were dried at 55°C for 48 hours and then at ambient temperature for 72 hours until final moisture content of 10% was achieved. The dried OFMSW was milled until a particle size of approximately 1 cm was obtained and, finally, the moisture was adjusted to 70–75% (25–30% in total solids concentration, which is characteristic of dry AD) with tap water, leachate from garbage, sludge, or combinations of these.

2.4. Analytical Techniques. For the control of the reactors, the following parameters were determined: the volume and composition of the biogas (H_2, O_2, N_2, CH_4, and CO_2), volatile fatty acids (VFA), total solids (TS), suspended total solids (STS), total volatile solids (TVS), suspended volatile solid (SVS), alkalinity, pH, dissolved organic carbon (DOC), ammonium, chemical oxygen demand (COD), and density. The analytical techniques were performed according to procedures described by Álvarez-Gallego [18].

3. Results and Discussion

3.1. Inoculum Preparation through Modified SEBAC Technology. The daily volume of leachate exchanged between the two modified SEBAC reactors must be between 5 and 10% of the initial volume of OFMSW for digestion [8]. For this reason, Reactor A controls the start-up phase, which is the *rate limiting step* of the process [19]. The theoretical calculation indicates that the volume of leachate that should be exchanged is approximately 600 mL. From the fourth day of operation until the conclusion of the experiment (hundredth day), the flow of leachate between the two reactors was maintained at 600 mL.

The minimum time required to obtain a suitable inoculum through modified SEBAC technology may be determined from the accumulated methane production curves generated in reactors A and B. As can be seen in Figure 2, the curves of both reactors present the maximum slope in 30 days of operation, more pronounced in reactor B (sludge). This fact indicates an exponential growth of the methanogenic Archaea in the system and, therefore, if the inoculum is taken in this moment, it will present a high methanogenic activity. Thus, the sludge from day 30 can be considered as a viable inoculum for the biomethanization of OFMSW at thermophilic-dry conditions. Finally, the initial and final compositions of wastes at the end of the assay are shown in Table 3.

TABLE 2: Composition of the wastes used to start-up the CSTR.

| Parameter	Leachate inoculum	Sewage sludge inoculum	OFMSW	OFMSW/Inoculum mixture
pH	8.62	8.35	7.78	8.70
Density (kg/m^3)	980	985	750	1116
Alkalinity (gCaCO$_3$/L)	21.78	16.54	4.29	5.14
Ammonium (gNH$_3$–N/L)	26.88	14.56	1.68	2.8
Total Nitrogen	25.66 gNH$_3$–N/L	21.46 gNH$_3$–N/L	207.2 gNH$_3$–N/kg	72.8 gNH$_3$–N/kg
gTSS/L	14.46	20.46	—	—
gVSS/L	10.73	9.16	—	—
gTS/g sample	—	—	0.90	0.31
gTVS/g sample	—	—	0.71	0.25
Total carbon (mg/g)	80.78	35.27	112.6	65.07
Total inorganic carbon (mg/g)	2.07	0.96	0.29	0.30
Total organic carbon (mg/g)	78.41	34.31	112.3	64.75
Acidity (mgAcH/L)	12403	17353	1440	356
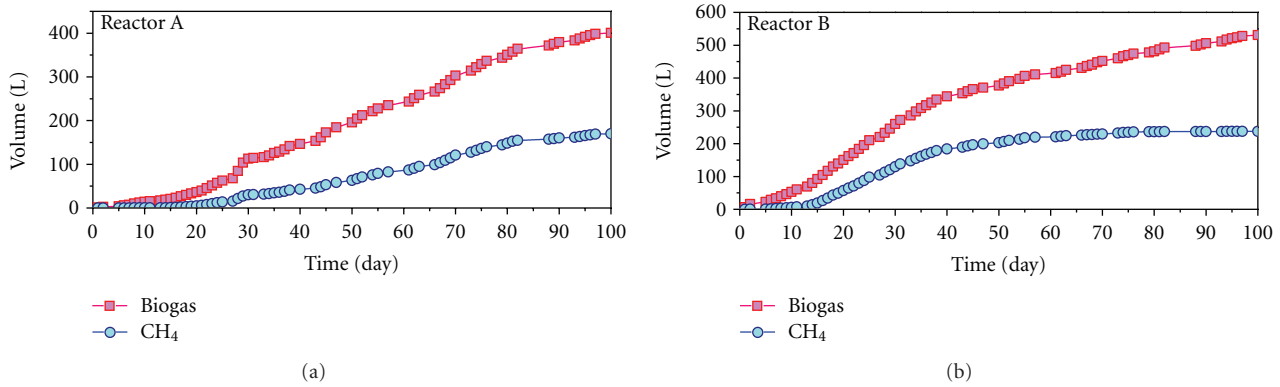
FIGURE 2: Accumulation of biogas and methane productions in the modified SEBAC reactors.

3.2. Start-Up and Stabilization of the Biomethanization Process. A continuously stirred tank reactor (CSTR) was started-up under thermophilic-dry conditions and a series of four solid retention times (SRT) was carried out in order to study the effect of the added organic loading rate (OLR$_0$) on the biomethanization performance at semicontinuous regime of feeding.

Along the four consecutive stages, the OLR$_0$ (expressed as mgDOC/L·d and mgTVS/L·d) was increased and it was maintained constant in each SRT. The SRT, OLR$_0$, and operation time data for each stage are shown in Table 4.

In the first stage the OLR imposed was relatively low (0.704 gDOC/L·day) in order to check if the system evolved appropriately. The results obtained in the first 14 days were favourable and, therefore, the OLR was increased to 0.805 gDOC/L·day. The OLR$_0$ used at stage 1 was different to the values reported in the literature. Bolzonella et al. [4] carried out start-up phase studies in the mesophilic range with an extremely low OLR—less than 0.16 gDOC/L·day—for approximately 40 days. It must be highlighted that, in this study, the start-up phase was carried out using the SEBAC inoculum, which had been previously adapted to the waste and operational conditions. This fact allows that the reactor may be operated at higher OLR.

3.2.1. Study of the Gas Productions. As can be seen from Figure 3, the biogas generated in stage 1 is not useful and this stage may be considered as a latency period in which the hydrolysis and colonization of the waste takes place. During stage 2, the specific methane yield reaches its maximum average values of 1.11 LCH$_4$/gDOC degraded and 0.51 LCH$_4$/gTVS degraded due to the biodegradation of the VFA accumulated in the previous stage. Finally, during stages 3 and 4, the methane yield coefficient stays constant at around 0.91 LCH$_4$/gDOC and 0.1 LCH$_4$/gTVS respectively, indicating stable biomethanization performance in the system.

On the other hand, the average specific methane yield in term of COD reaches the value of 0.42 LCH$_4$/gCOD in stage 2 and 0.34 LCH$_4$/gCOD in stages 3 and 4. However, in stage 1 the average specific methane yield is practically zero, 0.01 LCH$_4$/gCOD. In accordance with Bushwell and Mueller [20], the stoichiometric value for methane generation is 0.35 LCH$_4$/gCOD, which indicates that in stages 3 and 4 the reactor is working with a methane yield coefficient very close to the theoretical maximum. However, the value obtained for the 35-day SRT (stage 2) is higher than the theoretical maximum. This discrepancy is due to the fact that in this SRT, in addition to the degradation of the OLR added, the

TABLE 3: Initial and final compositions of the wastes.

Parameters	OFMSW		Pig manure		Sludge	
	Initial	Final	Initial	Final	Initial	Final
Density (kg/m³)	600	850	1200	1000	900	1000
Total solids (g/kg)	878	173	586	80	42	26.6
Total volatile solids (g/kg)	700.4	85	464.1	60	15	2.6
Suspended total solids (g/L)	0.5	7.9	3.9	5	20.2	11.4
Suspended volatile solids (g/L)	3.6	6.9	3.5	3.4	7.7	7.4
pH	0.2	8.1	7.1	8.4	8.3	8.35
Alkalinity (gCaCO₃/L)	7.6	8.4	50	75.4	20.1	16.5
Chemical oxygen demand (mgO₂/L)	112000	41558	14814	6509	10527	25526

TABLE 4: Initial organic loading rate (OLR_0) for each SRT.

Stage	SRT (day)	Operation time (day)	OLR_0	
			gDOC/L·day	gTVS/L·day
1	40	14	0.704	4.42
2	35	17	0.805	5.07
3	30	25	0.940	5.92
4	25	50	1.123	7.50
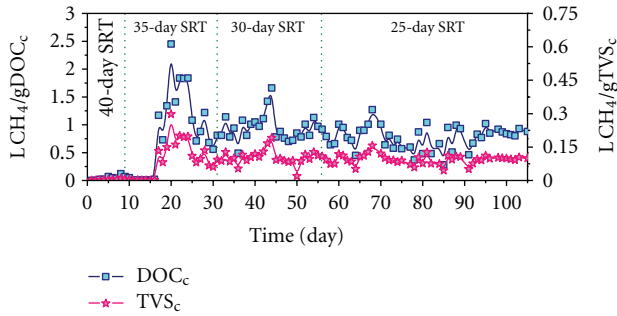
FIGURE 3: Evolution of the specific methane yield expressed as $LCH_4/gDOC_c$ and $LCH_4/gTVS_c$.

FIGURE 4: Daily biogas and methane productions expressed as $L/L_{Reactor}$·day.

FIGURE 5: Biogas composition expressed as percentage.

transformation of the organic matter accumulated in the system during the previous 40-day SRT takes place. As a consequence, the methane yield coefficient obtained is higher than its theoretical value.

As far as the daily biogas generation is concerned, during the first 3 days of stage 1 a significant level of production was observed due to the hydrolysis of the waste (Figure 4). The composition observed in this period is usual for hydrolytic phase: H_2 (20%) and CO_2 (80%), see Figure 5.

During the hydrolysis phase complex molecules are transformed into other simpler products, without methane production. For this reason, in Figure 5, stage 1 has been considered as a latency phase.

However, in stage 2, H_2 levels drop to zero due to the methanogenic activity while CH_4 and CO_2 converge at around 50%, which is typical behaviour of a stable biomethanization process. In this phase, the intermediate products generated in the hydrolysis are converted into CO_2 and CH_4 by the methanogenic Archaea and as consequence the daily
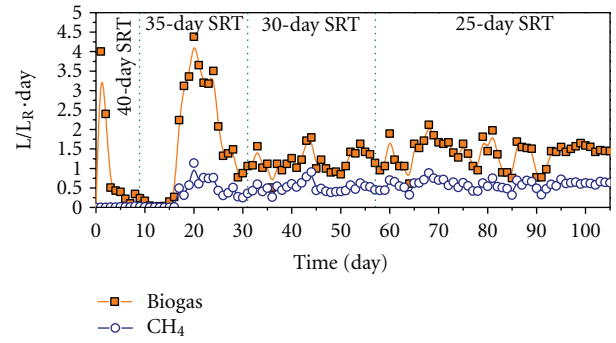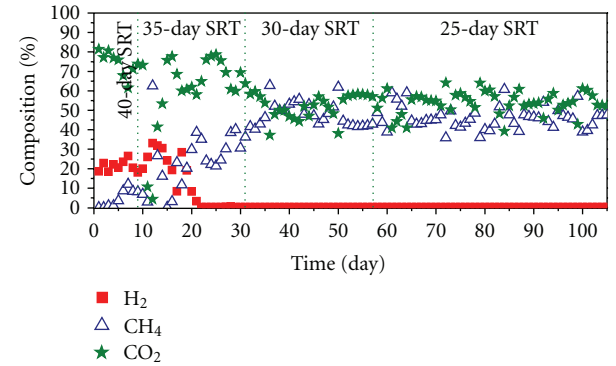
average biogas production reaches its maximum average value of $1.834\,L_{Biogas}/L_{Reactor}$·day an average stable methane production of $0.55\,LCH_4/L_{Reactor}$·day after 15 days of operation time. About the last value, $0.55\,LCH_4/L_{Reactor}$·day, it is higher than the result reported by Fernández et al. [21] in their dry AD studies of OFMSW using the same technology (CSTR) with similar SRTs. In that work, sewage sludge anaerobically digested at mesophilic regime of temperature coming from a full-scale WWTP was used as inoculums to start-up a CSTR. In that case, the system reaches a stable methane production of $0.48\,LCH_4/L_R$·day after 25 days of operation time and at 30-day SRT. In this work, the system reaches a stable methane production of $0.55\,LCH_4/L_R$·day after 15 days of operation time and at

35-day SRT (very positive result since higher SRTs are associated with low methane yields). Therefore, the start-up period is decreased about 40% with this strategy and, in addition, the methane production is improved around 15% although the SRT is higher (35 versus 30 days), and, therefore, the methane production should be lower.

In stage 3 the daily average biogas production decreases to 1.138 $L_{Biogas}/L_{Reactor} \cdot$ day since most of the initial waste which was loaded into the reactor has been degraded. Nevertheless, the composition of the biogas is stabilized with values of CO_2 and CH_4 at around 50%, which indicates that a balance between the different microbial populations involved in the digestion has been reached in the reactor.

Finally, in stage 4 the daily average biogas production increase to 1.768 $L_{Biogas}/L_{Reactor} \cdot$ d due to the OLR_0 increased, with a composition in CO_2 and CH_4 of 55 and 45%, respectively (Figure 5).

3.2.2. VFA Evolution. As can be seen in Figure 6, from day 90 at 35-day SRT, the total VFA and butyric and acetic acids concentrations reach very stable values of around 8000, 2500, and 400 mg/L, respectively. It must be noted that in this specific period (from 90 to 105 days), the stabilization of VFA concentrations matches with a stable specific methane yield, expressed in terms of DOC and TVS (Figure 3), and with a stable biogas and methane productions (Figure 4). In addition, removal percentages of 56% for TS, 89% for TVS, and 63% for DOC were observed. These values have been compared with literature values [8, 22] and they confirm that the biomethanization operates efficiently at stable conditions. Hence, it is possible to reach stable biomethanization performance in SRT that is appropriate for full-scale plants (25 days) in approximately 90 days.

4. Conclusions

As a general conclusion, a successful strategy for the start-up and stabilization phase of the biomethanization process of OFMSW in a CSTR operated at thermophilic-dry conditions has been developed. The new strategy allows stable operation in a reduced time versus other literature protocols. Taking into account the above main conclusion, the following specific conclusions may be established.

(1) In the first stage, a thermophilic anaerobic inoculum adapted to the OFMSW must be obtained by means of the modified SEBAC technology. This inoculum is used in the second stage to inoculate the CSTR. The semicontinuous reactor must be subsequently fed with milled OFMSW in a high SRT (40 days). When the system is stabilized, the SRT imposed can be progressively diminished until reaching 25-day SRT.

(2) The results obtained from the modified SEBAC reactors indicate that an incubation period of approximately 30 days is necessary to obtain an appropriate inoculum. From the day 30 of operation the system reaches a high biogas production with a high methane percentage.
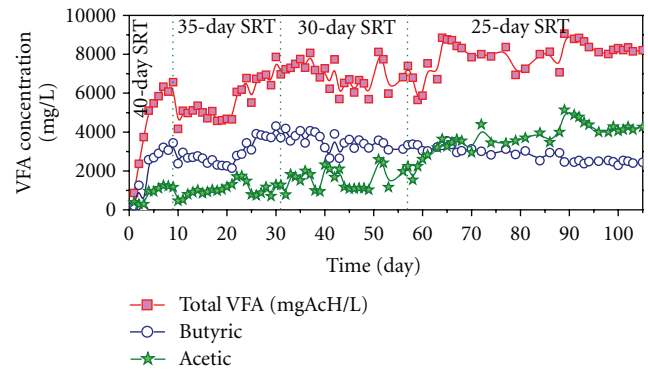

Figure 6: Evolution of total VFA, butyric, and acetic acids.

(3) The semicontinuous reactor can be inoculated with a 1 : 1 mixture of the effluents (leachate of OFMSW and sludge) from the modified SEBAC reactors and a period for the acclimatization of microorganisms is not required prior to feeding the system.

(4) A high retention time must be initially imposed (40 days) to avoid irreversible distortions in the process. The SRT is subsequently reduced progressively, which is associated with an increase in the OLR_0, until the required operational conditions are reached. The stabilization of the system, for an SRT of 35 days (OLR_0 of 0.805 gDOC/L·d), requires 30 days of operation. Under these conditions the maximum average methane productions is reached, 1.834 $L_{Biogas}/L_{Reactor} \cdot$ day.

(5) For a successful start-up of the system, it is necessary a period of 60 days at least (30 days to obtain the inoculum and 30 days to stabilize the system at 35-day SRT. In addition, it is possible to reach stable operation in times that are appropriate for industrial operation (25-day SRT) in approximately 90 days. These data compare favourably with literature results for similar reactors, where the start-up periods are higher than 245 days.

In summary, the preparation of an inoculum adapted to the solid waste and operational conditions by means of modified SEBAC procedure enables us to reduce the time necessary to start-up and stabilization of a CSTR for the thermophilic-dry AD of OFMSW by a factor of four (60 days versus 245) with respect to conventional strategies reported in the literature.

Acknowledgments

References

[1] K. F. Fannin, J. R. Conrad, V. J. Srivastava, D. E. Jerger, and D. P. Chynoweth, "Anaerobic processes," *Journal of the Water Pollution Control Federation*, vol. 55, no. 6, pp. 623–632, 1983.

[2] T. Akao, E. Mizuki, H. Saito, S. Okumura, and S. Murao, "The methane fermentation of *Citrus unshu* peel pretreated with fungus enzymes," *Bioresource Technology*, vol. 41, no. 1, pp. 35–39, 1992.

[3] K. K. Moorhead and R. A. Nordstedt, "Batch anaerobic digestion of water hyacinth: effects of particle size, plant nitrogen content, and inoculum volume," *Bioresource Technology*, vol. 44, no. 1, pp. 71–76, 1993.

[4] D. Bolzonella, L. Innocenti, P. Pavan, P. Traverso, and F. Cecchi, "Semi-dry thermophilic anaerobic digestion of the organic fraction of municipal solid waste: focusing on the start-up phase," *Bioresource Technology*, vol. 86, no. 2, pp. 123–129, 2003.

[5] S. Michaud, N. Bernet, P. Buffière, M. Roustan, and R. Moletta, "Methane yield as a monitoring parameter for the start-up of anaerobic fixed film reactors," *Water Research*, vol. 36, no. 5, pp. 1385–1391, 2002.

[6] D. Bolzonella, P. Pavan, S. Mace, and F. Cecchi, "Dry anaerobic digestion of differently sorted organic municipal solid waste: a full-scale experience," *Water Science and Technology*, vol. 53, no. 8, pp. 23–32, 2006.

[7] L. de Baere, "Anaerobic digestion of solid waste: state-of-the-art," *Water Science and Technology*, vol. 41, no. 3, pp. 283–290, 2000.

[8] T. Forster-Carneiro, L. A. Fernández, M. Pérez, L. I. Romero, and C. J. Álvarez, "Optimization of sebac start-up phase of municipal solid waste anaerobic digestion," *Chemical and Biochemical Engineering Quarterly*, vol. 18, no. 4, pp. 429–439, 2004.

[9] T. Forster-Carneiro, M. Pérez, L. I. Romero, and D. Sales, "Dry-thermophilic anaerobic digestion of organic fraction of the municipal solid waste: focusing on the inoculum sources," *Bioresource Technology*, vol. 98, no. 17, pp. 3195–3203, 2007.

[10] D. P. Chynoweth and R. LeGrand, "Apparatus and method for sequential batch anaerobic composting of high−solids organics feedstocks," Unites States Patent Number 5269634, University of Florida, 1993.

[11] D. P. Chynoweth, G. Bosch, J. F. K. Earle, R. Legrand, and K. Liu, "A novel process for anaerobic composting of municipal solid waste," *Applied Biochemistry and Biotechnology*, vol. 28-29, no. 1, pp. 421–432, 1991.

[12] L. T. Angenent, S. Sung, and L. Raskin, "Methanogenic population dynamics during start-up of a full-scale anaerobic sequencing batch reactor treating swine waste," *Water Research*, vol. 36, no. 18, pp. 4648–4654, 2002.

[13] S. Chugh, D. P. Chynoweth, W. Clarke, P. Pullammanappallil, and V. Rudolph, "Degradation of unsorted municipal solid waste by a leach-bed process," *Bioresource Technology*, vol. 69, no. 2, pp. 103–115, 1999.

[14] M. Kim, Y. H. Ahn, and R. E. Speece, "Comparative process stability and efficiency of anaerobic digestion; mesophilic versus thermophilic," *Water Research*, vol. 36, no. 17, pp. 4369–4385, 2002.

[15] C. Y. Lin and Y. S. Lee, "Effect of thermal and chemical pretreatments on anaerobic ammonium removal in treating septage using the UASB system," *Bioresource Technology*, vol. 83, no. 3, pp. 259–261, 2002.

[16] Q. Wang, M. Kuninobu, H. I. Ogawa, and Y. Kato, "Degradation of volatile fatty acids in highly efficient anaerobic digestion," *Biomass and Bioenergy*, vol. 16, no. 6, pp. 407–416, 1999.

[17] D. J. Martin, L. G. A. Potts, and A. Reeves, "Small-scale simulation of waste degradation in landfills," *Biotechnology Letters*, vol. 19, no. 7, pp. 683–685, 1997.

[18] C. J. Álvarez-Gallego, *Ensayo de diferentes procedimientos para el arranque de un proceso de co-digestión anaerobia seca de OFMSW y lodos de depuradora en rango termofílico [Ph.D. thesis]*, Universidad de Cádiz, 2005.

[19] T. E. Lai, A. Nopharatana, P. C. Pullammanappallil, and W. P. Clarke, "Cellulolytic activity in leachate during leach-bed anaerobic digestion of municipal solid waste," *Bioresource Technology*, vol. 80, no. 3, pp. 205–210, 2001.

[20] A. M. Buswell and H. F. Mueller, "Mechanism of methane fermentation," *Industrial and Engineering Chemistry*, vol. 44, no. 3, pp. 550–552, 1952.

[21] J. Fernández, M. Pérez, and L. I. Romero, "Effect of substrate concentration on dry mesophilic anaerobic digestion of organic fraction of municipal solid waste (OFMSW)," *Bioresource Technology*, vol. 99, no. 14, pp. 6075–6080, 2008.

[22] A. Davidsson, C. Gruvberger, T. H. Christensen, T. L. Hansen, and J. L. C. Jansen, "Methane yield in source-sorted organic fraction of municipal solid waste," *Waste Management*, vol. 27, no. 3, pp. 406–414, 2007.